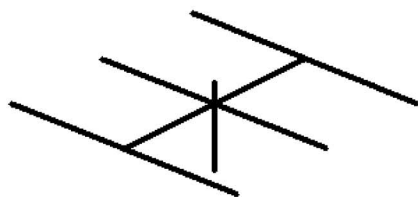
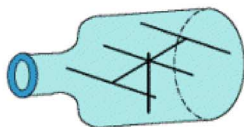


Antenna Modeling Notes



Volume 2



L. B. Cebik, W4RNL

Antenna Modeling Notes

Volume 2

L. B. Cebik, W4RNL

***Published by
antenneX Online Magazine***

<http://www.antennex.com/>

POB 271229

Corpus Christi, Texas 78427-1229 USA

Copyright 2003 by **L. B. Cebik** jointly with ***antenneX Online Magazine***. All rights reserved. No part of this book may be reproduced or transmitted in any form, by any means (electronic, photocopying, recording, or otherwise) without the prior written permission of the author and publisher jointly.

ISBN: 1-877992-55-0

Table of Contents

Dedication	6
Preface	7
26. The Scales of Equivalence	9
27. Modeling By Equation: A. A Beginning	21
28. Modeling By Equation: B. Bigger and Better Things	36
29. Modeling By Equation: C. Formulas and Blocks	57
30. Modeling By Equation: D. Scratch Pads & Coordinates ..	79
31. A Case Study: A 90' Wire	95
32. A Case Study: Rotating a Beam	109
33. A Clean Sweep	125
34. The Second Ground Medium	141
35. Notes on Using AZ-EL Plots Effectively	161
36. Getting a Grip on AZ/EL and Phi/Theta	179
37. Verticals: Using the MININEC Ground	199
38. Radials: Segmentation and Convergence	216
39. Radials: Complex Radial Systems	230
40. Resolution	244
41. Multiple-Feedpoint Loop Modeling	262
42. Moving and Rotating	276
43. Modeling Element Substitutes	292
44. Designing With NEC: A Case Study Part 1: The 4 Ss	308
45. Designing With NEC: A Case Study Part 2: Evaluation & Reality	323
46. A Load in Parallel With a Source	337

47. So You Want to Read a NEC-Deck	351
48. Radiation Plots: Polar or Rectangular; Log or Linear	366
49. Traps	380
50. The NEC-4 IS Card: Insulated Wires	391
Appendix: Antenna Models	406
Other Publications	408

Dedication

This volume of studies of antenna modeling is dedicated to the memory of Jean, who was my wife, my friend, my supporter, and my colleague. Her patience, understanding, and assistance gave me the confidence to retire early from academic life to undertake full-time the continuing development of my personal web site at the URL, <http://www.cebik.com>. The site is devoted to providing, as best I can, information of use to radio amateurs and others--both beginning and experienced--on various antenna and related topics. This volume grew out of that work--and hence, shows Jean's help at every step.

Preface

This collection of antenna modeling notes continues the compilation of the series that I began in 1998 in *antenneX*. It contains numbers 26 through 50 of the long-running series that is running even today. The time has come to collect these columns into a more convenient form for the reader. There is just too much material for a single volume, so I have broken the collection into three 25-column units. I have reviewed the text and graphics for each column to ensure as much accuracy as I can muster. However, I have also reviewed the sample models used in each column. That process permitted me to add something to these volumes that is not available in *antenneX* or at my own web site. The Appendix to each of these volumes contains a collection of antenna modeling files in three formats: .NEC (ASCII), .EZ (EZNEC), and .NWP (NEC-Win Plus). I have revised the text to include a file name for the applicable model in the Appendix. Therefore, should you wish to do so, you will be able to read a column in front of your computer and to test for yourself the ideas involved.

The 1980s and 1990s saw new implementations of MININEC and NEC: entry level programs, first in DOS and later in Windows. Every entry-level program makes a selection of what the developer considers to be the most essential features for basic antenna modeling. In MININEC programs, these features usually coincide with the limits of the calculating core itself, since it emerged as a basic modeling program for restricted-capability PCs of the earliest sorts. There are also advanced NEC programs, such as NEC-Win Pro (NEC-4) and GNEC (NEC-4) that offer the user advanced features. The advanced features include all of the geometry and command inputs of which the core is capable. The original FORTRAN programming of NEC allowed a very sizable number of possibilities and potentials.

Each program has its own personality, despite the fact that each accesses the NEC core. DOS versions of MININEC included MN (AO) and ELNEC, one striving to include every known feature, the other striving for user friendliness. These traits persist to this day in the Windows version of NEC called EZNEC and the recent descendent (by a different developer) of NEC-Wires called NEC2GO. Another NEC-2 implementation, NEC-Win Plus combines spreadsheet modeling by equation with

more standard entry-level features. Most NEC-2 implementations include corrections for the known NEC-2 weakness in dealing with stepped-diameter elements, a common method of construction for upper HF rotatable arrays. In the course of these three volumes, we shall have occasion to take a deeper look at some of these adjunct features. In this volume, we shall spend several columns on a tutorial that introduces the art and craft of modeling by equations using a spreadsheet format. See Volume 1 for the URL's of both NEC and MININEC programs.

In addition to adjuncts included within entry-level programs, there are also complete adjunct programs to perform special functions for the modeler. NEC-Win Synth from Nittany-Scientific (<http://www.nittany-scientific.com>) offers the modeler a program to simplify the process of developing wire-grid geometry structures to include within models. It even provides the user with some pre-set structures, such as vehicles and common geometric shapes used in microwave antennas, so that the user need only specify the frequency, the dimensions, and the level of segmentation required. A different sort of adjunct program is MultiNEC, an Excel application (<http://www.qsl.net/ac6la/index.html>). It permits the user to employ his or her NEC program within a spreadsheet shell to sweep numerous facets of a model's structure and other commands and to provide graphical and tabular outputs within the formatting capabilities of the shell.

Since both MININEC 3.13 and NEC-2 are public domain core programs, we can expect implementations to come and go over long periods of time. Some do both. For example, Antenna Model was an early DOS MININEC offering that disappeared, only to re-emerge in Windows dressing, accompanied by the most complete set of correctives for known limitations in the original core. AO and NEC-Wires disappeared a number of years ago, but their NEC-2 Windows descendent, NEC2GO (<http://www.nec2go.com>) is available today. We can expect this evolution to continue. Even more variable than the programs themselves are the Internet locations where you may obtain further information on them. Nevertheless, I hope that the principles discussed in this collection of modeling notes will be sufficiently general that they will apply beyond the boundaries of individual implementations of NEC and MININEC.

26. The Scales of Equivalence

Frequency scaling antennas consists of adjusting the dimensions of an antenna with a frequency F_1 to some other frequency F_2 . The process is very straightforward in some kinds of cases, and somewhat circuitous in others. Let's examine a case of each type so that we can become aware of when simple scaling may fail us and of the sorts of maneuvers we can perform to get the job done anyway.

Simple Scaling

The basic parameters of frequency scaling in its simplest form appear in **Fig. 26-1**.

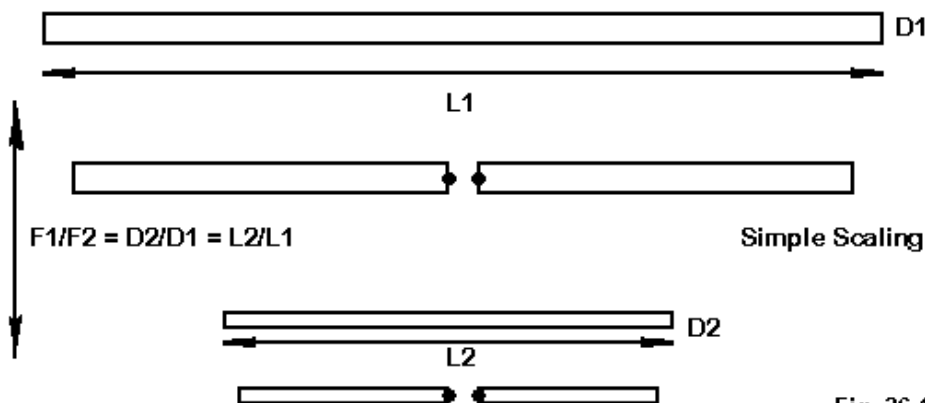


Fig. 26-1

Scaling involves not only element length adjustments, but also element diameter adjustments of the same magnitude. The adjustments we must make are simply the inverse of the ratio of the two frequencies. If the initial frequency is 28.35

MHz and the target frequency is 14.175 MHz, then the ratio is 0.5. All element lengths, spacing, and diameters must therefore be multiplied by the inverse of the ratio—in this case by 2—to arrive at the final antenna dimensions.

Let's examine the wire chart for a simple 2-element Yagi cut for 28.35 MHz.

2-el Al Yagi: 28.35 MHz

Frequency = 28.35 MHz.

Wire Loss: Aluminum – Resistivity = 4E-08 ohm-m, Rel. Perm. = 1

———— WIRES ————

Wire Conn.— End 1 (x,y,z : in) Conn.— End 2 (x,y,z : in) Dia(in) Segs

1	-95.250,	52.000,	0.000	95.250,	52.000,	0.000	1.00E+00	21
2	-105.75,	0.000,	0.000	105.750,	0.000,	0.000	1.00E+00	21

The element end coordinates are specified in the “X” columns; the element spacing is in the “Y” column; and the diameter is to the right. See model 26-1.

The modeled performance of this antenna is as follows.

Freq. MHz	Free-Space Gain dBi	Front-to Back Ratio dB	Feedpoint Z R +/- jX Ohms
28.0	6.29	11.32	31.18 - j 12.12
28.35	6.03	11.00	36.46 - j 0.13
28.7	5.80	10.35	41.55 + j 11.29

If we frequency scale this antenna to 14.175 MHz, all of the dimensions are multiplied by 2 to arrive at the following wire table.

2-el Al Yagi: 14.175 MHz

Frequency = 14.175 MHz.

Wire Loss: Aluminum – Resistivity = 4E-08 ohm-m, Rel. Perm. = 1

———— WIRES ————

Wire Conn.— End 1 (x,y,z : in) Conn.— End 2 (x,y,z : in) Dia(in) Segs

1	-190.50,	104.000,	0.000	190.500,	104.000,	0.000	2.00E+00	21
2	-211.50,	0.000,	0.000	211.500,	0.000,	0.000	2.00E+00	21

Because every dimension is exactly scaled, we expect the resultant antenna to perform along its new frequency range exactly as the initial model performed within its own range. We shall not be disappointed by the modeled antenna performance figures. See model 26-2.

Freq. MHz	Free-Space Gain dBi	Front-to Back Ratio dB	Feedpoint Z R +/- jX Ohms
14.0	6.29	11.32	31.15 - j 12.12
14.175	6.03	11.00	36.44 - j 0.14
14.35	5.81	10.37	41.52 + j 11.29

I have reported values to more decimal places than would be operationally significant in order to show the degree to which scaling can be precise. Unfortunately, not every case of scaling lends itself to such easy arithmetical treatment.

A More Difficult Scaling Task

Let's next tackle a slightly more interesting scaling task. Our task will be to scale a 20-meter Yagi with complex stepped diameter elements into a 10-meter Yagi with a simpler element scheme, as in **Fig. 26-2**.

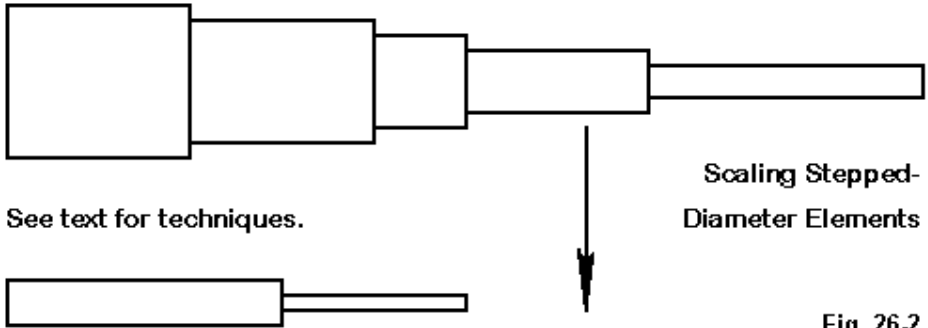


Fig. 26-2

The frequency ratio will be 2:1. As we shall discover, that fact does not come close to resolving the scaling challenge.

Suppose we begin with a 4-element 20-meter Yagi having the following wire structure. See model 26-3.

4-element 20M Yagi

Frequency = 14.175 MHz.

Wire Loss: Aluminum — Resistivity = 4E-08 ohm-m, Rel. Perm. = 1

———— WIRES —————

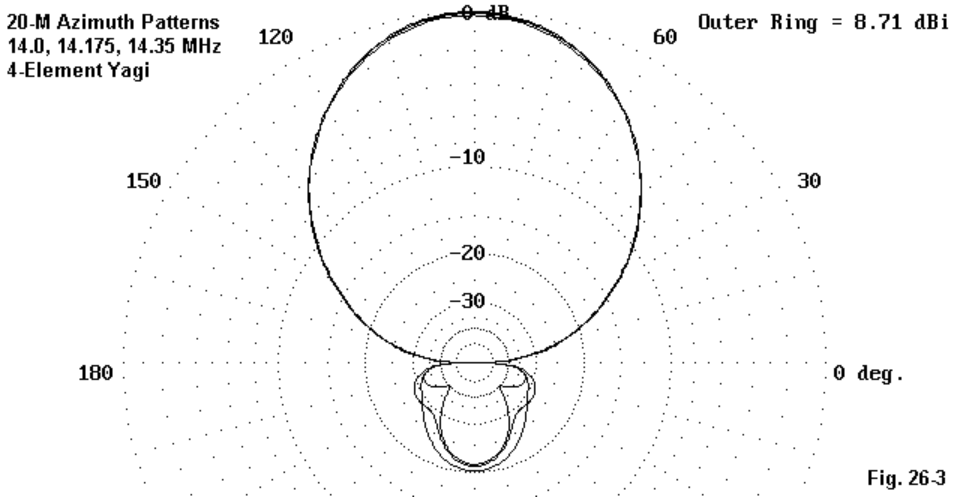
Wire Conn.--	End 1 (x,y,z : in)	Conn.--	End 2 (x,y,z : in)	Dia(in)	Segs
1	-217.50, 0.000, 0.000	W2E1	-154.00, 0.000, 0.000	5.00E-01	7
2	W1E2 -154.00, 0.000, 0.000	W3E1	-134.00, 0.000, 0.000	6.25E-01	2
3	W2E2 -134.00, 0.000, 0.000	W4E1	-92.000, 0.000, 0.000	7.50E-01	4
4	W3E2 -92.000, 0.000, 0.000	W5E1	-72.000, 0.000, 0.000	8.75E-01	2
5	W4E2 -72.000, 0.000, 0.000	W6E1	-48.000, 0.000, 0.000	1.00E+00	2
6	W5E2 -48.000, 0.000, 0.000	W7E1	48.000, 0.000, 0.000	1.25E+00	9
7	W6E2 48.000, 0.000, 0.000	W8E1	72.000, 0.000, 0.000	1.00E+00	2
8	W7E2 72.000, 0.000, 0.000	W9E1	92.000, 0.000, 0.000	8.75E-01	2
9	W8E2 92.000, 0.000, 0.000	W10E1	134.000, 0.000, 0.000	7.50E-01	4
10	W9E2 134.000, 0.000, 0.000	W11E1	154.000, 0.000, 0.000	6.25E-01	2
11	W10E2 154.000, 0.000, 0.000		217.500, 0.000, 0.000	5.00E-01	7
12	-211.00, 72.000, 0.000	W13E1	-154.00, 72.000, 0.000	5.00E-01	5
...					
22	W21E2 154.000, 72.000, 0.000		211.000, 72.000, 0.000	5.00E-01	5
23	-203.55,141.000, 0.000	W24E1	-154.00,141.000, 0.000	5.00E-01	5
...					
33	W32E2 154.000,141.000, 0.000		203.550,141.000, 0.000	5.00E-01	5
34	-190.56,306.000, 0.000	W35E1	-154.00,306.000, 0.000	5.00E-01	4
...					
44	W43E2 154.000,306.000, 0.000		190.560,306.000, 0.000	5.00E-01	4

For elements 2, 3, and 4, I have omitted the interior wires of the model, since they are identical to those in the first element. The design is adapted from a version created by N6BV. I have adjusted the dimensions so that the antenna properties are spread out across the 20-meter amateur band rather than being focused in the lower 200 kHz. Hence, the design-center frequency is 14.175 MHz for this model. As well, I have adjusted the driver length for resonance and adjusted the spacing so that the resonant impedance is close to 25 Ohms. Hence, the design can be fed with a 1/4-wavelength section of 35-Ohm cable from the main 50-Ohm feedline. All in all, this is a nice little design that would fit a 26' boom.

Tabularly, the performance of this example follows this pattern.

Freq. MHz	Free-Space Gain dBi	Front-to Back Ratio dB	Feedpoint Z R +/- jX Ohms
14.0	8.42	21.28	23.54 - j 6.99
14.175	8.53	22.80	26.26 - j 0.73
14.35	8.62	20.31	21.26 + j 4.89

More graphically, the overlaid free-space azimuth patterns for this antenna appear in **Fig. 26-3**.



Now let's scale the antenna directly, replacing every wire length, spacing, and diameter in the model with its half-size replacement for a design frequency of 28.35 MHz. Some programs, such as EZNEC, have an automatic scaling function associated with frequency selection. The scaling option applies to element length, spacing, and diameter, with one exception. If the user has specified the element diameter as an AWG wire gauge number, then the diameter remains constant. Other

programs that lack a scaling option, but that have the ability to model by equation, can achieve automatic scaling in a different way. Simply define all of the element parameters as a function of wavelength at the design frequency. The performance table is as follows. See model 26-4.

Freq. MHz	Free-Space Gain dBi	Front-to Back Ratio dB	Feedpoint Z R +/- jX Ohms
28.0	8.40	21.28	23.57 - j 6.97
28.35	8.51	22.76	26.27 - j 0.71
28.7	8.61	20.28	21.26 + j 4.95

The tabulated values tell us that **Fig. 26-3** makes as good a representation of the azimuth patterns for the scaled antenna as for the original. Hence, we can go directly to the wire table for the directly scaled 10-meter antenna.

4-element 10M Yagi-scaled

Frequency = 28.35 MHz.

Wire Loss: Aluminum - Resistivity = 4E-08 ohm-m, Rel. Perm. = 1

———— WIRES ————

Wire Conn.--	End 1 (x,y,z : in)	Conn.--	End 2 (x,y,z : in)	Dia(in)	Segs
1	-108.75, 0.000, 0.000	W2E1	-77.000, 0.000, 0.000	2.50E-01	7
2	W1E2 -77.000, 0.000, 0.000	W3E1	-67.000, 0.000, 0.000	3.13E-01	2
3	W2E2 -67.000, 0.000, 0.000	W4E1	-46.000, 0.000, 0.000	3.75E-01	4
4	W3E2 -46.000, 0.000, 0.000	W5E1	-36.000, 0.000, 0.000	4.38E-01	2
5	W4E2 -36.000, 0.000, 0.000	W6E1	-24.000, 0.000, 0.000	5.00E-01	2
6	W5E2 -24.000, 0.000, 0.000	W7E1	24.000, 0.000, 0.000	6.25E-01	9
7	W6E2 24.000, 0.000, 0.000	W8E1	36.000, 0.000, 0.000	5.00E-01	2
8	W7E2 36.000, 0.000, 0.000	W9E1	46.000, 0.000, 0.000	4.38E-01	2
9	W8E2 46.000, 0.000, 0.000	W10E1	67.000, 0.000, 0.000	3.75E-01	4
10	W9E2 67.000, 0.000, 0.000	W11E1	77.000, 0.000, 0.000	3.13E-01	2
11	W10E2 77.000, 0.000, 0.000		108.750, 0.000, 0.000	2.50E-01	7
12	-105.50, 36.000, 0.000	W13E1	-77.000, 36.000, 0.000	2.50E-01	5
...					
22	W21E2 77.000, 36.000, 0.000		105.500, 36.000, 0.000	2.50E-01	5
23	-101.77, 70.500, 0.000	W24E1	-77.000, 70.500, 0.000	2.50E-01	5
...					
33	W32E2 77.000, 70.500, 0.000		101.775, 70.500, 0.000	2.50E-01	5
34	-95.280, 153.000, 0.000	W35E1	-77.000, 153.000, 0.000	2.50E-01	4
...					
44	W43E2 77.000, 153.000, 0.000		95.280, 153.000, 0.000	2.50E-01	4

Once more I have omitted the interior structure of elements except for the reflector, since all 4 elements are the same in this respect. The problem posed by the scaled antenna is self-revealing from the truncated data: the stepped-diameter-tubing schedule would require the use of thin-wall tubing of sizes that are not available. In short, we are unlikely to want to build the directly scaled model.

Suppose that we wish simply to use for each element an interior length of 0.5" diameter tubing and an outer tip of 0.375" diameter tubing. The temptation would be to use our scaled outer dimensions for each element and simply change the remainder of the wire schedule. The final result might look like this.

4-element 10M Yagi

Frequency = 28.35 MHz.

Wire Loss: Aluminum - Resistivity = 4E-08 ohm-m, Rel. Perm. = 1

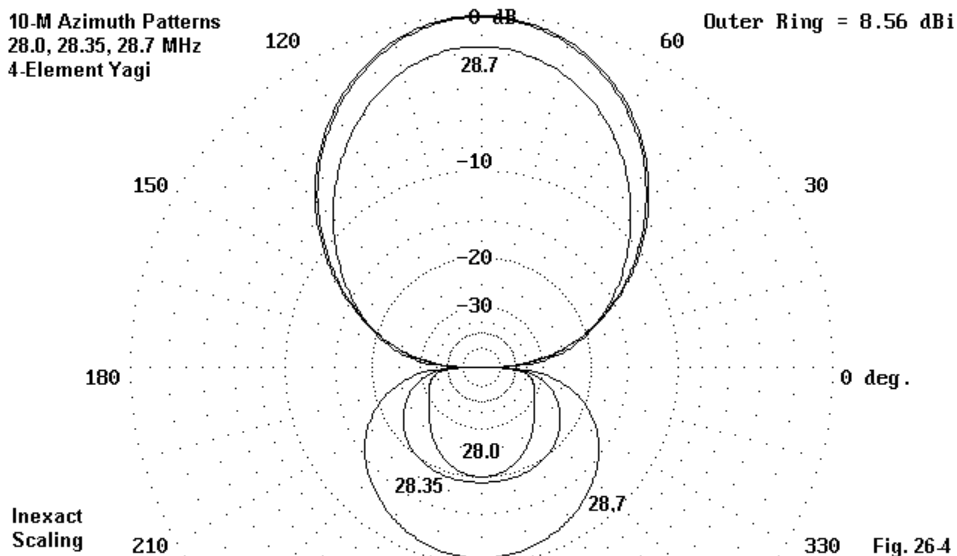
————— WIRES —————

Wire Conn.--	End 1 (x,y,z : in)	Conn.--	End 2 (x,y,z : in)	Dia(in)	Segs
1	-108.75, 0.000, 0.000	W2E1	-48.000, 0.000, 0.000	3.75E-01	6
2	W1E2 -48.000, 0.000, 0.000	W3E1	48.000, 0.000, 0.000	5.00E-01	9
3	W2E2 48.000, 0.000, 0.000		108.750, 0.000, 0.000	3.75E-01	6
4	-105.50, 36.000, 0.000	W5E1	-48.000, 36.000, 0.000	3.75E-01	6
5	W4E2 -48.000, 36.000, 0.000	W6E1	48.000, 36.000, 0.000	5.00E-01	9
6	W5E2 48.000, 36.000, 0.000		105.500, 36.000, 0.000	3.75E-01	6
7	-101.77, 70.500, 0.000	W8E1	-48.000, 70.500, 0.000	3.75E-01	5
8	W7E2 -48.000, 70.500, 0.000	W9E1	48.000, 70.500, 0.000	5.00E-01	9
9	W8E2 48.000, 70.500, 0.000		101.775, 70.500, 0.000	3.75E-01	5
10	-95.280,153.000, 0.000	W11E1	-48.000,153.000, 0.000	3.75E-01	5
11	W10E2 -48.000,153.000, 0.000	W12E1	48.000,153.000, 0.000	5.00E-01	9
12	W11E2 48.000,153.000, 0.000		95.280,153.000, 0.000	3.75E-01	5

If we check this model, we would obtain a performance table similar to the following one. See model 26-5.

Freq. MHz	Free-Space Gain dBi	Front-to Back Ratio dB	Feedpoint Z R +/- jX Ohms
28.0	8.54	19.90	20.24 + j 6.85
28.35	8.45	18.23	10.00 + j 20.49
28.7	6.91	8.32	3.56 + j 41.45

Graphically, the azimuth patterns would be those in **Fig. 26-4**. Something has one wrong with our scaling efforts. The elements are all too long. Unfortunately, many a home constructor of beams has been caught in this trap. Scaling an antenna's dimensions and then changing the stepped-diameter element schedule is a sure way to offset the performance curve of an antenna.



The Correction

The accuracy of NEC-2 (and to a lesser degree, NEC-4) depends upon the introduction of correction factors that substitute for stepped-diameter elements a uniform diameter element of the same impedance. Most NEC-2 software equipped with such correction factors use either the Leeson equations (EZNEC and NEC-Win Plus) or the Beezley equations (NEC-Wires). Let's compare the substitute uni-

form-element lengths and diameters of the elements for a. the impractical but exactly scaled 10-meter Yagi and b. the simplified but errant Yagi.

Element	Directly Scaled		Simplified	
	Length	Diameter	Length	Diameter
Reflector	104.094"	0.396"	106.985"	0.434"
Driver	100.990"	0.403"	103.765"	0.437"
Dir. 1	97.448"	0.410"	100.078"	0.440"
Dir. 2	91.317"	0.424"	93.663"	0.446"

The excess length of the Yagi with a simplified element structure is clearly apparent. However, there is no simple and sure means of shortening the uniform element lengths to the lengths used in the directly scaled version—at least not in extant implementations of NEC-2. However, there is a sure procedure to bring us very close indeed to the desired goal.

Every element in a Yagi has a self-resonant frequency. Using the directly scaled 10-meter beam as our guide (since we know its performance potential), let's find the self-resonant frequency for each element, using a reactance of under 1 Ohm to define resonance. Then, we shall adjust the length of the corresponding element in the simplified version of the antenna so that its self-resonant frequency is the same as in the directly scaled version. As a check on our work, we shall record the result—ant substitute uniform-diameter element. The final result looks like this.

Element	Freq.	New Length	Subs. Length	Subs. Diameter
Reflector	27.12	105.8"	104.062"	0.436"
Driver	27.96	102.6"	100.894"	0.439"
Dir. 1	28.94	99.1"	97.434"	0.442"
Dir. 2	30.86	92.9"	91.317"	0.449"

If we compare the substitute uniform-diameter elements in our revised model, we shall see how close they are to the substitute uniform-diameter elements for the directly scaled model in both length and diameter. Given that similarity, we shall not require any spacing adjustments in our newly revised model with its simplified element structure.

An alternative procedure is to adjust the element lengths in our 2-step element model until the substitute element lengths are the same as the substitute element lengths in the highly stepped directly scaled version of the antenna. The viability of

this method rests on two factors. One is the ease with which we can examine the uniform-diameter substitute element data, a factor that varies from one program to the next. The second factor is, once more, the similarity of the diameters of the uniform-diameter elements in the direly scaled and the new 2-step elements. Since the electrical properties of an elements depend both upon length and upon diameter, the diameters must be fairly close if the technique is to succeed.

The final wire table looks like this. See model 26-6.

4-element 10M Yagi-scale adj.

Frequency = 28.35 MHz.

Wire Loss: Aluminum — Resistivity = 4E-08 ohm-m, Rel. Perm. = 1

————— WIRES —————

Wire Conn.—	End 1 (x,y,z : in)	Conn.—	End 2 (x,y,z : in)	Dia(in)	Segs
1	-105.80, 0.000, 0.000	W2E1	-48.000, 0.000, 0.000	3.75E-01	6
2	W1E2 -48.000, 0.000, 0.000	W3E1	48.000, 0.000, 0.000	5.00E-01	9
3	W2E2 48.000, 0.000, 0.000		105.800, 0.000, 0.000	3.75E-01	6
4	-102.60, 36.000, 0.000	W5E1	-48.000, 36.000, 0.000	3.75E-01	6
5	W4E2 -48.000, 36.000, 0.000	W6E1	48.000, 36.000, 0.000	5.00E-01	9
6	W5E2 48.000, 36.000, 0.000		102.600, 36.000, 0.000	3.75E-01	6
7	-99.100, 70.500, 0.000	W8E1	-48.000, 70.500, 0.000	3.75E-01	5
8	W7E2 -48.000, 70.500, 0.000	W9E1	48.000, 70.500, 0.000	5.00E-01	9
9	W8E2 48.000, 70.500, 0.000		99.100, 70.500, 0.000	3.75E-01	5
10	-92.900,153.000, 0.000	W11E1	-48.000,153.000, 0.000	3.75E-01	5
11	W10E2 -48.000,153.000, 0.000	W12E1	48.000,153.000, 0.000	5.00E-01	9
12	W11E2 48.000,153.000, 0.000		92.900,153.000, 0.000	3.75E-01	5

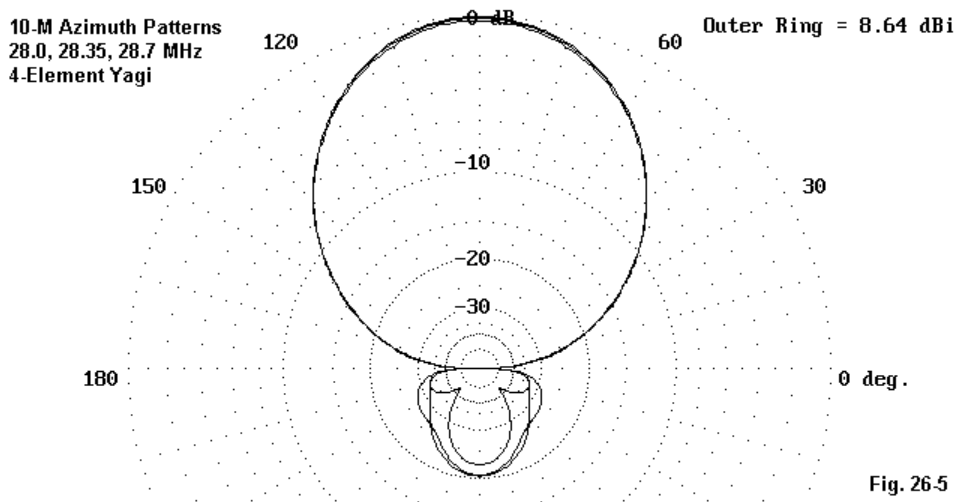
The proof of the method lies in performance, which NEC-2 reports in the following table.

Freq. MHz	Free-Space Gain dBi	Front-to Back Ratio dB	Feedpoint Z R +/- jX Ohms
28.0	8.41	21.84	23.20 - j 7.59
28.35	8.52	22.83	26.04 - j 1.37
28.7	8.61	20.39	20.39 + j 3.99

Do not expect the report numbers to be precisely the same as the originals to the last decimal place. The technique is close, but the resulting antenna is not an

exact clone of the original or the perfect scaling. Even perfect a scaling will show a small bit of variation, since skin effect does not vary linearly with frequency. However, the numbers will usually be within 1 to 2 percent, which is closer tolerance than most home workshops can achieve in the construction phase of a project such as this HF array.

In terms of azimuth patterns, **Fig. 26-5** provides the same data more dramatically.



There are other dimensions to the scaling project. For example, the operating passband for the scaling array is 28.0 to 28.7 MHz. However, 28.8 MHz is a popular frequency for a number of 10-meter activities. The modeler is faced with the question of whether simply to accept the beam design as modified as it is with whatever performance emerges above 27.7 MHz, or whether to further modify the design. Further modification might mean sliding the performance curve upward. The exact amount of sliding would depend upon the performance just above and just below the present edges of the defined passband. "Sliding," for course, would be a task

calling for a small frequency scaling of the element lengths and spacing. However, such small changes rarely require re-scaling of the element diameter.

Conclusion

Frequency scaling begins as a simple process. However, the more complex the antenna's structure, the more complex the process can become. I have used the example of changing the stepped-diameter structure of the elements for several reasons. First, in many instances, practical antenna construction demands element structures that differ from those of a directly scaled model. Second, many antenna constructors fall into the snare of simply changing element structures without first analyzing the potential consequences.

Third, the techniques required for restoring the poorly scaled antenna model to a much more usable state are typical of techniques that may be required in many other situations. For the general process of modeling, it is this last reason which is the most important. The exercise is not a cure-all for all difficulties in the process of scaling antennas. However, it should alert you to what may make a scaling task go astray and what sorts of techniques may bring the model back into the fold.

* * * * *

Models included: 26-1 through 26-6. (.NEC and .NWP model dimensions in meters; .EZ model dimensions in inches.)

27. Modeling By Equation: A. A Beginning

Most beginning modelers acquire the habit of simply placing physical wire dimensions into the structure grid of NEC and MININEC input systems. The wire geometry may be systematic or random, initially, but that is a problem we looked at in an early installment in this series. In this episode, I should like to start an exploration of another way to model antennas: by the use of variables and equations.

In MININEC programs, AO permitted the use of variables and equations. Of presently available NEC-2 programs, perhaps NEC-Win Plus offers the most versatile system of modeling in this way. For example, the input files for AO and Antenna Model (MININEC) or for NEC2GO (NEC) do not themselves show the physical values resulting from the use of variables and equations. However, the spreadsheet input screen of NEC-Win Plus allows the user to see, in alternative views of the structure spreadsheet, a. the numbers and equations used to set the values of variables, b. the values that result from those equations, c. the assignment of variables to the X, Y, and Z coordinates of the model structure, and d. the physical values of the X, Y, and Z coordinates that result from the preceding steps. So for this exercise, I shall make use of NEC-Win Plus to demonstrate a few (but by no means all) of the steps involved in modeling by variables—along with a couple of the advantages that accrue to the modeler. (In future episodes, we shall look at more complex structures and more complex ways of formulating variables.)

Fig. 27-1 represents our sample antenna—a simple quad loop. For simplicity, we shall begin with a free space model for 300 MHz, composed of #20 AWG (0.032" diameter) copper wire. A square quad loop consists of 4 equal sides. A simplistic approach to modeling by variables might simply let some variable A equal the physical length of a side and proceed from there.

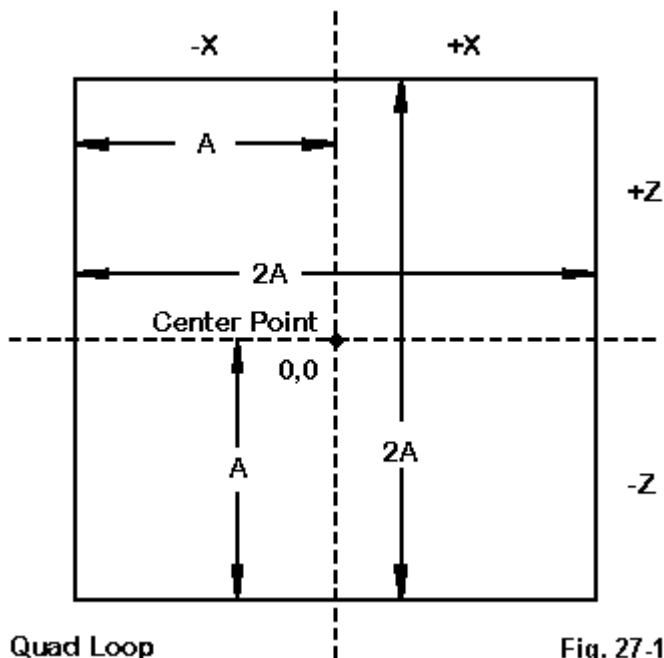


Fig. 27-1

Dimensions as Variables

However, when modeling by variables, it pays to do a preliminary inspection of the geometry of the antenna to see if one might obtain a more sophisticated and ultimately more useful selection of variables and values. **Fig. 27-1** shows that a square quad loop can be framed against a center point so that we can take advantage of the Cartesian reference system. The example takes the 2-dimensional square and assigns the horizontal dimension to the X axis and the vertical dimension to the Z axis. Initially, Y will always equal zero.

In a free-space model, we can keep the structure centered by using values of A as +/-X and +/-Z values. This will come in handy later when we move the antenna over real ground. For initial purposes, A becomes about 1/8 wavelength long to form the approximately 1 wavelength total loop circumference. For the present, we shall not be concerned with whether the loop should be exactly 1 wavelength long, since that is something we shall discover from our modeling. Unless otherwise specified, the dimensional units for our exercise will be inches.

The first step is to define a variable as 1/8 wavelength long. **Fig. 27-2** shows the NEC-Win Plus equations page, with A defined as W/8. (I shall by-pass the program-specific instruction set by which we accomplish this, but it follows standard spreadsheet procedures.) Two other variables are already assigned permanent values: F for the initial frequency (and in this case the only frequency) of test, and W for the wavelength. Note that the wavelength entry has a reference to model parameters. The parameter of relevance here is the conversion factor for changing the modeling units (inches in this instance) into the NEC core requirement of meters. The result is the wavelength in the unit of choice. See model 27-1

The lower half of **Fig. 27-2** shows the value of A in inches that results from establishing the equation that defines A. At the top of **Fig. 27-2** is a button labeled Fn. When highlighted, we see the equations. When dark, we see the values that the equations yield. In this model, we have let $A = W/8$, whatever the value of W might be. You may also note the header information that establishes this as a free-space ("No Ground") model at 300 MHz. At 300 MHz, A has a value of 4.91797. . ." because a wavelength is 39.34383. . ." long.

We might have defined the value of A in terms of frequency, but that would have required that we confine the units of measure to a single system, or that we define conversion variables. Defining A in terms of the wavelength will give us some versatility later on.

The next question is how to set up a structure that makes use of the variable A to determine the antenna dimensions.

NEC-Win Plus+ [eq1.nwp]

File Edit Configure Commands Help

Frequency (MHz) Start: 300 End: 300 Step Size: 1

Ground No Ground

Radiation Patterns 1° < Az < 360°, El = 1°, Step = 1°
0° < El < 180°, Az = 0°, Step = 1°

Geometry

Zo = 50 Ohm

Steepped inches

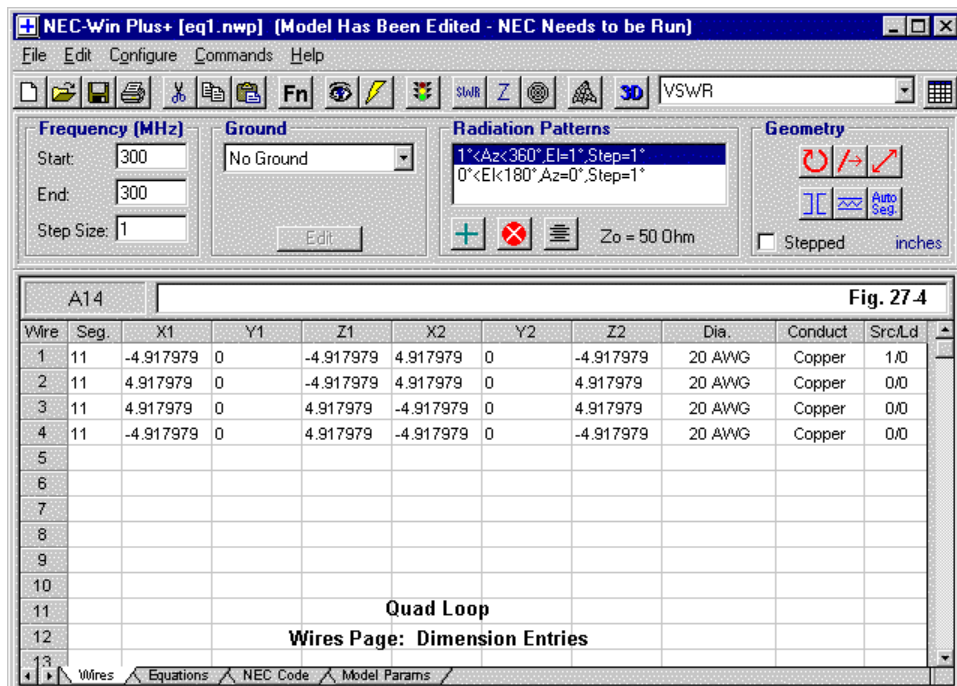
Fig. 27-2

	A	B	C	D	E	F	G	H
1	Var.	Value	Comment	Scratch Pad				
2	F =	300	Primary Frequency (MHz)					
3	W =	=299.8/B2/Model P	= "Wavelength(" & Model Params & B\$58"					
4	A =	=W/B	Initial trial value					
5	B =							
6	C =							
7	D =							
8	E =							
9	G =							
10	H =		Quad Loop					
11	I =							
12	J =		Equations Page					

Wires Equations NEC Code Model Params

	A	B	C	D	E	F	G	H
1	Var.	Value	Comment	Scratch Pad				
2	F =	300	Primary Frequency (MHz)					
3	W =	39.34383202	Wavelength(inches) = c / f					
4	A =	4.917979003						
5	B =							
6	C =							
7	D =							
8	E =							
9	G =							
10	H =							
11	I =		Equations Page					
12	J =		Values Version					

Wires Equations NEC Code Model Params

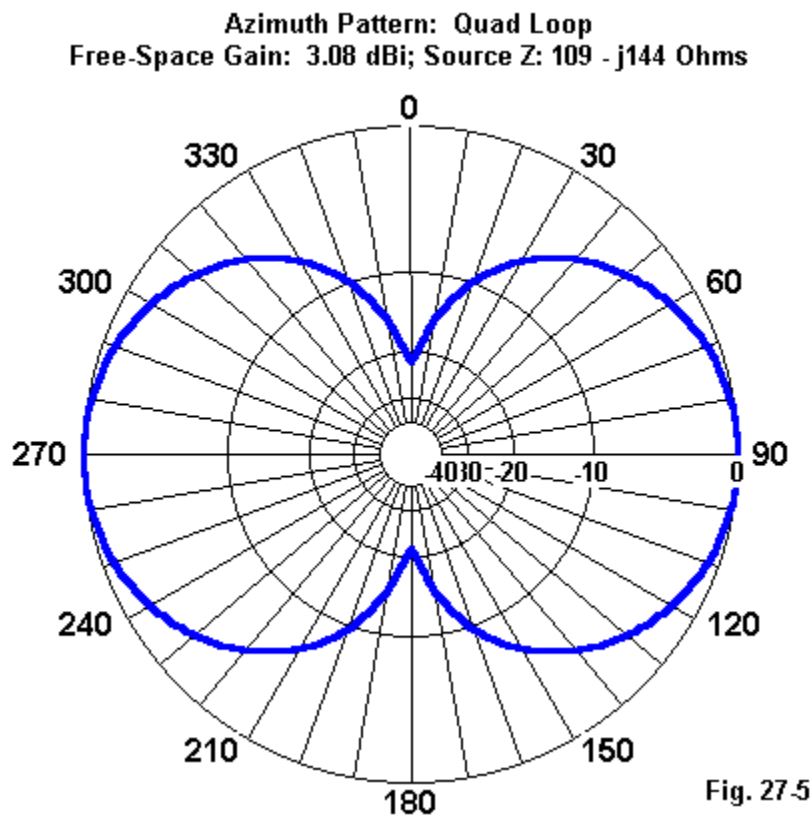


By flipping to the unhighlighted Fn version of the wires page (**Fig. 27-4**), we can view the values (in inches, our chosen unit of measure) for the variables in each position of the antenna structure. Perhaps the most difficult facet of this page to which we must grow accustomed is the number of digits in each value. We must remember that NEC programs are essentially calculating machines and do not choose the number of significant digits for us. We must do that according to the task at hand. For building this loop, we might round the figure for A into 4.92, and then translate that into 4 15/16" for measuring wire. Some other tasks involved in finding the trends in values might relevantly preserve additional decimal places. For now, we can simply accept the calculated value of A and focus on making sure that we

have constructed the loop correctly by checking appropriate End 1s and End 2s of each wire.

We characterized this model as a trial. So let's run the model and see what we get. **Fig. 27-5** places all of the data we need at this point on the free-space azimuth pattern—even though the data comes from different places in the program. For this exercise, the most essential figure to note is the source impedance: $109 - j144$ Ohms. Our loop is much too small to be a resonant quad loop for 300 MHz.

Had we entered our coordinate values in terms of individual numbers, we would now be faced with revising each coordinate value by the amount we think might move the quad loop toward resonance. To suggest that this is a time consuming procedure is to make a very serious understatement. We would have to revise 16 values however many times it takes to find a value that allows the loop to be resonant within an Ohm or two. I have found that many modelers enlarge the concept of resonance to encompass many Ohms of reactance, not because the task does not require close tolerances, but because they simply tire of adjusting coordinate values on the wires page. Some programs have shortcuts that permit adjusting junctions and wire groups together, but there are still multiple steps involved—and each becomes an invitation to drop, double strike, or transpose numbers along the way.

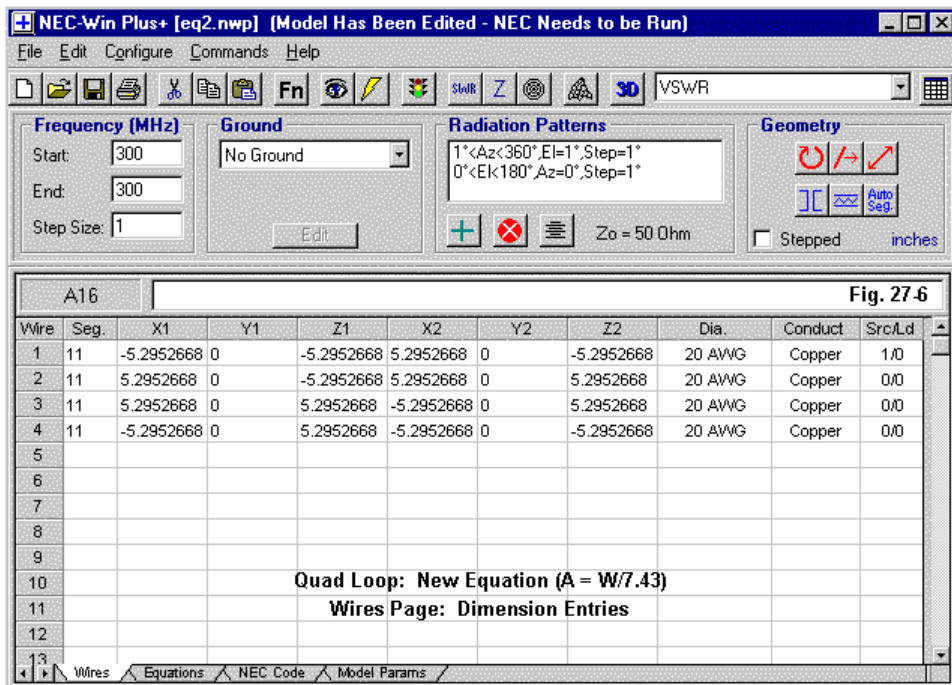


With our model-by-variable system in place, we shall change the loop dimensions by changing only one number. For this step, we return to the equations page and look back at **Fig. 27-2**. Where we had entered the value for A as $W/8$, we shall enter a new value. To make the loop larger, we should choose a smaller value than

8 as the denominator. To keep the story brief, let's replace 8 with 7.43. See model 27-2.

Had we exercised a preference for multipliers rather than divisors, we might have started with a value of $W \cdot 0.125$. Given that choice of equation formulation, to make the loop larger, we need a larger constant. The result would have been $W \cdot 0.1346$ or thereabouts.

The change we just made will make no difference to the version of the wires page that shows the assignment of variables to the coordinates of the structure. So we shall by-pass that version of the wires page and go directly to **Fig. 27-6**, the version of the wires page that shows the actual dimensions that result from the revised value for A.



The value for A is now (at 300 MHz) about 5.3, a full 7% larger than the value with which we made our trial start. Each side of the quad is now about 10.6" long. The question is whether we have achieved resonance. So let's run the model once more.

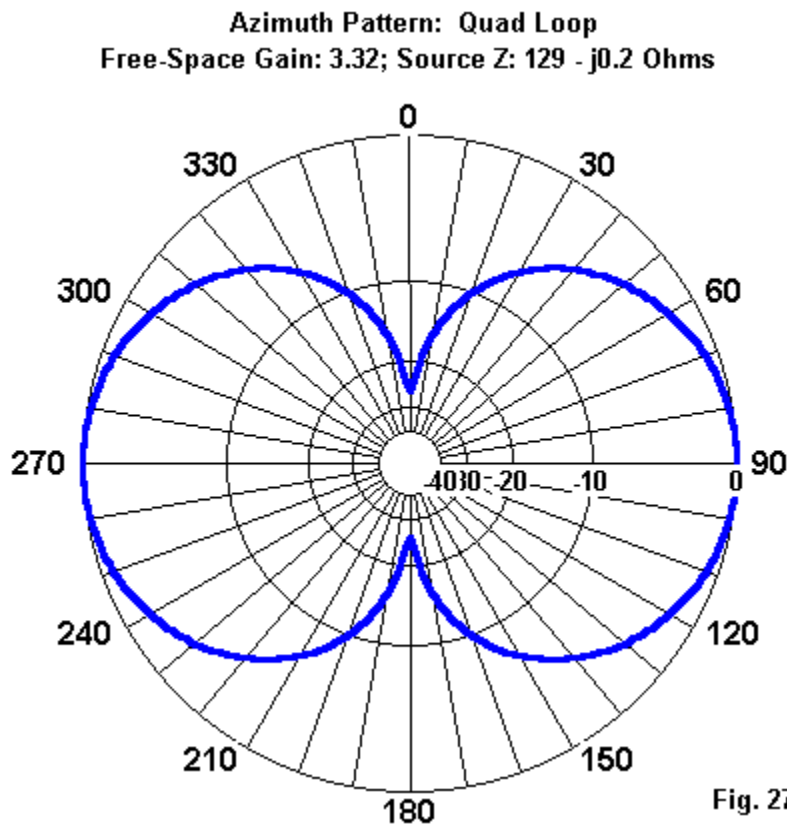


Fig. 27-7 shows the free-space azimuth pattern of the antenna, with the critical data added at the top. The loop achieves a resonant impedance of 129 Ohms, indicating that our initial task is complete. At this point, we should take a moment to appreciate the time we have saved in creeping up on the resonant dimensions of this simple loop. A little time spent with an initial analysis of the antenna geometry resulted in a much larger amount of time saved in the optimizing process.

Wire Diameter as a Variable

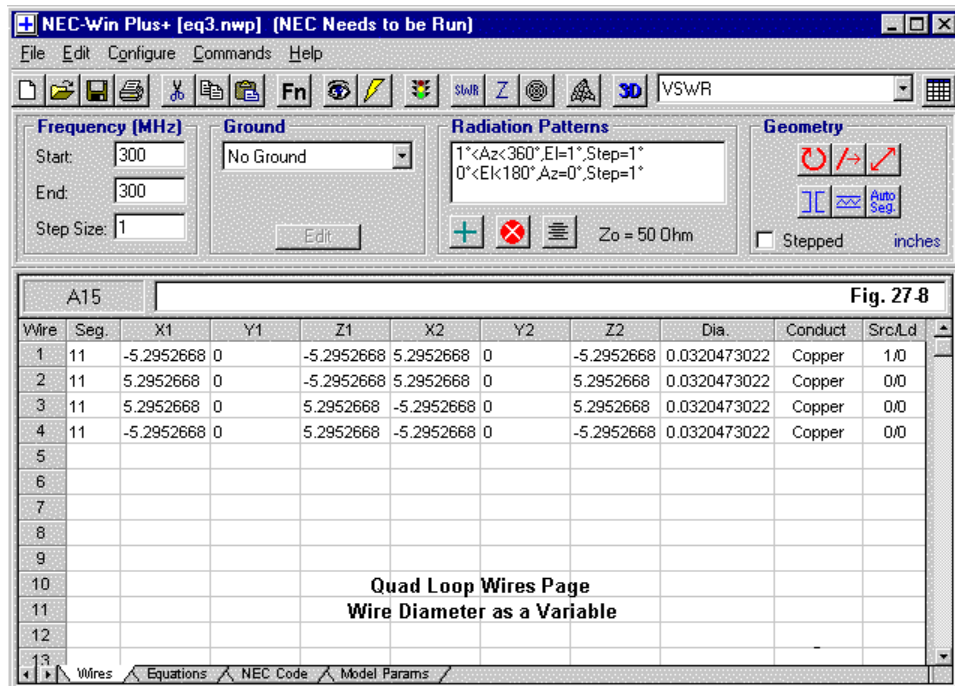
There is a limitation on the exercise we have just run. In order to focus on the aspects of dimensional modeling by the use of variables, we let the wire diameter become a constant. In virtually all programs, selecting a wire size from a chart—that is specifying the wire size in AWG values—creates a constant. For some purposes, it is better to make the wire size a variable. See model 27-3.

Therefore, let's return to **Fig. 27-2** and add a new variable B to our list. We might simply list the value of B as 0.032 or so to represent the diameter of #20 AWG wire. However, let's go to the trouble of making the wire size a function of a wavelength. If we let $B = W/1227.68$ (or $W \cdot .008145$), we shall have captured the diameter of #20 wire at 300 MHz. Wire size tables are readily available in many basic radio and electronics handbooks. Keeping a table handy at the computer is never a bad idea.

We must now go back to the “variables” version of the wires page and replace all of the wire diameter entries with “=B” to put the variable into effect. The end result on the dimensions version of the wires page will look like **Fig. 27-8**.

I shall not guarantee that the wire diameter shown is accurate for #20 AWG past the first 4 decimal places in inches, since paper tables end at that position. However, the wire size that is twice that diameter is listed at 0.0641, indicating the next digit in the #20 sequence is just below a 5. Some computer tables go much further—to 6 or more significant figures. Procedurally, one can seek out a value of the divisor (or multiplier) that yields a usable wire diameter value. Or, one can simply divide the wire size of #20 AWG by a wavelength. The actual wavelength is available on the equations page by clicking the Fn button. (For 300 MHz, the length is 39.34383202", according to the spreadsheet. If we divide .0320473 by this number, we arrive at about the same number for the divisor: 1227.68 or so. Once more, the

calculating machine provides more digits than would be useful to most operational tasks. 6 significant digits are far beyond relevance to any imaginable task.)

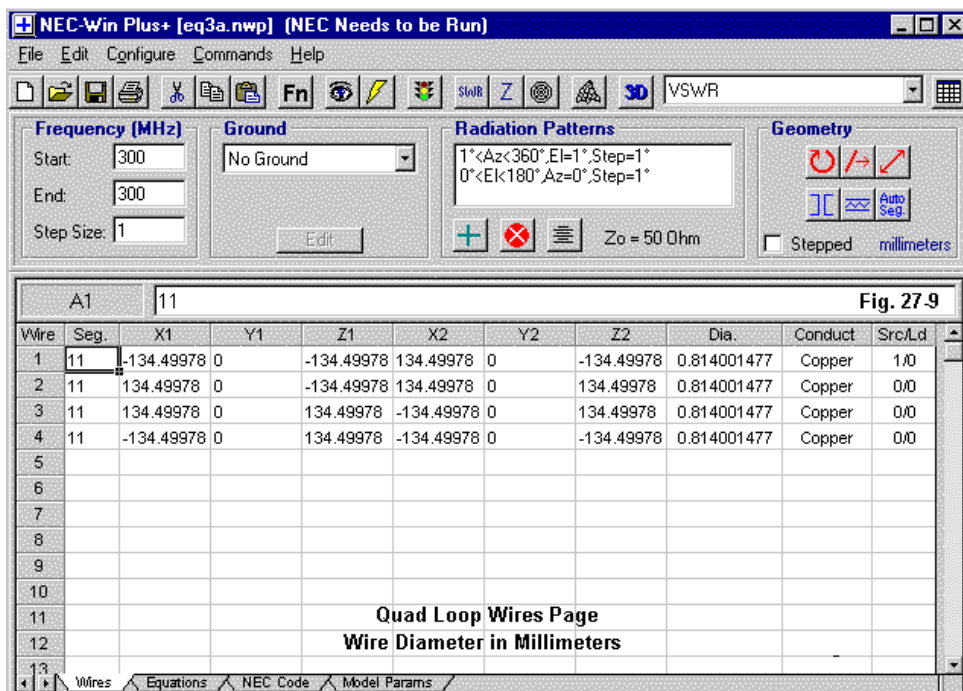


What we gain by making the making the wire diameter a function of a wavelength is a good bit more than the little trouble it took to create the variable and to put it into place on the wires page. Here are just two examples.

1. *Units conversion:* Programs vary in the manner in which they handle the conversion of units. When changing units in some programs, it may be possible to specify whether we convert all of the numerical values or whether we keep the numerical values and only change the units they represent. In other programs, a

change of units only changes the conversion factor for getting everything into meters for the NEC run. In such programs, any changes in numbers will be a task for the modeler.

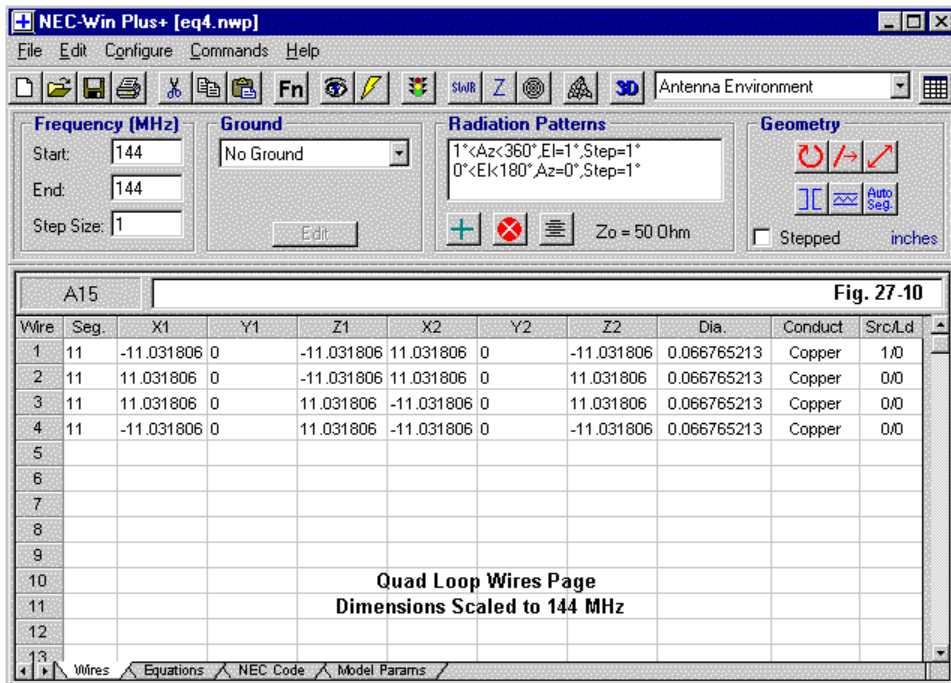
Design by variables and equations can change all of that. Since we defined all of our physical dimensions as functions of a wavelength, changing the units of measure will automatically change all of the physical values. If we remember from **Fig. 27-2**, the value for W, a wavelength, included adjustment into the currently selected units of measure by taking into account the adjustment factor for the eventual conversion into meters. Hence, the numerical value of W changes with each change we make in the units of measure. And if we change the value of W, then the values of A and B (the variables in our example) also change to the correct values for the selected unit of measure.



As an experiment, let us change from inches to millimeters. See model 27-4. The units of measure are listed in NEC-Win Plus at the right and above the geometry table. To see what happens with our change to millimeters, see **Fig. 27-9**.

The numerical difference in all of the values on the dimensions version of the wires page are instantly evident. Since the physical lengths and diameters have not changed, running the program from this version of the page would make no difference in the output. **Fig. 27-7** would still tell the same performance story. The NEC core input procedures would reconvert everything into meters for further processing.

2. *Frequency scaling*: Complete frequency scaling requires that we multiply every dimension of an antenna by the ratio of the old frequency to the new frequency. Hence, if we go lower in frequency, we obtain larger dimensions, and vice versa. There may be a very slight adjustment to be made for differences in skin effect, but if we scale the wire diameter as well as the wire lengths, we come as close to perfection as is possible.



If we fail to scale the wire diameter, we will find that the antenna at the new frequency may not perform as it did at the old frequency. The greater the frequency jump, the greater the difference in performance, if we simply let the wire size be a constant. For perfect scaling, we must make the wire diameter—like the wire lengths—a function of a wavelength.

Fig. 27-10 shows the dimensions version of the wires page of our quad loop. The only alteration made was to change (at the upper left corner) the frequency. We moved from 300 MHz to 144 MHz. On the equations page, since F changed, so to did W , the length of a wave, and so on through every variable defined in terms of W . The result is the series of numerical values shown in **Fig. 27-10**.

It is not necessary to show an azimuth pattern for this new antenna, since it is identical to that in **Fig. 27-7**. The reported source impedance is $129 - j0.4$ Ohms.

The wire diameter calls for comment. Our new diameter is 0.067", which does not coincide exactly with any AWG value. However, it is close enough to #14 AWG (0.0641") that using this size would likely turn up no measurable differences in loop dimensions—given the variables of physical construction.

The exercise does suggest that there is a limit to physically scaling antennas. When the wire diameter reaches unreasonably thin or thick values, it is time to redesign the antenna. If we scale our 300 MHz loop of #20 wire to 28 MHz, it calls for 0.343" diameter copper wire. This diameter is an unreasonably heavy wire for a quad loop (unless one simulates it with a double strand of thinner wire, spaced to achieve the same resonance with the same loop length). Nevertheless, the model shows a resonant loop with a source impedance of $128 - j0.8$ Ohms: a good model without any hope of direct implementation.

Is There More?

The exercise we have just run is only the beginning of modeling by the use of variables and equations. We took the process beyond the first step of merely assigning numerical values to our variables. By letting each variable be a function of a wavelength, we accumulated some advantages in addition to saving time in optimizing the antenna structure for a desired set of operating parameters. We gained

the ability to switch units of measure and operating frequencies with a simple choice in each case.

The type of modeling we have done—using wavelength as the key to our variables—can be simulated in other programs. For example, EZNEC allows direct conversion on its wires page from dimensional units either to other dimensional units or to wavelengths—with the wire diameter an additional option for this latter conversion. Much of what we have so far done can thus be accomplished in either popular NEC program.

There are instances where simpler schemes for assigning variables may be preferable, but they would not have been as interesting. In the other direction, there are two directions in which we should look before leaving the subject of modeling by variables. One is how we might deal with more complex antenna structures, for example, those involving numerous elements. The second direction involves more complex equations by which we might specify the dimensions of an antenna element. This latter task is restricted to programs that contain a complete equations-and-variables facility. We shall also want to take a longer look at the importance of conventions in making the task of modeling by variables and equations as efficient as possible.

* * * * *

Models included: 27-1 through 27-4. (Due to the nature of the models, they are available only in the .NWP format.)



28. Modeling By Equation: B. Bigger and Better Things

In the last episode, we took a look at modeling antennas through the use of variables and equations. Our antenna was a simple square quad loop. The technique we chose, from the many possible ones, was to define variables for element length and wire diameter in terms of fractions of a wavelength. For initial simplicity, we kept everything in free space.

In this installment, we shall move on to a moderately complex antenna—a 3-element quad. After we model it in free space, we shall move it over ground to see what that move might require by way of revisions to our variables and equations. Before we embark on this journey, let me throw in a few reminders about the importance of adopting conventions in your modeling.

The Many Faces of Conventions

Effective and efficient antenna modeling requires more than a random approach. The more systematic we become, the fewer things we have to decide in each modeling task. Not only do we save time, but as well, we are less likely to commit errors in the construction of our models.

The rules of the modeling programs set some boundary limits to the ways in which we can proceed. Within those limits, we have a good bit of flexibility. Sometimes, we need to make use of that flexibility and model some special structure in an unusual but correct way. Most of the time, however, we are more likely to speed success in our modeling efforts if we develop some good procedures and stick with them until the special case comes along. I tend to call these procedures conventions. There are several types.

1. *Structural procedures*: Creating a model, wire by wire, is best done by developing certain habits. For example, with linear elements, we can model from left to right or from right to left for each element. Either way permits us to track the currents along the element and easily read other portions of the NEC data output in

ways that modeling from the center outward only confuses. However, our linear progressions should always move in the same direction from model to model.

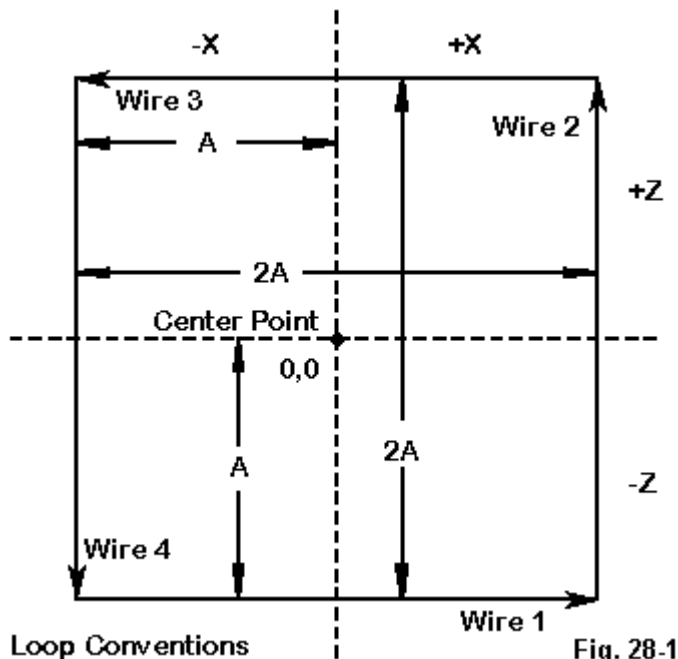


Fig. 28-1

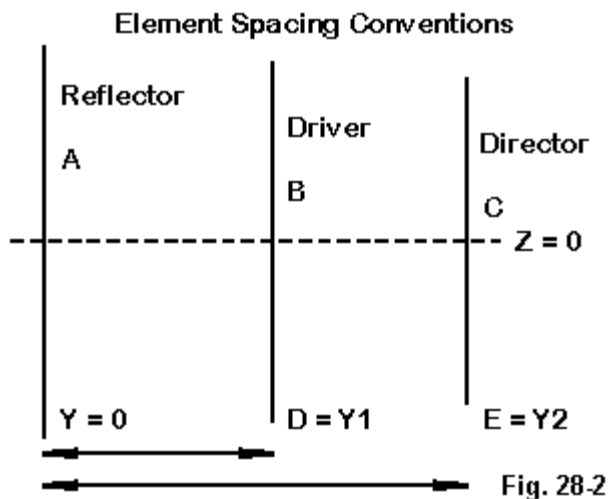
Loop elements, such as the one shown in **Fig. 28-1**, offer us additional opportunities to create conventions in our modeling. Since a loop is a continuous element composed of at least 4 wires, we shall normally encounter fewer confusions and errors if we model the circumference in a regular progression. The sketch shows a counterclockwise progression. Clockwise progressions are also good, but we should adopt one or the other for all of our loops.

Fig. 28-1 also shows the loop symmetrically placed around a center point. For initial free-space modeling, one should let the center point be 0,0, so that each dimension of the antenna involves A or -A for each coordinate point. The advantage of this procedure becomes evident as soon as we wish to place a second loop behind or ahead of the first, but to use a different set of dimensions at the same time. The 0,0-center point ensures that each loop is aligned with the next one.

A third facet of structural conventions involves the choice of coordinate axes for various antenna dimensions. The Z-axis handles vertical dimensions automatically. Some early programs for slower computers used the X-axis as the axis of symmetry, forcing the modeler to set elements as +Y and -Y dimensions. Those rules are largely defunct, and the modeler can place side-to-side dimensions across either the X or the Y-axis. The unused X- or Y-axis normally becomes the front-to-back axis, if the antenna has more than one element.

The example in **Fig. 28-1** uses the X-axis as the crossing point for the side-to-side dimensions of the loop. Hence, the wires that cross this axis will have +X and -X values. If we add further loops to form a beam, they will be spread along the Y-axis. My preference for this arrangement is personal: it places the most changed dimension—element length—in the left column of most wire geometry sheets for easy visual identification. However, using the Y-axis for side-to-side dimensions and the X axis for front-to-back dimensions is equally apt, and tends to align the forward lobe of most azimuth patterns with the zero-degree azimuth mark on plots. The goal is to pick one system (according to your modeling goals overall) and to stick with it so long as it serves well.

Fig. 28-2 shows a representative set of front-to-back conventions. In this sketch, all elements count their dimensions from the rear of the multi-element array, in this case, the reflector. It is set to zero. Each element will have a distance value that is positive, represented by the variables D and E in the sketch. The advantage of this scheme is that the total front-to-back dimension is always readily available to the modeler. The disadvantage is that distances from the second to the third element must be calculated.



An alternative procedure is to set the driver at 0 along the selected front-to-back axis. Then, the reflector will have a negative value and the director (or directors) will have a positive value. A third scheme occasionally used is to set the array in equal distances forward and behind the zero point. However, this system can only be put in place after the final front-to-back dimension is known.

For our work in this episode, we shall use the conventions shown in the sketches. I note this fact so that you can read the antenna structures directly from the screen captured graphics. If you model the subject antenna, give some thought to translating the model into the structural conventions you typically use. If you return to the model at a later date, you will be more likely to read the model correctly.

2. *Equation conventions:* When constructing values for the variables out of which you will build the antenna model, give some preliminary thought to the ways in which you will develop the variables. Of course, the simplest system is to simply assign variables a numerical value. This system permits multiple dimensional

changes with the change of a single value on the equations page. However, it is limited insofar as it does not permit full scaling of the antenna structure.

Let's look at a different sort of example.

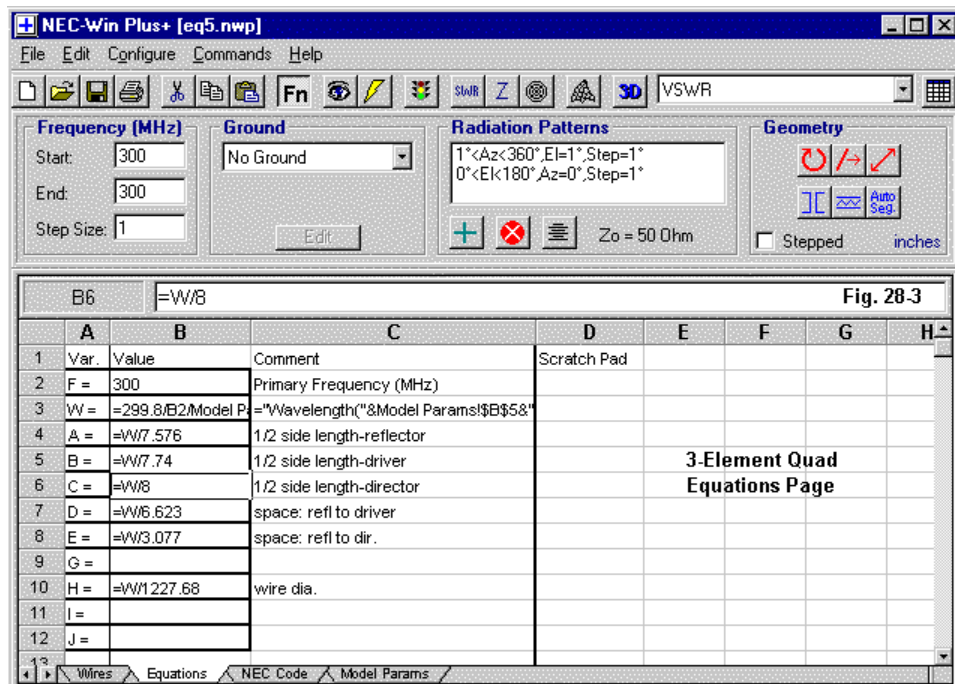


Fig. 28-3 shows the equation set for a 3-element quad beam consisting of a reflector, driver, and director. The page actually reveals a great deal of information about how the modeling is being conducted.

The equations all relate the antenna dimensions to a wavelength. One might choose to relate them to frequency. Although this latter scheme allows frequency scaling, it does not provide automatic numerical value changes with changes of units. Relating the numeric values to a wavelength provides both facilities.

The equations also arrive at the final values by dividing the length of a wave by a certain number. Alternatively, one might have multiplied a wavelength by the reciprocal of the divisor, if that scheme is more efficient for a given modeler.

There are also some conventions at work that logically group the values in the total set. A, B, and C are the variables controlling the reflector, driver, and director wire lengths, respectively. Note that each element has an independent equation related back to W, a wavelength. It is also possible to develop one variable, for instance, the driver, and then to key the reflector and director dimensions as functions of the driver.

Since the reflector will be set to zero along the Y-axis, D controls the reflector to driver spacing and E controls the reflector to director spacing. Even within the scheme used to assign values, one might have reorganized these variables. However, consistency from one model to the next reduces confusion and errors.

The wire diameter is assigned to H, with G reserved. Since the initial model will be in free space, no height equation is necessary. However, to keep the dimensional variables well grouped ahead of the wire diameter, G is reserved for later use, while the wire diameter moves to H. Later, when we move the model over ground, G will have a value. More importantly, you will be able more easily to correlate the components of the free-space model to those of the model over ground.

The end result is the use of A, B, and C for dimensions to be placed in the X column, D and E for dimensions to be placed in the Y column, and G for dimensions that go in the Z column. (Since the quad had a vertical dimension to begin with, using A in the Z column is, of course, inevitable.) Wire diameter comes last.

No magic attaches to this particular system. It serves to illustrate one of many possible orderly schemes that permit easy reading by both the modeler and others. Nonetheless, in the process of suggesting that each modeler develop conventions

that best facilitate modeling, I have also managed to explain the ones used in this exercise.

Onward to the 3-Element Quad

Fig. 28-1 and **Fig. 28-2** together showed the outline of a typical 3-element quad beam consisting of reflector, driver, and director elements. **Fig. 28-3** listed the design equations for the antenna. How these dimensions translate into values appears in **Fig. 28-4**, the equations page set to show numerical values.

NEC-Win Plus+ [eq5.nwp]

File Edit Configure Commands Help

Frequency (MHz) Start: 300 End: 300 Step Size: 1

Ground No Ground

Radiation Patterns 1°<Az<360°, El=1°, Step=1° 0°<E<180°, Az=0°, Step=1°

Geometry Z0 = 50 Ohm Stepped inches

	A	B	C	D	E	F	G	H
1	Var.	Value	Comment	Scratch Pad				
2	F =	300	Primary Frequency (MHz)					
3	W =	39.34383202	Wavelength(inches) = c / f					
4	A =	5.193219644	1/2 side length-reflector					
5	B =	5.083182432	1/2 side length-driver					
6	C =	4.917979003	1/2 side length-director					
7	D =	5.94048498	space: refl to driver					
8	E =	12.78642575	space: refl to dir.					
9	G =							
10	H =	0.03204730225	wire dia.					
11	I =							
12	J =							

3-Element Quad Equations Page Values Version

Wires Equations NEC Code Model Params

As we did with the simple quad loop, we have used 300 MHz and free space as the background for the antenna. See model 28-1. You may recognize the wire diameter as equivalent to #20 AWG. Also notable is the fact that adding to the number of elements in an array tends to multiply the number of variables required to fully describe the antenna.

Two items are notable about the page shown in **Fig. 28-4**. First, the variable G has been left blank, with the wire diameter registered as variable H. G will be used later to set a height value for checking the model over ground. Second, the variable E shows the total length of the antenna array from back-to-front. There would be no harm in defining further variables to provide instant calculation of the spacing from the driver to the director. By defining I (for example) as $E - D$, we would obtain that value, even though we do not plan to use the variable I in the set-up of the antenna geometry.

NEC-Win Plus+ [eq5.nwp]

File Edit Configure Commands Help

Frequency [MHz] Ground Radiation Patterns Geometry

Start: 300 End: 300 Step Size: 1

No Ground

1° < Az < 360°, El = 1°, Step = 1°
0° < El < 180°, Az = 0°, Step = 1°

Zo = 50 Ohm

Stepped inches

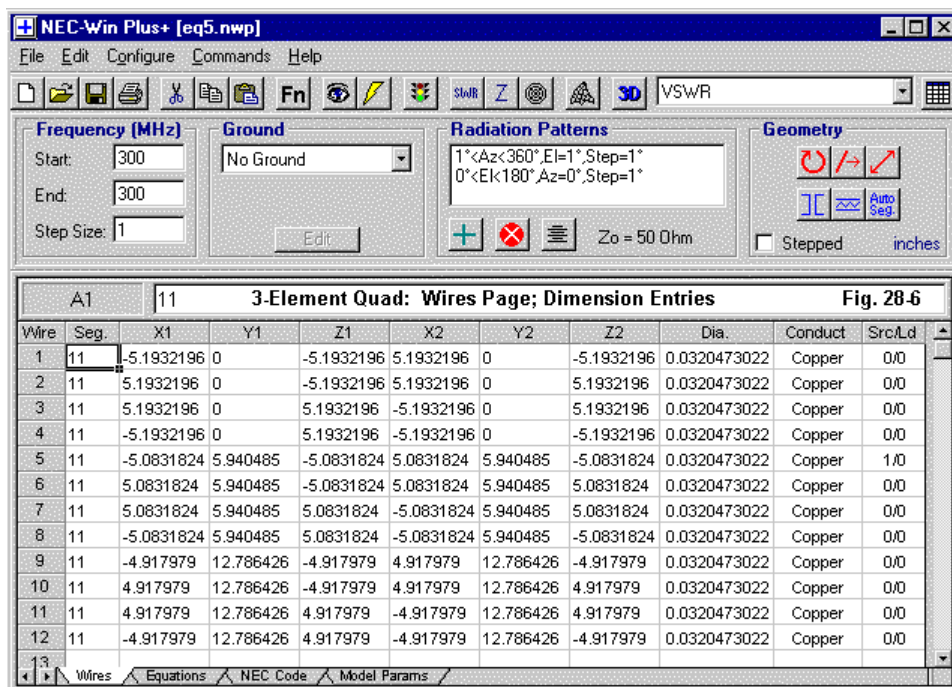
Fig. 28-5

Wire	Seg.	X1	Y1	Z1	X2	Y2	Z2	Dia.	Conduct	Src/Ld
1	11	=A	0	=A	=A	0	=A	=H	Copper	0/0
2	11	=A	0	=A	=A	0	=A	=H	Copper	0/0
3	11	=A	0	=A	=A	0	=A	=H	Copper	0/0
4	11	=A	0	=A	=A	0	=A	=H	Copper	0/0
5	11	=B	=D	=B	=B	=D	=B	=H	Copper	1/0
6	11	=B	=D	=B	=B	=D	=B	=H	Copper	0/0
7	11	=B	=D	=B	=B	=D	=B	=H	Copper	0/0
8	11	=B	=D	=B	=B	=D	=B	=H	Copper	0/0
9	11	=C	=E	=C	=C	=E	=C	=H	Copper	0/0
10	11	=C	=E	=C	=C	=E	=C	=H	Copper	0/0
11	11	=C	=E	=C	=C	=E	=C	=H	Copper	0/0
12	11	=C	=E	=C	=C	=E	=C	=H	Copper	0/0

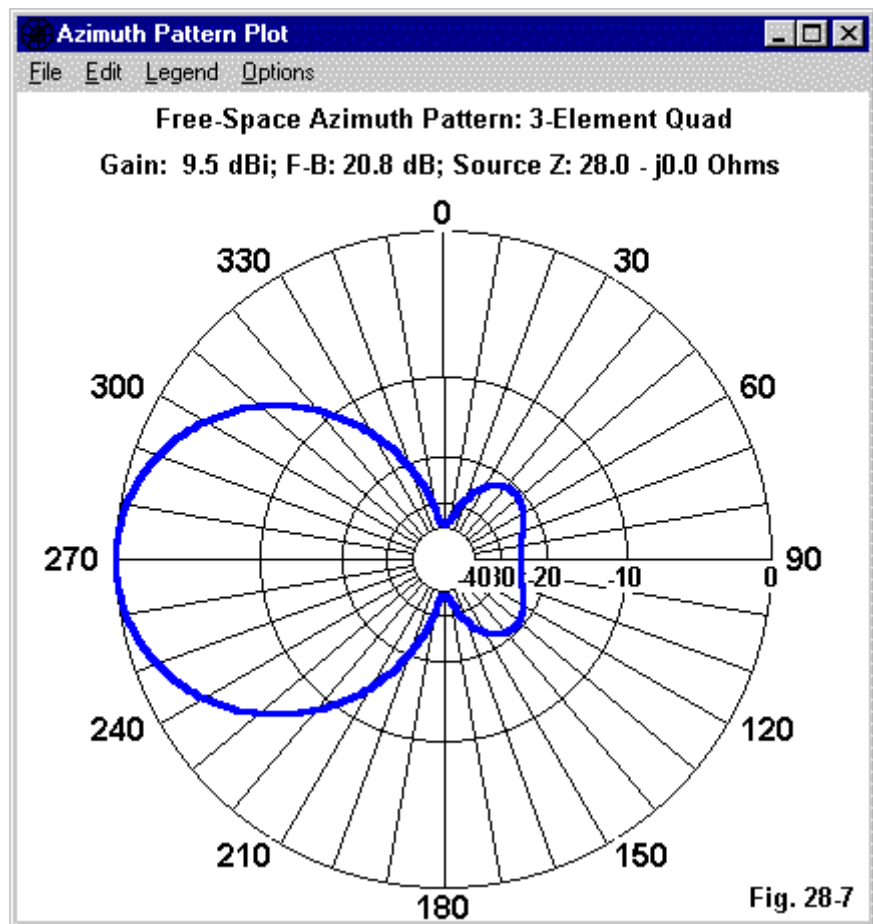
Wires Equations NEC Code Model Params

In addition, we might set other variables as ratios of the reflector to the driver length or the director to the driver length. Not every equation we define has to be used in the antenna geometry itself. **Fig. 28-5** shows the actual geometry of the 3-element quad, described in terms of the variables we have just defined. The Y columns have been assigned the back-to-front dimension. Recording the variables for these distances has the additional benefit of allowing us easily to identify which element is which.

The X and Z columns record the variables associated with each of the elements, expressed in terms of the half-length of each side of the quad. Note that each element follows identically the same pattern of development around the perimeter of the loop. Consistency of geometric layout is an aid to error detection as well as to later interpreting NEC output data.



The final step in preparing to run our model consists of looking at the actual dimensions on the wires page (**Fig. 28-6**). In that process, we also note that the antenna is of copper wire and that the source segment is placed on the lower horizontal wire of the second (driver) element. It now time to run the model.



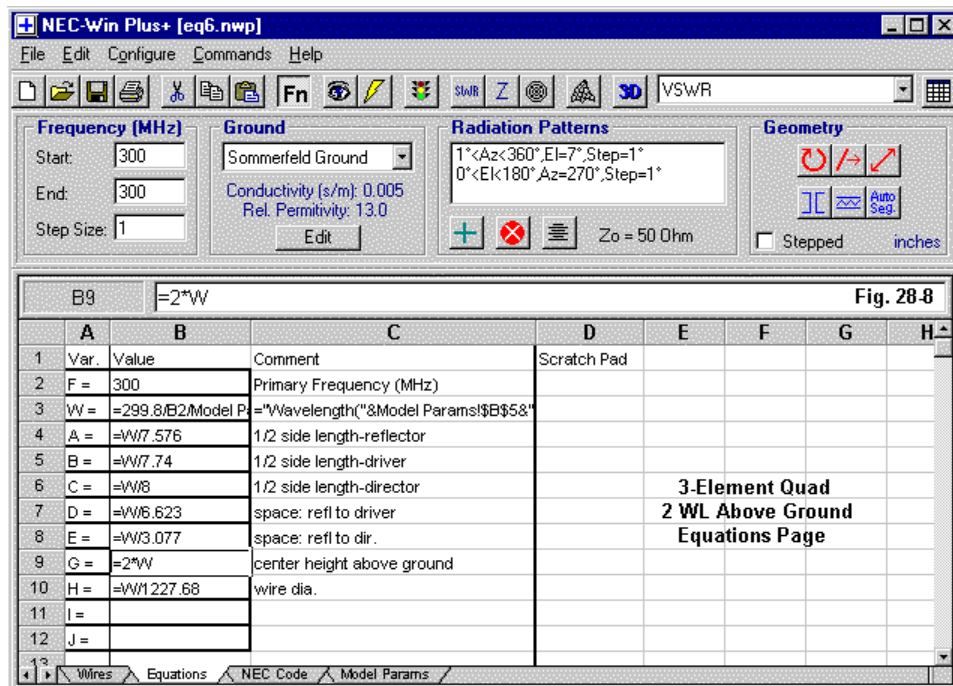
The data we gather from the NEC core output is gathered together in **Fig. 28-7**. The free-space gain of this quad is about 9.5 dBi, a very respectable value for a monoband 3-element quad design. The gain is about 1.4 dB better than a 3-element Yagi having the same boom length and configured for a similar front-to-back value in excess of 20 dB. Given the smaller diameter of the wires in the quad relative to what would be typical for a Yagi at the same frequency, the modeled quad achieves as much as possible of the theoretical gain of quads over Yagis.

The front-to-back figure should be referenced to the azimuth pattern. Although the pattern does not show trace lines that would identify the bearing for the front-to-back ratio, the value shown is clearly related to the strongest rearward lobes. In fact, early versions of the program used (NEC-Win Plus) routinely provided the worst-case front-to-back ratio. The more common 180-degree front-to-back ratio can be extrapolated from the pattern itself and approaches 25 dB. More exacting figures can be derived by comparing the forward gain (heading 270 in the example) with the rearward gain (heading 90 in the example).

Above Ground

To place the antenna above a desired ground requires two steps. The first is to define a ground. **Fig. 28-8** shows the selection of the Sommerfeld-Norton ground, using the values for good ground (conductivity = 0.005 S/m; dielectric constant or relative permittivity = 13.0). Since the antenna is configured for horizontal polarization, the actual ground values chosen will not have a very significant effect upon antenna performance at heights greater than 1 wavelength above ground. See model 28-2.

Fig. 28-8 also shows how we plan to establish the antenna at a certain height above the ground we have just defined. The variable we earlier reserved is now assigned the value of 2*W, indicating a height of 2 wavelength. However, this entry does not say how we shall implement the height. Let us assume that the 2-wavelength height represents the height of the center of the quad structure. This is a common practice—and a good reason for centering each of the elements of the quad array on the same axis line.



On the equations page, we could have used variable G to define several further variables. We might let $I = G - A$ to cover the lower reflector element and $J = G + A$ to handle the upper reflector element. We would need 4 more variables to cover all of the quad elements. However, there is a simpler method, shown in **Fig. 28-9**, the wires page using the variable entries version.

When entering the antenna geometry as a set of variables, we are not limited to single letter assignments. We can enter more complex equations involving those variables. The equations can involve complex functions, but in the present case, we only need simple addition and subtraction involving the variable for the antenna

height and the loop dimension variable. Lower wires will be below the value of G and upper wires will be above the value of G. Note that values in the X and Y columns are unaffected: everything we need to modify in order to place the antenna above ground occurs in the Z axis column.

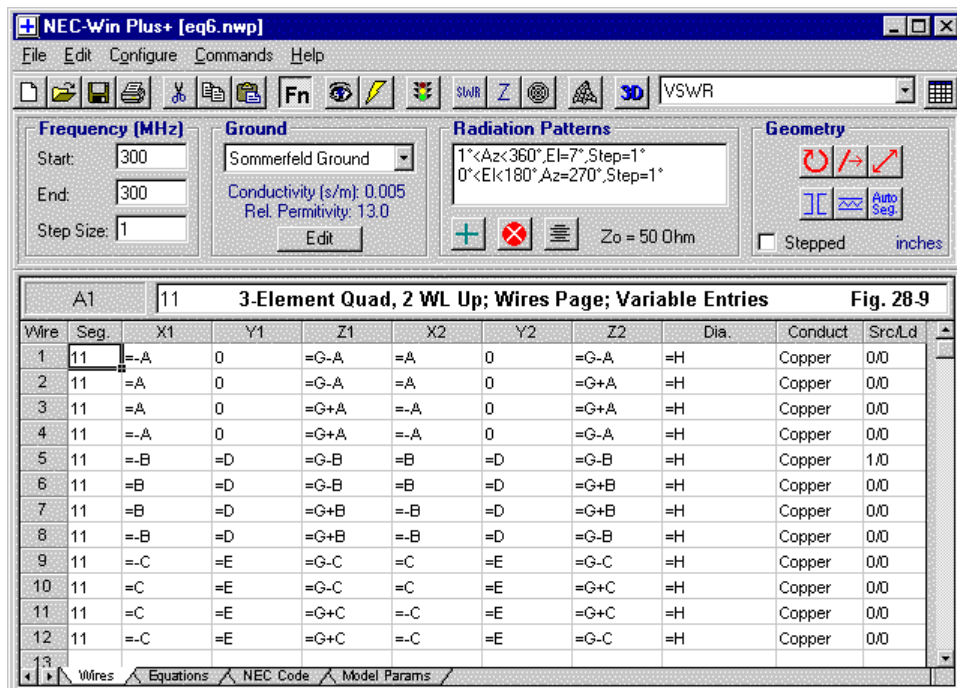
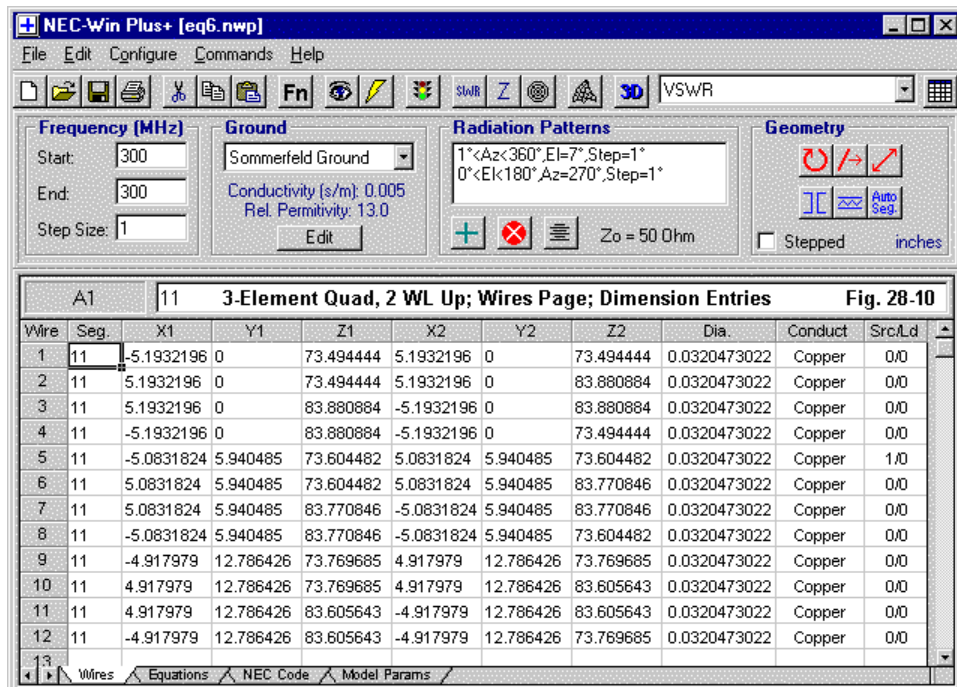


Fig. 28-10 shows the results of our new variable and our revised symbolic structure in the dimensions version of the wires page. The center of the antenna is about 6.5' above ground, with the upper and lower horizontal wires less than 6" distant from the center position. Of course, at this point (or any other point in the model development process), we could have selected other dimensional units. Any read-

ers outside the U.S. will prefer millimeters for the dimensional unit for an antenna at 300 MHz.



The final element to note before running the antenna model is the revision made to the azimuth pattern request. Only free-space NEC models should request an elevation angle of zero degrees. In this case, the elevation angle will be 7 degrees, the angle of maximum radiation or take-off angle.

Fig. 28-7 captured the shape of the azimuth pattern of the antenna placed 2 wavelength above average ground. Only the detailed information requires revision. The array shows a gain of 15.1 dBi, with a worst-case front-to-back ratio of 20.7 dB. The feedpoint impedance is $29 - j0.0$ Ohms.

Since the model uses #20 wire at 300 MHz, it can be reasonably scaled to other VHF and UHF frequencies commonly used in amateur radio. Scaling to 2 meters will permit the use of #14 wire. However, scaling down to 6 meters will require something close to #4 wire to preserve the exact balance of factors in the design. Changing to a more common wire size—#12 or #14 AWG—will require adjustment of at least the variable for the driver wire length. You may also wish to experiment with the values for the reflector and director to see if changes in their dimensions result in better or worse overall antenna performance. From that point, you may wish to do some further scaling and adjusting to optimize the array for HF performance (on any band from 20 through 10 meters). In the process, you will certainly note the greater ease that variables and equations lend to the process of manually optimizing an antenna relative to having to change each dimension entry individually. If you like the results of your scaling and adjusting work, be sure to save the results under different file names for each version you wish to preserve.

Same Song, Different Key

Rather than detail the potential for scaling the quad (which is only an example in this context, but a pretty good example), let's take the same antenna and look at it in another way. **Fig. 28-11** provides the first step.

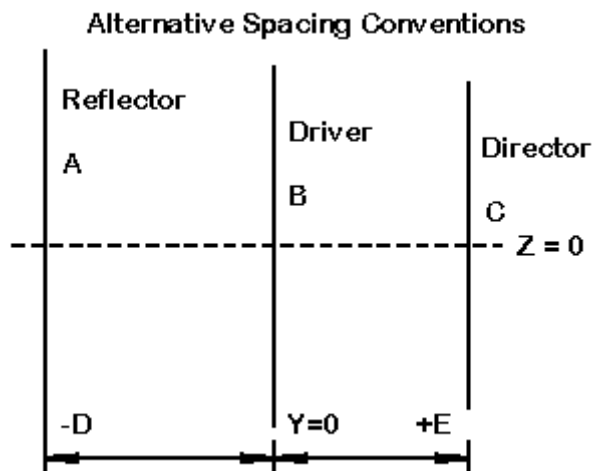


Fig. 28-11

In this view of the antenna, we shall treat the driver as the central element and place it at the zero point on the Y -axis. The reflector will use a negative value to record its position behind the driver, while the director will be placed ahead of the driver with a positive value.

At the same time, we shall let the driver be the central element in another sense. We shall define the length dimensions for the reflector and the director in terms of the driver length. To keep our focus upon these elements of designing by variables and equations, let's place the antenna back into free space.

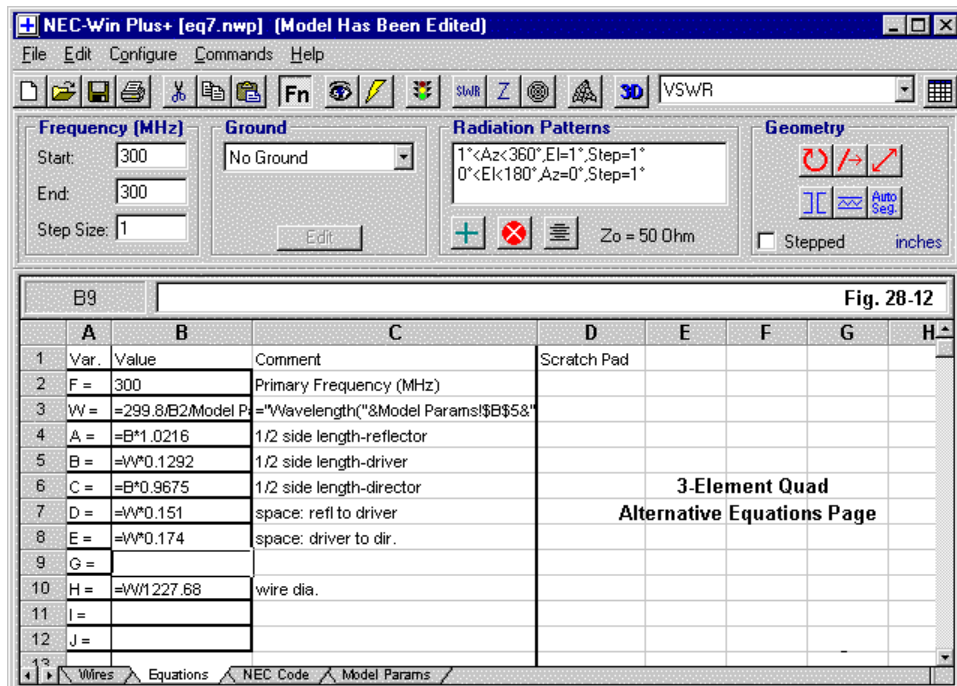
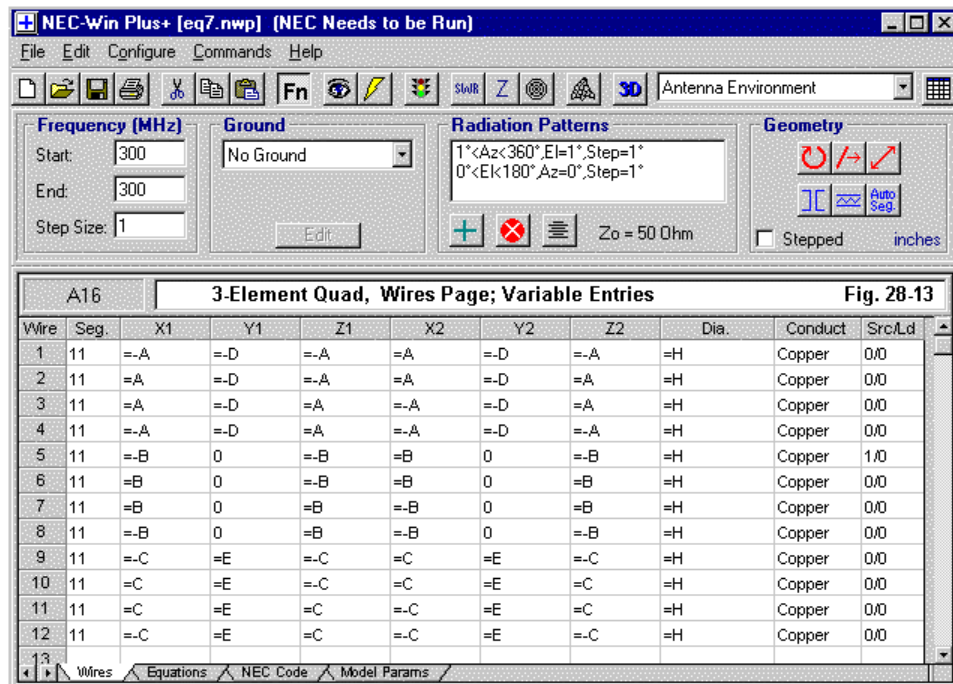
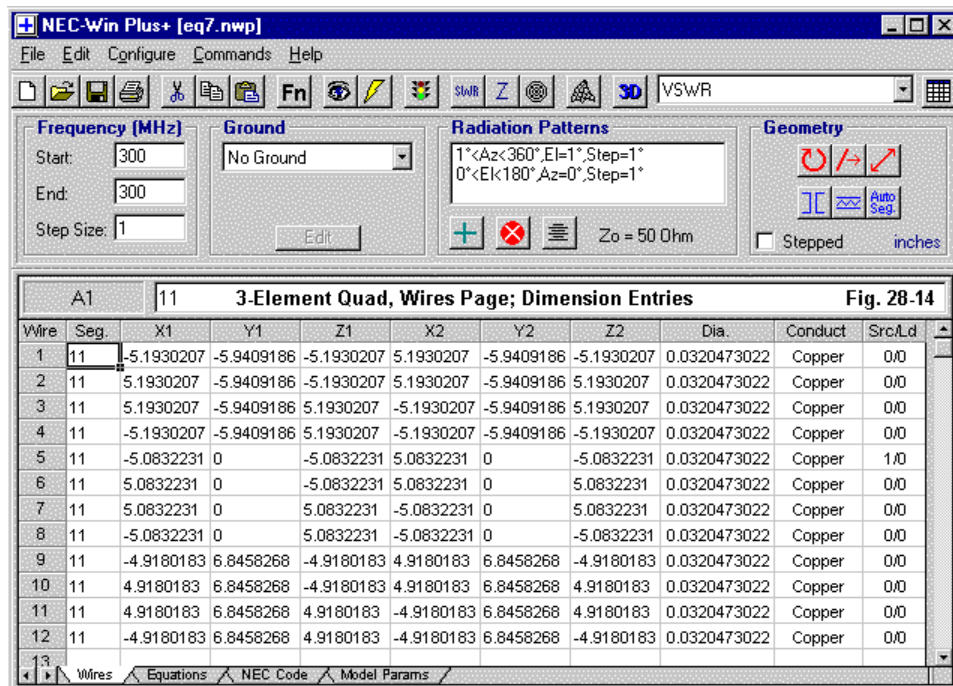


Fig. 28-12 shows the results of our work, at least with respect to defining the basic variables we shall use. Note that the values for A and C are defined in terms of B. The order of definition does not make a difference: the spreadsheet form will find B and use it to determine the numerical value of A (as well as C). In this exercise, I have also changed from the use of denominators to the use of multipliers to set the values. See model 28-3.

In addition, the spacing is now defined in the terms set forth in **Fig. 28-11**. If we wish to know the total array length, we can always define an extra variable as the sum of D and E.



The changes we have made to the equations page will require some revisions to the variable entries version of the wires page. See **Fig. 28-13**. Actually, only the variables assigned to the Y columns require change from the earlier example. The reflector is at -D, while the director is at +E. Using negative values for variables on this page allows us to simplify the equations page by letting most, if not all, of our basic equations be expressed in positive values.



Flipping to the dimension entry version of the wires page shows that the resulting antenna is virtually identical to the earlier version. Compare **Fig. 28-14** to **Fig. 28-6**. The numerical values for the two models are the same through 3 decimal places—which is at least one more than any practical application would call for when the dimensions are in inches. Consequently, we can expect the performance reports from the NEC core to be virtually identical for the two models.

We have not explored all of the permutations and combinations of ways in which we can construct models using variables and equations. The procedure with which you become most comfortable may not coincide with either of the variants we have

explored. However, developing a consistent procedure—except where a specific task may dictate otherwise—will go a long way toward naturalizing the process of modeling in this way. The larger the model, the more crucial it is to adhere to conventions that yield the quickest error detection, the clearest readout of your work, and the greatest ease in modifying the model en route to the perfect antenna.

Once you have developed a sense of the conventions of modeling that work best for you, the door is open to the use of more complex equations. The ones we have explored have been of the simplest kind. Indeed, the more complex that modeling tasks grow, the more important it becomes to adopt—and to record—a set of conventions that all models will use.

Within many engineering corporations, there is an A³ manual: Abbreviations and Acronyms. All corporate staff, including management, engineering, and technical writing, are expected to use abbreviations and acronyms according to the manual, even though the task of cleaning up after careless staff members usually falls to the technical editing group. If antenna modeling becomes a standard tool within engineering, an “AMC” (antenna modeling conventions) manual should become as much a part of the work environment as the A³ manual. Work passes from hand to hand in the process of development and review. Vital (and costly) man-hours can be saved if everyone works in the same direction, that is, according to the same modeling conventions. For the individual, an equivalent saving of time and energy accrues to the consistent use of conventions. Reviewing efforts that are several months (or years) old is much easier if the earlier work adheres to the same conventions currently in use. It certainly would not hurt the individual—even the casual—modeler to keep a notebook to record conventions that emerge as projects grow more complex.

We have so far employed only simple equations to set up our models. We have hardly taxed even the rudimentary levels of what a spreadsheet can provide. Therefore, let’s take one more look at the process of modeling with variables and equations in the next column. We shall keep a sharp eye out for what we can do with slightly more complex equations and model set-ups.

* * * * *

Models included: 28-1 through 28-3. (Due to the nature of the models, they are available only in the .NWP format.)



29. Modeling By Equation: C. Formulas and Blocks

We have been looking at some of the elements of modeling via the use of variables and equations in slow motion for the benefit of newer modelers who have never modeled in this manner before. Our progress into new territory will be equally patient, since there are better and worse ways of getting to various ends—and we want always to choose the better way. Since we are working with the variable and equation provisions of a specific program—in this case, NEC-Win Plus—it is inevitable that certain aspects of the work will be program-specific. The more detail we understand about the processes, the easier it will be to adapt the procedures to other programs having the same capability.

This is the third episode of this sequence (but perhaps not the last word that will ever be said in this series about modeling by equation). We shall look at the rudiments of other mathematical techniques used to define variables—leaning especially on a little trigonometry as applied to spreadsheet formulations. In addition, we shall also explore ways to cut long repetitive model-creation tasks down to simple work. Finally, we shall look at when and how to freeze a design that we initially create for frequency-scaling purposes.

A Little Trig

Many antenna designs are amenable to trig-treatment. Theoretically, most antenna designs can be handled with trig, since we can transform almost any geometry into a collection of angles and triangles. For example, a linear element can be viewed as two lines with a 180-degree angle. This way of thinking, of course, gets into the extremes of the unnecessary, although there are always a few folks who live by the motto, “Stop! Look! There must be a harder way!”

More realistically, loop antennas—especially triangles or “deltas”—are most apt for trig-treatment. So let’s pick one and see what we might do with it.

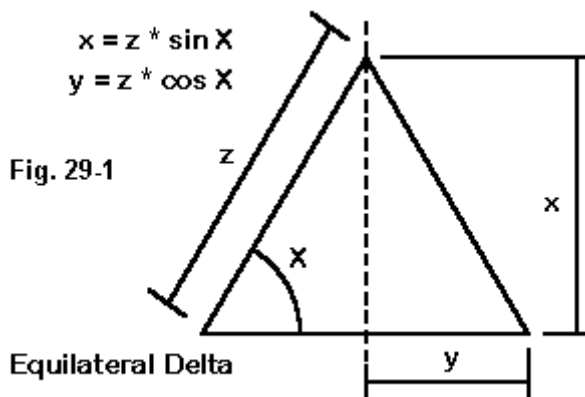


Fig. 29-1 shows a typical equilateral delta, much used on the lower HF bands. The antenna consists of 3 sides of equal length (z). Since the angles of every triangle add up to 180 degrees, each corner angle is 60 degrees. Now we can appeal to basic trig functions to determine the values of $+/-y$ and x so that we can model the antenna within 2 of the 3 cartesian dimensions that form the basis of model construction in NEC. Note that we have cut the equilateral triangle in half along a vertical line to get two equal right triangles. This conversion makes the calculation of dimensions much easier.

The two most important trig functions to absorb are sine and cosine (abbreviated “sin” and “cos”). The sine of an angle in a right triangle (or $\sin X$ in the sketch) is simply the length of the side opposite to the angle (X) divided by the hypotenuse (z). The cosine of that same angle, or $\cos X$, is the side adjacent to the angle (y as equaling half the length of the base) divided by the hypotenuse. Now, if we know the angle and the hypotenuse, we can derive the length and hence the coordinates of the remaining sides. Of course, we also need to know some values for sines and cosines.

Many modelers keep a few handy trig values in their head for rough calculations. The sine of 30 degrees is 0.5, which is also the cosine of 60 degrees. The

sine of 60 degrees is about 0.866, which is also the cosine of 30 degrees. With an angle of 45 degrees, the sine and the cosine are equal: 0.707. These familiar numbers are handy and deserve commission to memory. However, if we model using variables and equations, we only need the numbers to check up on our work—an error detection system.

Since a delta loop has a circumference of about 1 wavelength, we know that each side is about 1/3 wavelength long. We also know that the equations for half the base and the overall height shown in **Fig. 29-1** are simple transformations of the basic trig relationships. Now, we can let the spreadsheet equations-system of the program help us create a perfectly general delta loop. See model 29-1.

Fig. 29.2

	A	B	C	D	E	F	G	H
1	Var.	Value	Comment	Scratch Pad				
2	F =	7	Primary Frequency (MHz)					
3	WV =	=299.8/B2/Model P	= "Wavelength(" & Model Params!\$B\$5 & "					
4	A =	=WV/2.84	Delta Side Length					
5	B =	=A*SIN(6.2832/6)	Delta Height (Z)					
6	C =	=A*COS(6.2832/6)	1/2 Delta Base (+/-X)					
7	D =							
8	E =							
9	G =							
10	H =							
11	I =							
12	J =							

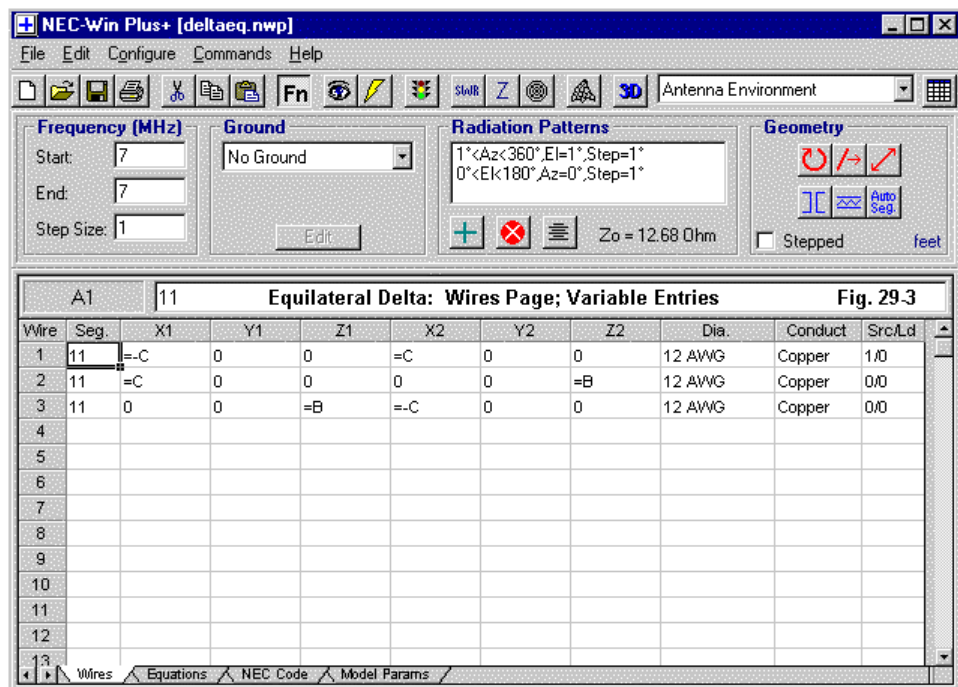
Equilateral Delta Equations Page

Fig. 29-2 shows the equations page for an equilateral delta loop. And nothing seems to correlate with what we have just said. The length of the hypotenuse (A) is not shown as $W/3$, but as $W/2.84$. The loop is larger than a wavelength in circumference, as it was with the quad loops we looked at earlier. Actually, the denominator of the equation for A was derived by resonating the final model—which used #12 AWG copper wire in free space—to a source impedance of $117 - j0.4$ Ohms at 7 MHz. (We can by-pass absolute generality of design with the wire size specified in terms of a wavelength for this exercise. However, that option is always open to the modeler.)

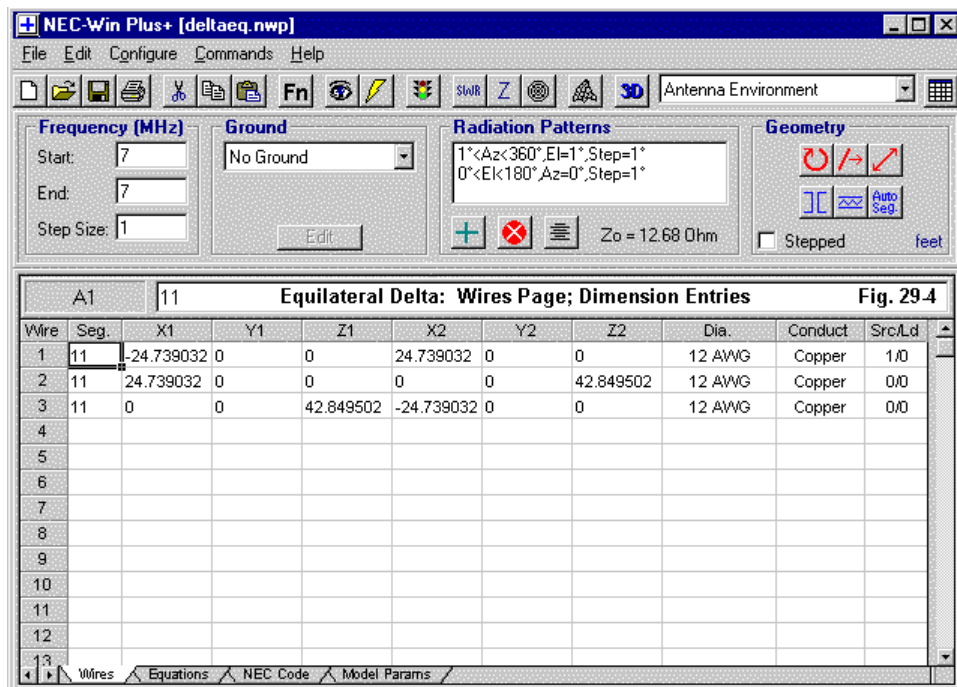
The second deviation from our initial discussion includes the equations for B and C, the height and half-base length equations. The deviation results from the fact that spreadsheet math is a derivative of Basic, a programming language that does all its angles in radians rather than degrees. To use radians effectively requires that we remember just one fact: a circle has 2π radians or 360 degrees. Hence, to convert an angle from degrees to radians, we simply divide 2π by the result of $360/\text{angle}$, where “angle” is the angle with which we are concerned. Since our equilateral triangle uses an angle of 60 degrees, $360/60 = 6$. π is about 3.1416, so 2π is about 6.2832. Hence, our angle in radians is $6.2832/6$. We shall let the spreadsheet finish the calculation, but we know the angle is a little over 1 radian.

Remember: if you forget to make the conversion into radians, your results will not make any sense at all. As well, you may do some of the conversion calculations on the scratch pad facility available on the equations page of NEC-Win Plus.

We can construct our equilateral delta by using the variables we have just defined, as shown in **Fig. 29-3**. The baseline of the delta lies along the X-axis (at $Z = 0$) from $-C$ to $+C$, with the source centered. The two angled wires go to or from these end points to a common height, B. This is the easiest part of the process.



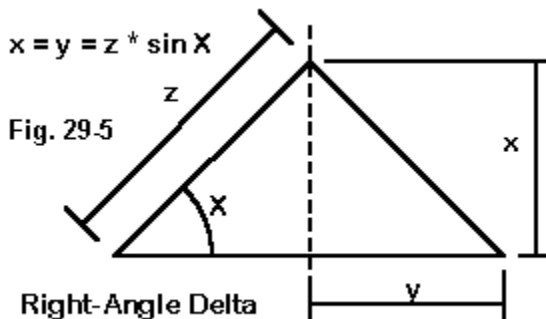
Flipping from the variables version of the wires page to the dimensions version in **Fig. 29-4**, we find the final results of our modeling. Note that this will not necessarily be the first set of values you see if you begin the process by setting $A = W/3$ and then refine the denominator by checking for resonance. However, at 7 MHz and using #12 AWG copper wire in free space, this is where you will end up.



Sometimes, trig can simplify our equations more than we might initially expect. Consider the right-angle delta, an alternative version of the delta we just explored. We shall retain the same wire size and material, and we shall keep the antenna in free space. Our interest will be in the angles, shown in **Fig. 29-5**.

First, let's think about the perimeter of the right-angle delta. If we start with a wavelength, it is divided into three legs, but only 2 of them are equal: z . However, we know that a right triangle has two 45-degree angles and a 90-degree angle. The length y is the cosine of angle X times Z . Since the sin of 45 degrees is 0.707, y is $.707 * z$, and the total length of the base is $1.414 * z$. (We can also use the old right-

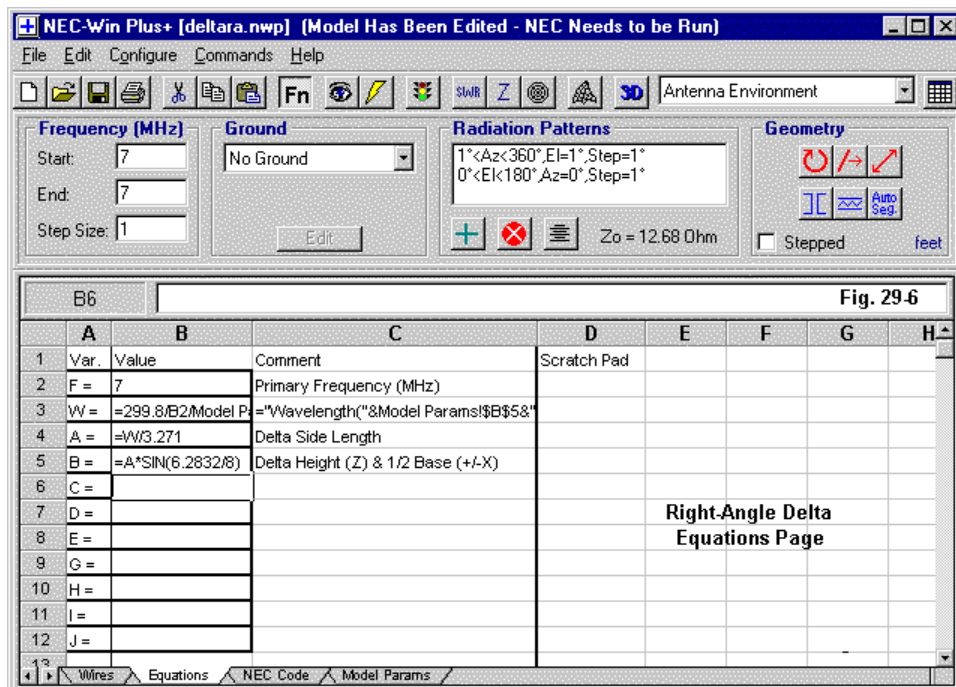
angle theorem from plane geometry: the square root of the sum of the squares of the two sides of the entire right triangle is the length of the entire base, which is the hypotenuse. The base is still $1.414 \cdot z$.) So in terms of z , the total perimeter is $3.414 \cdot z$. In terms of a wavelength, the length of z will be $W/3.414$ as a starting value.



One of the conveniences of a right triangle is that the sine and the cosine of 45 degrees are both 0.707. Hence, we can define our right-angle delta with only two equations, one to define z in terms of a wavelength and one to define both the lengths x and y . Let's now turn to the equations page of our spreadsheet.

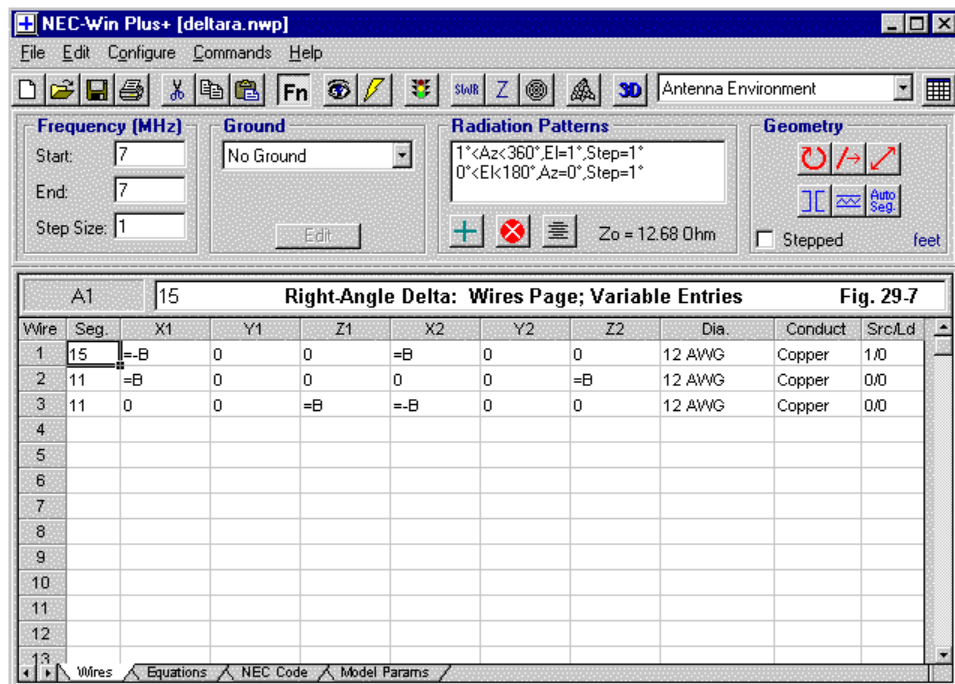
In **Fig. 29-6**, we find the final equations for the right-angle delta. See model 29-2. Values for the X - and Z -axes appear in the equation for variable B . This follows the same pattern we used earlier in converting from degrees to radians. We recognize the value of $2 \cdot \pi$. The denominator of 8 derives from dividing 360 degrees by 45 degrees.

The final value for A comes from adjusting our initial denominator of 3.414 until the antenna achieved resonance with a source impedance of $196 + j0.6$ Ohms. Once more, for a loop, the final size to give 1-wavelength resonance will be physically longer than 1 wavelength.

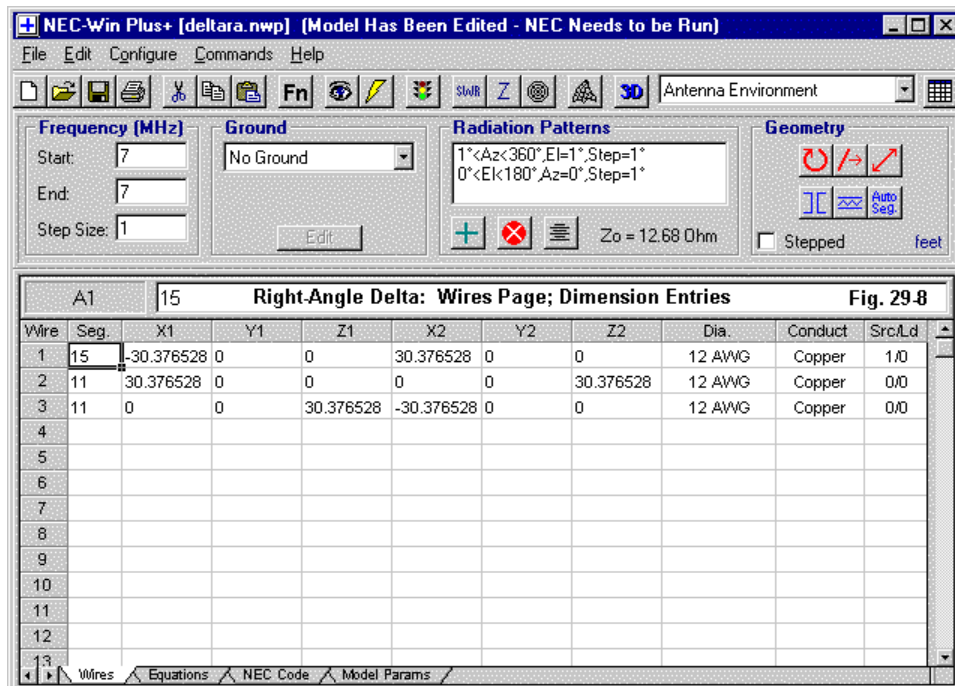


The simplification of our set-up also shows up in the variables version of the wires page, **Fig. 29-7**. For a right triangle, we only need to set the baseline ends at -B and +B, and the height will be +B. For both deltas, we set the baseline at zero on the Z-axis. Should we wish to center the model vertically, using +/-Z values that are the same, we shall have to wait until we know the final physical dimensions, or we shall have to create a further equation for this purpose to the short list on the equations page. For example, we might have defined C as 1/2 the value of B and then specified Z coordinate of the baseline as -C and the peak as +C. Once we start down the road of modeling by equation, we can get as sophisticated as we desire. The key questions are these: Do we need the added fanciness? Will the resulting

model be easy to read in the future? For this example, a baseline of zero on the Z-axis will do just fine. If we develop a special need later on, we can adjust the equations. For example, a particular project might set a maximum height. In that case, we can revise the equations to work downward from that height.



The final dimensions for the resonant right-angle delta appear in **Fig. 29-8**. As always, round off the excess precision to the level appropriate to the task at hand.



Something Bigger: A Helical Dipole

We have lingered over the basics of using trig functions in a spreadsheet model-by-equations system to prepare ourselves for larger tasks. The larger task I have chosen as an exercise is the creation of a helical dipole for 10 meters. What I wish to achieve is a helical dipole that is under 10' from end to end for a frequency of 28.5 MHz, using #12 wire. Since I might run into difficulties with the limits of NEC if I wind the helix too tightly, I shall specify a radius of 4".

NEC must create a helix from straight wires. In fact, NEC has an input card that will automate the creation of a helix, but that card is normally not available on entry-level commercial versions of the program. No matter: manually creating a helix will give us some understanding of what goes on when we implement that card in an advanced NEC program.

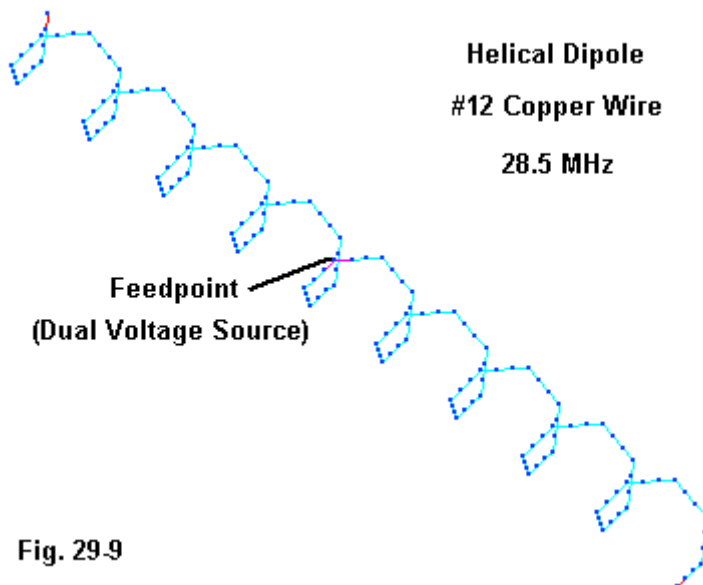


Fig. 29-9 shows us an outline of the helical dipole. Almost any representation of a helix made from straight wires will give some visual distortion of what is actually happening to the wire, and **Fig. 29-9** is no exception. However, we can see the straight wire sections of each turn of the helix. Each one forms part of the circumference and also proceeds part way down the line from one end to the other. Since

each wire is the same length, the increment of movement along the total length will also be the same for each successive wire.

For the example, the total number of wires turned out to be an even number. Hence, I specified a split feed, using the last segment of one wire (28) and the first segment of the next wire (29). We shall look at the consequences of placing the source in this manner later on. First, we need to figure out how to make up the turns of the helix.

Elements of a "Straight-Wire" Helix

Fig. 29-10

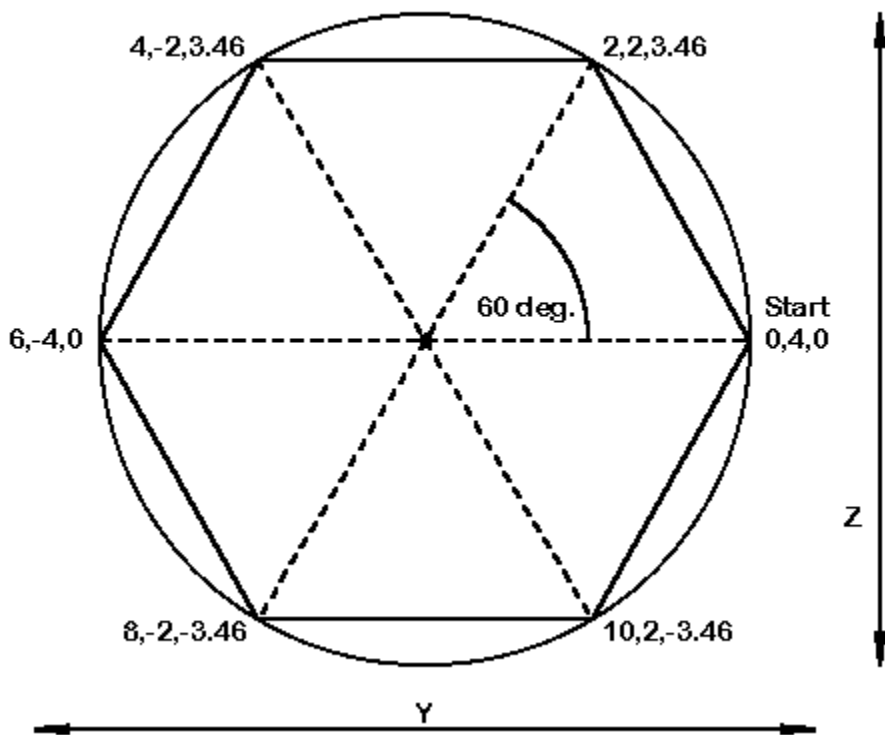


Fig. 29-10 shows the cross section of one complete turn of the helix. Since the length of the entire assembly will lie along the X-axis, the turns will be defined for the Y- and Z-axes. The circle shows the true helical shape. For this exercise, I have chosen to use a hexagon as the substitute. An octagon would have been truer to the circle, but the hexagon is more interesting for our purposes. Obviously, when translating the final model into a physical antenna, we would likely discover that a true circular radius a bit under 4" will best capture the model.

A hexagon can be subdivided into a collection of equilateral triangles. If we let the radius lie along the Y-axis, the first set of X, Y, Z coordinates will be 0, 4, 0, indicating no progress along the length of the antenna, and a peak of +4" on the Y axis.

The angle between successive points of the hexagon is 60 degrees. Therefore, we can use the same subdivisions of each triangle that we used with the equilateral delta. The value of Y for the second point will be half the base, or 2". The height of the triangle will be the sine of 60 degrees (0.866) times the radius, which becomes the hypotenuse of the triangle. The result is 3.46 for the Z-axis. The value of X increases by 2", which is half the radius.

Continuing counterclockwise, the values for X increase regularly. However, the values for Y and Z are simple repetitions of the values already derived, with some sign changes depending on which side of the axis the value falls. Consequently, we can define our helical dipole with very few equations.

Fig. 29-11 shows the equations page for the final helical dipole. See model 29-3. The values used in the equations are fussy beyond belief—simply because I wished the subsequent wires page to have simple numbers. The radius is defined in terms of a wavelength at 28.5 MHz. The extended decimal value is simply what was necessary to get a radius of 4.0000000". Likewise, the value of $2 \cdot \pi$ is carried out to many significant figures so that the equation shown on the working line (B5) would yield exactly 2.000000". You may truncate these values to practical sizes—if you are willing to live with longer decimals on the wires page.

The equations page also involves a small fudge, intentionally placed there to illustrate a point. The denominator for variables B and C is 12. The number is the result of dividing 360 by 30. However, since the sine of 30 degrees = the cosine of

60 degrees, and vice versa, we simply assign the cosine of 30 to the Z-axis and the sine of 30 to the Y-axis to arrive at correct values. Familiarizing yourself with a little trig is very handy in antenna design. However, not in every case can you get away with doing something backwards.

Fig. 29-11

	A	B	C	D	E	F	G	H
1	Var.	Value	Comment	Scratch Pad				
2	F =	28.5	Primary Frequency (MHz)					
3	W =	=299.8/B2/Model P	= "Wavelength(" & Model Params!\$B\$5&"					
4	A =	=0.00965843896*W	helix radius					
5	B =	=A*COS(6.283185)	+/- Z value					
6	C =	=A*SIN(6.283185)	+/- Y value					
7	D =	=0.5*A	increment					
8	E =							
9	G =							
10	H =							
11	I =							
12	J =							

Helical Dipole Equations Page

The variables we have just defined complete one turn of the helix. The next question is how we create the total structure of the entire dipole.

Fig. 29-12 partially reveals a wires page, showing the variables through wire 29 of the 56 total wires in the model. There are just enough lines to show the source assignments. The wires table has some features we have not shown to this point.

NEC-Win Plus+ [helix.nwp] (NEC Needs to Be Run)

File Edit Configure Commands Help

Antenna Environment

Frequency (MHz)
 Start: 28.5
 End: 28.5
 Step Size: 1

Ground
 No Ground

Radiation Patterns
 1°<Az<360°,El=1°,Step=1°
 0°<Ek180°,Az=0°,Step=1°
 Zo = 12.68 Ohm

Geometry
 Stepped inches

Helical Dipole: Wires Page; Variable Entries **Fig. 29-12**

Wire	Seg.	X1	Y1	Z1	X2	Y2	Z2	Dia.	Conduct	Src/Ld
1	3	=A	=A	=D	=C	=B	12 AWG	Copper	0/0	
2	3	=B1+D	=C	=B	=E1+D	=-C	=B	12 AWG	Copper	0/0
3	3	=B2+D	=-C	=B	=E2+D	=-A	0	12 AWG	Copper	0/0
4	3	=B3+D	=-A	0	=E3+D	=-C	=-B	12 AWG	Copper	0/0
5	3	=B4+D	=-C	=-B	=E4+D	=C	=-B	12 AWG	Copper	0/0
6	3	=B5+D	=C	=-B	=E5+D	=A	0	12 AWG	Copper	0/0
7	3	=B6+D	=A	0	=E6+D	=C	=B	12 AWG	Copper	0/0
8	3	=B7+D	=C	=B	=E7+D	=-C	=B	12 AWG	Copper	0/0
9	3	=B8+D	=-C	=B	=E8+D	=-A	0	12 AWG	Copper	0/0
10	3	=B9+D	=-A	0	=E9+D	=-C	=-B	12 AWG	Copper	0/0
11	3	=B10+D	=-C	=-B	=E10+D	=C	=-B	12 AWG	Copper	0/0
12	3	=B11+D	=C	=-B	=E11+D	=A	0	12 AWG	Copper	0/0
13	3	=B12+D	=A	0	=E12+D	=C	=B	12 AWG	Copper	0/0
14	3	=B13+D	=C	=B	=E13+D	=-C	=B	12 AWG	Copper	0/0
15	3	=B14+D	=-C	=B	=E14+D	=-A	0	12 AWG	Copper	0/0
16	3	=B15+D	=-A	0	=E15+D	=-C	=-B	12 AWG	Copper	0/0
17	3	=B16+D	=-C	=-B	=E16+D	=C	=-B	12 AWG	Copper	0/0
18	3	=B17+D	=C	=-B	=E17+D	=A	0	12 AWG	Copper	0/0
19	3	=B18+D	=A	0	=E18+D	=C	=B	12 AWG	Copper	0/0
20	3	=B19+D	=C	=B	=E19+D	=-C	=B	12 AWG	Copper	0/0
21	3	=B20+D	=-C	=B	=E20+D	=-A	0	12 AWG	Copper	0/0
22	3	=B21+D	=-A	0	=E21+D	=-C	=-B	12 AWG	Copper	0/0
23	3	=B22+D	=-C	=-B	=E22+D	=C	=-B	12 AWG	Copper	0/0
24	3	=B23+D	=C	=-B	=E23+D	=A	0	12 AWG	Copper	0/0
25	3	=B24+D	=A	0	=E24+D	=C	=B	12 AWG	Copper	0/0
26	3	=B25+D	=C	=B	=E25+D	=-C	=B	12 AWG	Copper	0/0
27	3	=B26+D	=-C	=B	=E26+D	=-A	0	12 AWG	Copper	0/0
28	3	=B27+D	=-A	0	=E27+D	=-C	=-B	12 AWG	Copper	1/0
29	3	=B28+D	=-C	=-B	=E28+D	=C	=-B	12 AWG	Copper	1/0

Wires Equations NEC Code Model Params

Let's begin with the easy part. Note that the Y and Z columns repeat themselves periodically, in fact, every 6 lines. To create the first 6 lines in each column, we manually enter the variables. Then we copy that block of 6 lines in the column and paste them to the next six lines. We can continue to paste until we reach line 54, the last line divisible by 6. The final step is to copy only the first two lines and past them to lines 55 and 56.

Of equal ease is the specification of the wire diameter and material conductivity, since each can be selected in a single block operation encompassing all 56 lines of the model.

We have covered every part of the model except the progression of the helix along the X-axis. Here we use another spreadsheet facility. We enter the values of X on line 1. Then we set an equation on line 2 for the X-entries that, in each case, references the first line box and the increment defined by variable D. The values for X1 occur in column B, so the first formula become $=B1+D$. Likewise, for X2, in the E column, we get $=E1+D$. The spreadsheet knows to read "D" as a variable from the equations page and to read "B1" and "E1" as the values within the boxes with those names.

So much for the hard work. Spreadsheets have a special function that works this way. Let's place the heavily outlined box onto line 2 and the column with the X1 values, which is B. We can now type CTL-C for "copy." The value goes to what Windows calls the "clipboard." Now, with the mouse, block the entire column from B3 (the next line) down to B56, the end of the model. Next, type CTL-V, which pastes the value on the clipboard to the boxes in the block. However, remember that this is a spreadsheet, and the special function is at work. Each new box value created will have the same form as the original formula: it will use the preceding B line and add D to it for the box at hand. Hence, the progression of values increases regularly from line 1 to line 56. We do the same for the X2 column, which is column E on the spreadsheet.

Had we wished to keep the precise value within box B2, we would have had to signal that with a special sign. On this spreadsheet, surrounding B1 with \$s (dollar signs) fore and aft would have done the job. Other spreadsheets may use other symbols.

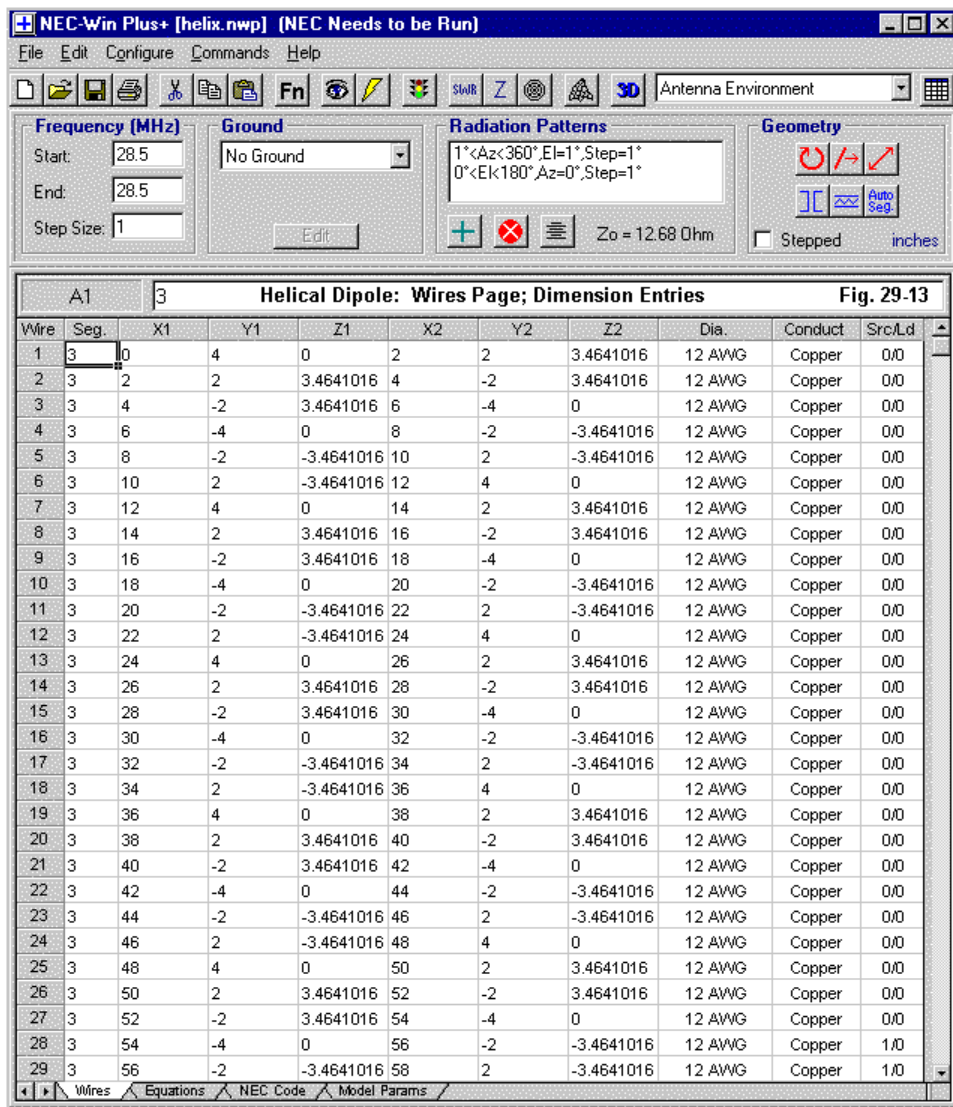
In the end, the laborious task of manually entering even the simple variables for the model is reduced to about a 5-minute job. As well, we have reduced the potential for entry errors of all sorts. If an error appears, we know to look back to the equations page or to the equations we entered on the variables version of the wires page. Hence, error correction also becomes a short-order task.

Fig. 29-13 replicates the portion of the wires page shown in **Fig. 29-12**, but with the dimensions rather than the variables. My fussiness with the equations makes this page easy to read as an example. The increment of progression along the X-axis is clear, and we can extrapolate that the total number of wires is 56, with a total antenna length of 112". This value is under the 10' limit set out as a requirement for the antenna. As well, the regular cycles of the turns in the helix are also clear, as they repeat themselves every 6 wires.

If we run the model at 28.5 MHz, we will obtain two values of impedance, each of which is about $12.68 + j2.69$ Ohms. The impedance of the antenna for a single feed is simply the sum of the resistances and reactances: $25.5 + j5.4$ Ohms, which is close to resonance. Although incidental to this exercise, the free-space gain of the helical dipole is 1.74 dBi, about 0.4 dB below a full-length linear dipole for the same frequency. Helical dipoles are certainly usable, but even as open a helix as this one shows losses in dipole use. Had we tightened the increment or shrunk the diameter, we would have seen even lower gain.

Nonetheless, the helical dipole has allowed us to create an extensive structure using the equations and variables provisions of a spreadsheet entries page for our model geometry. Other types of equations are certainly possible for other geometries, but the trig relationships we used allowed us to draw out some of the features of spreadsheet use. As well, the long repetitive structure of the helix gave us the occasion to use some of the time-saving features that spreadsheets offer.

However, before we close the book on modeling by equations and variables, we have one more question to pose. When is maximum generality too much generality?



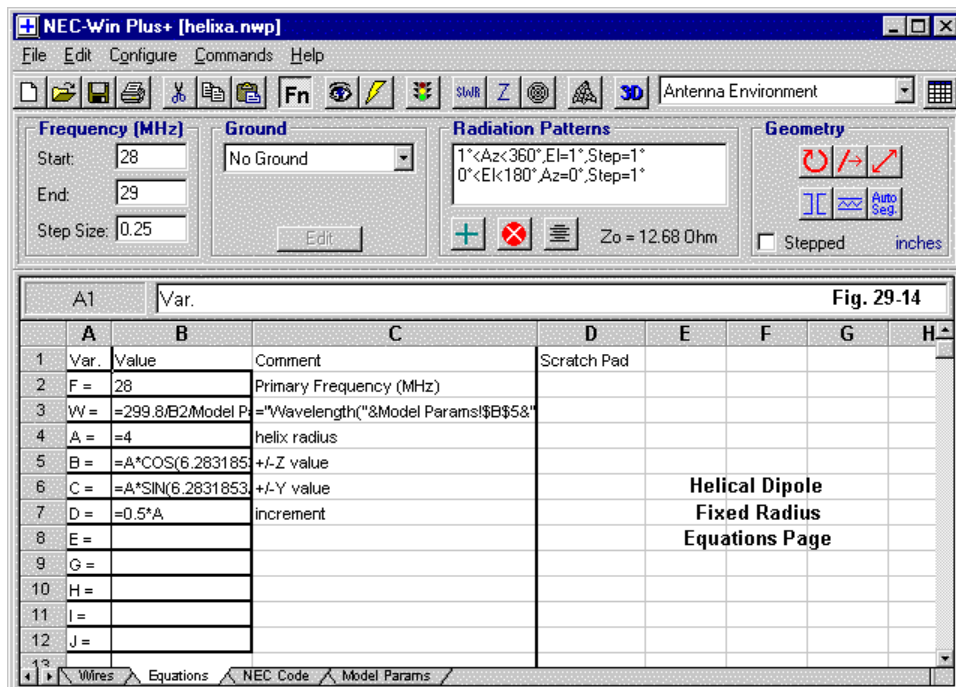
Confining Our Models

Suppose we wished to do a frequency sweep for the range from 28 to 29 MHz of the helical dipole we just designed for 28.5 MHz. Models designed by equations and variables are linked to the “Start” frequency (in the upper left corner of any of the screen captures shown) in NEC-Win Plus. Remember that we defined the variable A in terms of a wavelength and then defined the other variables in terms of the value of A. If we change the start frequency from the design frequency of 28.5 MHz down to 28 MHz, the dimensions of the antenna will change.

To preserve the dimensions of the design we just created, we must “freeze” it. This task involves only one change in the equations page, and the change appears in **Fig. 29-14**. See model 29-4.

Note that we have changed the value of A from a wavelength-dependent value to a constant. The value of 4 (inches) derives from the dimensions on the wires page that proved successful when we ran the model. Now, all of the other variables depend on the set value of A and are independent of the frequency. At this point, we can set the frequency sweep with a start frequency of 28 MHz, an end frequency of 29 MHz, and any desired interval for the sweep check frequencies.

There is a technique for retaining all of the variables as wavelength-dependent equations and still making the design frequency independent of the program “start” frequency. Using the technique allows us to perform frequency sweeps without altering the dimensions for each change of the sweep starting frequency. We shall look at that technique in a future episode.



Incidental to this exercise, but relevant to the modeling task at hand, is the fact that the impedance against which SWR will be calculated has been set to the design frequency source resistance for each of the sources (12.68 Ohms). The resulting SWR curve will track a composite curve set to the value we might have used had we specified only a single source for the antenna (that is, an impedance of about 25.36 Ohms). The helix, relative to the source resistance at or near resonance, shows a 2:1 SWR curve that is about 700 kHz wide, slightly reduced from the curve we might obtain from a full-length linear dipole of #12 AWG copper wire. These curves will generally track the 50-Ohm SWR curve we might create with most com-

mon, relatively lossless matching circuits between the actual antenna connection point and a coaxial cable.

If our interest in this particular design goes beyond the modeling session, we should save the revised model under a new file name. As a file in .NWP format, the model will retain its model-by-equation features. However, we may freeze the model as a simple set of coordinates by saving it as a .NEC file. Such files are useful for transport from one program to the next. However, they contain only the result of the spreadsheet calculations and not the equations themselves. For a simplified file in .NWP format without the equations, we can always open the .NEC-format file that we just saved under its new name and then re-save the file in the .NWP format.

The upshot of the move that made the helix radius 4" instead of a wavelength-dependent variable is to note that there are limitations to designing models by equations and variables for maximum generality. For every task, there is an appropriate level of generality somewhere between the maximum and, at the other extreme, specifying each dimension as simply a number on the wires page. It is not possible to say in advance of knowing the task parameters what the proper level of generality should be. However, with some practice in both "normal" modeling with numbers and modeling with equations and variables, the modeler gains a sense of the level of generality that works best in each circumstance.

In these three episodes, we have certainly only begun the process of modeling by equations and variables. However, by combining the techniques covered, we can branch out into many directions. For example, we might wish to create a 2-element Yagi consisting of 2 helical elements. However, even the trig involved in the helix pales compared to the complexity of equations that we might invoke to set the coordinates of very complex geometries.

There is also another option. There are wire-grid programs, that is, programs (such as NEC-Win Synth) which offer a large number of pre-set shapes. We need only enter the dimensions specified by a shape option, along with the frequency of operation and the segmentation density. The program then creates a collection of wires in the designated shape. These wires do not appear as variables, but instead as a sequence of basic geometry (GW) entries that are fixed. Changing the entries requires that we re-create the wire-grid from scratch. (Of course, once we have the wire structure, we must add all of the other features that go into making a complete

model, for example, a source, wire conductivity, and pattern request.) Given the alternatives of modeling by equation or of synthesizing a complex shape with a helping program, the modeler must give serious thought to which technique is best for a given set of modeling tasks.

Although we could extend this series almost indefinitely with equation-based models, each of which might add a bit to our insight into the process, we must draw a line call “conclusion” somewhere in the sands of words. Next month, we shall close the series by looking at a pair of examples that show a. there is always more than one way to formulate a model via equations, and b. the scratch pad facility can come in handy at times.

* * * * *

Models included: 29-1 through 29-4. (Due to the nature of the models, they are available only in the .NWP format.)



30. Modeling By Equation: D. Scratch Pads & Coordinates

In this small series of columns devoted to modeling by equation, we have looked at the very basics and then proceeded to topics that may help us refine our techniques. The object has been to make maximum use of the facilities offered to us by any program containing a model-by-equation option, even though we have had to confine ourselves to a single program in order to sensibly link the various moves we have made.

So far, we have explored the need to develop modeling conventions, even within the use of equations to define variables, so that the task of modeling remains orderly and unconfused. We have also examined a few more complex models in order to reach decisions about what part of the work best appears on the equations pages of the spreadsheet and what of the work best appears on the wire pages.

In our exploration of modeling by equations, the examples we have so far used have all focused on the geometry of the antenna as either a function of wavelength or as a function of a physical structure. There are further options that lead us to use some other facilities within a modeling-by-equation system. In this column, we shall focus on two diverse examples that are especially suited to exploit these facilities. As in previous notes, we shall use the equations spreadsheet within NEC-Win Plus for our examples. But in this episode, we shall examine the utility of having a “scratch pad” at our disposal within the equations pages.

A scratch pad is simply an area on the spreadsheet in which we may store data and equations. The data and equations will be those that are necessary in the process of deriving the values for the variables that will appear on the wire coordinate page. However, the data and equations in question do not directly define these variables. In simple models, we may not need the scratch pad, but as models become more complex—either in structure or in the mathematics used to define the structure—reserving variables for use on the wires page and placing supplementary data and calculations on the scratch pad can be very useful. (There is a technique within our sample program for getting around the limited number of allowed variable, but it will not be needed for our sample models.)

Another Look at the Quad Loop

Let's return to the quad loop with which we began, as shown in **Fig. 30-1**.

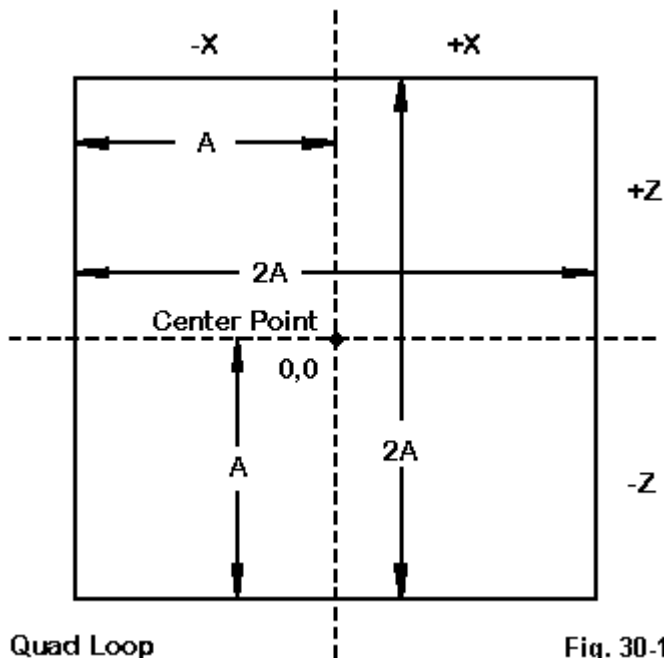


Fig. 30-1

We have thought of the quad loop in terms of letting the value of A be a constant or a simple function of wavelength. However, we can also look at the dimensions as a function of wire diameter. If we give the wire diameter as a fraction of a wavelength, then the resonant circumference for any frequency, also in wavelengths, can be approximated by the following equation:

$$QL_{wf} = 1.0413 + (\log^2(d_{wf} * 1E5) * 0.0128) \quad (1)$$

QL is the circumference/perimeter of the quad loop in wavelengths and d_{wf} is the wire diameter as a fraction of a wavelength. The log is to the base 10. (The spreadsheet in NEC-Win Plus knows the difference between LOG, also known as the “common” logarithm, and LN, known as the “natural” logarithm. In contrast, GW Basic, still a useful programming language for simple utility programs, knows only natural logs, and the user must program in a conversion factor to derive common logs.) A restriction upon this approximation equation is that it applies with under 2% error for wire sizes from 10^{-5} to 10^{-2} wavelengths in diameter. Although the equation appears to be quite adequate for wires that are thinner than the lower defined limit, using the equation on fatter wires will rapidly yield inaccurate results. Most physically constructed quad loops will have wires falling within the equation limits.

Since the equations page already provides the wavelength in the selected units (W), implementing the required equations for the model becomes very straightforward. The first step is to set a variable to the wire size. (Wire size here refers to wire diameter. Although NEC calculates using the wire radius, most NEC programs permit the user to input a wire diameter, since that value is normally better known. Conversion to the radius becomes an internal function of the user-to-core interface programming.) Since the wire size ultimately must be in the same units as we use for the wire-end coordinates, here is a handy conversion chart for common AWG wire sizes, given in inches, feet, and mm.

AWG Size	Dia. Inches	Dia. Feet	Dia. mm
18	.0403	.00336	1.0236
16	.0508	.00423	1.2903
14	.0641	.00534	1.6281
12	.0808	.00673	2.0523
10	.1019	.00849	2.5883

We can enter the desired wire size directly, or we might use up a bit of scratch pad or equation variable space by entering the diameter in a common unit (such as inches) and then converting it to the value in the desired units (in this example, feet). Suppose we enter .0641 as our wire diameter and let it equal A. Then B might equal this value divided by 12 to obtain a value in feet, the chosen unit of measure for the

model. Finally C might equal B divided by W (the wavelength). I have taken this route only because we have plenty of pre-defined variables at our disposal for this small problem.

We can now let D be the perimeter/circumference as defined in **Equation 1** above, where d takes the value of variable C, as we have just derived it. In this example, we have used #12 AWG wire with a diameter of 0.0808" as the wire size. Note that in the upper portion of **Fig. 30-2**, the entry for the variable D follows **Equation 1** exactly, although the notations differ.

However, for developmental purposes we may wish to follow a different procedure in setting up the equation for D. In the lower portion of **Fig. 30-2**, we can see that the equation for D refers to D2, D3, and D4. These are values entered into column D, in the "scratch pad" area of the equations page. The entries in column E identify the values placed in column D. The equation for the variable D uses the active values in rows 2-4 of column D at the designated places.

An advantage of using the scratch pad is that the modeler can make adjustments to the numerical values in the equation for variable D without having to rewrite the equation. Compare models 30-1 and 30-2, which correspond to using the scratch pad for reference only and for active data. In fact, adjustments were made in the development of the algorithm in question. The initial value in D2 was 1.0416 and the value in D4 was 0.0131. Further adjustments, including varying the exponent, to bring the curve further into alignment with NEC calculations for resonant quad loops would be a routine matter.

NEC-Win Plus+ [301eq.nwp] (NEC Needs to be Run)

File Edit Configure Commands Help

Antenna Environment

Frequency (MHz)
 Start: 28.5
 End: 28.5
 Step Size: 1

Ground
 No Ground

Radiation Patterns
 1°<Az<360° El=1°, Step=1°
 0°<Ek<180°, Az=0°, Step=1°
 Zo = 127.6 Ohm

Geometry
 Stepped

Fig. 30.2

B7 = $1.0413 + (\text{LOG}(C \cdot 10^5))^2 \cdot 0.0128$

A	B	C	D	E	F	G	H
1	Var. Value	Comment	Scratch Pad				
2	F = 28.5	Primary Frequency (MHz)					
3	W = $=299.8/B2/Model P$	Wavelength ("&Model Params;\$B\$5&")					
4	A = $=0.0808$	Wire Diameter Inches					
5	B = $=A/12$	Wire Diameter Feet					
6	C = $=B/W$	Wire Diameter Wavelengths					
7	D = $=1.0413 + (\text{LOG}(C \cdot 10^5))^2 \cdot 0.0128$	Perimeter Wavelengths					
8	E = $=D \cdot W$	Perimeter Feet					
9	G = $=E/8$	1/8 Perimeter					
10	H =						
11	I =						
12	J =						
Quad Loop Equations Page							

Wires Equations NEC Code Model Params

B7 = $D2 + (\text{LOG}(C \cdot 10^5))^2 \cdot D3 \cdot D4$

A	B	C	D	E	F	G	H
1	Var. Value	Comment	Scratch Pad				
2	F = 28.5	Primary Frequency (MHz)	1.0413	base	Scratch Pad Holds Active Data		
3	W = $=299.8/B2/Model P$	Wavelength ("&Model Params;\$B\$5&")	2	exponent			
4	A = $=0.0808$	Wire Diameter Inches	0.0128	multiplier			
5	B = $=A/12$	Wire Diameter Feet					
6	C = $=B/W$	Wire Diameter Wavelengths					
7	D = $=D2 + (\text{LOG}(C \cdot 10^5))^2 \cdot D3 \cdot D4$	Perimeter Wavelengths					
8	E = $=D \cdot W$	Perimeter Feet					
9	G = $=E/8$	1/8 Perimeter					
10	H =						
11	I =						
12	J =						
Quad Loop Equations Page							

Wires Equations NEC Code Model Params

B7		=1.0413+(LOG(C*10^5)^2*0.0128)					Fig. 30-3	
	A	B	C	D	E	F	G	H
1	Var.	Value	Comment	Scratch Pad				
2	F =	28.5	Primary Frequency (MHz)					
3	W =	34.51326568	Wavelength(feet) = c / f					
4	A =	0.0808	Wire Diameter Inches					
5	B =	0.006733333333	Wire Diameter Feet					
6	C =	0.000195094066	Wire Diameter Wavelengths					
7	D =	1.062608541	Perimeter Wavelengths					
8	E =	36.67409087	Perimeter Feet					
9	G =	4.584261359	1/8 Perimeter					
10	H =		Quad Loop					
11	I =		Equations Page					
12	J =		Values Version					
<div> <div>Wires</div> <div>Equations</div> <div>NEC Code</div> <div>Model Params</div> </div>								

We can convert the value of variable D (initially calculated in wavelengths) to a value in the selected units of measure by letting E equal D times W, the length of a wave in those units of measure. **Fig. 30-3** shows the numerical values that result for a frequency of 28.5 MHz.

The only additional step we need to take is to set up the coordinates. We have some choices here, one of which is to pre-convert the total perimeter length into +/- values for the 4 wires in the single square loop. So we can let G equal E divided by 8. (Note that, in the NEC-Win Plus spreadsheet used for our examples, F and W are preset variables for frequency and wavelength, respectively. Hence, our own list of variables will jump from E to G.) **Fig. 30-4** shows the wires page that corresponds to the prescribed variables we have just described.

A14		Wires Page: Variable Entries								Fig. 30.4	
Wire	Seg.	X1	Y1	Z1	X2	Y2	Z2	Dia.	Conduct	Src/Ld	
1	11	=G	0	=G	=G	0	=G	=B	Copper	1/0	
2	11	=G	0	=G	=G	0	=G	=B	Copper	0/0	
3	11	=G	0	=G	=G	0	=G	=B	Copper	0/0	
4	11	=G	0	=G	=G	0	=G	=B	Copper	0/0	
5											
6											
7											
8											
9											
10											
11											
12											
13											

Wires

Equations

NEC Code

Model Params

From this set of variables entered on the wires page, we get the numerical values shown in **Fig. 30-5**.

A14		Wires Page: Dimension Entries							Fig. 30.5	
Wire	Seg.	X1	Y1	Z1	X2	Y2	Z2	Dia.	Conduct	Src/Ld
1	11	-4.5842614	0	-4.5842614	4.5842614	0	-4.5842614	0.0067333333	Copper	1/0
2	11	4.5842614	0	-4.5842614	4.5842614	0	4.5842614	0.0067333333	Copper	0/0
3	11	4.5842614	0	4.5842614	-4.5842614	0	4.5842614	0.0067333333	Copper	0/0
4	11	-4.5842614	0	4.5842614	-4.5842614	0	-4.5842614	0.0067333333	Copper	0/0
5										
6										
7										
8										
9										
10										
11										
12										
13										

Wires

Equations

NEC Code

Model Params

G16		Wires Page: Variable Entries								Fig. 30-6	
Wire	Seg.	X1	Y1	Z1	X2	Y2	Z2	Dia.	Conduct	Src/Ld	
1	11	=E/8	0	=E/8	=E/8	0	=E/8	=B	Copper	1/0	
2	11	=E/8	0	=E/8	=E/8	0	=E/8	=B	Copper	0/0	
3	11	=E/8	0	=E/8	=E/8	0	=E/8	=B	Copper	0/0	
4	11	=E/8	0	=E/8	=E/8	0	=E/8	=B	Copper	0/0	
5											
6											
7											
8											
9											
10											
11											
12											
Wires Equations NEC Code Model Params											

G16		Wires Page: Dimension Entries									
Wire	Seg.	X1	Y1	Z1	X2	Y2	Z2	Dia.	Conduct	Src/Ld	
1	11	-4.5842614	0	-4.5842614	4.5842614	0	-4.5842614	0.0067333333	Copper	1/0	
2	11	4.5842614	0	-4.5842614	4.5842614	0	4.5842614	0.0067333333	Copper	0/0	
3	11	4.5842614	0	4.5842614	-4.5842614	0	4.5842614	0.0067333333	Copper	0/0	
4	11	-4.5842614	0	4.5842614	-4.5842614	0	-4.5842614	0.0067333333	Copper	0/0	
5											
6											
7											
8											
9											
10											
11											
12											
Wires Equations NEC Code Model Params											

Even on the wires page, we have options. The definition of variable G was unnecessary, although for many purposes it is convenient. We might have done our division by 8 on the wires page itself, thus saving the use of one variable. In the present simple case, we have plenty of variables to use, but in more complex cases.

We might wish to use the least number possible to ensure that all entries needing a variable have one. **Fig. 30-6** shows our revised wires page variable entries, along with the dimension entries to verify that we achieve the same results as we obtained with our previous procedure.

Learning to use all of the facilities at our disposal in the most efficient and effective manner takes some time, and the simple example only scratches the surface of the scratch pad.

The Moxon Rectangle

The Moxon Rectangle is a 2-element parasitic array with the ends of the elements folded to point toward each other. The mutual coupling of the elements and the coupling between the tips of the tails yields a nearly cardioidal pattern with a very high front-to-back ratio. **Fig. 30-7** shows the general outline of the Moxon rectangle, with identifications for all of the key dimensions.

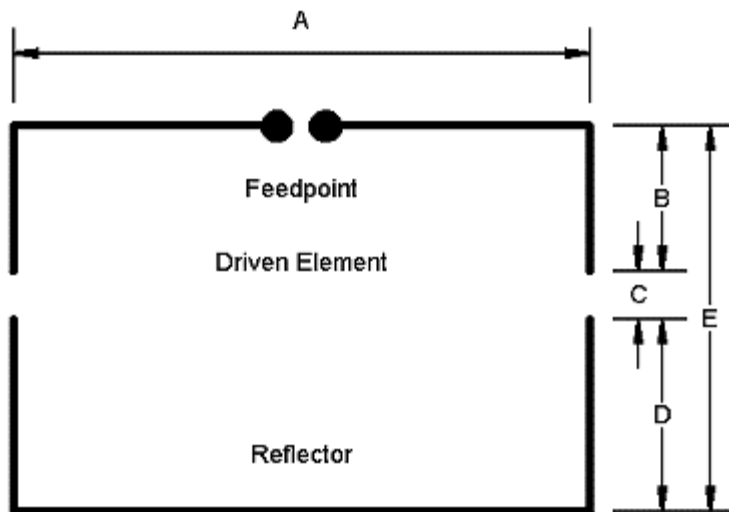


Fig. 30-7

Moxon Rectangle Outlines

The critical dimension is the gap between the tips of the tails (dimension C). The other dimensions then determine the resonant frequency of the array (close to 50 Ohms) and the frequency of maximum front-to-back ratio. I once optimized a series of models using #14 copper wire for all of the HF bands from 40 meters to 10 meters. Barbara Craig, KC8KJA, performed a series of regressions on this data to develop a sequence of equations defining Moxon Rectangle dimensions for #14 bare copper wire, with results that are usable even at 2 meters.

The following GW Basic utility program provides a listing of the equations that resulted from the regression analysis. Lines 40-80 supply the mathematics, using the design frequency that the user enters in line 20 and the constants defined in line 30.

```

10 PRINT "Program to calculate the dimensions of"
12 PRINT "a #14 AWG Bare Wire Moxon Rectangle"
14 PRINT "Analysis by Barbara Craig, KC8KJA"
16 PRINT "Output dimensions in Feet"
20 INPUT "Enter frequency in MHz:";F
30 A0=6.19653:B0=1.00058:A1=6.126836:B1=.99437:A2=6.19966:B2=1.00033:GA=.72
40 A=GA*((EXP(A2)/F)^(1/B2))
50 B=.5*((EXP(A1)/F)^(1/B1))-.5*A
60 D=((1-GA)/2)*((EXP(A2)/F)^(1/B2))
70 E=((EXP(A0))/F)^(1/B0)-A
80 C=E-(B+D)
90 PRINT "A = ";A
100 PRINT "B = ";B
110 PRINT "C = ";C
120 PRINT "D = ";D
130 PRINT "E = ";E
140 END

```

Fig. 30-8 shows one way in which we can enter the equations into the equations page of NEC-Win Plus. The spreadsheet mathematical forms here follow the Basic forms exactly. As the representative equation (for variable A, which corresponds to dimension A in **Fig. 30-7**) shows, we can enter the set of constants that emerged from the exercise in regressions directly into the equations. On the scratch pad, we have entered solely for reference the values of gamma and of alpha0-2 and beta0-2. However, the variable equations themselves contain all of the requisite information for dimension calculation. Variables A-E correspond to the dimensions in **Fig.**

30-7. See model 30-3. (Although Basic requires rigorous serial calculation, which places the derivation of variable and dimension C last, the spreadsheet permits the user to list the variables in almost any desired order.)

Frequency [MHz]
Start: 28.5
End: 28.5
Step Size: 1

Ground
No Ground

Radiation Patterns
1° < Az < 360°, El = 1°, Step = 1°
0° < Ek < 180°, Az = 0°, Step = 1°
Zo = 127.6 Ohm

Geometry
Stepped

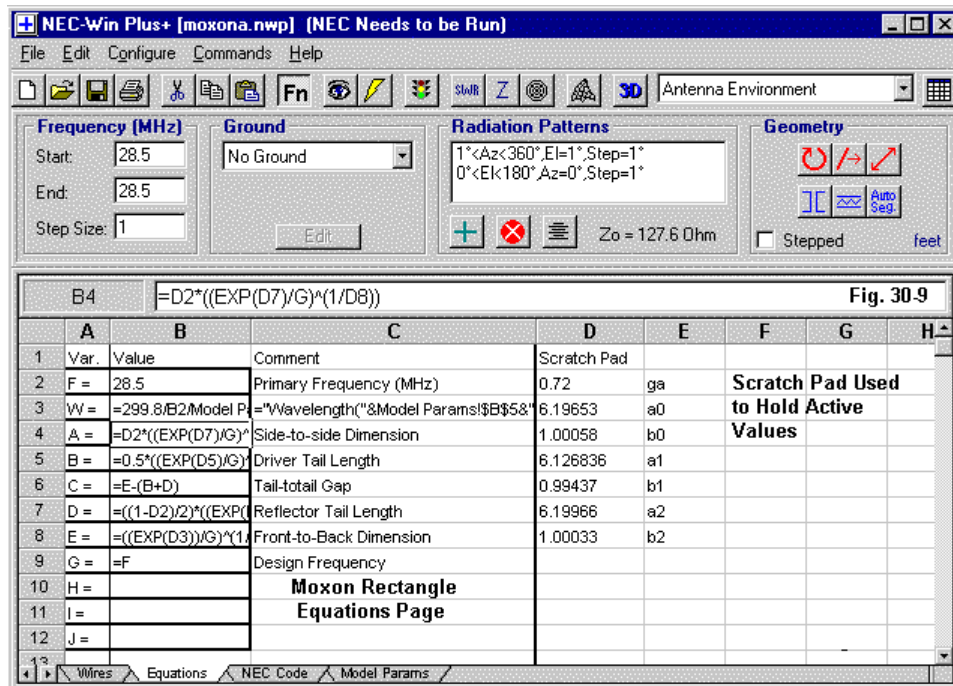
Fig. 30.8

	A	B	C	D	E	F	G	H
1	Var.	Value	Comment	Scratch Pad				
2	F =	28.5	Primary Frequency (MHz)	ga = .72	Scratch Pad Used for Reference Only			
3	W =	=299.8/B2	Model P = "Wavelength"&Model Params	a0 = 6.19653				
4	A =	=0.72*((EXP(6.19966)/G)^(1/1.00033))	Side-to-side Dimension	b0 = 1.00058				
5	B =	=0.5*((EXP(6.12683)/G)^(1/1.00033))	Driver Tail Length	a1 = 6.126836				
6	C =	=E-(B+D)	Tail-to-tail Gap	b1 = .99437				
7	D =	=(1-0.72)/2*(EXP(6.19966)/G)^(1/1.00033)	Reflector Tail Length	a2 = 6.19966				
8	E =	=(EXP(6.19653)/G)^(1/1.00033)	Front-to-Back Dimension	b2 = 1.00033				
9	G =	=F	Design Frequency					
10	H =		Moxon Rectangle Equations Page					
11	I =							
12	J =							

Wires Equations NEC Code Model Params

The equations apply only to antennas using #14 bare copper wire. The actual relationships among the dimensions is somewhat complex, since a fatter wire will require a wider gap. The resultant increase in dimension E will change the feedpoint impedance, as will the fatter wire itself. Elongating the array will restore the near-50-Ohm feedpoint impedance, but there will be adjustments to the overall length of both the driver and reflector elements to place the maximum front-to-back ratio at

the design frequency. Hence, the relationships among the element dimensions will shift as we move to #10 wire or to aluminum tubing in the 0.5" to 1" range.



With the prospect that regression analysis would produce differing constants for other wire diameters, a more useful way of entering the equations appears in **Fig. 30-9**. Here, the values in column D represent active values that we draw into the variable equations by means of column and row references. The sample equation for dimension A illustrates the method and may be compared directly with the sample equation in **Fig. 30-8**. D2, D7, and D8 replace the constants in the earlier version of

the equation. Column E now holds reference data to identify each of the values in column D. See model 30-4.

B4		=D2*((EXP(D7)/G)^(1/D8))						Fig. 30-10	
	A	B	C	D	E	F	G		
1	Var.	Value	Comment	Scratch Pad					
2	F =	28.5	Primary Frequency (MHz)	0.72	ga				
3	W =	34.51326568	Wavelength(feet) = c / f	6.19653	a0				
4	A =	12.43247172	Side-to-side Dimension	1.00058	b0				
5	B =	1.945912205	Driver Tail Length	6.126836	a1				
6	C =	0.4053338801	Tail-to-tail Gap	0.99437	b1				
7	D =	2.417425056	Reflector Tail Length	6.19966	a2				
8	E =	4.768671141	Front-to-Back Dimension	1.00033	b2				
9	G =	28.5	Design Frequency						
10	H =		Moxon Rectangle Equations Page Values Version						
11	I =								
12	J =								

Let us suppose that we have a new set of values for gamma and for A0-2 and B0-2 for some new wire size. We need not create an entirely new model. One option would be to replace the values in column D with the new values and to save the model under a new name. Another option would be to place the new values in column F and then to use further spreadsheet capabilities to let the equations page select the appropriate column of values, depending upon the wire size, which we might enter as a variable. Such possibilities go beyond the scope of these introductory exercises. However, if modeling by equation becomes a routine task, then exploring the full limits of the spreadsheet's language becomes an important part of the learning curve.

Fig. 30-10 shows the set of values that emerge from either method of entering the equations. Variable G is useful for this and other sample models, because it gives us the option of setting the design frequency either to the current frequency of the model or to some specific frequency. The latter type of frequency assignment is useful when we wish to run a frequency sweep with the design frequency at neither end of the frequency range that we sweep.

A14

Wires Page: Variable Entries

Fig. 30-11

Wire	Seg.	X1	Y1	Z1	X2	Y2	Z2	Dia.	Conduct	Src/Ld
1	7	=A/2	=E-B	0	=A/2	=E	0	14 AWG	Copper	0/0
2	45	=A/2	=E	0	=A/2	=E	0	14 AWG	Copper	1/0
3	7	=A/2	=E	0	=A/2	=E-B	0	14 AWG	Copper	0/0
4	9	=A/2	=D	0	=A/2	0	0	14 AWG	Copper	0/0
5	45	=A/2	0	0	=A/2	0	0	14 AWG	Copper	0/0
6	9	=A/2	0	0	=A/2	=D	0	14 AWG	Copper	0/0
7										
8										
9										
10										
11										
12										
<div> <div>Wires</div> <div>Equations</div> <div>NEC Code</div> <div>Model Params</div> </div>										

A14

Wires Page: Dimension Entries

Wire	Seg.	X1	Y1	Z1	X2	Y2	Z2	Dia.	Conduct	Src/Ld
1	7	-6.2162359	2.8227589	0	-6.2162359	4.7686711	0	14 AWG	Copper	0/0
2	45	-6.2162359	4.7686711	0	6.2162359	4.7686711	0	14 AWG	Copper	1/0
3	7	6.2162359	4.7686711	0	6.2162359	2.8227589	0	14 AWG	Copper	0/0
4	9	-6.2162359	2.4174251	0	-6.2162359	0	0	14 AWG	Copper	0/0
5	45	-6.2162359	0	0	6.2162359	0	0	14 AWG	Copper	0/0
6	9	6.2162359	0	0	6.2162359	2.4174251	0	14 AWG	Copper	0/0
7										
8										
9										
10										
11										
12										
<div> <div>Wires</div> <div>Equations</div> <div>NEC Code</div> <div>Model Params</div> </div>										

Fig. 30-11 displays the two forms of the wires page for this example. Note that it is necessary to decide several matters regarding the axes for the model. In this case, the X-axis uses +/- A values, requiring us to use half of the value of A. The Y-axis provides the front-to-back dimensions, with the reflector set a Y=0. All other values are positive. Only the tip of the driver tail requires a “complex” formulation, and dimension C is not referenced at all on the wires page (despite its importance to the antenna design). You may wish to reference the side-to-side dimensions to the Y-axis and the front-to-back dimensions to the X-axis. To capture a vertically oriented Moxon, the side-to-side dimensions would be referenced to the Z-axis, with

the front-to-back dimensions referenced either to X or Y. To place the antenna at some specific height above ground would require the use of one more variable for the antenna height. In this case, the wires page variable entries would become a mixed function of the new height variable and the variable A, using techniques noted in previous episodes.

Conclusion

Together, the quad and Moxon examples illustrate two of the many uses of the scratch pad facility. Not only is it a place to enter reference data, it also serves as an active data pad that the variable equations can routinely reference. The scratch pad data need not be just a series of constants, but may also consist of equations. Indeed, any equation that is not used on the wires page may best be placed on the scratch pad. In addition, we may also use the scratch pad area for identifying notes and labels to ensure that the data we place there today can be interpreted months later. As an exercise to ensure mastery of these matters, you may wish to go through all of the examples in these 4 episodes, transferring to the scratch pad all data and equations that are not directly needed to specify a variable used on the wires pages.

Since I first wrote these notes, I have developed through regression analyses self-calculating models for two versions of the Moxon rectangle: a standard 50-Ohm version and a special purpose 93-Ohm version. Using similar techniques, I also developed self-calculating models for monoband quad antennas from 1 to 4 elements (with wide-band and higher gain versions for 3-element quads). The 1-element model will replace with higher accuracy the quad loop models used here. All of these models—on the equations page—only require entry of a design frequency and the wire diameter in the active unit of measure.

The frequency entry is supplemented by a repetition of the equation under W to arrive at a wavelength variable that is independent of the starting frequency on the main NEC-Win Plus page. Hence, the dimensions will remain stable regardless of what main-page frequency entries you use. To illustrate that function, I am including the collection of NEC-Win Plus quad and Moxon models with this chapter. However, they will retain their generic file names in order to be more self-identifying. The only difficulty might occur with the 3-element quads. Q3LE is the wide-band version, while Q3LEA is the high-gain version.

We could carry on this series of columns on modeling by equation almost indefinitely. However, I hope the selection of examples used in this and the preceding columns provides enough background and ideas to permit you to develop your own best methods of using this versatile adjunct to creating effective models. Although these notes have focused exclusively on elements that we may model through the use of equations, we must also remember that none of the requirements and limitations of NEC are set aside in the process. Segmentation, source placement, load placement and type, convergence testing, and average gain testing all remain important concerns to the modeler, no matter how simple or complex the equations of the model.

* * * * *

Models included: 29-1 through 29-4. (Due to the nature of the models, they are available only in the .NWP format.) See also the following models (all .NWP): Q1LE, Q2LE, Q3LE, Q3LEA, Q4LE, MOXGEN50, and MOXGEN93.



31. A Case Study: A 90' Wire

I assisted another amateur radio operator in analyzing his antenna, since it had largely evaded modeling. The purpose of the exercise was to provide some general information on the modeled performance of the antenna across the MF-HF amateur frequency spectrum for a typical amateur radio wire antenna fed by an antenna tuner. The purpose was not to be overly precise, and indeed, the input data and modeling conditions would have precluded precision. However, even carefully constrained modeling of a general nature can be useful. The following exploration is a case in point.

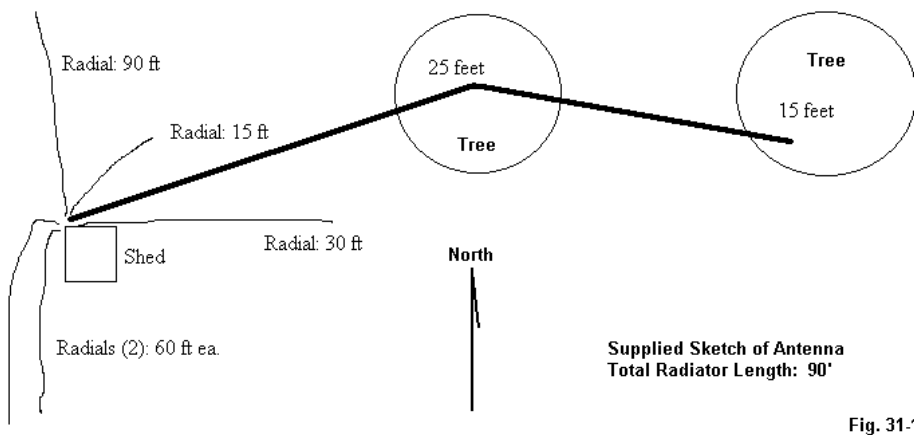


Fig. 31-1

The basic antenna is shown in **Fig. 31-1**. The radiator is about 90' long and runs from near the ground at the left (shed) to a maximum height of 25' about 50' from the shed and then down to a height of about 15' at the far right tree. It is fed at the base of the wire at the junction with the buried radial wires. The antenna may be

variously classified as an end-fed random wire or as the type of antenna to which it most closely corresponds at each frequency of operation.

The sketch supplied was incomplete. Therefore, I made a few assumptions that will not materially affect the modeled outcomes. First, I assumed that true north was straight up the page of the sketch. If north has a different bearing, one will have to adjust the azimuth headings in this report accordingly. I had to use a compass to approximate the angles of the wire.

Second, the owner did not specify the wire size. I assumed #12 AWG copper wire. For the number of approximations required by this exercise, a small change in wire size will produce no radical changes in the patterns or the impedance reports.

Third, the owner did not specify the conductivity and dielectric constant of the soil in his area. Maps suggest that the conductivity is about 0.002 Siemens per meter, which corresponds to the class of soil listed as “poor.” The corresponding dielectric constant is about 13. However, it may in fact be lower than this level, depending upon subsoil structure. For example, the dielectric constant of shale is about 7. Nonetheless, given other approximations, the difference will not alter projected performance by much.

Before looking at the model of this antenna, let me note something about what this report can and cannot tell. What the NEC-2 models of the antenna provide is a general portrait of anticipated performance characteristics with the assumption of a level homogenous soil beneath the antenna. There are limitations to the data that emerges.

1. NEC-2 cannot account for variations in the patterns created by the immediate terrain. The subject terrain is likely to be quite hilly, but not mountainous. An immediate hill may yield a stronger signal in the direction from the hill through the antenna, but this cannot be assured without the application of supplementary software into which topographical features can be placed. However, an awareness of one’s immediate topography can assist one in accounting for differences in the model and actual operation.

2. NEC-2 cannot place radials on or beneath the ground, as they are at the subject site. However, placing radials very close to the ground provides a very

reasonable approximation of in-ground radial performance, with errors well within the limitations of other approximations made in this report.

3. The antenna owner has chosen EZNEC as his modeling vehicle. Two factors limit the ability of this program to model both natural and constructed structures beyond the antenna wires. First, EZNEC permits only 500 segments, which limits the available segments for such structures. Second, the program allows only a single wire loss (or conductivity) value for all wires. Secondary structures in the vicinity of the antenna may require many different conductivity values for their approximating wire-grid structures. However, since no data on secondary structures was provided, modeling must do without them. The effects of such structures must remain an estimate used in conjunction with this report.

The Model

The EZNEC model for NEC-2 analysis of the antenna requires 8 wires, as shown in the side and top views of **Fig. 31-2**. The following model description has been annotated for correlation with **Fig. 31-2**.

Wire Loss: Copper — Resistivity = 1.74E-08 ohm-m, Rel. Perm. = 1

WIRES									
Wire Conn.--	End 1 (x,y,z : ft)	Conn.--	End 2 (x,y,z : ft)	Dia(in)	Segs				
Radiator wires									
1	W3E1	0.000, 0.000, 0.200	W2E1	45.500, 21.000, 25.000	# 12	50			
2	W1E2	45.500, 21.000, 25.000		82.607, 7.500, 15.000	# 12	40			
Radials									
3	W4E1	0.000, 0.000, 0.200		30.000, 0.000, 0.200	# 12	30			
4	W5E1	0.000, 0.000, 0.200		10.607, 10.607, 0.200	# 12	15			
5	W6E1	0.000, 0.000, 0.200		0.000, 90.000, 0.200	# 12	90			
6	W7E1	0.000, 0.000, 0.200		0.000, -60.000, 0.200	# 12	60			
7	W1E1	0.000, 0.000, 0.200	W8E1	-10.000, 0.000, 0.200	# 12	10			
8	W7E2	-10.000, 0.000, 0.200		-10.000, -50.000, 0.200	# 12	50			

SOURCES						
Source	Wire Seg.	Wire #/Pct Actual	From End 1 (Specified)	Ampl.(V, A)	Phase(Deg.)	Type
1	1	1 / 1.00	(1 / 0.00)	1.000	0.000	V

Ground type is Real, high-accuracy analysis
Conductivity = .002 S/m Diel. Const. = 13

MEDIA					
Medium	Conductivity(S/m)	Dielectric Const.	Ht(ft)	R Coord(ft)	
1	2.000E-03	13.00	0 (def)	0 (def)	

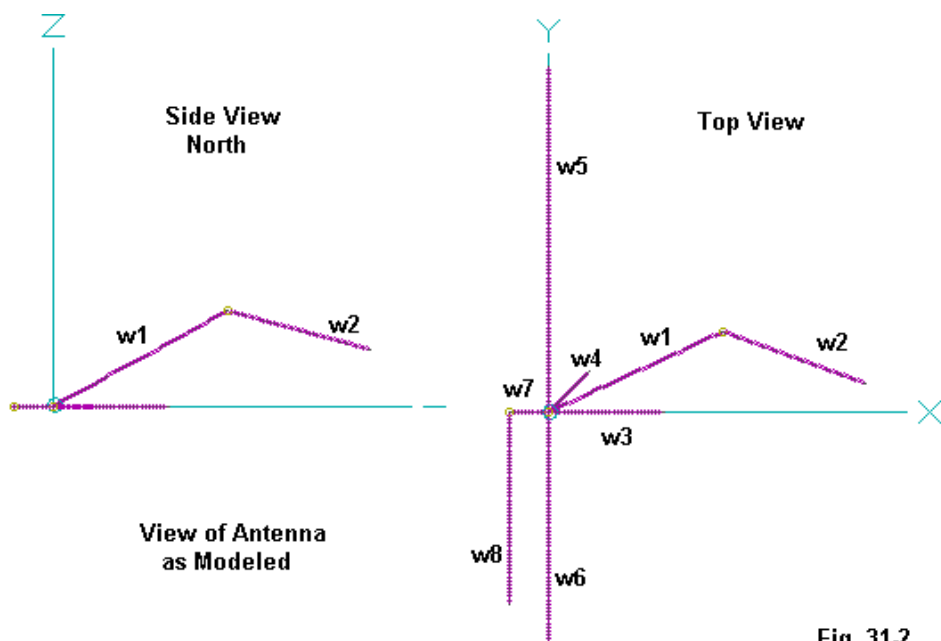


Fig. 31.2

The direction of each radial is an estimate based upon the original sketch. The two 60' radials have been arranged so that one is straight, while the other moves west for 10' and then south for the remaining 50'. This is as close to accurate as the sketch would permit.

In NEC modeling, longer wires are subdivided into segments to permit the accurate calculation of mutual impedances, currents, and other output data. The segmentation of wires that NEC-2 recommends is approximately 9-11 segments per half wavelength (with a minimum of about 5 per half wavelength) at the shortest wavelength used. At 28.5 MHz, a wavelength is about 34.5' long, and the radiator is

about 2.6 wavelengths long. Since the wire (#12) is thin, additional segmentation density is allowable and was used in the model to assure convergence, given the non-standard geometry of the assembly. A uniform segment length of 1' was used throughout the model. The result is a model using 345 segments.

The antenna source or feedpoint is the lowest segment of the radiator wire nearest the junction of the radials. This approximates the actual feed system, which employs an automated tuning system.

What the Model Suggests

Given the numerous approximations required to model the antenna, the modeling output data must be taken as suggestive and indicative, but not precise. The following table provides a summary of the data for 160 through 10 meters (with 80-75 sampled at 3.6 and 3.9 MHz). The TO angle is the elevation angle of maximum radiation. It is a function of taking an elevation pattern in the azimuth heading of strongest radiation. The maximum gain in dBi is the gain at this elevation angle and azimuth angle. There are three exceptions. On 80 and 40 meters, the TO angle exceeds all but NVIS use, and so an alternative angle of 50 degrees was also used to sample gain. Comparing the TO angle gain value with the arbitrary lower angle value gives some idea of the rate of gain decrease as the signal angle departs from the TO angle.

There are two azimuth headings. The first corresponds to the heading provided by EZNEC, which actually counts azimuth in “phi” angle terms, that is counterclockwise. The second heading presumes that the compass heading of North is straight up the page, in accord with the original sketch. Therefore, the heading is a compass bearing resulting from that assumption. Finally, the table provides a report of estimated feedpoint impedance. Given the assumptions of the model, the actual values of resistance and reactance may easily vary by 20% from the listed figures.

Frequency MHz	TO angle	Max. Gain dBi	EZNEC azimuth	Compass azimuth	Feedpoint Z (R +/- jX Ohms)
1.8	38	-6.7	169	281	25 - j 330
3.6	61 (50)	-3.0 (-3.1)	215	235	180 + j 510
3.9	63	-2.6	213	237	310 + j 760

	(50)	(-2.8)			
7.1	79	3.5	266	184	60 - j 180
	(50)	(2.8)			
10.1	53	3.0	48	42	2300 - j 790
14.1	44	3.1	314	136	245 + j 390
18.1	45	3.2	91	1	135 + j 70
21.1	40	4.5	343	107	470 - j 660
24.9	35	5.0	343	107	660 + j 590
28.5	32	4.0	346	104	220 + j 110

The table contains some interesting data patterns. First, only on 30 meters does the antenna system offer a feedpoint impedance that may challenge the capabilities (or efficiency) of an automatic tuner. Second, except on the lowest bands, the antenna offers a reasonably constant gain. However, tables do not tell the entire story and should be read in conjunction with relevant azimuth and elevation patterns for the antenna. The following patterns and commentary employ an azimuth pattern taken at the TO angle except for the three cases listed as exceptions in the table. The elevation patterns are taken at the azimuth heading of maximum gain, which may require the user to orient himself to see properly what those patterns show.

1.8 MHz: Fig. 31-3 supplies the patterns for this frequency. The solid line represents the total pattern. The blue line represents the horizontal component, and the red line represents the vertical component. At 160 meters, note that the vertical component dominates the total pattern. Maximum radiation is in the direction opposite the length of the wire, that is, toward the west, using the conventions set forth earlier. A gain figure of -6.7 dBi seems low, but only about 2 S-units below the value that might emerge from a dipole that was set at least 1/2 wavelength above the ground. Because lower frequency RF penetrates the ground more deeply, and the ground is often stratified, the effects of the modeled ground may vary from those of real ground.

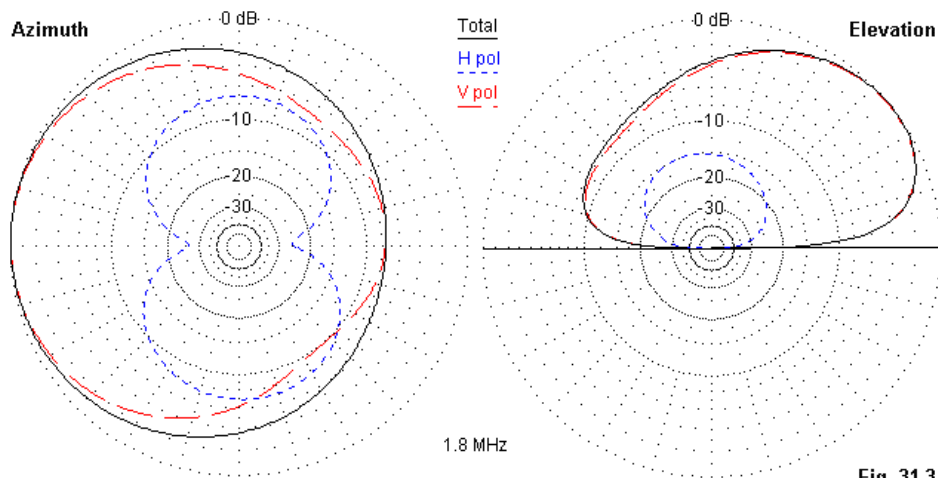


Fig. 31.3

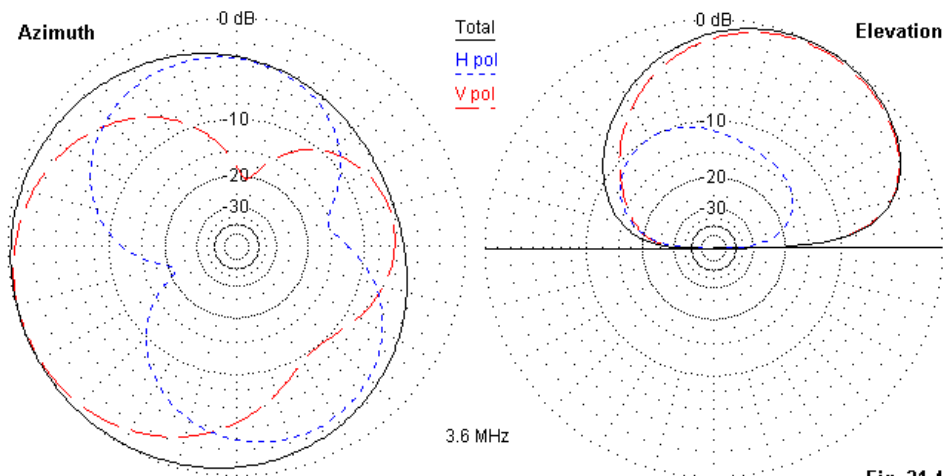


Fig. 31.4

3.6 MHz: In Fig. 31-4 we find azimuth and elevation patterns for 80 meters. The strengthening of the horizontal component broadside to the wire (but weakly along the length of the wire) tends to circularize the overall pattern. There is much high-

angle radiation, but note in the elevation pattern the slow rate of decrease with the lowering of the elevation angle. Hence, performance at lower angles is likely to be consistent with higher angle performance.

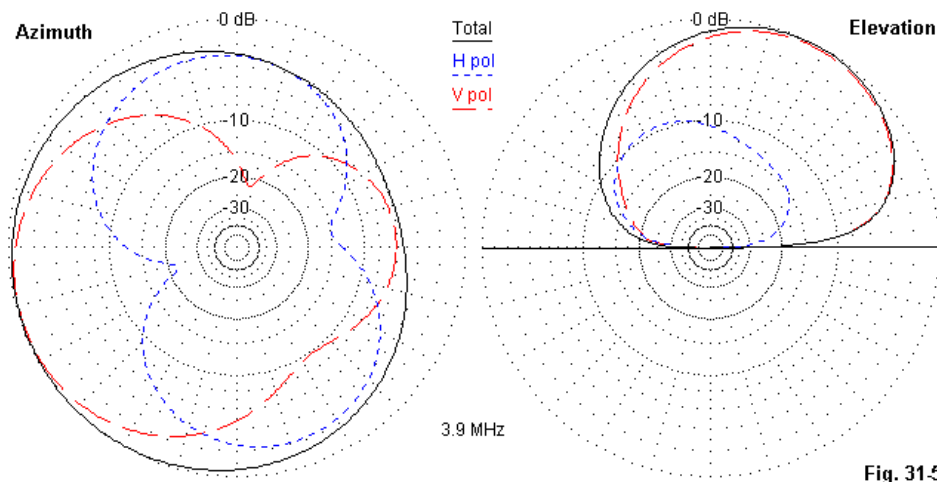


Fig. 31-5

3.9 MHz: The similarity of the patterns in **Fig. 31-5** to those in **Fig. 31-4** suggests that only small changes in performance occur across the span from 80 to 75 meters. There is actually a slight gain decrease that results from the fact that the antenna is in a transition from dominance by the vertical component to dominance by the horizontal component. However, the wire is very low for a horizontal wire at this frequency, resulting in a higher TO angle.

7.1 MHz: On 40 meters, as shown in **Fig. 31-6**, the antenna begins to perform somewhat like an end-fed $1/2$ wavelength wire, and the length is actually less than $3/4$ wavelength. The proximity to the earth yields a high TO angle, but the increasingly dominant horizontal component yields a pattern roughly broadside to the bent wire radiator, favoring North-South paths (given the initial conventions of the study).

The near $3/4$ wavelength of the radiator yields a feedpoint impedance against the ground plane that has an expected low resistive component.

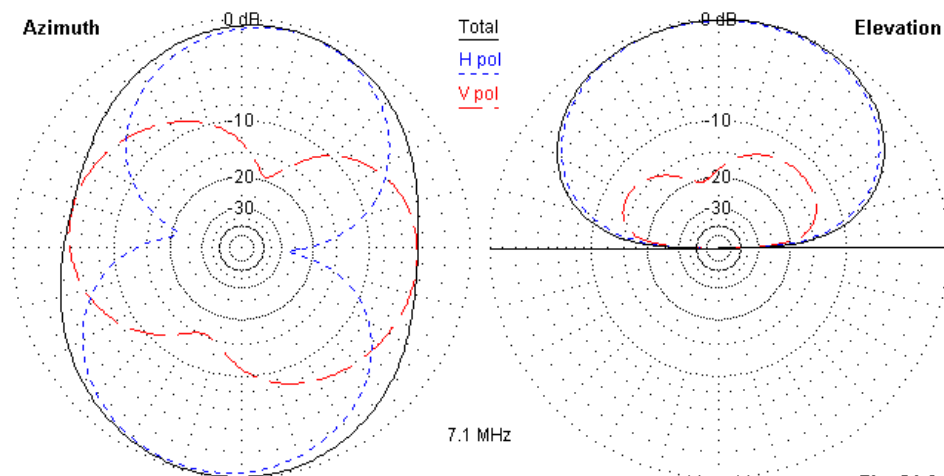


Fig. 31.6

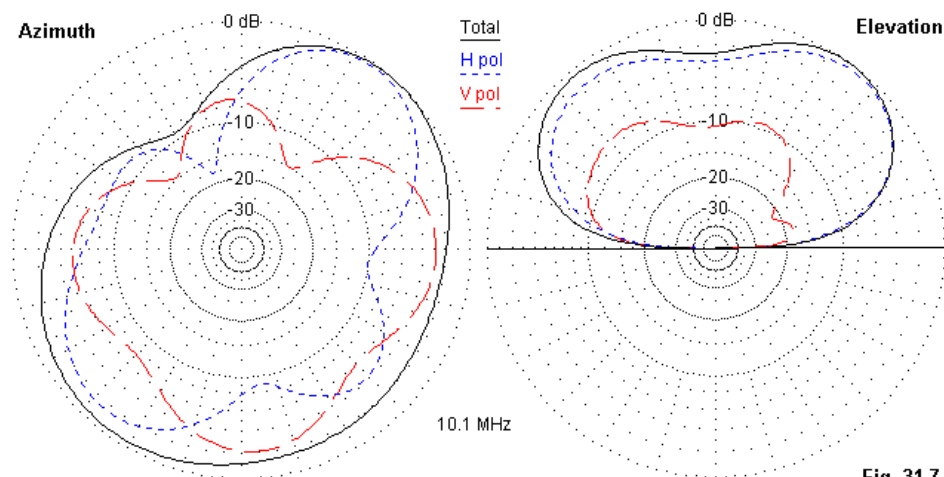


Fig. 31.7

10.1 MHz: On 30 meters (**Fig. 31-7**), the radiator is nearly 1/2 wavelength long, and like end-fed half-wavelength antennas in general shows a high impedance. The pattern is a curious mix of horizontal and vertical component elements, with the horizontal component becoming increasingly dominant. However, both the wire slant and bend combine to give the antenna a NE-SW orientation. Drawing a line across the azimuth pattern on this axis will yield the elevation pattern.

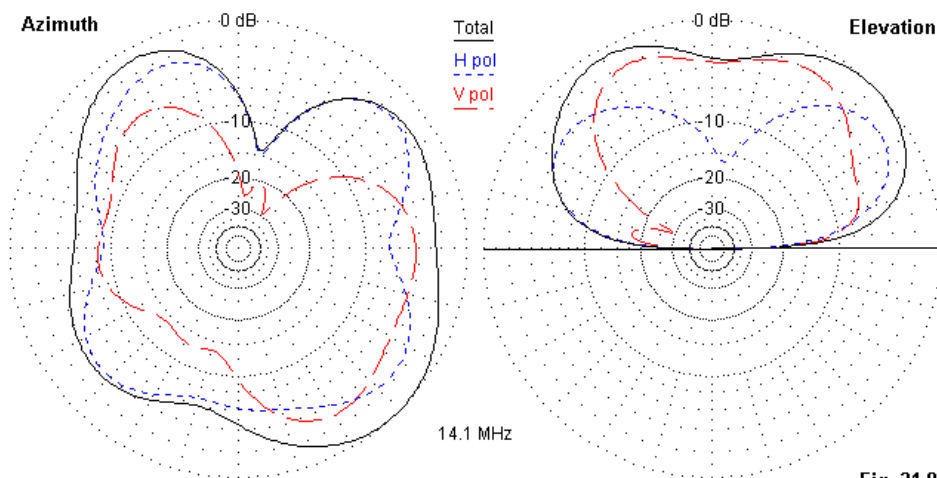


Fig. 31-8

14.1 MHz: **Fig. 31-8** is the beginning of two phenomena of note. One is the final domination of the horizontal component of the total pattern. The other is the development of multiple lobes. Since the antenna is now about 1.5 wavelengths long, additional lobe structures are to be expected. However, the slope and bend of the antenna yield fewer deep nulls than a pure horizontal doublet. Fewer deep nulls also tend to be accompanied by less strong major lobes. Hence, the pattern is nearly omni-directional, but at a modest gain level.

18.1 MHz: The lobe structure becomes more apparent in **Fig. 31-9** for the 17-meter band. This band also shows a danger in reading only tabular data. The stron-

gest lobe is nearly due north. However, that lobe is fairly narrow. Almost as strong is the very broad lobe to the southeast, which is likely to yield more impressive coverage in actual operation. (This note, of course, does not take into consideration the potential effects of terrain and surrounding structures.)

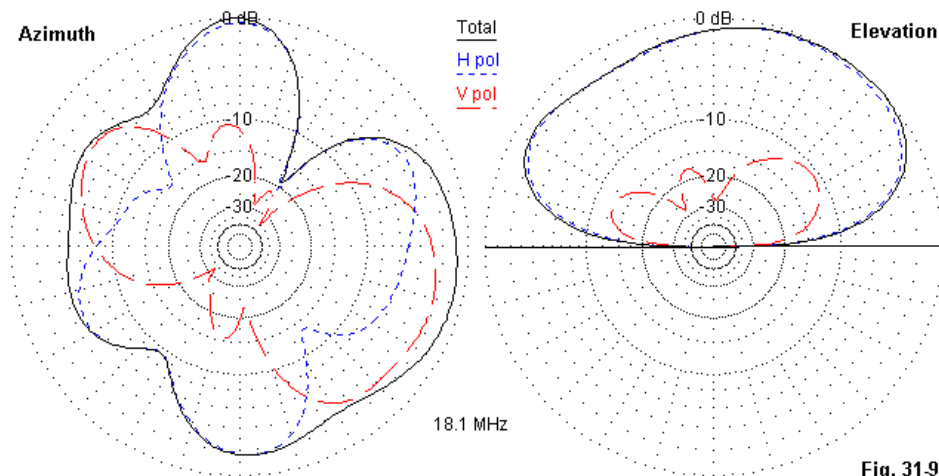
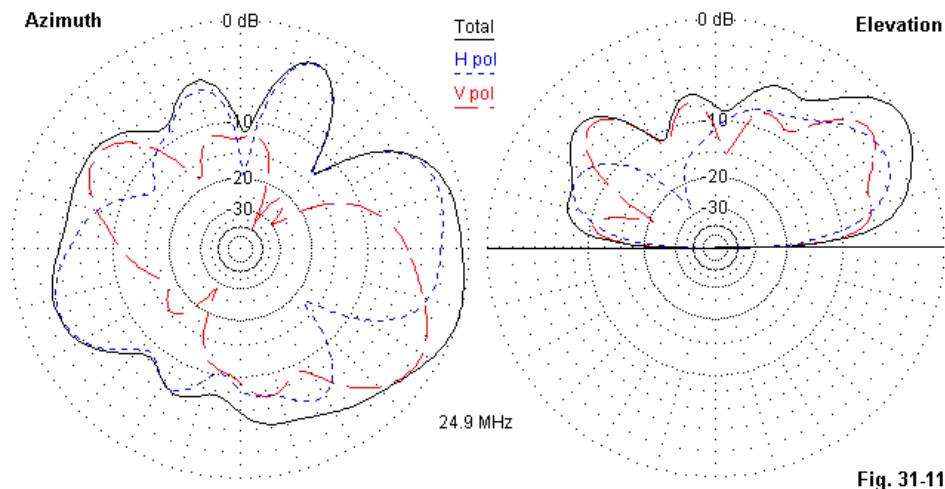
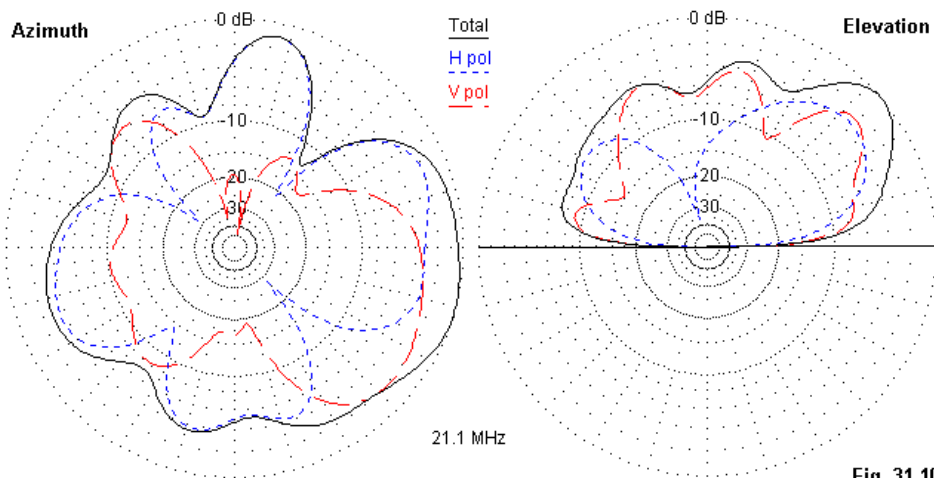


Fig. 31.9

21.1 MHz: The 15-meter patterns in **Fig. 31-10** reveal the continued evolution of lobe and null structures as the antenna becomes longer as a function of the wavelength in use. The low height of the antenna, relative to the dominance of the horizontal component, yields a fairly high TO angle. However, as the elevation pattern shows, the rate of gain decrease with a lower angle is slow, and there remains usable gain to quite low elevation angles.

24.9 MHz: Once more the patterns in **Fig. 31-11** show further development of lobes and nulls. However, overall, the patterns for 15 and 12 meters are very reasonably coincident. This fact permits one to anticipate strong and weak paths from one band to the next. As the frequency continues to increase, the antenna shows a distinct east-west orientation of major lobes.



28.5 MHz: The 10-meter patterns in **Fig. 31-12** are simply more complexly wrinkled versions of those for 15 and 12 meters. The east-west orientation—along the length of the radiator—dominates, but without many deep nulls away from the main lobes.

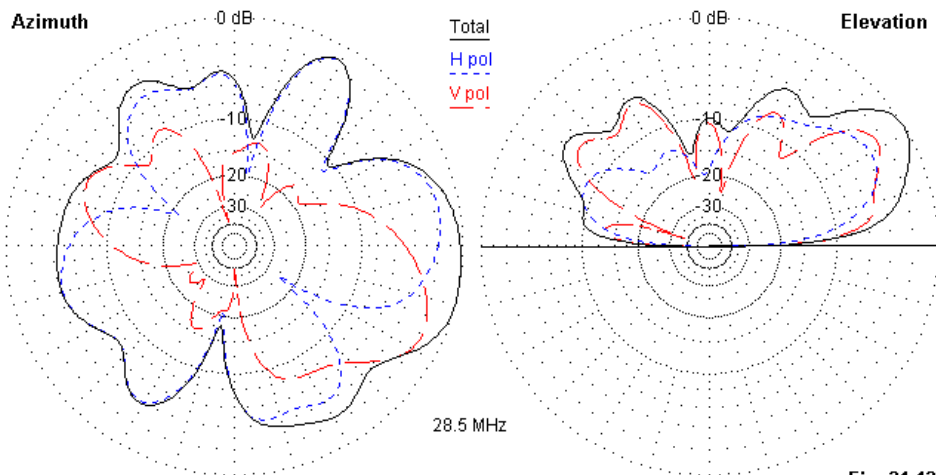


Fig. 31-12

Of What Use Is the Analysis?

The modeled analysis of the antenna provides a generalized picture of how the antenna is likely to perform, once the data is adjusted for terrain and other interfering factors. It also shows the evolution of the antenna's patterns with increasing frequency. The end result is something like this: the antenna provides modest gain and performance potential within the matching abilities of an automated tuner on virtually all of the amateur bands from 160 through 10 meters—with only the impedance on 30 meters being potentially problematical.

The model is also useful when placed in conjunction with other models of possible system alterations or improvements. For example, suppose one were to erect

a wooden vertical support at the shed, perhaps 30' tall. Would such a structure yield a better or worse antenna? One option would be to run the initial length of the wire up the support and then over to the trees. However, one might limit the total length to 90' or one might use about 120' of wire in the radiator. Determining which of these options, if either one, offers better performance than the current radiator would be indicated (but not guaranteed) by modeling the options.

Another potential change in the system would be the addition of either more or longer radials—or both. Just how much, if any, improvement one might garner from an improved radial field can be loosely estimated from modeling various possibilities in this area.

Besides measuring alterations to the present antenna system, one might also use the analysis of the current antenna as a baseline for considering other antenna types. In large measure (but not absolutely), comparisons among antenna types and configurations equally affected by local terrain and ground clutter will remain valid.

Nonetheless, in using the numbers and patterns that have emerged from the analysis, one must be mindful of the limitations outlined early in the report. Terrain and secondary structures not accounted for, and there are numerous approximations in the model. Consequently, the model is best used for the trends it shows and not for the absolute values of the output numbers. However, even in a more modest role, the analysis is both useful in itself and potentially useful when contemplating system alterations.

* * * * *

Model included: 31-1. (.NEC and .NWP model dimensions in meters; .EZ model dimensions in feet.)



32. A Case Study: Rotating a Beam

Another request for assistance yielded a case with some interesting possibilities for modeling by equation. It involves a common situation: two stacked beams. The problem arose when the individual noted that one of the beams would be fixed in position. The other would rotate. What would be the effect, if any, on the patterns when the beams were not in alignment? To answer this question, he was faced with the prospect of remodeling the rotating beam every time he wished to check another angle of divergence between the two.

There is a solution to this problem, and its form depends on the software in use. The solution can be applied to a spreadsheet or other calculating program, with the new rotating beam coordinates used to create a new model. If the software has a “modeling by equation” facility, the solution can be plugged into the software and the process of remodeling automated.

The following notes will step through the problem—very likely in too much detail for some and too little detail for others. However, it will indicate what a modeler can do to rotate one antenna relative to another.

Step 1: Simplify the design details.

Well-designed horizontal arrays for the HF spectrum use tapered element schedules for each wire. Although the solution to be shown can be applied to every element step, that process introduces needless tedium into the process. So the first step is to simplify the beam design so that it uses uniform diameter wires for each element.

NEC-2 programs, such as NEC-Win Plus and EZNEC for Windows provide Leeson corrections for calculating the properties of arrays with linear elements having symmetrical stepped diameter structures. The correction produces equivalent elements having a uniform diameter. Since these substitute elements form the basis of calculation, the user should access the dimensions of these elements and use them for the project ahead.

Step 2: Center the beam on the boom.

Once we have a beam with uniform diameter elements, we should then place the beam mounting position at coordinates 0,0. There are numerous conventions used by modelers to develop antennas. Some place the reflector either at $Y=0$ or at $X=0$, so that all distances along the boom are cumulatively positive. Other modelers use a plus-minus system, so that the extreme elements are at the same distance from zero—whether or not the mid-point along the boom is the mounting point.

Fig. 32-1

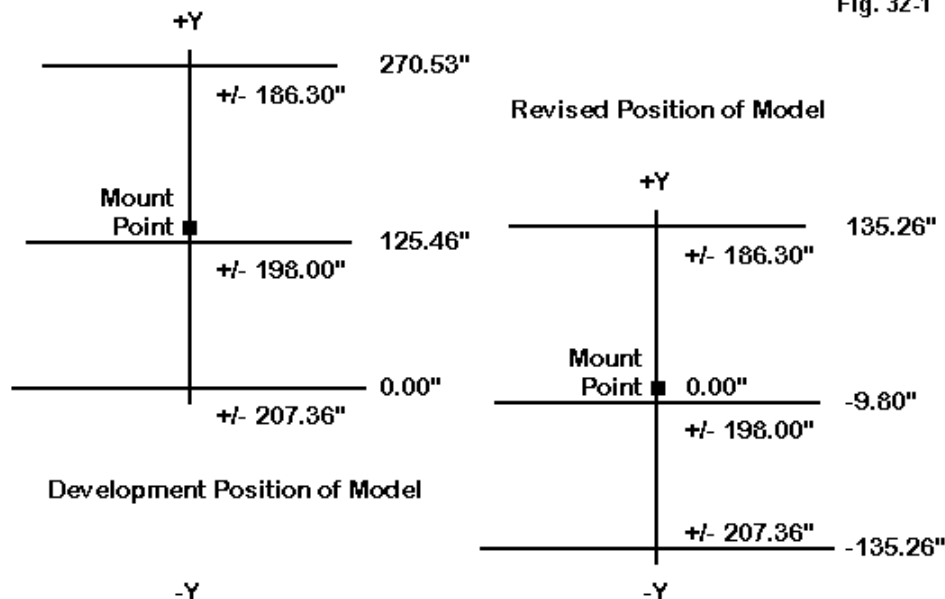


Fig. 32-1 shows a model transformed from the first convention to the second. The second convention is closer to the desired goal of having 0,0 represent the mounting position. In the absence of a precise location of the true mounting point,

the second convention can be used without introducing significant error into the resulting modeling tests.

Fig. 32-1 also shows the dimensions of the beam that we shall use as our running example. It is a 3-element 20-meter Yagi with 1" diameter elements. One of the merits of the model is that none of the elements will fall at 0,0 in our transformation of position.

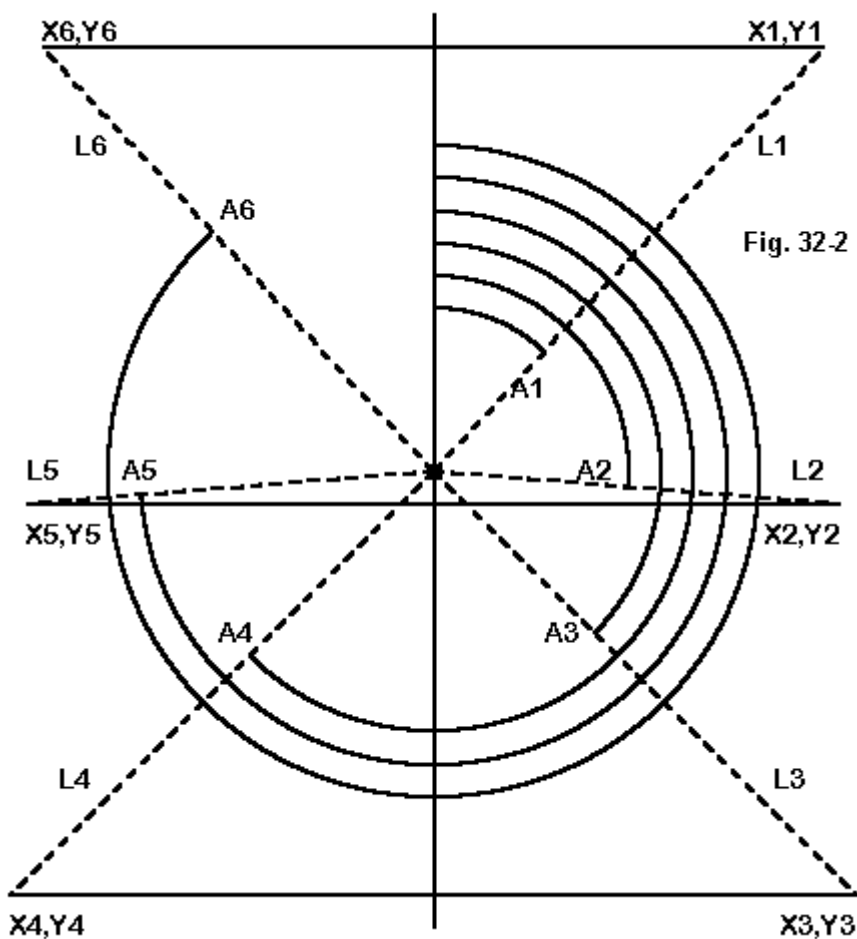
Step 3: Rethink the coordinates of the element ends.

We normally think of a beam as a set of linear elements with end coordinates. For the moment, we need think only of the end coordinates and ignore the wire between them. What we shall develop is a method of accurately producing end coordinates for any angular position of the beam. Then, by placing those coordinates in the correct places in the modeling wires table, a correctly dimensioned beam will result—pointed just where we desire.

Fig. 32-2 holds the key to rethinking the coordinates. From the mounting position (0,0), let each coordinate set (6 of them in this case) be a function of a (dotted) line of length L with an angle A relative to the initial boom axis. Note that we are using angles from 0 to 360 degrees. More accurately, we shall be using angles from 0 to 2PI radians, since most spreadsheets know angles only in terms of radians. However, we can always convert an angular measure in degrees to one in radians (or back again) by the conversion equations

$$A_{\text{radians}} = \frac{A_{\text{degrees}} \pi}{180} \quad A_{\text{degrees}} = \frac{180 A_{\text{radians}}}{\pi} \quad (1)$$

where PI is carried to as many decimal places as you can stand.



Step 4: Calculate L1-Ln and A1-An

We may calculate the length of each radial (L1 through Ln) and angle (A1 through An) from the existing coordinates of our model that is centered on the mounting point. The necessary equations are basic trig:

$$L_n = \sqrt{X_n^2 + Y_n^2} \quad A_n = \arctan \frac{X_n}{Y_n} \quad (2)$$

where X and Y are the coordinates for any of the point, A is the angle relative to the axis of reference, and L is the length of the radial from the mounting point (0,0). For the beam we are using as our example, we derive the following table for the 6 points. Since you may be using a hand calculator, use whatever shortcuts you know that are allowed by trig to place the angles in the proper quadrant.

Coordinate Identification	Ln (")	An (degrees)	An (radians)
Director End 1 (1)	230.2	54.0	0.943
Director End 2 (6)	230.2	306.0	5.340
Driver End 1 (2)	198.2	92.8	1.620
Driver End 2 (5)	198.2	267.2	4.663
Reflector End 1 (3)	247.6	123.1	2.149
Reflector End 2 (4)	247.6	236.9	4.134

For a given beam design, the lengths in the L_n column will remain constant.

Step 5: Calculate coordinates for a new angle.

To rotate the beam—in a clockwise fashion—we need only add to each angle the number of degrees (or radians) of rotation and then recalculate the coordinates. From the length of the radial and the angle, we may calculate the coordinates with equally basic trig equations:

$$X_n = \sin A'_n \cdot L_n \quad Y_n = \cos A'_n \cdot L_n \quad (3)$$

where A' is the new angle resulting from the rotation.

Let's rotate our beam by 20 degrees and look at the new coordinates for the elements. 20 degrees is 0.349 radians. So we may simply increase the angles in the table above by this amount.

Coordinate Identification	A_n (radians)	X_n	Y_n
Director End 1 (1)	1.292	221.3	63.4
Director End 2 (6)	5.689	-128.8	190.8
Driver End 1 (2)	1.970	182.7	- 76.9
Driver End 2 (5)	5.012	-189.4	58.5
Reflector End 1 (3)	2.499	148.4	-198.1
Reflector End 2 (4)	4.483	-241.1	- 56.4

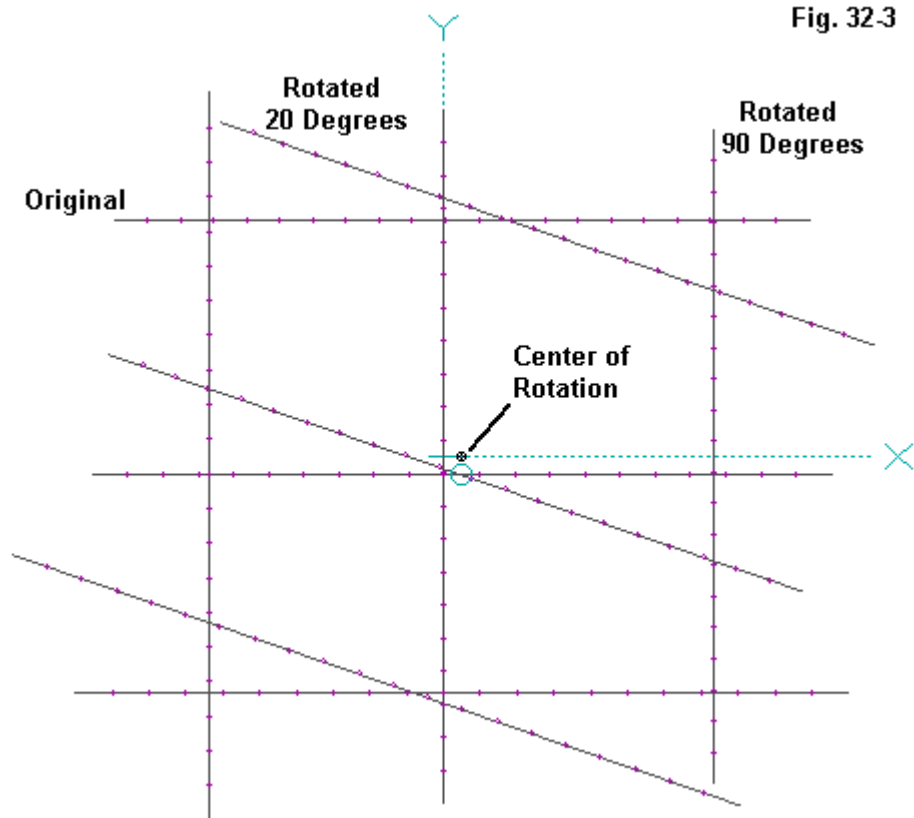
If we rotate the beam another 70 degrees, we shall end up with a total 90-degree or 1.571-radian rotation. In this case, our dimensions will become those in the following table.

Coordinate Identification	A_n (radians)	X_n	Y_n
Director End 1 (1)	2.514	135.2	-186.3
Director End 2 (6)	6.911	135.2	186.3
Driver End 1 (2)	3.191	- 9.8	-198.0
Driver End 2 (5)	6.235	- 9.8	198.0
Reflector End 1 (3)	3.720	-135.2	-207.4
Reflector End 2 (4)	5.706	-135.2	-207.4

In other words, the antenna has its original dimensions, with the X- and Y-axes transposed.

Fig. 32-3 shows a top view of the three antennas: the original, with 20-degrees rotation, and with 90-degrees rotation to verify that the results indeed rotate around a common mounting point.

Fig. 32-3



Step 6: Automate the model.

Although we can use the basic trig equations and our reformulation of the model coordinates to create new models for any orientation about the mounting point, systematic modeling of a rotating beam can be much simplified. However, the requirement is a software package with a “model-by-equation” facility, such as NEC-Win Plus. We may simply plug our design data and equations into the equations and wires pages of the built-in spreadsheet.

The screenshot shows the NEC-Win Plus+ software window with the title bar "NEC-Win Plus+ [yagirot.nwp]". The menu bar includes File, Edit, Configure, Commands, and Help. The toolbar contains various icons for file operations and simulation. The main interface is divided into several panels:

- Frequency (MHz):** Start: 14.175, End: 14.175, Step Size: 1.
- Ground:** No Ground (dropdown menu).
- Radiation Patterns:** 0° < Az < 359°, El = 1°, Step = 1°; 0° < El < 180°, Az = 0°, Step = 1°.
- Geometry:** Includes icons for rotation and a checkbox for "Stepped" (checked).
- Zo:** 26.26 Ohm.

Below these panels is a spreadsheet titled "Rotation Equations" (Fig. 32.4). The spreadsheet has columns A through H and rows 2 through 14. The data is as follows:

	A	B	C	D	E	F	G	H
2	F =	14.175	Primary Frequency (MHz)	=230.22606	L1/6	=(F3*PI()/180)	deg-rad	
3	W =	=299.8/B2/Model P	"Wavelength(" & Model Params \$B\$5 & "	=198.24257	L2/5	=20	rotation de	
4	A =	=D5+F2	Dir X1/Y1	=247.57511	L3/4			
5	B =	=D6+F2	Dir X2/Y2	=0.9427971	A1			
6	C =	=D7+F2	Driver X1/Y1	=5.3403882	A6			
7	D =	=D8+F2	Driver Xi/Y1	=1.6202509	A2			
8	E =	=D9+F2	Refl X1/Y1	=4.6629344	A5			
9	G =	=D10+F2	Refl X1/Y1	=2.1495876	A3			
10	H =	=D2	Dir length	=4.1335977	A4			
11	I =	=D3	Driver length					
12	J =	=D4	Refl length					
13								
14								

The bottom of the window shows tabs for Wires, Equations, NEC Code, and Model Params.

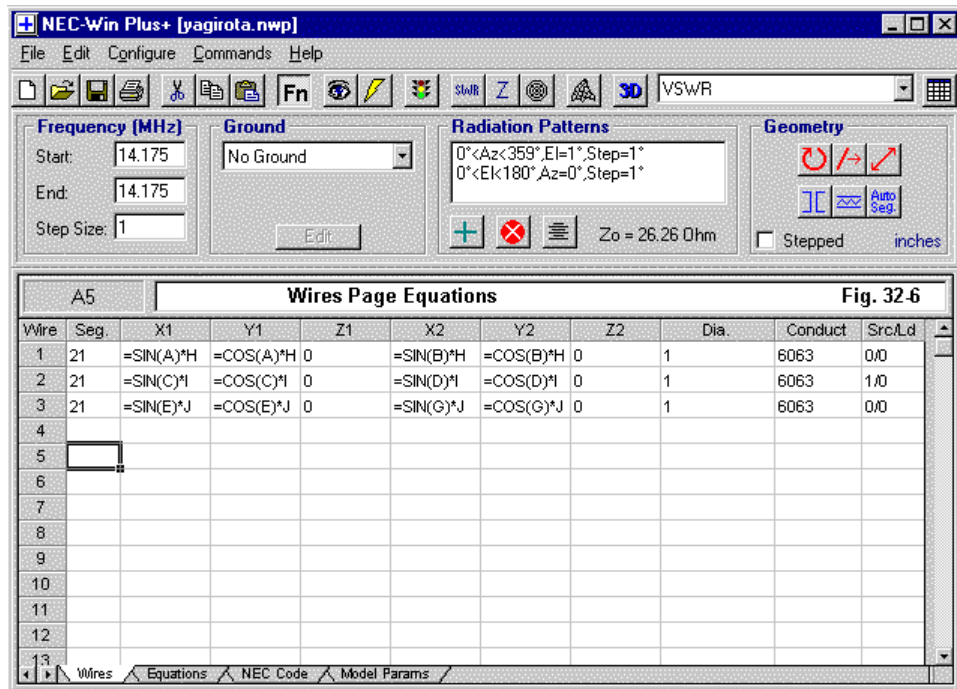
Fig. 32-4 illustrates the initial stage of the project. Column D becomes a reference column for the design's radial lengths and the angles from 0 to 360 degrees, but given in radians, the calculating basis for spreadsheets. Column E identifies each of the D-entries in terms of the designations in the figures we have used so far. Column F contains 2 entries: a converter for changing entries in degrees to radians and a place (F3) to enter the rotation of the Yagi from its initial setting. Since most of us are accustomed to thinking in terms of degrees, the entry is in those terms.

Column B provides values for the pre-assigned variables A-J. A-G simply add the design angles to the additional rotation angle. H-J repeat the radial lengths as a matter of convenience.

Rotation Equation Values						Fig. 32.5
	A	B	C	D	E	F
2	F =	14.175	Primary Frequency (MHz)	230.22606	L1/6	0.3490659
3	W =	832.6736936	Wavelength(inches) = c / f	198.24257	L2/5	20 rotation deg
4	A =	1.29186295	Dir X1/Y1	247.57511	L3/4	
5	B =	5.68945405	Dir X2/Y2	0.9427971	A1	
6	C =	1.96931675	Driver X1/Y1	5.3403882	A6	
7	D =	5.01200025	Driver Xi/Y1	1.6202509	A2	
8	E =	2.49865345	Refl X1/Y1	4.6629344	A5	
9	G =	4.48266355	Refl X1/Y1	2.1495876	A3	
10	H =	230.22606	Dir length	4.1335977	A4	
11	I =	198.24257	Driver length			
12	J =	247.57511	Refl length			
13						
14						

The page shows an entry of 20 degrees as the rotation of the basic 3-element Yagi. The Equations Values page, in **Fig. 32-5**, shows the calculated values for each of the adjusted angles, in column B. You can compare these values to those in one of the tables shown earlier. See model 32-1.

We did not calculate the coordinates on the equations page, since we may do that on the Wires page through equations (**Fig. 32-6**). All X values will involve a sine, while all Y values require a cosine. H, I, and J are the appropriate radial lengths used to determine the values of the coordinates.



The values yielded by the equations—both those on the equations page and those on the wires page—appear in **Fig. 32-7**. Since we are working with a free space model, Z is zero. However, for a real problem involving stacked beams—one of which is fixed, Z would take a positive value. In fact, one may add further lines to this model to create the fixed beam using numerical values throughout—since it is a constant. Then, simply by placing a new value in degrees in F3 on the equations page, one can rotate the movable beam to find the pattern consequences of this form of stacking.

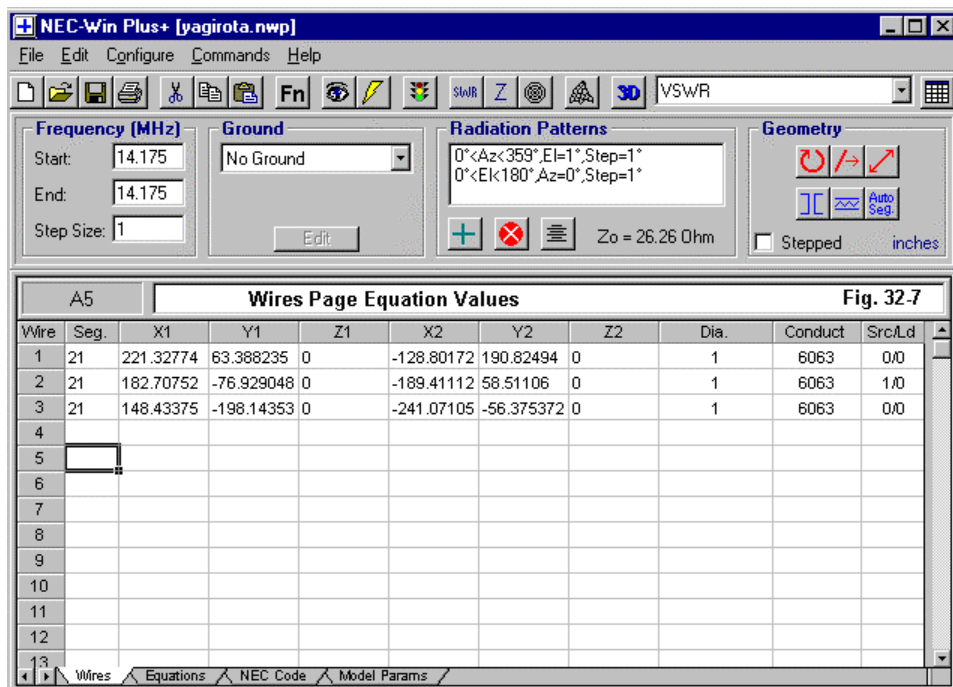


Fig. 32-8 shows the pattern of the rotating beam when moved 20 degrees from its initial orientation. The pattern values (gain and front-to-back ratio) plus the impedance data make a quick check on whether we have formulated our equations correctly.

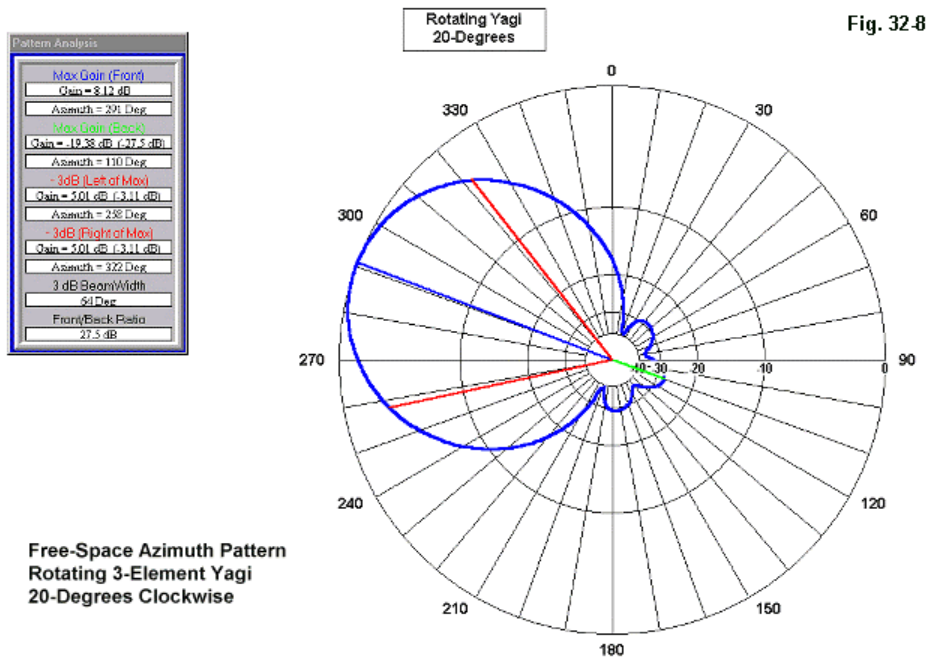
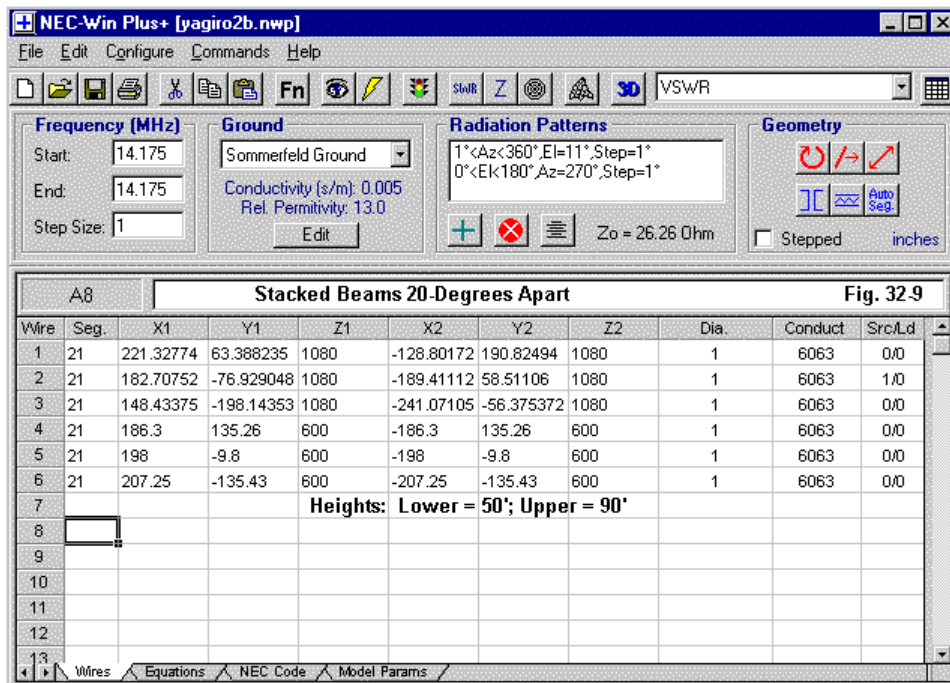


Fig. 32-8

Putting the rotating beam to use involves simply assigning a set of ground conditions and adding the fixed beam. **Fig. 32-9** shows the wires page for a sample situation. An identical beam to the rotating one has been added in lines 4-6. It has been left inert, on the premise that the upper rotating beam will be active alone when it is not aligned with the lower beam. Of course, the modeler is certainly free to

change this premise, as well as the 50- and 90-foot heights assigned to the beams. See model 32-2.

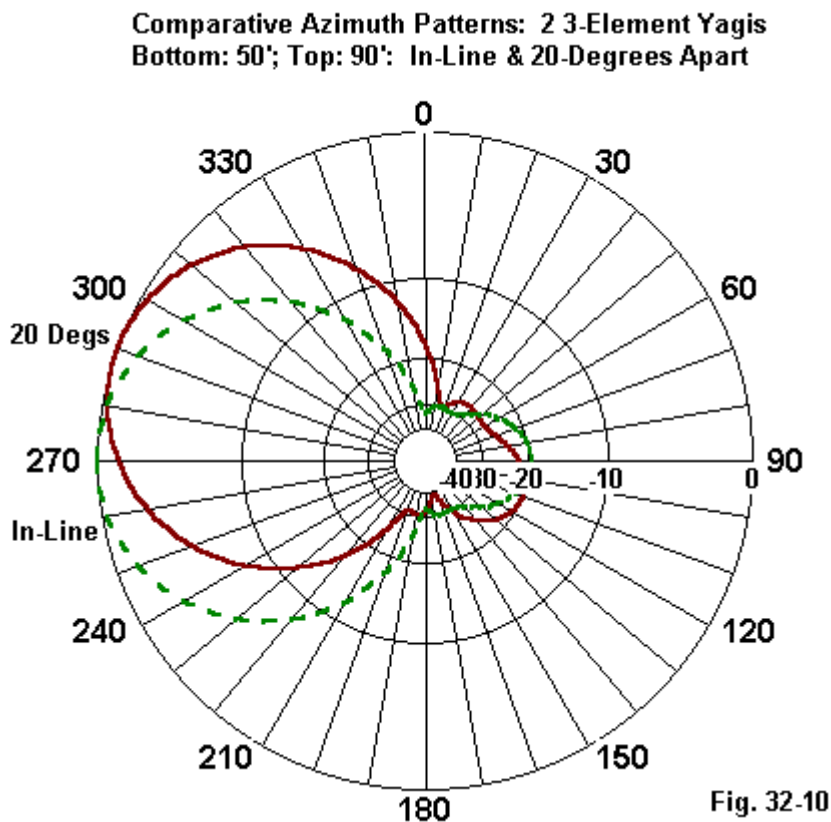
In fact, it may be well for a modeler to investigate what happens within a site-specific model when the fixed beam driver is either closed or open at the feed point. The condition in the model is closed when no source is assigned to the driver wire. To open the driver, insert a very high resistive load (1E10) at the normal feed position on the wire.



For our simple sample, the inert lower driver is closed. **Fig. 32-10** combines azimuth patterns for the active upper antenna when in line with the lower antenna and when 20 degrees off clockwise. Nothing radical happens in this case. The gain differential is insignificant, as is the front-to-back ratio. However, as the figure reveals, there is some small distortion of the rear pattern as the antenna departs from

the in-line condition. The source impedance shows a 2-Ohm change in reactance for this situation relative to the impedance of the upper antenna in isolation.

There is no requirement that the two beams in the stack be identical. In fact, one can combine beams of many sorts simply by cutting and pasting entry lines. However, it is wise to ensure that the various beams in the stack use segments of roughly equal lengths to ensure that there are enough segments per half wavelength at the highest frequency tested.



Although deriving and entering the equations needed to create a rotating beam takes three times as long as entering a single model, the net time saved will be considerable. If we take readings every 10 degrees, for example, the equations can save us about 80% of the time required to introduce individual models for each step of the way. The more complex the individual antenna models, the more time saved by the use of equations.

Sometimes it is worth the effort to develop some models by equation.

An Alternative Procedure

The procedure that we have examined for rotating a model antenna allows the modeler to rotate one or more antennas from within the model. The user specifies by a rotation entry on the equations page the amount of rotation for each covered structure. For many purposes, this procedure may be overly complex. A number of current NEC-2 programs offer other means of rotation.

NEC-Win Plus has a rotation control on its main page. Use the mouse to block out the lines of the antenna structure to be rotated. Next, click on the rotation control to open a dialog box. In the box, select the axis of rotation, the amount of rotation, and the direction of rotation (clockwise or counterclockwise). The box shows the resulting coordinates of the first wire in the group as a check on the selections before implementing them. Not until approval and departure from the dialogue box do the coordinates resulting from the rotation go into effect.

When using this method of rotation, you must save the altered file under a new file name if you wish to preserve both the original model and the revised model.

EZNEC has a similar facility that appears among the wires-page options. With the wires page open, select the “Rotate Wire” dialog box. The dialog calls for you to indicate the first and last wires of the group to be rotated. Then select the rotation angle, direction, and axis. Upon approval, the selected wires have new coordinates reflecting the rotation selections. As with NEC-Win Plus, you must save the file under a new name to preserve it while leaving the original model unaffected.

In both programs, the initial model must be set up so that the center of rotation is at $X=0$ and $Y=0$. Otherwise, rotating the models will result in a distortion to the relative antenna positions.

The rotation controls do simplify one special operation. In many VHF and UHF applications, you may wish to analyze the potential antenna performance with the antenna horizontal and with it vertical. Without a rotation facility, you must rewrite the model, transferring the side-to-side dimensions from their original axis (either X or Y, depending upon modeling habits or conventions) to the Z-axis. If the antenna boom is a certain height above ground, you must add the height to the element end coordinates before entering them in the Z-axis column.

The availability of a rotation facility simplifies the process immensely. If the beam's boom is aligned along one axis, then you only need to rotate the antenna around that axis by 90 degrees to go from horizontal to vertical (or vice versa). The position of the antenna along its boom axis does not matter in this case. Of course, you will want to save as separate model files both the horizontal and the vertical versions of the model.

You may also rotate the beam along the axis that crosses the boom. This action is useful if you wish to check for changes in performance with slight tilts. It is also useful for understanding the antenna patterns that emerge when pointing an array directly at an elevated target, such as the moon or a satellite position.

* * * * *

Models included: 32-1 through 32-2. (Due to the nature of the models, they are available only in the .NWP format.)



33. A Clean Sweep

It would not be uncommon to find an antenna advertisement of the following sort: 2-element antenna—peak gain 6.8 dBi free space, peak front-to-back ratio >32 dB, SWR >1.1:1 at design frequency. Such notices are common and have carried over into casual modeling practices. We design an antenna for a single frequency, even if we intend to use across a span of frequencies, for example, one of the amateur bands. So perhaps a short exercise in the utility of performing frequency sweeps might not be out of place.

NEC cores (both -2 and -4) are set up for frequency sweeping, although the core set-up and common commercial program set-ups will look different. The basic FR (frequency) input line or “card” looks something like this:

FR	0	5	0	0	24.90	0.05
Type of Stepping	No. of FQs				Start FQ	Increment

The Type of Stepping can be zero for normal linear stepping. If the entry is a “1”, then the stepping is multiplicative. The next entry lists the number of frequency steps in the sweep. Either a 1 or a 0 in the entry gives a single frequency output. Following two inactive “zero” entries, we come to the sweep start frequency in MHz. The final entry is the increment between steps.

In the example, the model would have produced output data for 24.90, 24.95, 25.00, 25.05, and 25.10 MHz.

The most commonly used NEC-2 programs, NEC-Win Plus (NW+) and EZNEC for Windows (EZW) use the same variant input system for performing a frequency sweep.

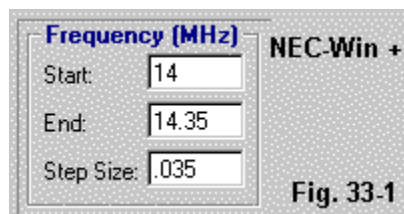


Fig. 33-1

Fig. 33-1 shows the NW+ upper-left-corner frequency-entry portion of the main screen. Instead of inputting a start frequency, the number of steps, and the increments, we put in start and stop frequencies as well as the increment. If the increment or “Step Size” creates a frequency value higher than the “end” frequency, the nearest lower frequency in the sequence is the upper limit for the sweep. The program translates the user input into the data needed for the FR card.

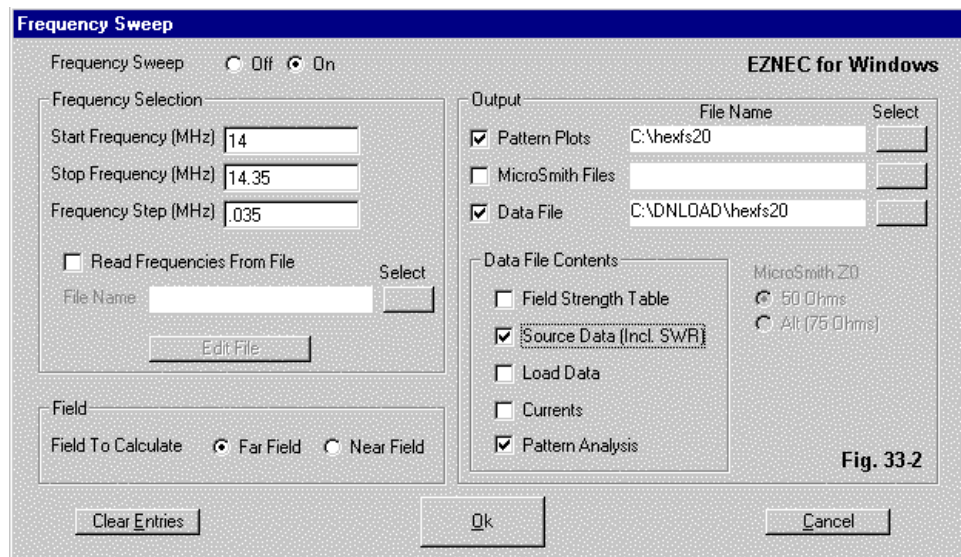


Fig. 33-2

EZW's window is more complex, but the frequency selection process is identical to that of NW+, as shown in the left portion of **Fig. 33-2**. (The remainder of the frequency sweep box represents a difference in software design philosophies of the two packages. NW+ produces output data for every frequency of a sweep from 1 to n steps. The user can then print or save the data he may need. EZW normally operates in a single frequency mode, with a frequency sweep called up as a special function. Hence, sweep output data is selected by the user and placed into special files. Both systems work equally well in yielding sweep data.)

Frequency sweeps yield data at regular frequency intervals. Very often, it is useful to transfer this data to a spreadsheet with graphing capabilities, since the data of interest can exceed the internal graphing capabilities of NEC programs. I routinely transfer the entire data set to a spreadsheet such as EXCEL, Quattro Pro, or Lotus. (The graphs in this column are from Quattro Pro, although almost all spreadsheets have quite adequate graphing capabilities. There is also a program called EZPlots, a special Excel application that reads EZW sweep files and graphs the results according to user specification of data. A single graph will handle up to 4 lines.)

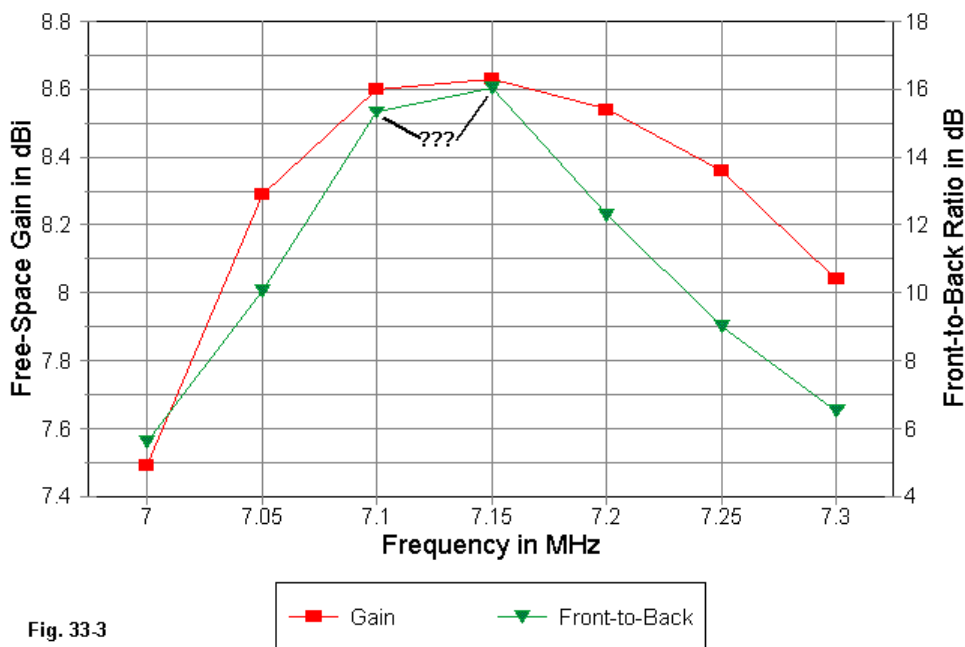
Sweeps and “Mini-Sweeps”

Usual practice tends to call for the use of frequency increments that end in zero or five. For most of the wider HF amateur bands, the start frequency is usually an integer, which makes the practice seem natural.

Consider a 40-meter 3-element quad array. We might generate a frequency sweep to determine the antenna's potential across the band from 7.0 to 7.3 MHz in 0.05 MHz increments. If we combine gain and front-to-back curves, the results might look something like **Fig. 33-3**. Model 33-1 is an approximation of the one used to generate the graph.

There is useful data in this graph. Note the smooth gain curve. The absence of corner squaring suggests that it is an adequate representation of the gain across the band, ranging from 7.5 dBi free space gain at the low end of the band to a little over 8.0 dBi at the upper band edge, with a peak at mid-band. Curve smoothness suggests that interpolated values will be close to those we might find in a model output file for any intermediate frequency along the way.

3-Element 40-Meter Quad Beam Free-Space Gain & Front-to-Back Ratio



The front-to-back curve presents an interpretive problem. Many quad designs, but certainly not all of them, show a very sharp and narrow-band front-to-back peak. The graphed values for 7.1 and 7.15 MHz suggest that there might be a peak somewhere between them. The only way to know for certain is to run a “mini-sweep” between 7.1 and 7.15 MHz, perhaps in 0.005 MHz increments.

3-Element 40-Meter Quad Beam Mini-Sweep: Gain & Front-to-Back Ratio

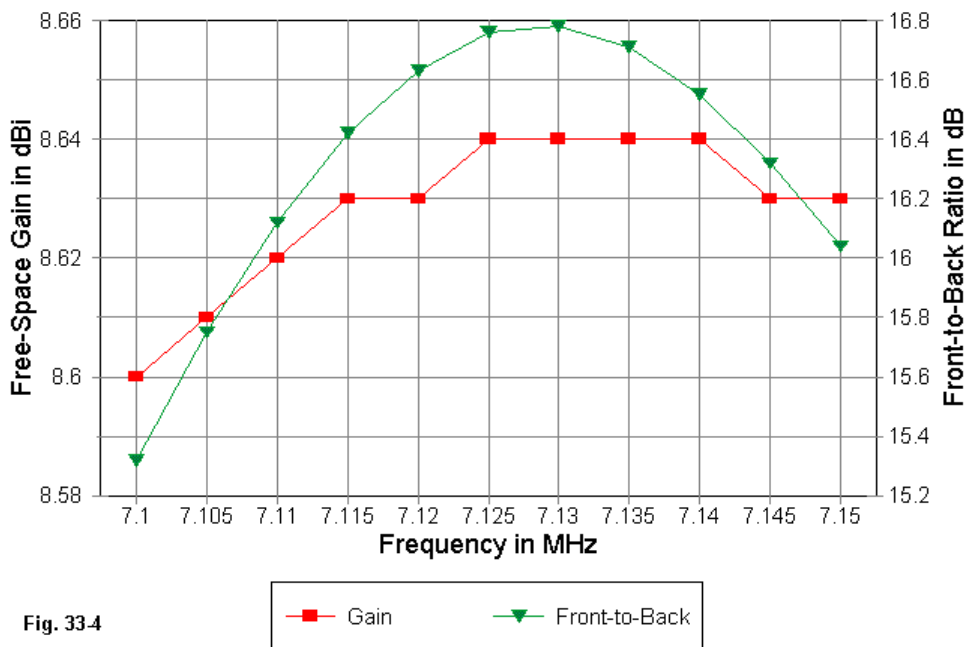


Fig. 33-4

Fig. 33-4 shows the results of such a sweep in graphical form. The gain values show steps, since the output data was limited to 2 decimal places and the overall change across the new set of frequency limits is very small. The potential front-to-back value peak turned out to be only a small rise in value, approaching 16.8 dB at 7.13 MHz. Other designs have shown equally narrow peaks well over 20 dB. The mini-sweep was the only way to ascertain the nature of this design's front-to-back behavior at its peak.

In general, whenever the data leaves potentially significant operating parameters ambiguous or vague, performing supplementary frequency sweeps over narrower frequency ranges is the easiest means of clarification. The ambiguities may not occur solely between graphed points of a sweep. Sometimes initial sweep data will raise questions regarding performance at the edges of the passband, calling for supplemental sweeps—or sometimes, simply for wider sweeps than are indicated by the intended limits of operation.

3-Element 40-Meter Quad Beam 50-Ohm VSWR: 7-7.3 MHz

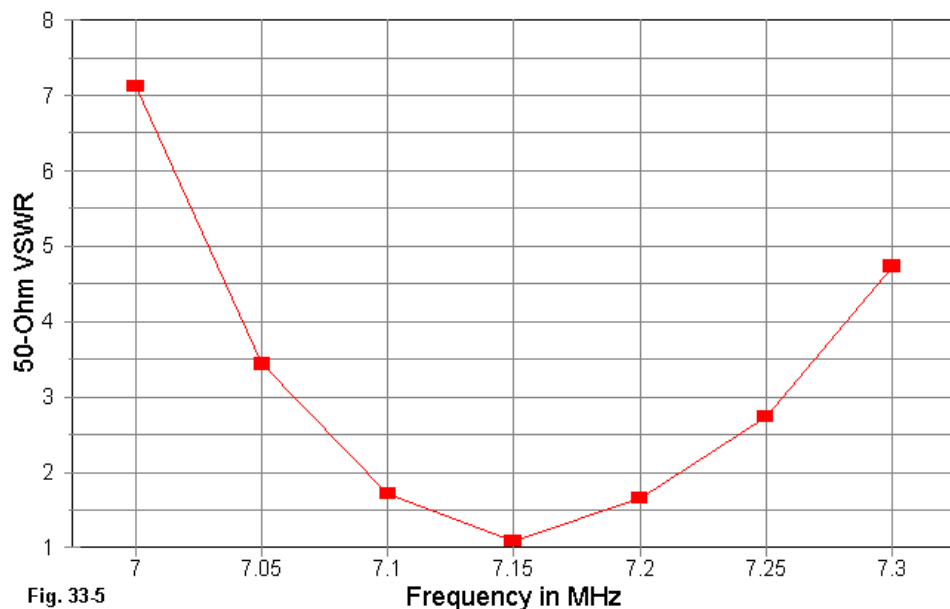


Fig. 33.5

Fig. 33-5 shows the 50-Ohm VSWR sweep of the subject quad model. I insert it here for two reasons. First, it completes the data set most commonly developed by a frequency sweep. However, on occasion, the modeler may find it useful to record (and graph) both the resistive and reactive components of the source impedance. The rates of change of resistance and reactance are often good indicators of the potential of a design for wide-band operation or for the addition of compensatory components to achieve a given source impedance. For example, in some lower HF wire antennas, the resistive component changes very little, while the reactance changes rapidly and almost linearly with frequency. By making such an antenna inductively reactive throughout its range, one may add a series variable capacitor to compensate for the inductive reactance of the antenna, thus achieving a relatively constant resistive impedance that matches a feedline of choice. Second, the SWR sweep in the present case is unambiguous in its indication of the narrow-band operation of the modeled antenna.

Comparing Antennas via Sweeps

Frequency sweeps are often very useful in comparing “competing” antenna designs for a given purpose. To illustrate the technique, I shall use a model of a hexbeam and a model of a Moxon rectangle. Neither model is a representation of a commercial antenna. Thus, no conclusions about the inherent potential or limitations of any such design can be drawn from the illustration. Both antenna types are generally interesting because they are compact and employ semi-closed geometries involving coupling between element ends as well as between parallel portions of the elements. The hexbeam looks like two “W” elements with the open ends facing each other. The rectangle is—well, rectangular. Both are 2-element arrays employing a driver and a reflector. See models 33-2 and 33-3.

Performing a frequency sweep of two antennas requires that we take account of normal sweep matters. We should use the same start and stop frequencies, as well as the same frequency increment throughout. Moreover, we should use enough frequency steps to obtain a relatively unambiguous picture of the antenna performance across the passband of interest. Let’s use the range of 14.0 to 14.35 MHz as our passband, with an increment of 0.035 MHz. This increment provides 10 steps—or 11 total checkpoints—of operation.

In addition, the modeler should note any other relevant factors that may affect the interpretation of the comparative output. For example, the hexbeam model in question has a design frequency of 14.10 MHz, while the Moxon was designed for a 14.15 MHz design center. The hexbeam is normally constructed from wire, so #12 AWG wire composes the elements. In contrast, a 20-meter Moxon can be easily fabricated from aluminum tubing, so its model employs 1" diameter elements.

Hexbeam and Moxon Rectangle Free-Space Gain: 20 Meters

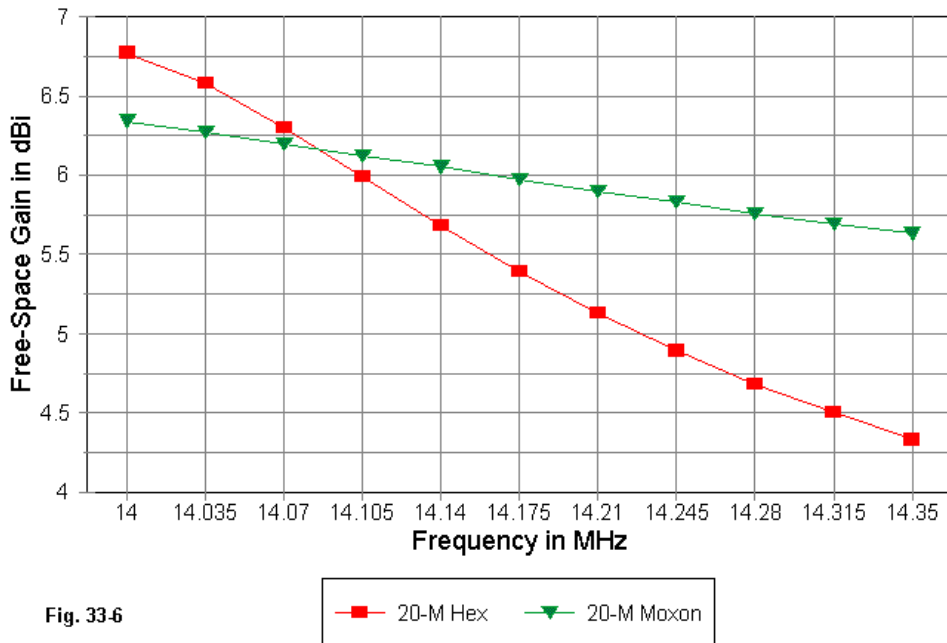
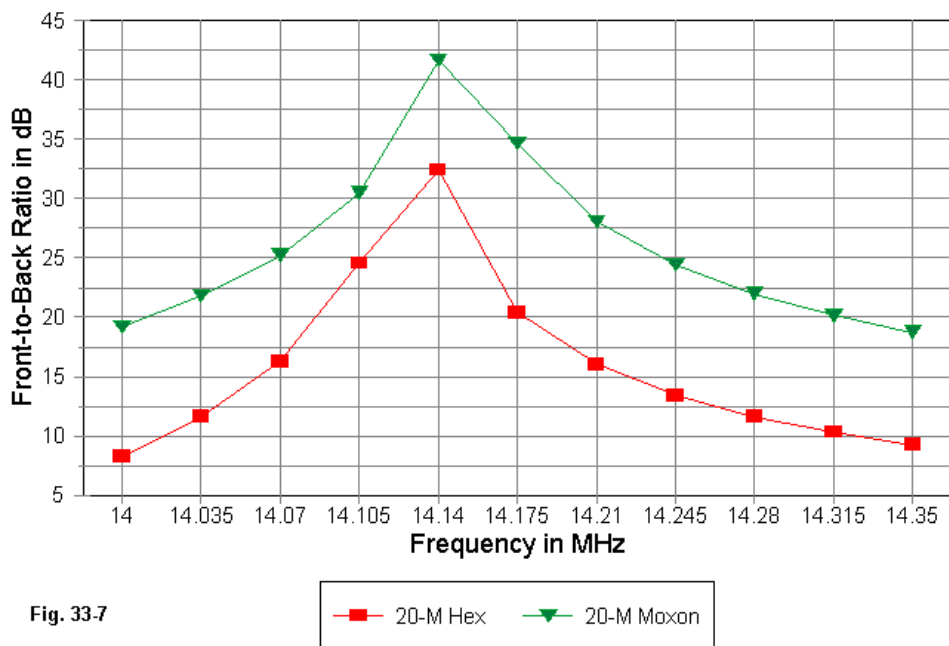


Fig. 33-6 shows the comparative free-space gain curves for the two models. Although the hexbeam has a higher gain at the low end of the passband, the rate of decrease in gain is much higher than that of the Moxon. Hence, the Moxon shows a 1-dB gain advantage at the upper end of the band.

Notice the flattening of the curve of the hexbeam as it reaches the lowest frequency of the sweep. One might raise a question of whether the hexbeam reaches peak gain close to or far from the low end of the band. Hence, supplementary sweeps might be useful over the range from 13.5 to 14 MHz to answer this question.

Hexbeam and Moxon Rectangle Front-to-Back Ratio: 20 Meters



In **Fig. 33-7** we find the 180-degree front-to-back curves for the two antennas over the prescribed range of frequencies. Both antennas exhibit the sharp front-to-back peak that marks semi-closed geometries (among others). Whether the absolute peak is higher than the graphed peaks makes less difference to the comparison of designs than the front-to-back ratio as one approaches the passband edges. A difference of 10 dB makes more difference here than at a frequency where the differential is between 30 and 40 dB.

Hexbeam and Moxon Rectangle 50-Ohm VSWR: 20 Meters

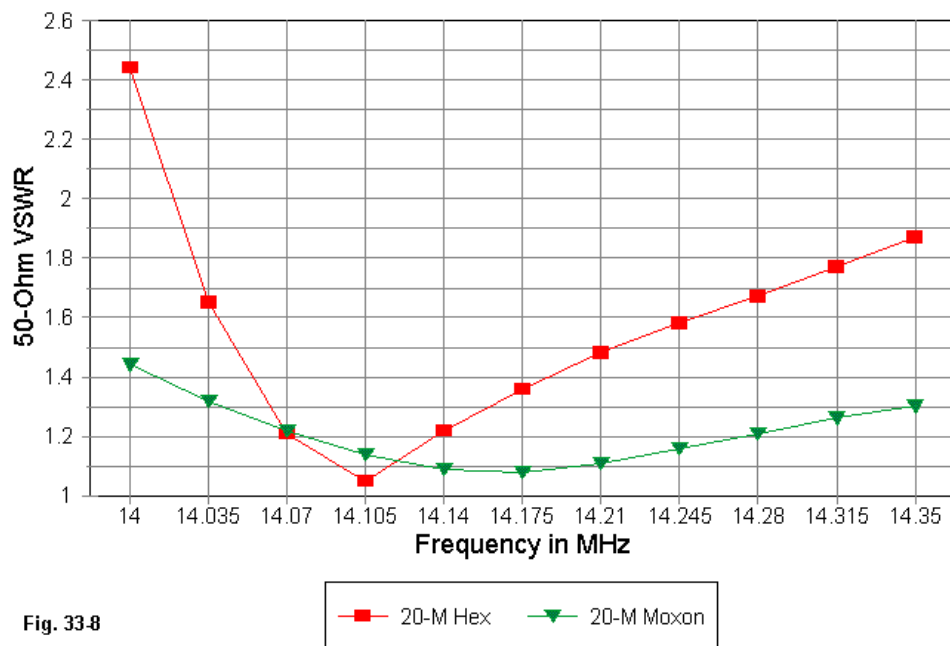


Fig. 33-8

The 50-Ohm SWR curves for the two models under comparison appears in **Fig. 33-8**. Here we can most clearly see the attempt to design one antenna for 14.1 MHz and the other for 14.15 MHz. Although one design shows much steeper curves than the other, both exhibit the properties of closed and semi-closed geometries wherein the curves are noticeably steeper below the design frequency than above it. As well, the fact that one model uses thin (#12 AWG) wire and the other employs 1" tubing also is evidenced in the differences between the curves.

The exercise has so far been geared toward a comparison of two designs, as if one had only a choice between the two. Of course, one may enter into the graphs as many designs as one likes, taking into account other properties of the antennas that do not show up in performance figures. For example, the total area (or volume) of an antenna may play a role in determining whether a design is a candidate at all. Additionally, one may place variants of the two designs into the picture in order to optimize each. None of these decisions will make any sense without first having a set of design specifications in hand to define what better and worse may mean.

The one major exception to the need for a set of design criteria has also shown up in our small foray into comparative frequency sweeping. In the process of looking at the differences between the models, we also noted a number of family resemblances borne by all members of the close and semi-closed group of 2-element antennas. For some modelers, these characteristics may be common expectations; for others, they may amount to discoveries about the class of antennas involved. Modeling is not solely for design and analysis—it can also be for learning about antennas.

Antennas on Different Bands

Suppose we frequency scale the Moxon rectangle from 20 to 10 meters. We shall approximately halve the element lengths. As well, for proper scaling, we shall halve the element diameter down to 0.5". Now let's define 10-meter coverage as extending from 28 to 29 MHz. Let's use a design center frequency on 10 of 28.5 MHz. Compare models 33-3 and 33-4.

In recording a comparative frequency scan, we should do two things. First, we shall set up the 10-meter scan in the same number of steps as the 20-meter scan.

The 10-step, 11-checkpoint scan is convenient on 10 meters where the increment become 0.1 MHz.

Second, when we graph the results, we should use some sort of common scale. In this case, the checkpoints are each 10% of the total frequency span. Therefore, a percentage scale becomes very useful.

20-Meter and 10-Meter Moxon Rectangles Free-Space Gain

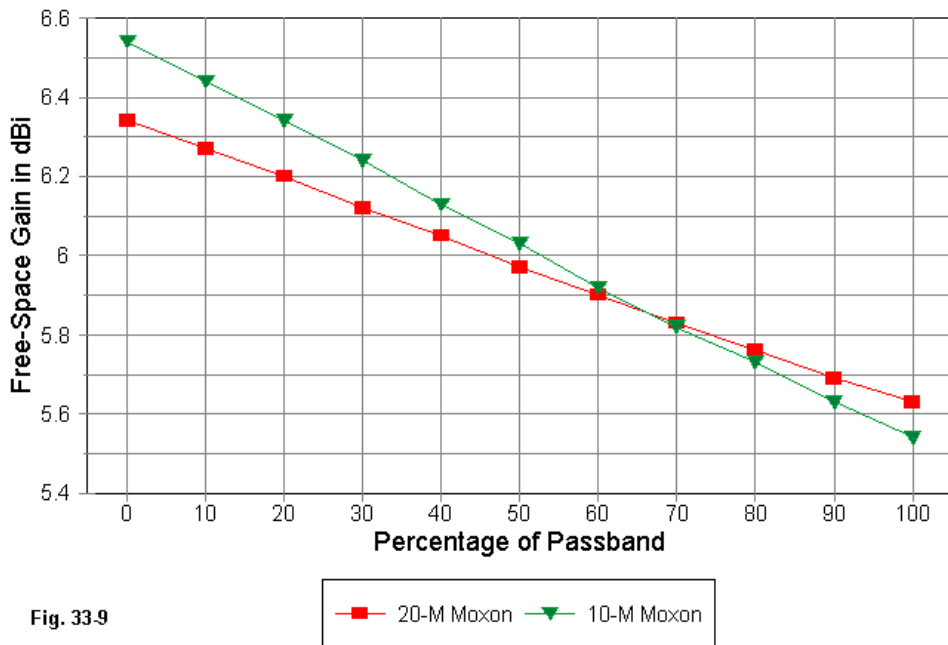
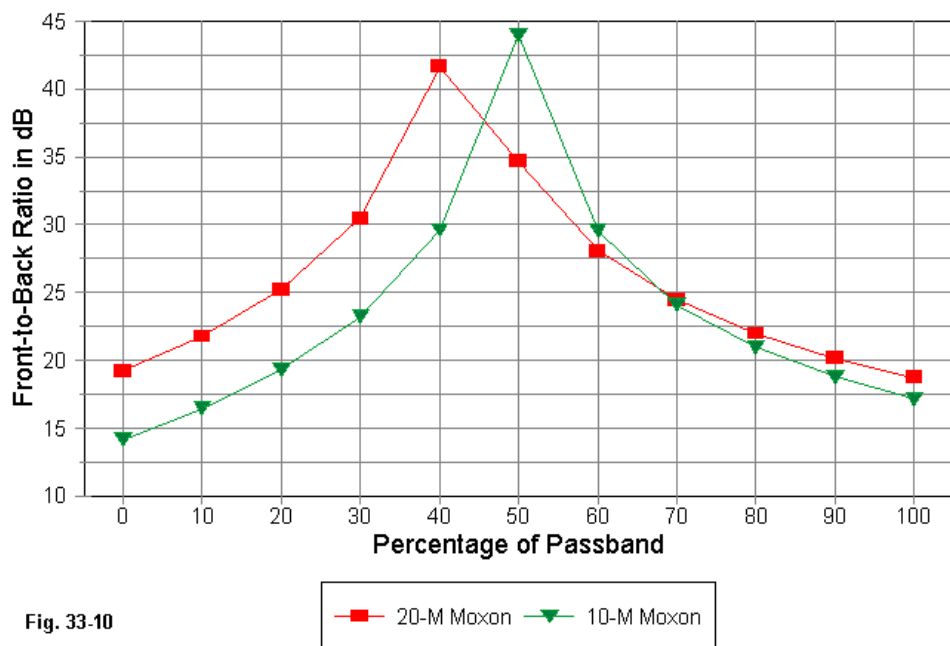


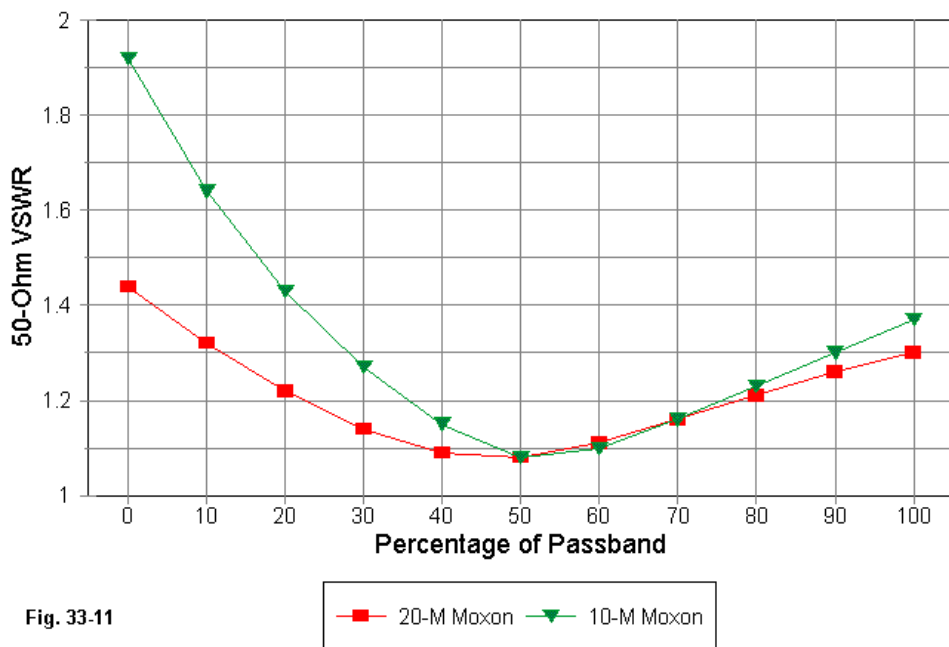
Fig. 9 shows the gain curves for the two antennas. Initially, we might think that the two scales should overlap or at least closely parallel each other. However, the size of the passbands differs, not only in total width, but as well as a percentage of the center frequency. The 20-meter amateur band is about 2.47% of its center frequency, while the first MHz of the 10-meter band is 3.51% of the center frequency—a 42% difference. Consequently, over the defined passbands, the gain on 10 meters will show a larger total variation than on 20 meters. In fact, designs that are adequate for 20-meter coverage may require significant alteration if they are scaled and adjusted to cover 28-29 MHz.

20-Meter and 10-Meter Moxon Rectangles Front-to-Back Ratio



The front-to-back sweeps for the 20-meter and 10-meter Moxons appear in **Fig. 33-10**. These curves tell us a great deal about both the performance of the antenna in question and about the design parameters for each model. For example, the 20-meter version used a design frequency of 14.15 MHz, about 42% up from the lower end of the band. Setting the design frequency lower than mid-band takes into account the fact that, for this design, the curves are steeper below the design frequency than above it. Displacing the design frequency permits the designer to achieve roughly equal front-to-back ratios at each band edge. In contrast, the 10-meter design was set for 28.5 MHz for 28-29 MHz coverage. As a result, the low-end front-to-back ratio is somewhat lower than the high-end value.

20-Meter and 10-Meter Moxon Rectangles 50-Ohm VSWR



As well, we can clearly see the consequence of operating the antenna over a frequency range that is a larger percentage of the design frequency, as it is on 10 meters. The average band-edge deficit in front-to-back ratio on the wider band is about 3 dB. Whether this amount is operationally significant is a design-evaluation decision that would require a set of project goals against which to measure the modeled values.

In **Fig. 33-11**, we have the 50-Ohm SWR curves for the two antennas. Once more, the relative displacement of the design frequency on the lower band shows up as a much more “centered” SWR curve than the one for the upper band. On 10 meters, the use of the exact passband center as the design frequency results in higher SWR values at the low end of the band. (Remember that the antenna used as an example here is designed for a direct connection to a 50-Ohm feedline, so adjustment of the curve via a matching network is not part of the project.) Besides the offset of the two SWR curves, we can see further evidence of the consequences of using the design over a frequency span that is a higher percentage of the design frequency.

Linear vs. Multiplicative Steps

We have looked at only some of the applications of frequency sweeps. Since a frequency sweep yields a NEC core run that produces all of the output data, we also have access to these data, ordinarily in tabular form. Among the most significant data that we might examine are the current magnitudes and phases, perhaps on the parasitic elements of a Yagi. These values may go a long way toward explaining the behavior of an array across an intended operational passband. Additionally, the change of source resistance and reactance across a passband is also valuable information to extract from a frequency sweep. Such data are useful in comparing two designs as well as in designing feedpoint matching systems.

Most of the work we wish to do with frequency sweeps can be done using linear frequency steps. Therefore, entry-level NEC-2 programs may limit the user to this option. However, the basic NEC core input system permits another type of sweep. Let’s re-examine the frequency input card once more.

FR	1	13	0	0	14.00	1.00206
Type of Stepping	No. of FQs		Start FQ		Increment	

We have modified the FR entry relative to the entries used throughout the exercise so far by changing the “Type of Stepping” value from 0 to 1. A zero indicates linear stepping, but a 1 activates multiplicative stepping. The start frequency is 14.0 MHz in the example. We can calculate the increment via the following equation:

$$M.F. = \sqrt[N-1]{\frac{f_{HI}}{f_{LO}}}$$

where M.F. is the multiplying factor, N is the number of frequency steps, f_{HI} is the highest frequency of the sweep, and f_{LO} is the lowest frequency (the “start” frequency). In the example, the 12th root of the ratio of 14.35 to 14 is about 1.0020598.

For most common purposes, we mentally extrapolate from linear sweeps those performance factors that are functions of a percentage of design frequency rather than strict linear frequency functions. However, on some occasions, it may be useful to view NEC output data more directly in these terms. In such cases—assuming one’s program permits the use of multiplicative frequency sweeps—the use of this alternative input may prove beneficial.

In this small foray into sweeping frequencies with antenna modeling programs, we have certainly not covered all of the potential uses. However, I hope that there is enough here to either get you started on the road toward making good use of the facility.

* * * * *

Models included: 33-1 through 33-4. (.NEC and .NWP model dimensions in meters; .EZ model dimensions in inches.)



34. The Second Ground Medium

Way back in the 11th column of this series (Volume 1), I discussed the use of the various types of ground available in both NEC and MININEC. What we by-passed at that time was the fact that these calculating cores permit the use of two ground media. Perhaps it is time to fill in that gap—at least partially. In this episode, we shall look at the use of using 2 ground media to define the ground beneath and away from the antenna.

In order to keep the discussion focused on using more than one ground medium, I shall restrict the discussion to Sommerfeld-Norton (S-N) high accuracy grounds found in NEC. Multiple media can be defined for both MININEC and NEC real grounds of all sorts, and it is even possible to place a NEC perfect ground beneath the immediate vicinity of the antenna. However, for the sake of focus, I shall stay with the one ground calculation system and concentrate on the 2 ground media possible within NEC.

To define a single S-N ground, we simply follow the program directions for selecting the ground type and then plug in the values of conductivity (in Siemens per meter) and relative dielectric constant (or permittivity) that define a single medium. This medium pervades and defines the entire ground surface from coordinates 0, 0, 0 to the limits of the antenna's far field. In raw NEC terms, a typical card or entry would look like the following line (spaced out for identification of the entries):

GN	2	0	0 0	13	.005
Card	Gnd	Nr of	Zeros	D.C.	Cond.
Type	Type	Radials			

The “GN” card identifies both the ground type and medium. A type 2 ground is the Sommerfeld-Norton type. We set the number of NEC radials at zero (mandatory for an S-N ground). The following two columns are always zeros. The last two columns specify the relative dielectric constant and the conductivity: the values shown are those for what is commonly taken to be average ground. Note that the GN card accepts the values defining the medium in the reverse order of entry relative to the

input system of most commercial implementations, which specify the entry of conductivity first. The ground definition is called in the NEC manual “an infinite ground plane,” since it extends in every direction indefinitely. There are further columns, but if they are empty—as in this example—the program presumes that they have zero values. In many places around the NEC core, a zero value is interpreted as an absent value that then plays no role in the calculations or that triggers certain ways of handling the user input.

As a refresher on the general classification of ground values used in most common sources, I shall repeat a table appearing in the earlier column on grounds. Always substitute more precise values wherever known. The table represents an adaptation of values found in *The ARRL Antenna Book* (p. 3-6), which are themselves an adaptation of the table presented by Terman in *Radio Engineer's Handbook* (p. 709), taken from “Standards of Good Engineering Practice Concerning Standard Broadcast Stations,” *Federal Register* (July 8, 1939), p. 2862. Terman's value for the conductivity of the worst soil listed is an order of magnitude lower than the value shown here.

Soil Description	Conductivity in S/m Constant)	Permittivity (Dielectric	Relative Quality
Fresh water	0.001	80	
Salt water	5.0	81	
Pastoral, low hills, rich soil, typical from Dallas, TX, to Lincoln, NE	0.0303	20	Very Good
Pastoral, low hills, rich soil, typical of OH and IL	0.01	14	Good
Soil Description	Conductivity	Permittivity	Quality
Flat country, marshy, densely wooded, typical of LA near			

the Mississippi River	0.0075	12	
Pastoral, medium hills, and forestation, typical of MD, PA, NY (exclusive of mountains and coastline)	0.006	13	
Pastoral, medium hills, and forestation, heavy clay soils, typical of central VA	0.005	13	Average
Rocky soil, steep hills, typically mountainous	0.002	12-14	Poor
Sandy, dry, flat, coastal	0.002	10	
Cities, industrial areas	0.001	5	Very Poor
Cities, heavy industrial areas, high buildings	0.001	3	Extremely Poor

As a reminder, the ground beneath a NEC model is homogenous, whatever the degree of ground penetration by a signal. Real ground may be stratified within the region of ground penetration, especially from the lower HF to the VLF portions of the radio spectrum. Penetration more significantly affects the propagation of signals from vertically polarized antennas than from horizontally polarized ones, but both types are affected to some degree. Any errors created by the difference between modeled homogenous ground and real stratified ground, however, tend to be greater for vertical antennas.

Fig. 34-1

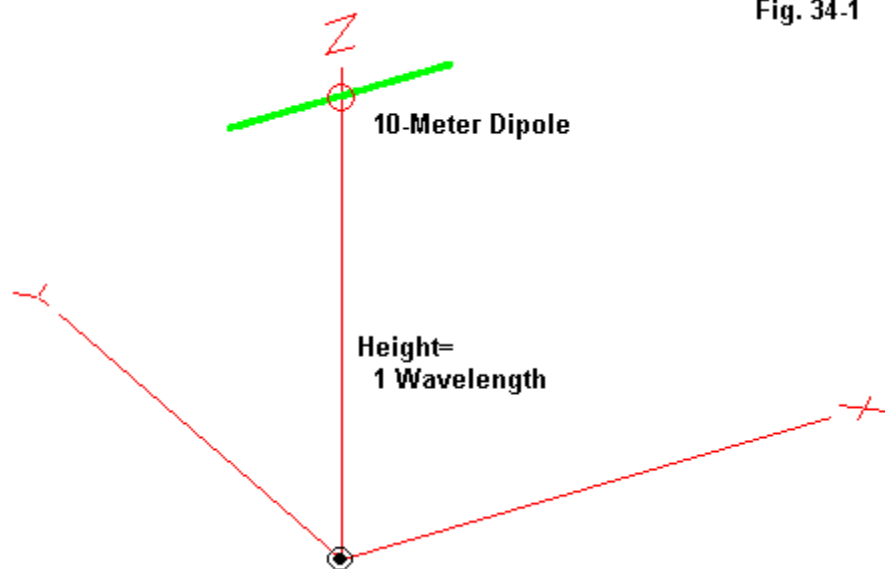


Fig. 34-1 shows a 10-meter dipole at a height of 1 wavelength above ground. With a single ground medium, we obtain an elevation pattern like the one shown in **Fig. 34-2**. Everything in the pattern—including the gain, the elevation angle of the lowest lobe, and the number of lobes—should be familiar to even relatively new modelers.

So far, we have a modeling situation of no great interest or significance. However, there are numerous circumstances in which we may wish to simulate multiple ground media. As one hypothetical case, let's assume that the dipole we just examined is about 1 wavelength from the ocean.

10-Meter Dipole
Height = 1 wl
1 Ground Medium

Cond. = 0.005 S/m
DC = 13

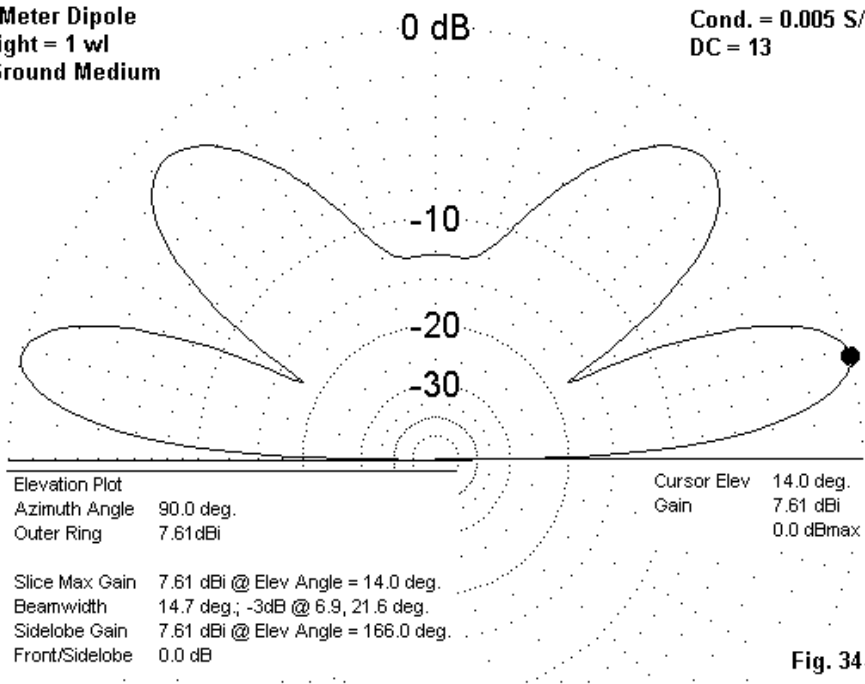


Fig. 34.2

Let us restrict ourselves for the moment to using a circle to define the limits of the inner medium. There are other possibilities, but mastering them one at a time will be the order of the day. If we happen to be interested in the radiation toward an inland location, we can use the single medium model. If we are interested in the radiation out to sea and beyond, we can use the next model to emerge.

When we use more than one medium, NEC calculates the current distribution and source impedance of the antenna based on the inner medium. The combined media play a role in the far field calculations. To specify a second medium, our GN card might look like the following entry:

GN	2	0	0	0	13	.005	81	5	10.7
Card	Gnd	Nr of	Zeros	D.C.	Cond.	D.C.	Cond.	Boundary	
Type	Type	Radials		[Inner Med.]		[Outer Med.]		Radius	

This card specifies two media, an inner and outer, with the inner medium having average soil values and the outer one having salt-water values. The boundary radius tells us how far (in meters) from the coordinate system origin that the outer medium begins. Note that boundaries are always specified in terms of distance from the 0, 0, 0 point of the coordinate system, not necessarily from the antenna. Since we can alter the coordinates of the antenna elements, we can place it anywhere in the inner medium region.

10-Meter Dipole
Height = 1 wl
2 Ground Media

0 dB

Inner Medium to 1 wl
Cond. = 0.005 S/m, DC = 13
Outer Medium
Cond. = 5, D.C = 81

-10

-20

-30

Elevation Plot
 Azimuth Angle 90.0 deg.
 Outer Ring 8.15dBi

Cursor Elev 14.0 deg.
 Gain 8.15 dBi
 0.0 dBi max

Slice Max Gain 8.15 dBi @ Elev Angle = 14.0 deg.
 Beamwidth 14.8 deg.; -3dB @ 7.2, 22.0 deg.
 Sidelobe Gain 8.15 dBi @ Elev Angle = 166.0 deg.
 Front/Sidelobe 0.0 dB

Fig. 34.3

To obtain a far field NEC-2 plot that takes account of the outer medium, we have to make a change in the requested plot or RP card. The normal mode has a value of 0 in the first integer slot of the RP card. For a radial boundary between 2 ground media, we change this number to 3. There are other values, but for 2 media with a radial boundary—the limits of this column—the 3 will cover all our work. (If we leave the value at 0, the far field will be calculated in NEC-2 using only the inner medium, as if it extended indefinitely. Wherever a commercial program does not ask for a user change to the radiation pattern set-up, it is made automatically when the user specifies a second medium.) See model 34-1.

Fig. 34-3 provides an elevation plot for the antenna in its new environment. Note the increase in gain for the lobe at 14 degrees. Note also the nearly “knife-edge” change in gain value within the second lobe. Reality would not likely in this kind of case provide such a sharp change in gain. However, the boundary between modeled ground media is a sharp change and shows up as such in the calculations. The lower values of signal strength at higher angles result from reflection from within the inner medium (at least in part). The approximate 45-degree elevation changeover point for the 1 wavelength boundary radius is no accident.

In this example, both ground media are at the same level, namely $Z=0$. However, we can go a step further in defining media by placing the outer level at a lower height by a defined amount. Let's assume that our salt water is a full wavelength below the ground beneath the antenna itself, which is above the ground by a wavelength. Then our GN card takes on this appearance:

GN	2	0	0 0	13	.005	81	5	10.7	10.7
Card	Gnd	Nr of	Zeros	D.C.	Cond.	D.C.	Cond.	Boundary	Neg.
Type	Type	Radials		[Inner Med.]		[Outer Med.]		Radius	Outer
									Height

The new number (again in meters, even if the user interface entry is in other units) represents the distance by which the outer medium surface is below the inner medium surface. A commercial program might call for a negative number as an input to remind the user that the outer medium can never be higher than the inner medium. However, the NEC card requires that this value of lower ground be entered on the card as a positive distance downward. 10.7 meters is about 1 wavelength at the 28 MHz test frequency for the model we are using.

10-Meter Dipole
Height = 1 wl
2 Ground Media
Outer = 35' Down

0 dB

Inner Medium to 1 wl
Cond. = 0.005 S/m; D.C. = 13
Outer Medium
Cond. = 5; D.C. = 81

-10

-20

-30

Elevation Plot
Azimuth Angle 90.0 deg.
Outer Ring 8.17 dBi

Cursor Elev 7.0 deg.
Gain 8.17 dBi
0.0 dBmax

Slice Max Gain 8.17 dBi @ Elev Angle = 7.0 deg.
Beamwidth 7.2 deg.; -3dB @ 3.6, 10.8 deg.
Sidelobe Gain 8.17 dBi @ Elev Angle = 173.0 deg.
Front/Sidelobe 0.0 dB

Fig. 34.4

Fig. 34-4 presents the modeled elevation pattern for our old dipole in its revised environment. Note that the lowest lobe has dropped to 7 degrees, since the antenna is now about 2 wavelengths above the medium most affecting far field patterns at elevation angles below 45 degrees. At that angle, the inner medium exerts the dominant effect. The model once more shows the knife-edge effect presented by the models sharp boundary—something unlikely in reality. However, the lower lobes are likely to be reasonably accurate with respect to a real situation.

Let's change the scenario to explore some other modeling results that you may expect from NEC calculations with multiple media. The first move is the change our dipole into a vertical dipole for 30 MHz and to set its lowest point about 3' above ground. **Fig. 34-5** shows the general scheme.

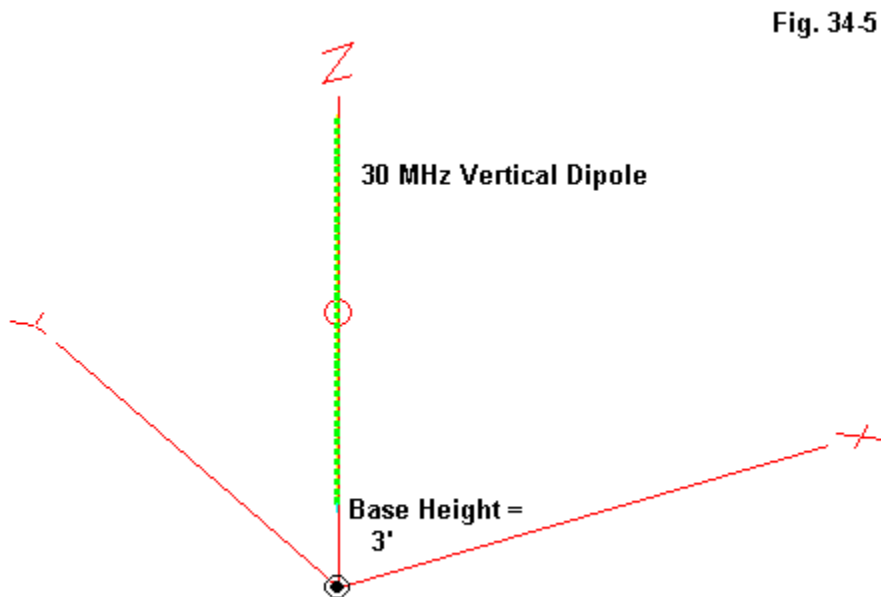


Fig. 34-5

Initially, let's set the antenna over a single ground medium defined as "very poor" (Cond. 0.001 S/m; D.C. 5).

Fig. 34-6 presents the elevation pattern of the antenna over its very poor soil. Note the very modest gain figure for the antenna under these conditions.

30-MHz Vertical Dipole
Base Height = 3'
1 Ground Medium

Cond. = 0.001 S/m
D.C. = 5
(Very Poor Soil)

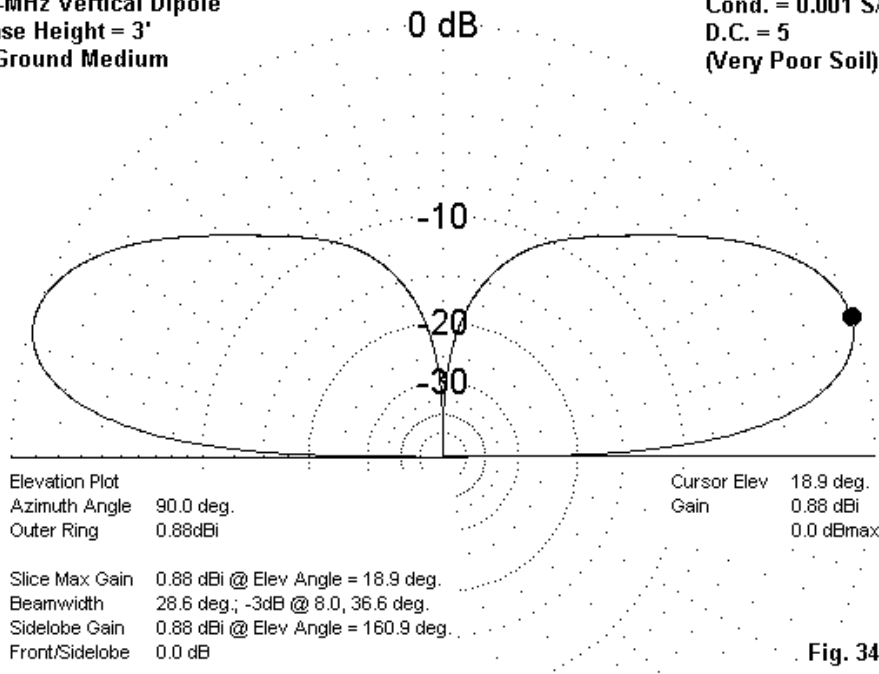


Fig. 34-6

Next, let's make a change. Let's place a modest ground screen or ionizing salts in the ground in an effort to improve its quality. Let's estimate that the result is ground that qualifies as very good (Cond. 0.0303 S/m; D.C. 20). We shall leave the overall playing field level, but make the radial boundary 1/4 wavelength from the point beneath the antenna. Outside the boundary, the ground values remain at the very poor level. See model 34-2.

Now, a warning. What follows is what the NEC model reports and no more. No claim about reality is made for the purposes of this note.

30-MHz Vertical Dipole
Base Height = 3'
2 Ground Media

0 dB

Inner Medium to 0.25 wl
Cond. = 0.0303; D.C. = 20
Outer Medium
Cond. = 0.001; D.C. = 5

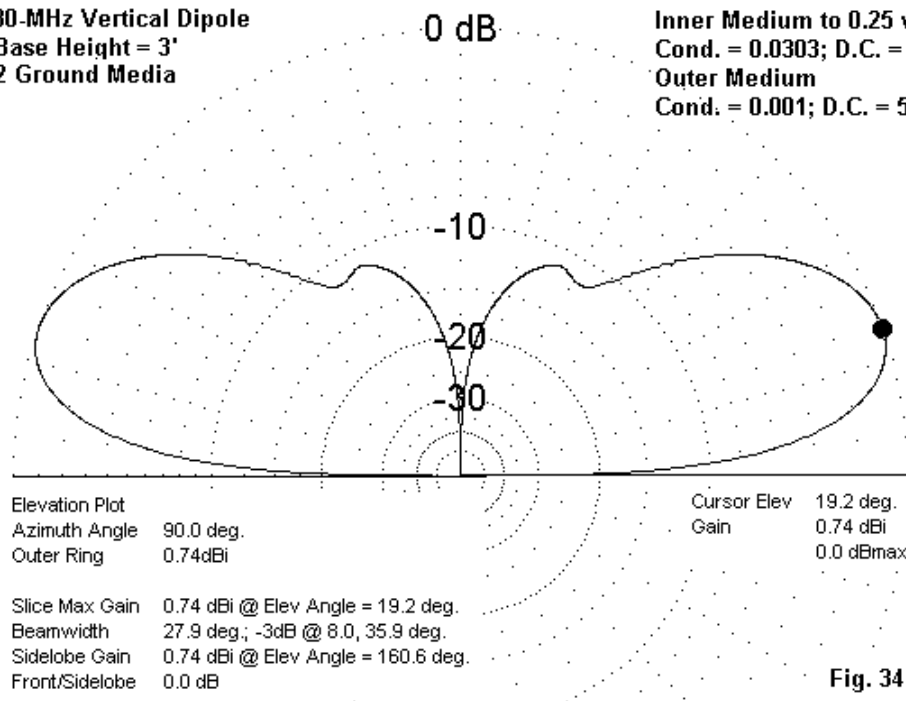


Fig. 34-7

Fig. 34-7 shows the elevation pattern of the antenna with the revised soil conditions. The antenna shows a tad less gain and a slight increase in the elevation angle of maximum radiation. The ground improvement did not extend to the major portion of the Fresnel or reflection zone of the antenna and hence does not show an improvement in radiation at low levels. This result is typical of modeling outputs for vertical antennas that do not use a set of radials as both a ground plane and antenna element completion, such as the group of 1 wavelength loops fed as vertically polarized antennas. As a useful exercise to acquaint yourself with multiple ground media, you may wish to change the inner medium values across a range of values, including but not exceeding those for salt water. There are some reports that values higher than those for salt water may yield inaccurate modeling results.

For our next example, let's increase the frequency of our vertical dipole to 300 MHz to simulate another common situation: the placement of an antenna over a building top. To simplify matters, we can work in meters, since the nearly resonant vertical dipole is a bit shorter than 0.5 meters. Initially, we shall place the base of the antenna 5 meters above a single ground medium consisting of very good ground (Cond. 0.0303; D.C. 20).

300 MHz Vertical Dipole
Base Height = 5 m
1 Ground Medium

0 dB

Cond. = 0.0303;
D.C. = 20

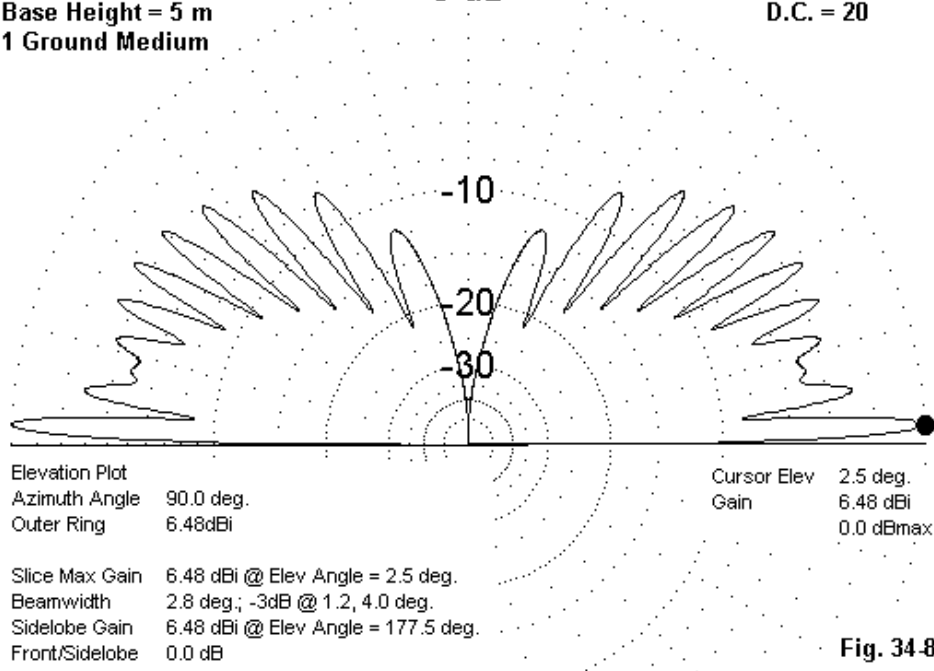
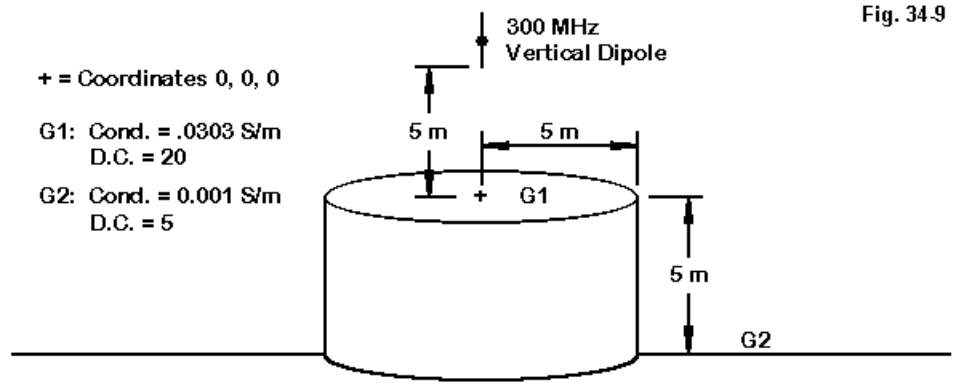


Fig. 34-8

Fig. 34-8 shows the elevation pattern for this model. Note the gain of nearly 6.5 dBi at an elevation angle of 2.5 degrees. (In working with antenna more than a very few wavelengths above the ground, you will often obtain greater accuracy by reducing the pattern steps from 1 degree to about 0.1 degree, especially for elevation patterns.) These values are typical for VHF vertical dipoles.

Now, let us make the case interesting. Let us assume that the antenna is 5 meters above a modestly tall building, perhaps 5 meters high. We shall assume—in order to preserve our simplified RP value of 3—that the building is circular and has a diameter of 10 meters, with the antenna mounted in the exact center. Beyond the building, the soil is very poor (Cond. 0.001; C.D. 5). **Fig. 34-9** illustrates that situation.



The GN card for this antenna looks something like the following lines:

GN	2	0	0 0	20	.0303	5	.001	5	5
Card	Gnd	Nr of	Zeros	D.C.	Cond.	D.C.	Cond.	Boundary	Neg.
Type	Type	Radials		[Inner	Med.]	[Outer	Med.]	Radius	Outer
									Height

Fig. 34-10 provides the modeled elevation pattern for our VHF antenna atop the building. The “cliff” (as it is called in NEC manuals) results in a 1.2 dB gain for the antenna, with nearly half the elevation angle for the main lobe. As well, the increased radius (as a function of a wavelength) results in a lower angle for the transition between dominance by the inner and by the outer media—about 25 degrees. See model 34-3.

300 MHz Vertical Dipole
Base Height = 5 m
2 Ground Media
Cliff Scenario

0 dB

Inner Medium to 5 m
Cond. = 0.0303; D.C. = 20
Outer Medium 5 m lower
Cond. = 0.001; D.C. = 5

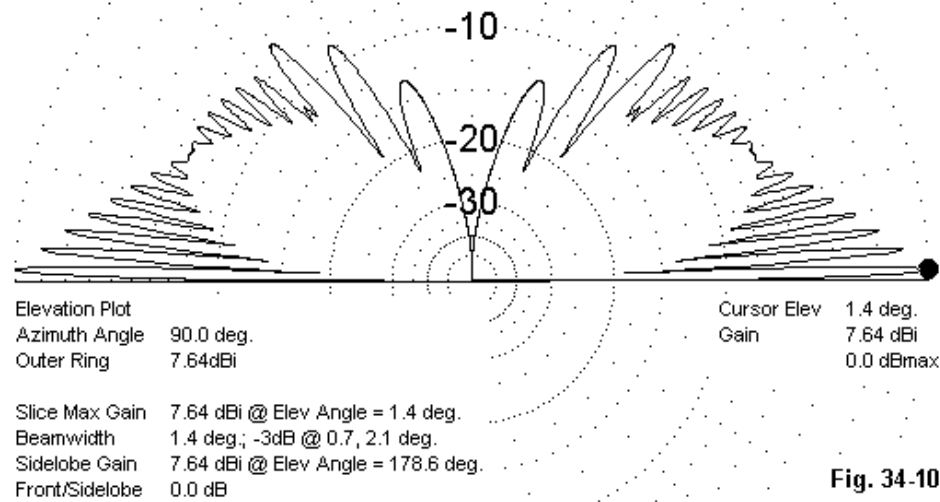


Fig. 34-10

As an exercise, to increase further your familiarity with modeling results using 2 media, you might place antennas of various sizes (or resonant frequencies)—both horizontal and vertical—over this building and compare the results with their counterparts using a single medium. For some HF antennas, do not be surprised to get knife-edge effects that cut a lobe into a stronger and a weaker part.

Once more, reality may or may not exhibit the sharp change in pattern lobes. Remember that the rooftop was considered a homogenous ground material having enough metal in it to simulate very good soil. Real buildings may range from very poor to even better than very good, depending on their composition and the fre-

quency of the antennas involved. I chose the very good rating for the example with the assumption of there being a good bit of metal in the upper structure under the roof. In reality, both the amount and the arrangement of the metal may play a significant role in determining how good a ground medium that a given roof top makes.

Let's perform an additional experiment. Remember that the coordinates for a ground medium must be 0, 0, 0, the coordinate system origin. However, there is no restriction on where we place our antenna. Therefore, let's return to the 30 MHz vertical dipole and place it about 1 meter (3') above the inner medium, which simulates a circular rooftop. Next, let's place it 0.1 m from the building edge by changing the X or Y coordinate by 4.9 m.

30 MHz Vertical Dipole
Base Height = 1m
Base Position = .1 m
from "Cliff" edge
2 Ground Media

Inner Medium to 5 m
Cond. = 0.0303; D.C. = 20
Outer Medium 5 m lower
Cond. = 0.001; D.C. = 5

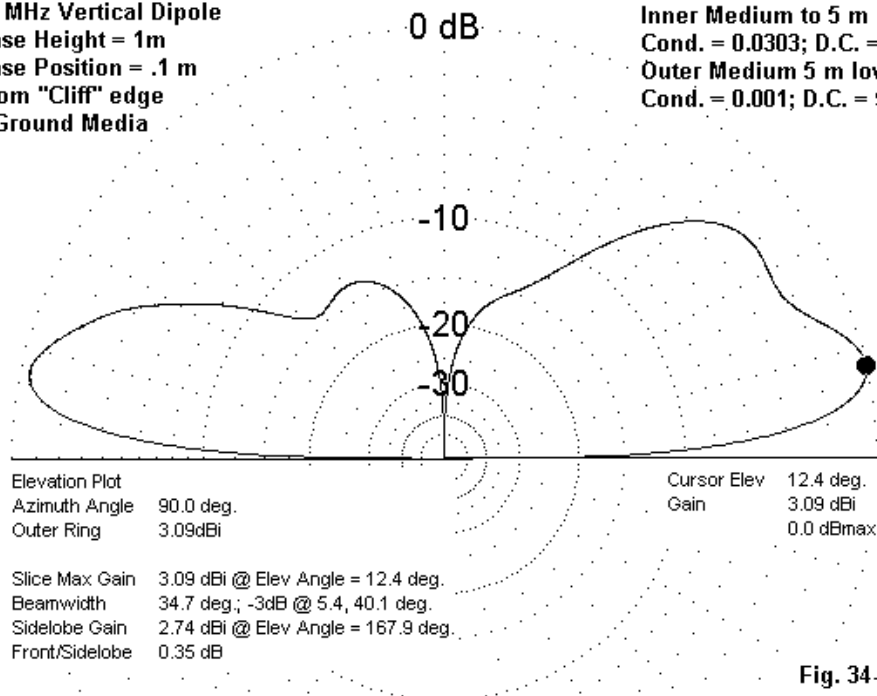


Fig. 34-11

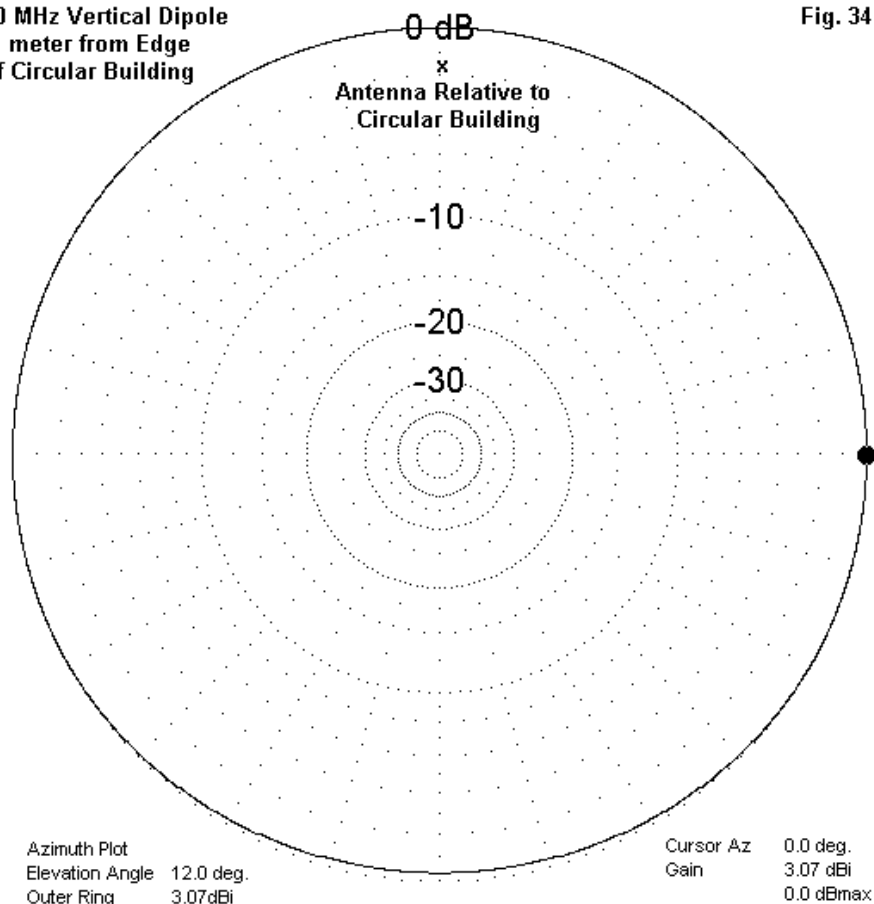
Fig. 34-11 shows the results of our move in an elevation pattern for the antenna. The shift in antenna position results in a pattern displacement over the edge of the building. At the same time, we see the emergence of higher-angle energy in the direction over the building edge. Although the displacement is—for most purposes—hardly fatal to the new antenna placement, the practice of modeling the antenna position as exactly as possible over or on the inner medium shows its merits. However, beware of placing the antenna beyond the inner medium. Because NEC will calculate the impedances and current distribution based on the inner medium, the results may not be accurate.

We can specify the boundary between media as either a radius or a linear boundary. In NEC-2, the difference appears in the RP card, where the mode is specified as 2 rather than 3. The linear boundary occurs parallel to the Y-axis as a value for X. To see the difference, let's look at two azimuth patterns of our 30 MHz vertical dipole. First, we shall examine a circular or radial cliff. With the antenna near the edge of the building—at 0.1 meter from the building edge, which is point X on **Fig. 34-12**—the alteration produced by the antenna position is a slight offset in the circular azimuth pattern.

When the “cliff” is linear, it extends indefinitely and creates a larger change in the far field azimuth pattern. **Fig. 34-13** illustrates the pattern from our 5-meter tall building with the antenna 0.1 meter from the edge. As an exercise, one might wish to run a selection of models in which the only difference is the type of boundary between the inner and outer ground media.

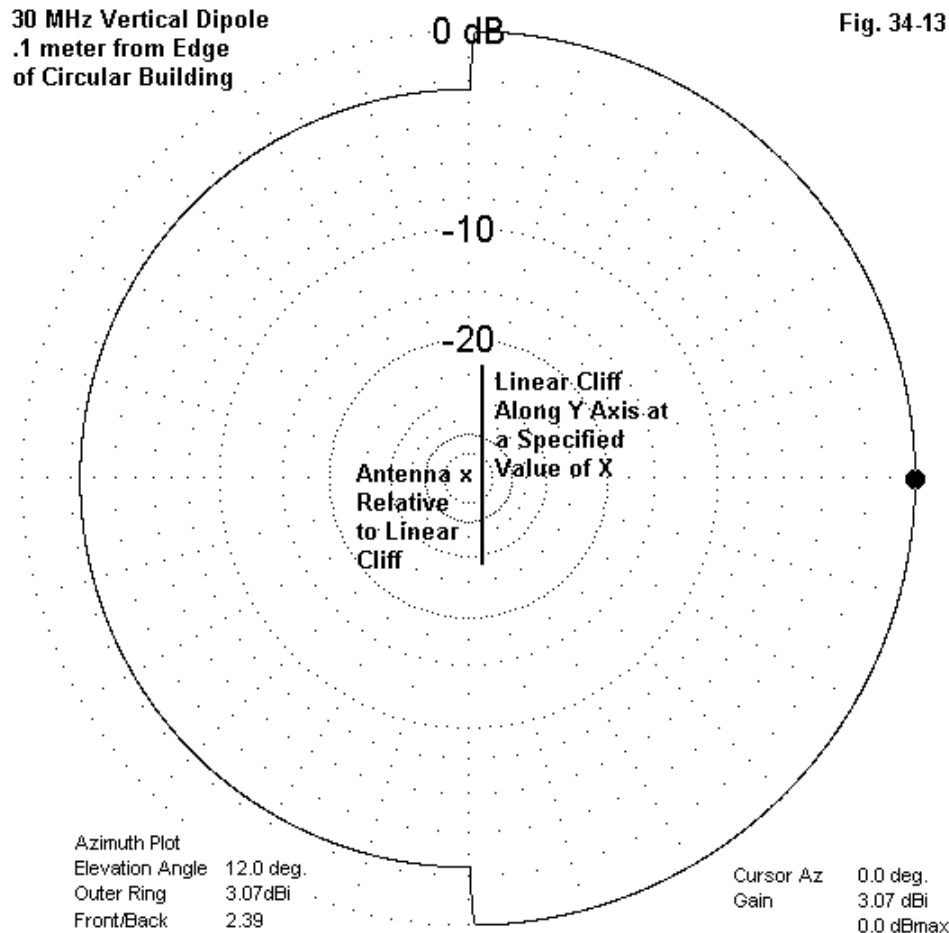
30 MHz Vertical Dipole
.1 meter from Edge
of Circular Building

Fig. 34-12



30 MHz Vertical Dipole
.1 meter from Edge
of Circular Building

Fig. 34-13



We have restricted ourselves to S-N ground using two media with a radial boundary between them. These are not the only possibilities that NEC offers. For example, if we change to the NEC fast or reflection coefficient ground system, we can create a set of radials beneath the antenna. We can also add our second medium by the use of a GD (Ground Description) card instead of expanding the content of the GN card. For example, if the 2-media GN card were to look like this:

GN	2	0	0 0	20	.0303	5	.001	5	5
Card	Gnd	Nr of	Zeros	D.C.	Cond.	D.C.	Cond.	Boundary	Neg.
Type	Type	Radials		[Inner Med.]		[Outer Med.]		Radius	Outer
									Height

Then the corresponding pair of (NEC-2) GN and GD cards would have this appearance:

GN	2	0	0 0	20	.0303		
Card	Gnd	Nr of	Zeros	D.C.	Cond.		
Type	Type	Radials		[Inner Med.]			

GD	0 0 0 0	5	.001	5	5
Card	(Zeros)	D.C.	Cond.	Boundary	Neg.
Type		[Outer Med.]		Radius	Outer Height

(Note: in NEC-4, the first GD integer position—a zero in NEC-2—uses a 1 for a linear boundary, a 2 for a circular boundary, and a 0 for no second medium. This system replaces the options found in the RP card for NEC-2. A NEC-4 card for the current outer medium would begin GD 2 0 0 0. . ., with the remainder as shown. This note is an example of some of the easily missed entry requirement differences between NEC-2 and NEC-4. Although many models developed in NEC-2 will run without alternation in NEC-4, it pays to keep on hand a list of commands whose requirements change between the two cores. As well, a good practice when going from one core to the other is to do a thorough inspection of the model input file. The larger the file, the more important that inspection becomes in terms of the long partial run times that may occur before the core rejects the model or turns out improbable results.)

Whether one uses a single GN card or a GN-GD pair, the calculations would provide the same output. Some commercial implementations of NEC tend to favor the use of the GD card for the second medium. Not all low-end programs allow the

full spectrum of ground potentials. Multiple ground media may require advancement to a professional version of some programs.

Although we have not surveyed all of the ground type and descriptions available in NEC, perhaps this much of a start may be useful. It pays to be well grounded in NEC's multi-media potentials.

* * * * *

Models included: 34-1 through 34-3. (All model dimensions in meters.)



35. Notes on Using AZ-EL Plots Effectively

The most common use for azimuth (AZ) and elevation (EL) plots might be summed up in the following example:

Suppose that we have a 3-element Yagi designed for 28.5 MHz composed of 1/2" diameter elements placed at a height of 35' above average ground. The 3-element Yagi would look, in outline, like **Fig. 35-1**.

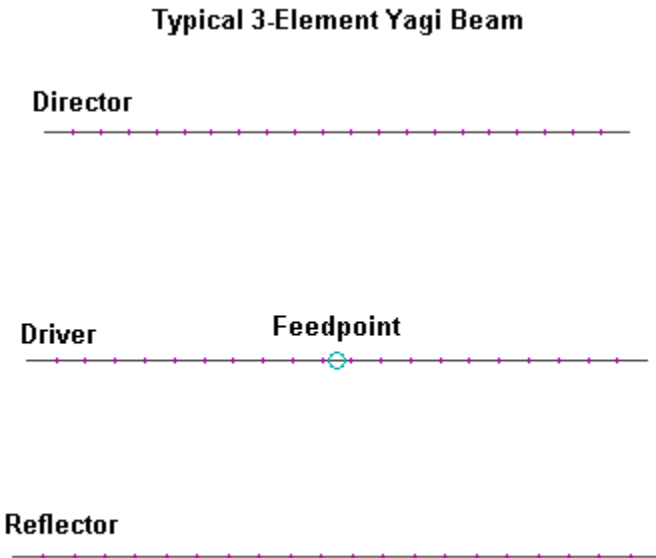


Fig. 35-1

The following table describes the model (35-1) of this antenna.

3 el Yagi 1/2" al elements

Frequency = 28.5 MHz.

Wire Loss: Aluminum (6061-T6) — Resistivity = 4E-08 ohm-m, Rel. Perm. = 1

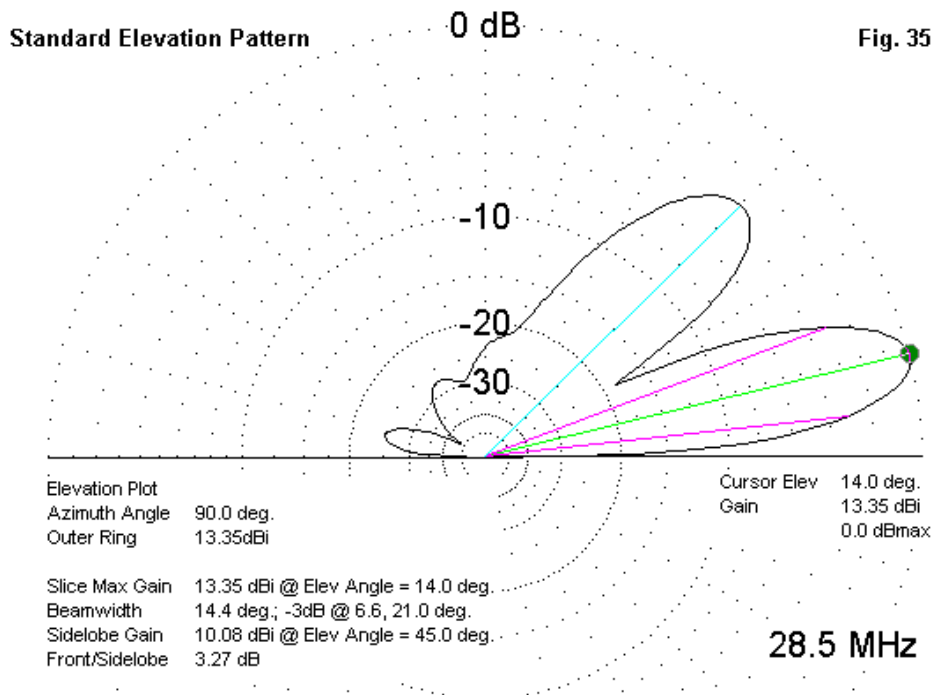
No.	End 1			End 2			Dia (in)	Segs
	X	Y	Z	X	Y	Z		
1	-8.595,	0,	35	8.595,	0,	35	0.5	21
2	-8.207,	5.2,	35	8.207,	5.2,	35	0.5	21
3	-7.722,	11.212,	35	7.722,	11.212,	35	0.5	21

Total Segments: 63

No.	Specified Pos.		Actual Pos.		Amplitude (V/A)	Phase (deg.)	Type
	Wire #	% From El	% From El	Seg			
1	2	50.00	50.00	11	1	0	V

Most of us have grown accustomed—perhaps too much so—to examining the AZ-EL plots for only a small amount of information: maximum gain, front-to-back ratio, and elevation angle of maximum radiation. Since we know that the maximum forward gain of the antenna is (literally) straight forward, we can begin with an elevation plot by setting the azimuth angle for it along the axis we chose as the front-back direction. In this case, let's assume that the elements stretch from end-to-end along the X-axis, which makes the Y-axis the standard beam direction. So we shall set the AZ heading to 90 degrees. The resulting EL pattern looks like **Fig. 35-2**.

From **Fig. 35-2**, we pick up the maximum gain figure (13.35 dBi) and the take-off (TO) angle (elevation angle of maximum radiation): 14 degrees. The next step is to call for an AZ plot, setting the elevation angle to 14 degrees. The result looks like **Fig. 3**.



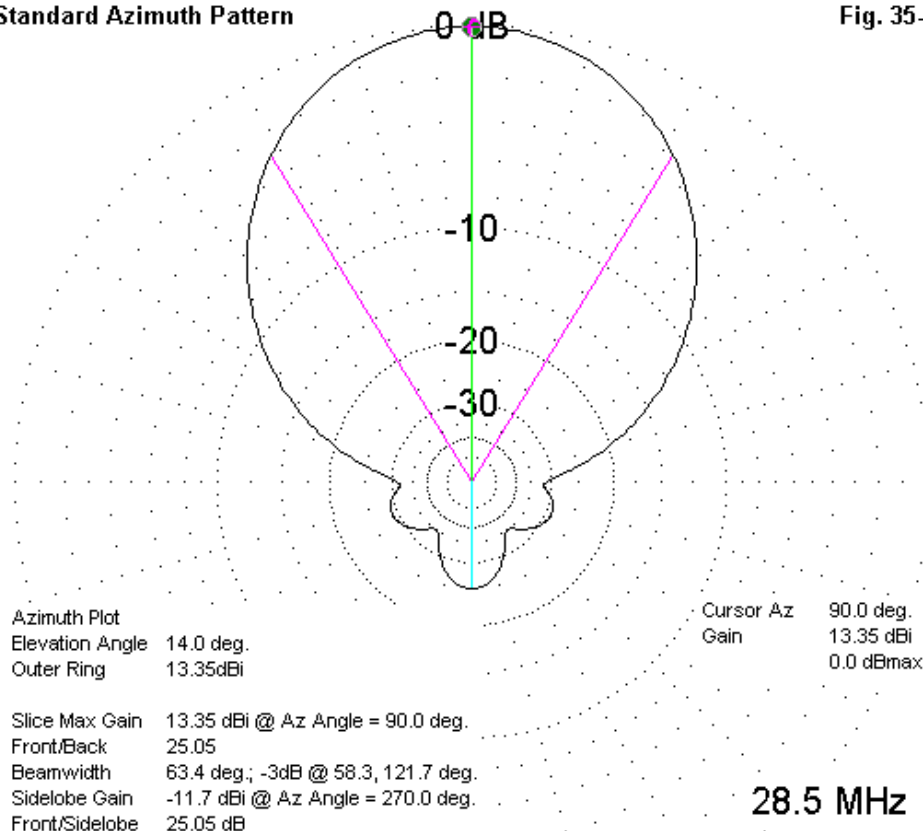
An examination of **Fig. 3** yields a confirmation of the maximum gain as well as the front-to-back ratio: 25.05 dB in 180-degree F-B terms.

Very often, we neglect much of the information that is also included on these plots. For example, the horizontal beamwidth to the -3 dB or half-power points is 63.4 degrees. This data gives us some idea of the coverage of the antenna without having to change beam heading. It should also inform us of why it is a fairly futile exercise to try to orient a beam such that the reference heading of our rotator is correct to under 1 degree.

The EL plot informs us that the vertical beamwidth to the -3 dB points is 14.4 degrees. Although the horizontal beamwidth was composed of symmetrical pattern portions left and right of the centerline, we should never assume that the same is true of a vertical beamwidth value. In this instance, the symmetry around the centerline is not severely distorted. The upper -3 dB point is 6.6 degrees above the TO angle and 7.8 degrees below the TO angle. Our coverage to the half-power points ranges from 6.6 to 21 degrees, covering most of the skip angles we are likely to encounter on 10 meters.

Standard Azimuth Pattern

Fig. 35-3



Also notable in the elevation pattern is the secondary lobe at a higher angle. The plot informs us that its angle of maximum radiation is 45 degrees and that it is more than 3 dB weaker than the main lobe.

How we use this information to evaluate the potential performance of the antenna involves a number of factors that go beyond what the model tells us. First, we have to determine the weight to give each element of the information relative to the purpose for which we might install this antenna. Second, we must factor in information that may alter the reliability of the modeled numbers relative to the actual site situation of the antenna itself. For example, terrain variations may require special treatment outside the realm of NEC modeling to determine more precise expectations of the antenna when pointed in various directions.

Having said this much about AZ and EL plots, we tend to stop our investigation. In doing so, we often deny ourselves useful data that might be supplied by a few supplementary plots. Here are a couple of examples—using the same initial model—of what we might learn.

Case 1—an alternative direction: Suppose that we have the 3-element Yagi set on a certain heading, perhaps the primary direction for communications. Now further suppose that there is a secondary heading about 20 degrees to the right of the primary bearing—with the new heading indicating a station or set of stations with which we wish to communicate.

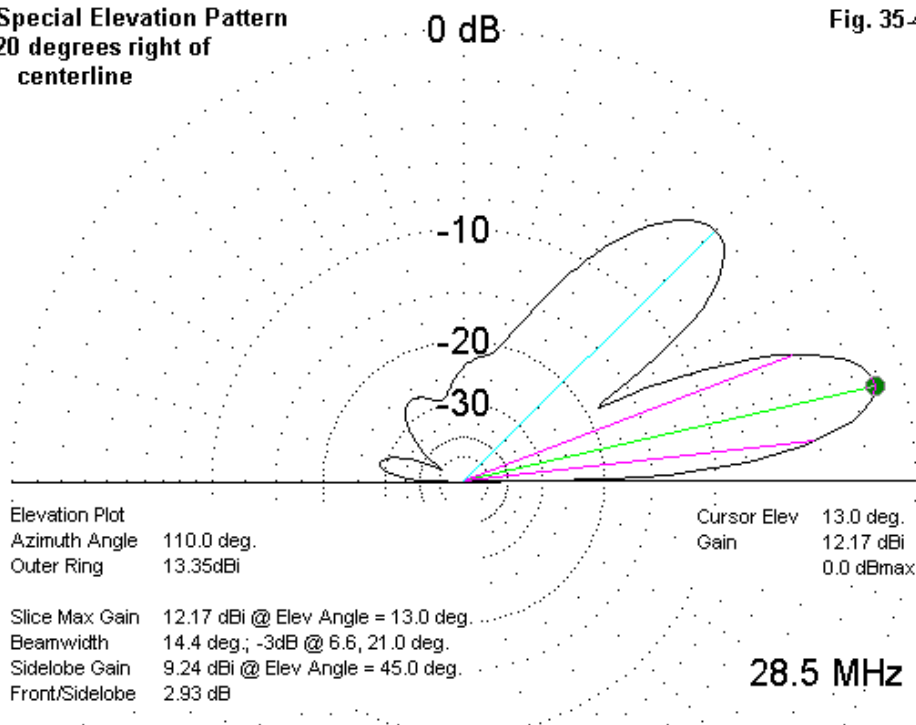
One solution to this situation is to move the beam heading by 20 degrees. However, one might wonder whether this solution is necessary. The ultimate answer to the question might well involve the type of operation involved. Casual contact leaves the operator plenty of time to change the antenna direction. However, there are contest and similar operational contexts in which every movement that can be classified as unnecessary is eliminated as part of the operational strategy. Hence, for some contexts, the decision to move or not to move the antenna heading may acquire some significance.

One important piece of data that might enter into the decision process is how much signal strength we might lose by not moving the antenna. Alternatively, we can ask how much signal strength we would have in the secondary direction if we

leave the heading in the primary direction. The answer is as simple as requesting a new elevation plot using a heading that is in the secondary direction.

Special Elevation Pattern
20 degrees right of
centerline

Fig. 35-4



For such plots, it is useful to set the outer ring of the plot at the maximum gain obtained from our initial elevation plot—in this instance, 13.35 dBi. The resulting elevation plot will then show graphically as well as numerically the difference in signal strength. **Fig. 35-4** shows the new plot.

From the EL plot, we can discover that the gain in the secondary direction is 12.17 dBi, down 1.18 dB from the primary direction. Although we might have estimated these values from the initial azimuth plot, the ability to request alternative EL plots for any AZ bearing can provide a table of values that can contribute either to operational planning or to an evaluation of the potential antenna performance.

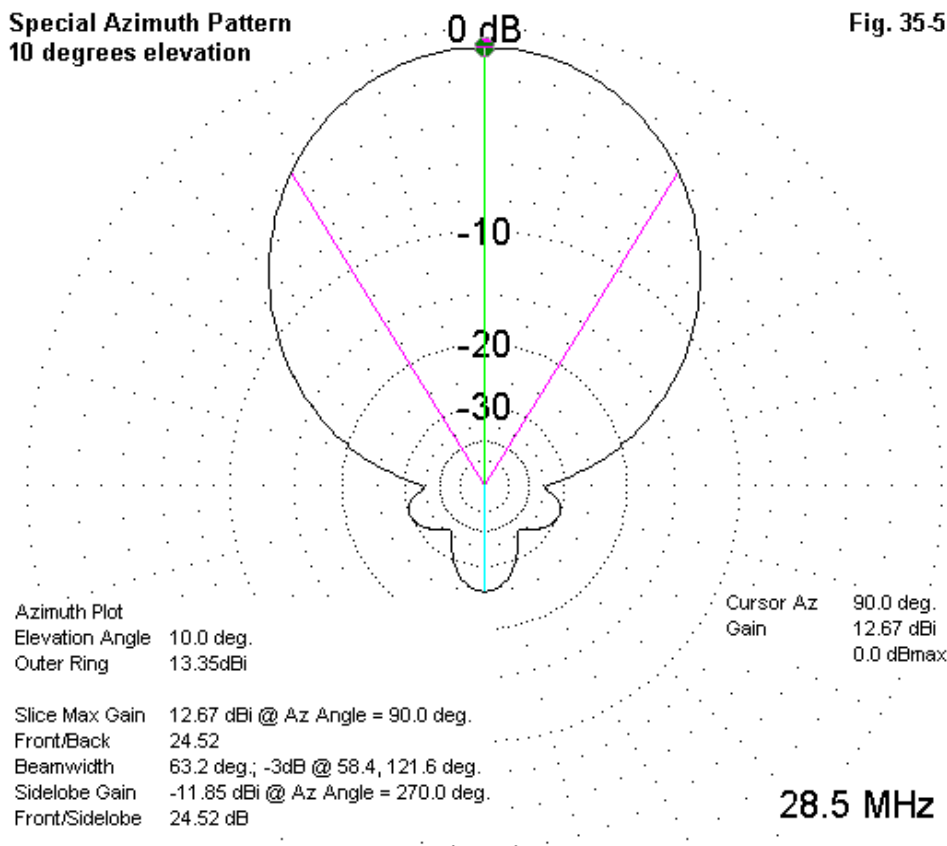
Case 2—an alternative elevation angle: The TO angle or elevation angle of maximum radiation is not the only elevation angle that is important. Adjunct to many types of operation are programs and other sources that predict propagation. The predictions may also include estimated skip angles for different frequencies. These predictions in the short term may open the question of just how effective our subject antenna might be at its present height. Over a longer term, we might question whether or not it would be useful to change the antenna height to obtain better results.

Suppose, then, that we are interested in a skip angle of 10 degrees—4 degrees lower than the TO angle that we initially obtained from our general analysis of the 3-element 10-meter Yagi. We can simply set the elevation angle for an AZ plot to the 10-degree mark. Once more, it is useful to set the outer ring of the AZ plot to the maximum gain level from our initial analysis—13.35 dBi. Then, the new AZ plot will graphically as well as numerically show the difference in signal strength. The result appears in **Fig. 35-5**.

From **Fig. 35-5**, we learn that the forward gain at a 10-degree angle is 12.67 dBi, about 0.68 dB less than at the TO angle. We may also note in passing that the front-to-back ratio changes by only an insignificant amount. Just how we factor this information into the overall operational and construction planning will depend on all of the additional factors we have so far noted. Since we can request AZ plots for any elevation angle, we can develop detailed information across a spectrum of possible skip angles. Of course, all such data must be adjusted for any terrain affecting signal propagation to the antenna and its site.

Special Azimuth Pattern
10 degrees elevation

Fig. 35-5

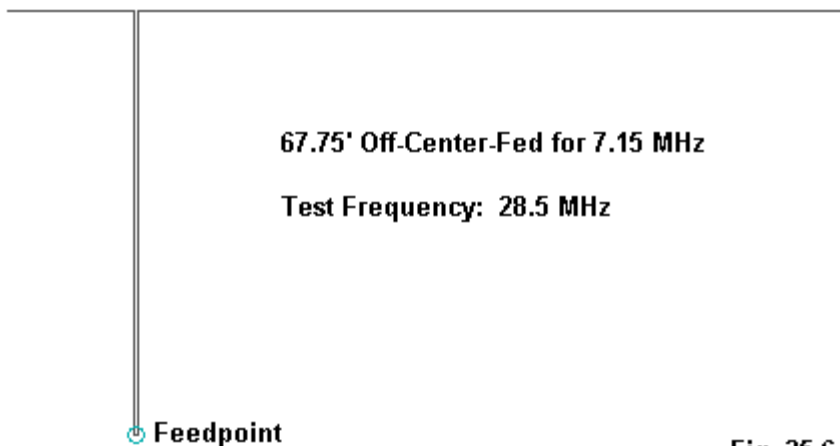


These two cases are only the beginning of the kind of information that we can gather if it is useful to us. For example, if we propose to raise the height of the antenna—anywhere from the present height of 35' to an upward limit of 200'—we may wish to develop detailed data about beamwidths and angles. The higher we raise the antenna in terms of wavelengths above ground, the more elevation lobes we shall encounter. Even though the lowest lobe is usually the main lobe of interest, we must also note that each lobe will have a narrower beamwidth as we increase the antenna height. This factor should be added into the data mix we obtain relative to potential skip angles we may encounter in operation. If the antenna surpasses certain heights (in terms of wavelengths above ground), we may discover that the

null between the two lowest lobes potentially deprives us of possible communications paths on some occasions.

For some of the necessary planning data, tables of values may suffice. In other instances, overlaying elevation plots can provide a graphic portrayal of both advantages and disadvantages.

The cases we have been examining were based upon simple variations upon an initial determination of the antenna's maximum gain and the elevation angle at which it occurs. For many types of antennas whose general properties at a given frequency are well established, this procedure works well and leads us quickly to the desired supplementary information. However, not all antenna properties are well known in advance for some frequencies of operation.

**Fig. 35-6**

As a case in point, consider the antenna in **Fig. 35-6**. It is a 40-meter off-center-fed antenna, with the transmission line set at approximately the 300-Ohm position on 7.15 MHz. The antenna is of #14 wire and models a transmission line of about 410 Ohms, that is, 1" wire separation. The line is 35' long, with the antenna positioned 70' above average ground.

The question we might pose is what the maximum gain might be for the antenna and at what TO angle, if we operate the antenna on 28.5 MHz. For our exercise, we shall present the antenna along the X-axis so that in the plots to follow, it would appear as a line from left to right across the center of the azimuth plots.

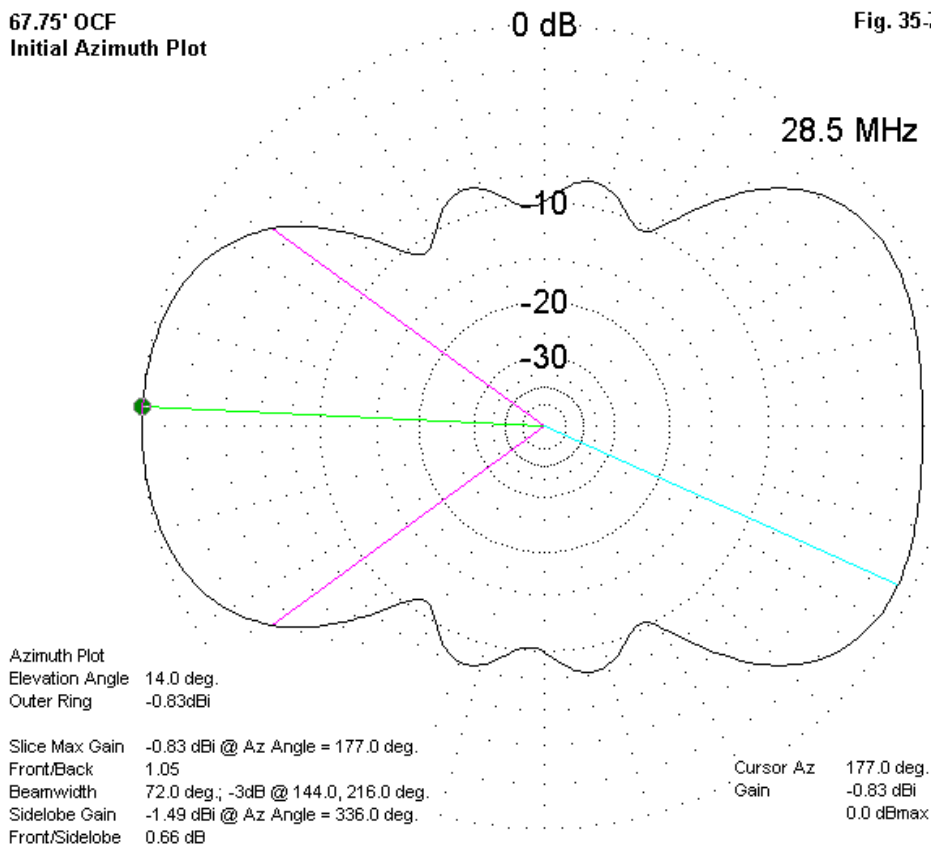
We shall quickly discover that the antenna pattern is neither broadside to the wire nor off the wire ends at the frequency of operation. In order to answer our questions, we shall have to develop a procedure that allows us to “creep up” on the values for maximum gain and TO angle.

In many instances, experience with similar antennas may let us start the process fairly close to the final values. However, for illustrative purposes, let's choose an arbitrary beginning point. We shall take an azimuth pattern at 14 degrees elevation and see where it leads. The pattern appears in **Fig. 35-7**.

From the azimuth pattern we obtain 2 critical pieces of data. For reference, we shall record the gain (a low value of -0.83 dBi). As well, we shall record the azimuth angle of maximum radiation: 177 degrees.

67.75' OCF
Initial Azimuth Plot

Fig. 35-7



The next step is to request an elevation pattern at the azimuth angle of 177 degrees. From this elevation pattern, we obtain a new elevation angle of maximum radiation, 141 (or 39) degrees. So we request an AZ pattern, using the new EL angle value. We continue the process until the AZ and EL patterns provide the same gain value and until the EL and AZ angle coincide on the respective plots. For this exercise, the following table summarizes the steps that led to final values.

Preset Angle Type	Preset Angle	Current Pattern Type	Max. Gain dBi	Angle of Max. Gain
EL	14	AZ	- 0.83	177
AZ	177	EL	6.20	141 (39)
EL	39	AZ	6.60	19
AZ	19	EL	7.11	22
EL	22	AZ	9.02	34
AZ	34	EL	9.76	7
EL	7	AZ	9.90	37
AZ	37	EL	9.90	7

**67.75' OCF:
Final Azimuth Plot**

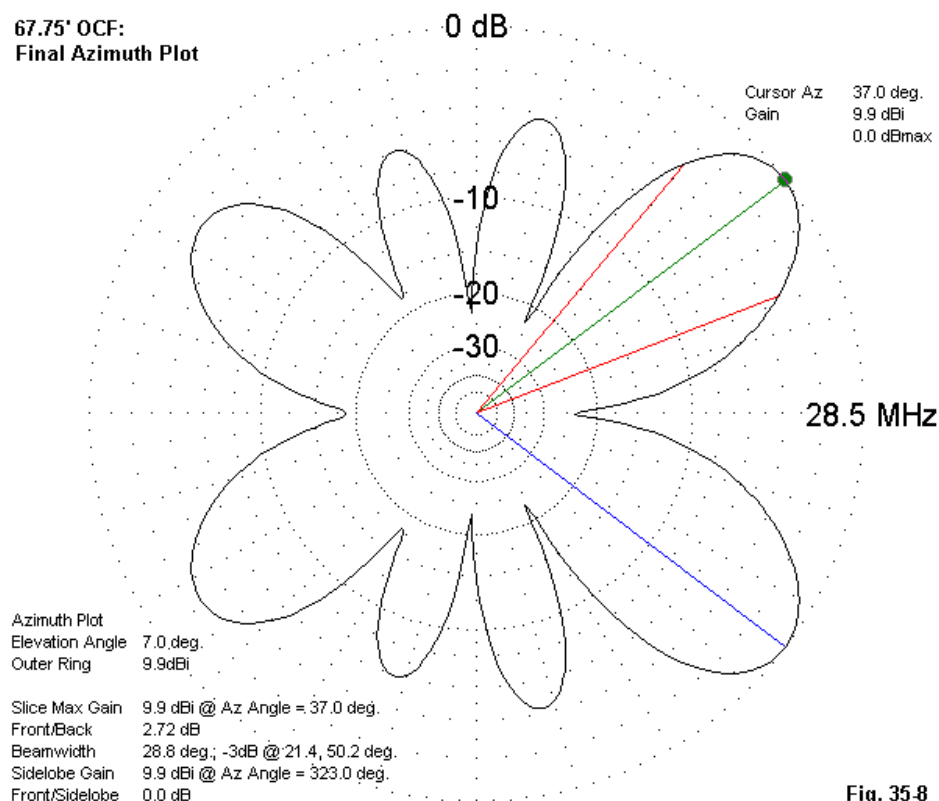


Fig. 35-8

Note first that the last two steps in the table replicate the maximum gain. As well, each plot uses the other's angle of maximum radiation as the preset angle. This is generally the sign that one has arrived at the correct gain and angle values. There are some patterns so complex that it may be necessary to sample other regions of the overall plot fields, but these tend to be rare. Ordinarily, the number and placement of lobes will be a guide to suggesting further exploration.

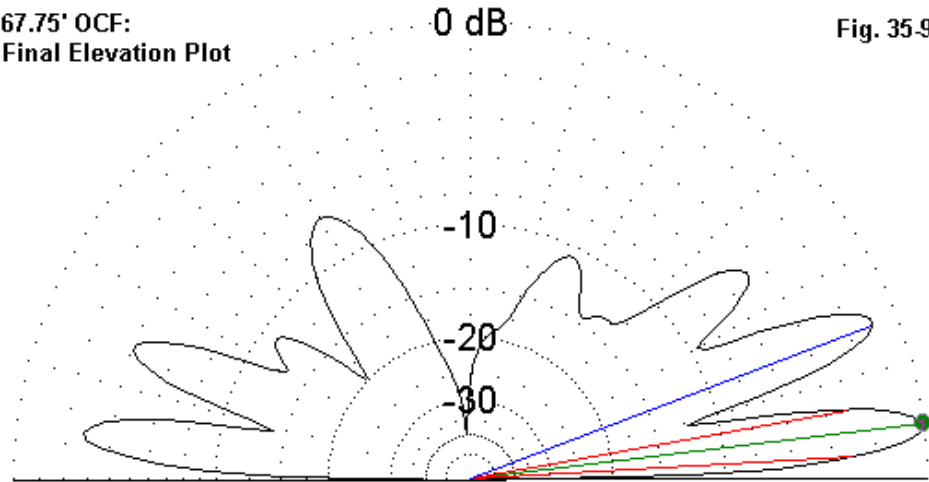
Fig. 35-8 provides a second factor to note. The AZ pattern clearly shows a null in the final pattern just where the initial pattern shows a lobe maximum. In the exploration of complex radiation pattern structures, it is never wise to assume that an AZ pattern retains a particular shape as we change the elevation angle. Although the antenna we used in the exercise seemed to be simple in geometry, it was actually fairly complex. The horizontal portion consisted of a 2-wavelength collinear element. Since the parallel feedline does not have equal currents at its terminals, the line is unbalanced and makes a net contribution to the overall radiation pattern. The result is a complex radiation pattern whose elevation plots change with every change of azimuth bearing.

Part of the pattern complexity appears in **Fig. 35-9**. We should note that the AZ heading for this plot is 37 degrees, that is, an angle that is neither along the plane of the wire nor broadside to it. In any data presentation, it is often useful to mention this fact, since viewers tend to make erroneous assumptions about the azimuth bearings of elevation plots unless the correct bearing is called to their attention. It is for this very reason that I have moved the data from outside the plot region directly into the plot area.

In addition, we may note that the special elevation angle that was counted on a 0-180 degree scale. When counted above the horizon, the angle of 141 degrees translated to 39 degrees. Some programs restrict elevation angles to the range of 0 through 90 degrees. Had we used the 141-degree angle, the maximum gain heading would have appeared on the opposite side of the plot. That position might well have led to wrong conclusions about the actual direction of maximum radiation.

67.75' OCF:
Final Elevation Plot

Fig. 35.9



Elevation Plot
Azimuth Angle 37.0 deg.
Outer Ring 9.9dBi

Cursor Elev 7.0 deg.
Gain 9.9 dBi
0.0 dBmax

Slice Max Gain 9.9 dBi @ Elev Angle = 7.0 deg.
Beamwidth 7.1 deg.; -3dB @ 3.4, 10.5 deg.
Sidelobe Gain 8.9 dBi @ Elev Angle = 21.0 deg.
Front/Sidelobe 1.0 dB

28.5 MHz

One technique for sorting out the various lobes, nulls, and oddities (if any) of the overall radiation pattern of a given antenna is to use a 3-D plot. 3-dimensional plots are commonly found in commercial implementations of NEC (and MININEC). They generally use a larger step size between azimuth and elevation pattern readings than might be used in 2-dimensional AZ and EL in order to speed the execution of the plot. However, they can be valuable adjuncts to the detailed information provided by standard AZ and EL plots.

3-D Oblique View:
Wire is Along the
X-Axis

Fig. 35-10

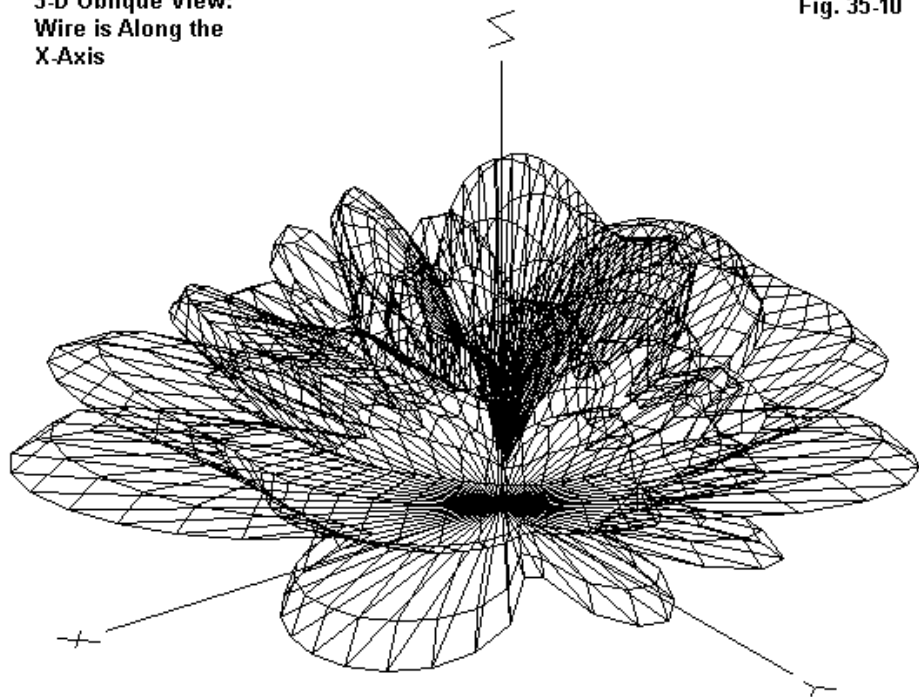


Fig. 35-10 provides an oblique view of the OCF that we have been exploring. Although the wider step size changes smooth curves into sharp angles, we can clearly see the exceptionally complex structure of the lobes and nulls at most elevation and azimuth angles. The pattern is oriented to place the strongest lobes, as revealed by the AZ and EL plots in **Fig. 35-8** and **Fig. 35-9**, in the foreground. (Hence, the axis letters appear as mirror images.)

3-D View End-On
Along the Plane of
the Wire

Fig. 35-11

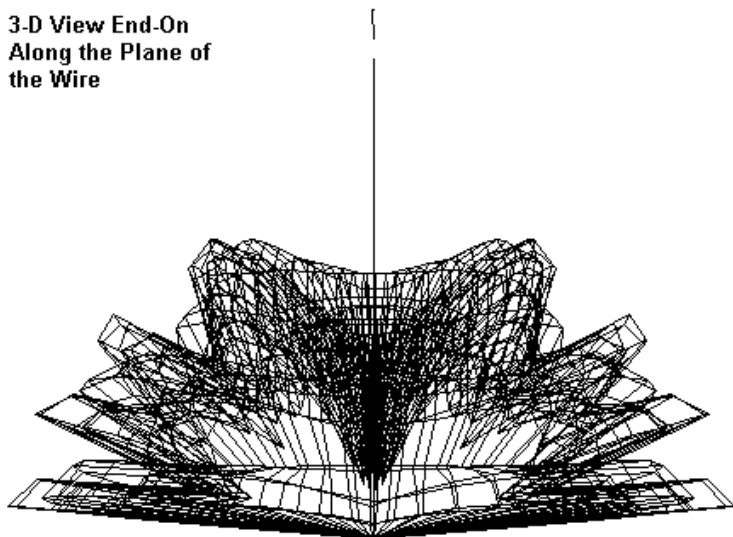
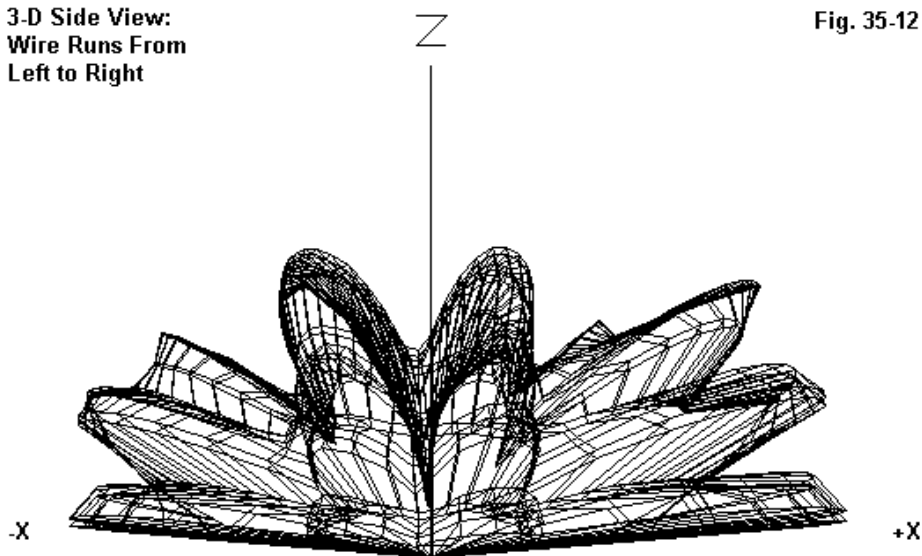


Fig. 35-11 presents a 3-D view of the patterns as viewed down the antenna wire from its end. This view is useful to establish that there are no broadside patterns stronger than the one we identified as the lobe of maximum gain. As well, we can see that there are no significant lobes below the angle of maximum radiation.

Fig. 35-12 presents a 3-D view of the pattern with the wire running directly from left to right. This view gives us a sense of the strength of the pattern off each of the antenna ends, with the long side of the antenna obviously yielding the strongest pattern. The view also confirms that there are no lobes at upper levels stronger than the one identified as the lobe of maximum radiation.

**3-D Side View:
Wire Runs From
Left to Right**

Fig. 35-12



Some programs enable the user to specify a 2-D pattern from within the context of the 3-D pattern. To use this provision, one simply specifies graphically the “slice” desired for the 2-D view. In many cases, using both 3-D and 2-D patterns in conjunction can resolve more quickly the problem we set for ourselves of identifying the lobe of maximum radiation strength.

With some antennas—for example, VHF antennas at large heights above ground, the multiplicity of elevation lobes may elude 3-D analysis and yield a false picture of the radiation pattern structure. A pattern, whether 2-D or 3-D, simply connects the dots between readings. 5 degrees is barely sufficient for lobe identification at the frequency and height of the present antenna. For 2-D patterns, 1-degree steps between readings generally suffice for most HF antennas at any reasonable height and for VHF antennas at lower heights. Above about 5 wavelengths in height, the use of a 0.1-degree step is advisable in 2-D plots in order to ensure that you capture all elevation lobes.

The cases we have examined in no way exhaust the potentials for AZ-EL plots to provide the modeler with useful information. However, they hopefully provide a start toward making new and productive use of this facility for those whose work has not yet gone beyond the “standard” sorts of patterns with which we began.

* * * * *

Models included: 35-1 through 35-2. (.NEC and .NWP model dimensions in meters; .EZ model dimensions in feet.)



36. Getting a Grip on AZ/EL and Phi/Theta

Among the unappreciated subtleties of NEC (in any version from -2 to -4) is the fact that the radiation pattern outputs make use of different conventions from those we ordinarily apply to antennas in both amateur and field engineering work. We tend to think of the horizontal dimensions for an antenna pattern in azimuth terms, which correspond to the headings on a standard compass. For elevation, we count from the ground upward.

However, the NEC core does its work with radiation patterns using the conventions of phi and theta angles. Folks using “raw” NEC must either adopt the phi/theta angle counting scheme or be ready to make conversions into azimuth/elevation (AZ/EL) on a scratch pad. Those using commercial implementations of NEC have access to pre-conversions that show up as AZ/EL headings in the graphical and tabular outputs of NEC programs. In some programs, users may have a choice of graphical labels for some plots.

However, not everything may be as it seems, that is, as pure elevation and azimuth plots. Therefore, perhaps it may be useful to start at the beginning and carry ourselves into the conventions used by at least a couple of commercial programs. In this way, we can become prepared for almost anything.

In the course of our discussion, we shall uncover some implementation schemes that use the term “azimuth” but which are not quite pure azimuth structures. Our purpose in noting these departures is not to be critical. Very often, there are good programming reasons for the variants. We need to understand what is before us and how to interpret it well, and that will be our primary goal in looking at the structures of pattern plots.

Elevation and Theta

The simple beginning in our effort to get a handle upon both theta angles and elevation angles is to differentiate the two systems. The rule of thumb goes something like this: theta angles count downward from the zenith heading (directly over-

head along the Z-axis on the coordinate system). Elevation angle count from the horizon upward. Hence, for starters, we can think of a horizon as 90 degrees theta or zero degree elevation. Likewise, directly above the antenna is zero-degrees theta and 90-degrees elevation.

This simple convention works well for some purposes. For example, when we specify the elevation angle in a commercial version of NEC, we enter a value between 0 and 90. Likewise, if we specify a theta angle, we normally specify a value between 90 and 0. This practice is necessary when requesting an azimuth pattern for an antenna over real ground.

However, this step is only the beginning of our understanding of how NEC counts. Examine **Fig. 36-1**. The circle in **Fig. 36-1** represents a free-space 360-degree set of bearing that is possible for an antenna in free space. (The proper name for a free space pattern in this set of directions is an H-plane pattern, if the antenna is a horizontally oriented Yagi that would be parallel to the earth's surface—if there were an earth with a surface.) For antennas above ground, we use only the upper half of the circle. To understand how the NEC calculating core performs its radiation pattern duties, let's look on the inside of the circle. By convention, the direction to the right is the primary heading for theta (and for elevation) angles, and its theta value is +90. As we move up the circle, the angle decreases to 0. Moving back down the circle to the left, we find -90 as the value. This scheme is convenient, since for antennas above the horizon line, we have values between 0 and 90 in both directions.

The situation becomes somewhat more complex if we extend the circle to the full 360 degrees for a free space pattern. By the time we return to our starting point, the inner circle reads -270. In many ways, this is a perfectly sensible scheme, since we can simply specify +90 degrees as the finish point for any theta pattern, whether over ground or in free space. The starting point then becomes 90 degrees minus 180 degrees for patterns over ground or 90 degrees minus 360 degrees for patterns in free space. (Remember that for NEC-2 patterns over ground, direct horizontal values (+90 and -90 degrees theta) are illicit.)

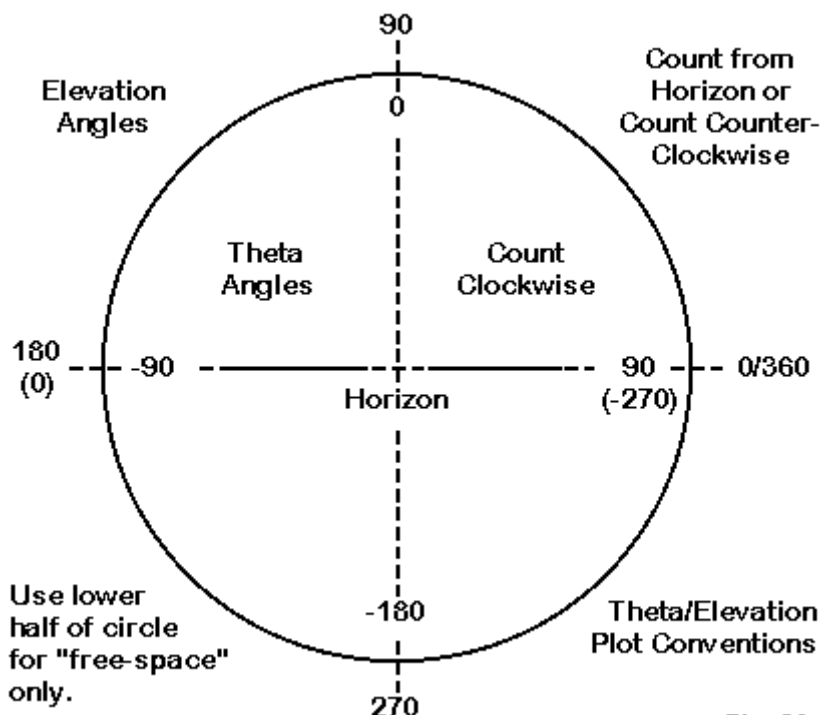
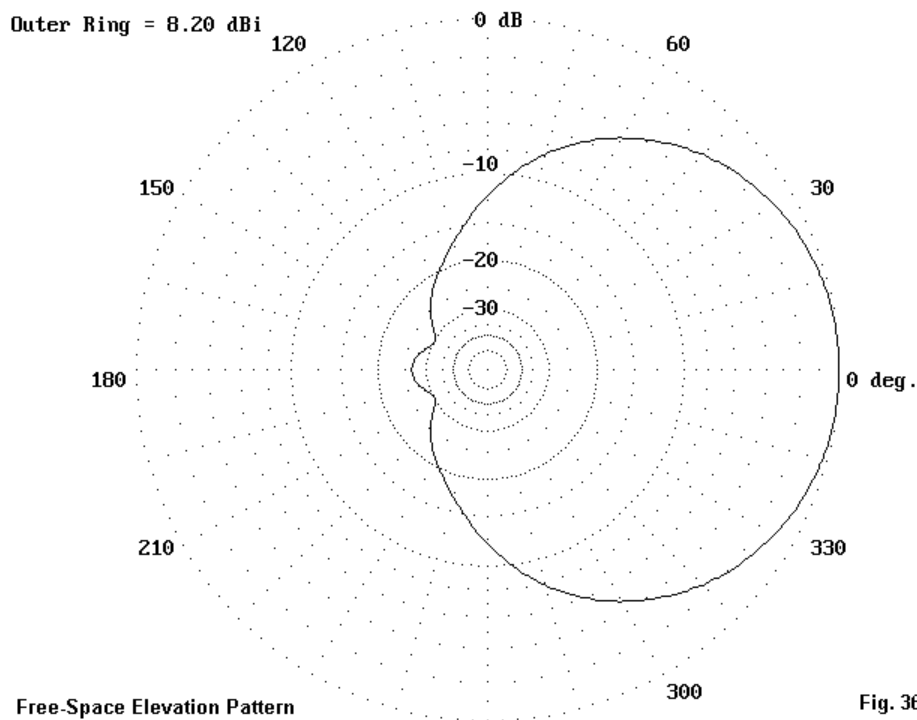


Fig. 36-1

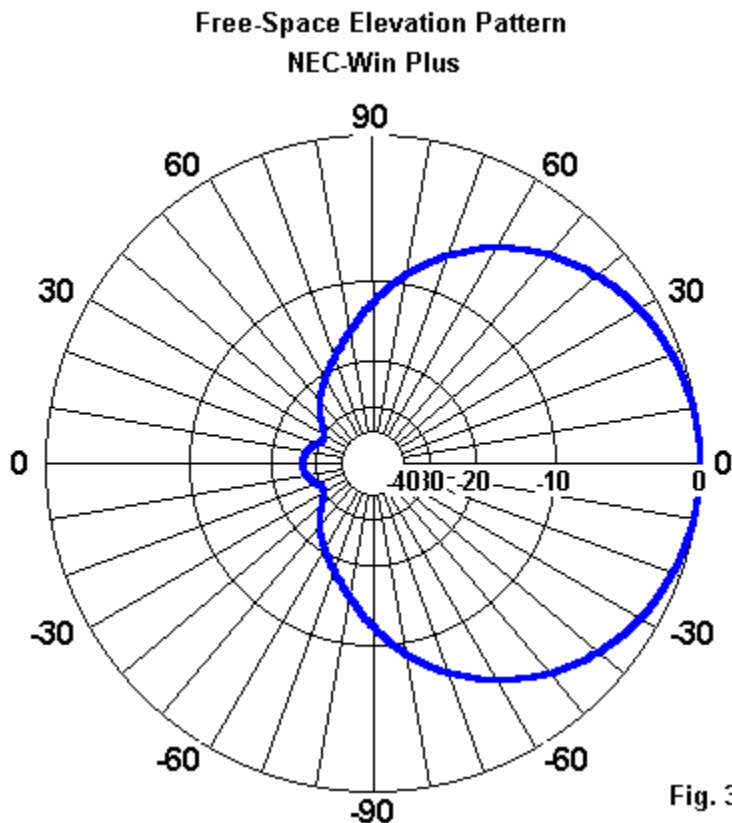
If we turn our attention to the labels outside the circle, we encounter the conventions applicable to elevation patterns. Over ground, we have two choices, in the main. We can count upward from the right from 0 to 90 degrees overhead and back down to 0 at the left horizon point. Alternatively, we can count from 0 to 180 degrees moving from the far right to the far left. This latter scheme is useful when we wish to deal with a free-space pattern, since we can continue the count to the low point value of 270 and then back to 360 or 0 degrees.

Notice that on a circle, theta values increase in a clockwise direction, while elevation values increase in a counterclockwise direction—if we adopt the convention of placing the prime direction or orientation to the right on the graph.

One of the commercial implementations of NEC that I use, EZNEC, uses elevation angles instead of theta angles, since elevation is the standard used by most practical antenna folks. The program's graphical output for elevation patterns of all types uses a single set of labels, shown in the free-space pattern for a 3-element Yagi in **Fig. 36-2**.



The EZNEC scheme exactly follows the conventions shown in the general scheme in **Fig. 36-1**. Incidentally, version 2 of EZNEC is used for this exercise, since the patterns show the labels at all times. Version 3.0 is now available for Windows, and it uses the same scheme. However, the graphical angles are not labeled.



Another NEC program that I regularly use is NEC-Win Plus. It offers the user a choice of theta or elevation angles for the plots. Moreover, the user can also select from 4 different sets of labels for elevation/theta plots (with the designations arranged from left to right on the actual graphic):

1. -90/0/90 (theta)
2. 180/90/0 (elevation)
3. 0/90/180
4. 0/90/0

The first two selections replicate the standard theta and the elevation scheme also used by EZNEC. The third option is useful for reversed patterns. The fourth provides elevation angles in simple numbers for both directions away from the zenith. **Fig. 3** provides a sample of a free-space pattern using the 0/90/0 scheme. Notice that area below the hypothetical horizon uses negative values, with the lowest point using a -90 degree value.

Differences in the conventions used—either as provided by the software writer or as selected by the user—begin to show up in elevation patterns for antennas above ground. Let's set our 3-element Yagi about 1 wavelength above ground. See model 36-1. In the EZNEC scheme, the new elevation pattern looks like **Fig. 36-4**.

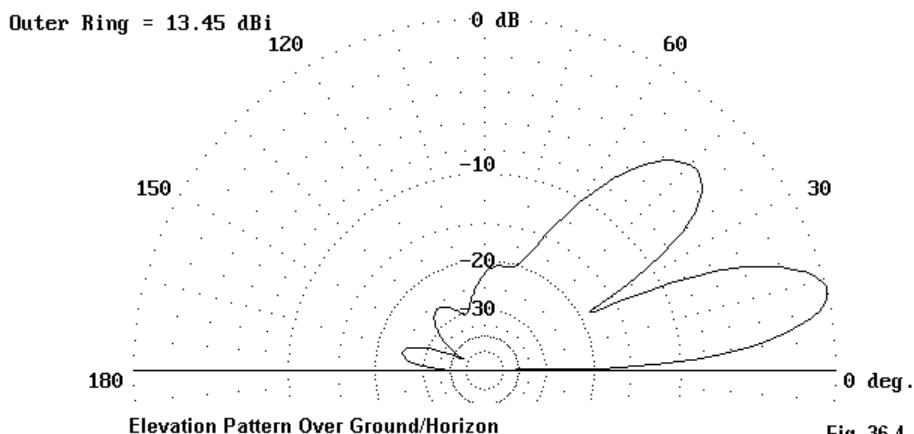
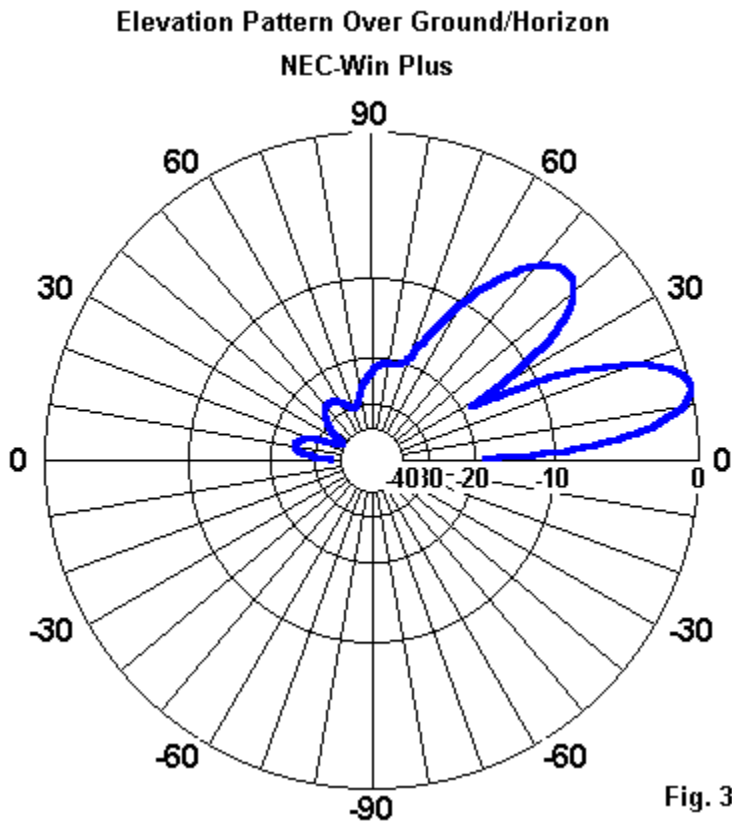


Fig. 36-4

The 0-90-180 degree counting scheme (from right to left) requires that the user do some mental or pencil arithmetic to determine the elevation angle of the lowest rear lobe in the figure—which happens to be 13 degrees—the same as the main forward elevation angle. Not all antennas yield such symmetry.



The NEC-Win Plus pattern (**Fig. 36-5**), using the 0/90/0-degree elevation scheme obviates the need for the simple arithmetic, although accurate location of the rear lobe angle would require that I alter the graphic by choosing 1. thinner lines for the plot and 2. a full screen plot that would be too large for easy replication in the format used in these columns. Both programs offer a wide selection of color and line widths to suit user preferences and specific applications of the graphics.

In general, the differences between implementations of elevation pattern heading conventions are too slight to make a difference in how we use the programs. In all cases, we can easily arrive at the elevation angle we need to use in the overall antenna analyses we perform.

Azimuth and Phi

Theoretically, the differences between azimuth and phi angle systems are less complicated than the ones for elevation and theta. With azimuth and phi patterns, we always count a full 360 degrees around a circle, as shown in **Fig. 36-6**. We simply count in different directions. However, the use of the upper point of the circle as the starting or zero point is arbitrary.

The inner part of the circle shows the phi counting scheme (used by the NEC core), which moves counter-clockwise around the circle. The outer labels show the standard azimuth scheme, which counts clockwise around the circle. The two schemes coincide at zero and 180 degrees.

Since free-space phi or azimuth patterns of antennas that would be horizontal if over ground closely resemble the patterns of those same antennas at their take-off or TO angle, we can by-pass a sample. However, the proper name of such free-space patterns is E-plane patterns. To avoid an undue multiplication of labels, NEC programs simply carry the pattern names applicable over ground into free space.

Some small difficulties of user orientation arise when implementations of NEC develop the azimuth pattern graphics for their programs. Then we begin to see some variations on the standard azimuth scheme. Most of the variations result from the fact that converting a phi pattern requires—for complete conversion to azimuth conventions—a full conversion of the data table that NEC produces. A simple re-labeling of the headings will not suffice to do a complete job. Hence, we find some shortcuts.

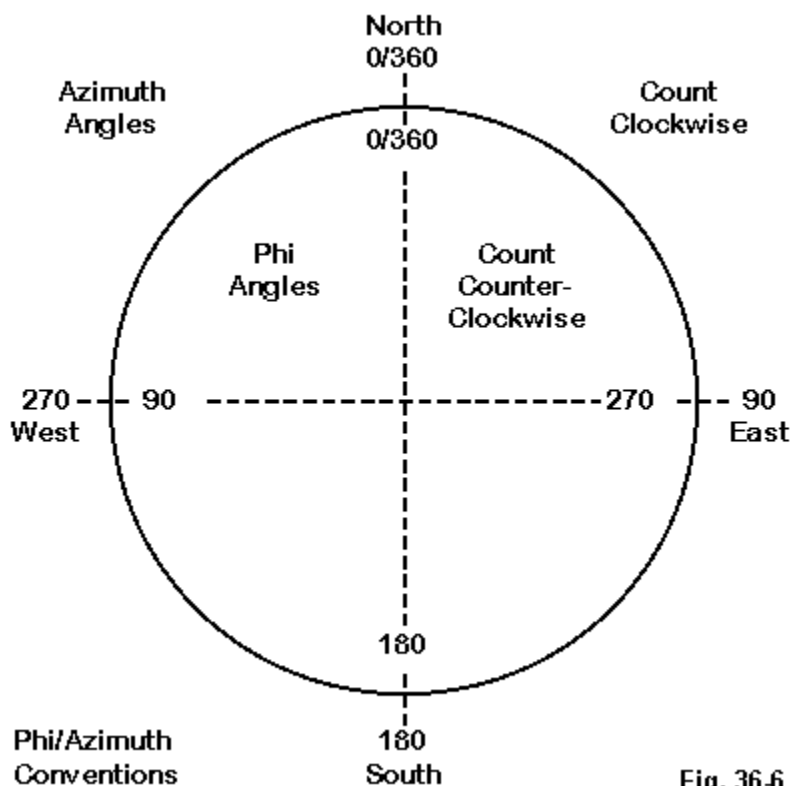
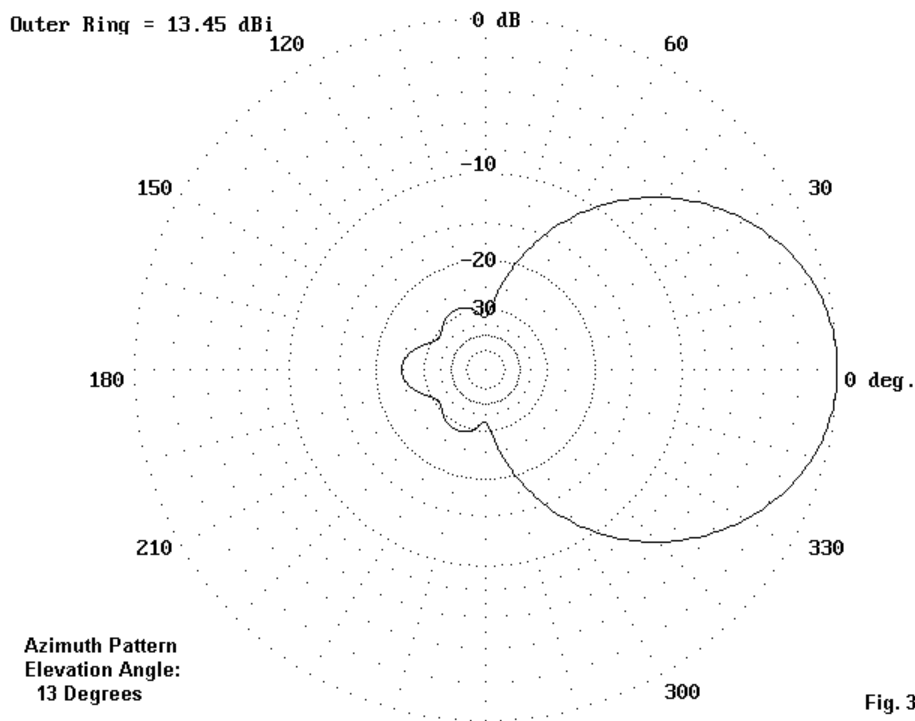


Fig. 36-6

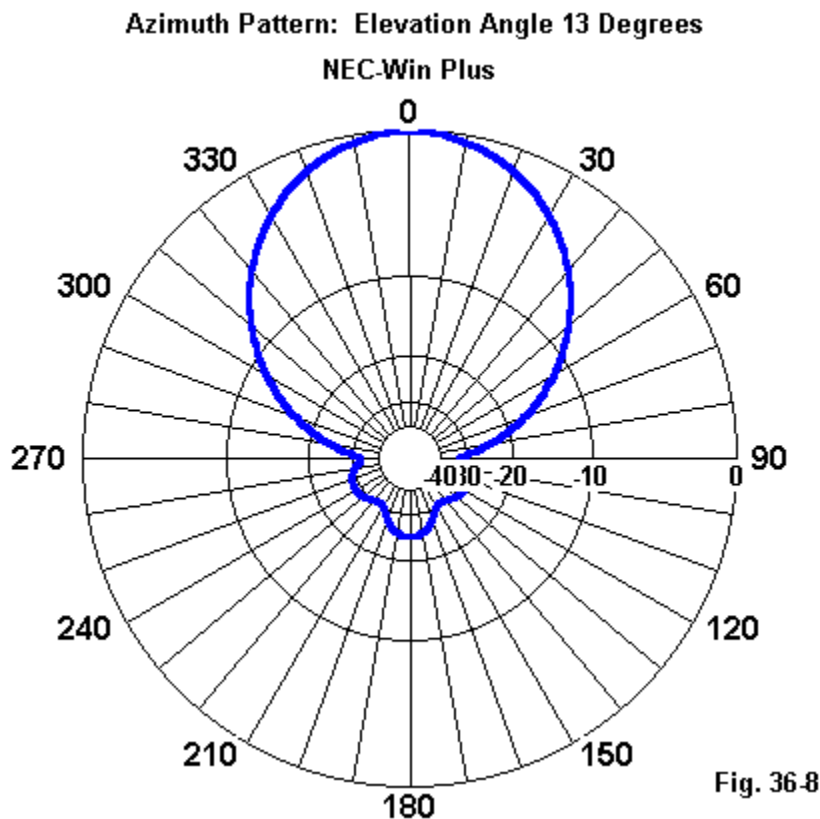
Fig. 36-7 shows the azimuth pattern of our 3-element Yagi at a height of 1 wavelength above ground. By setting the elevation angle to the “take-off” angle or the angle of maximum radiation (13 degrees in this case), we obtain an azimuth pattern. Note that EZNEC (Version 2) sets the zero point to the right. In this manner, the

background graphical setting, consisting of dots and heading numbers, is the same for both azimuth and elevation patterns. However, 90 degrees is not clockwise to the left of the zero point, but counter-clockwise to the right of the zero point. EZNEC's azimuth patterns are actually phi patterns.



In the latest (Windows) version of EZNEC, the label-less pattern grid avoids the problem of orienting oneself to either phi or azimuth conventions. The user has a choice between counting counter-clockwise from zero (the phi convention) or using compass bearing (the azimuth convention), but this choice shows up only in data entries.

In **Fig. 36-8**, we see the NEC-Win Plus azimuth pattern for the same antenna under the same conditions. NEC-Win Plus sets the zero point at the top of the graph and labels everything in standard azimuth terms. So far, it appears that orientation in the azimuth scheme presents no problem at all.



The question of orientation toward the graphical pattern outputs does not become readily apparent until we decide to construct models in alternative ways to those most often used. For example, all of the models of the 3-element Yagi we have so far examined extend their linear elements along or parallel to the Y-axis. The forward portion of the antenna (or the front end of the boom) has a positive value on the X-axis, while the rear has a negative X-value.

Now let's reverse the procedure. We shall model the same antenna with the linear elements extended left and right along or parallel to the X-axis. The front of the array will have a positive Y value, and the rear will have a negative Y-value. If we run this model, it will show exactly the same gain, front-to-back ratio, source impedance, and element currents as the first model. So the only remaining question is how it will appear in the azimuth pattern graphics.

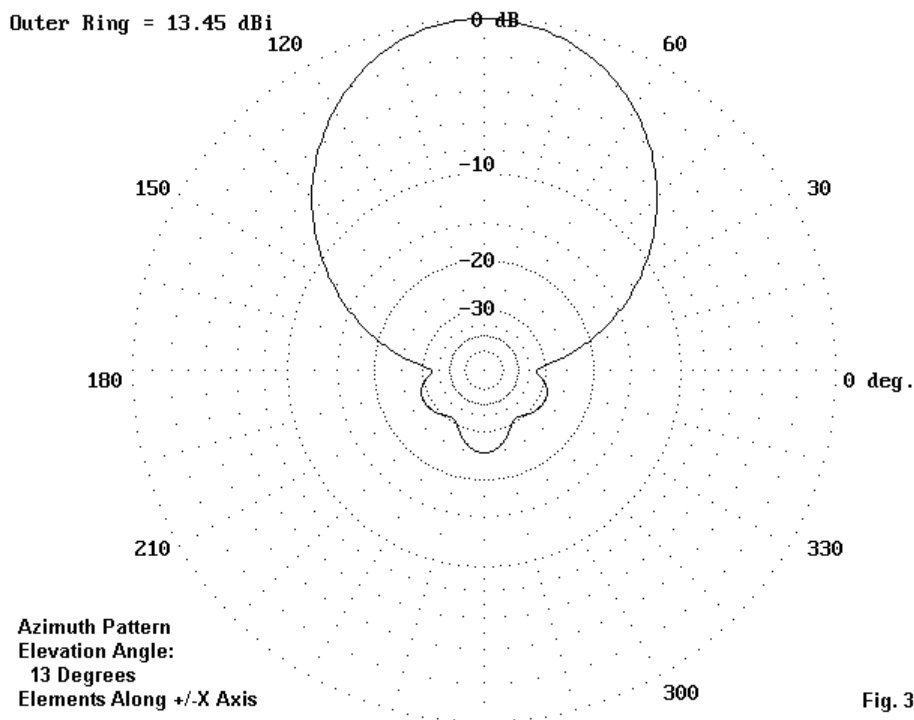
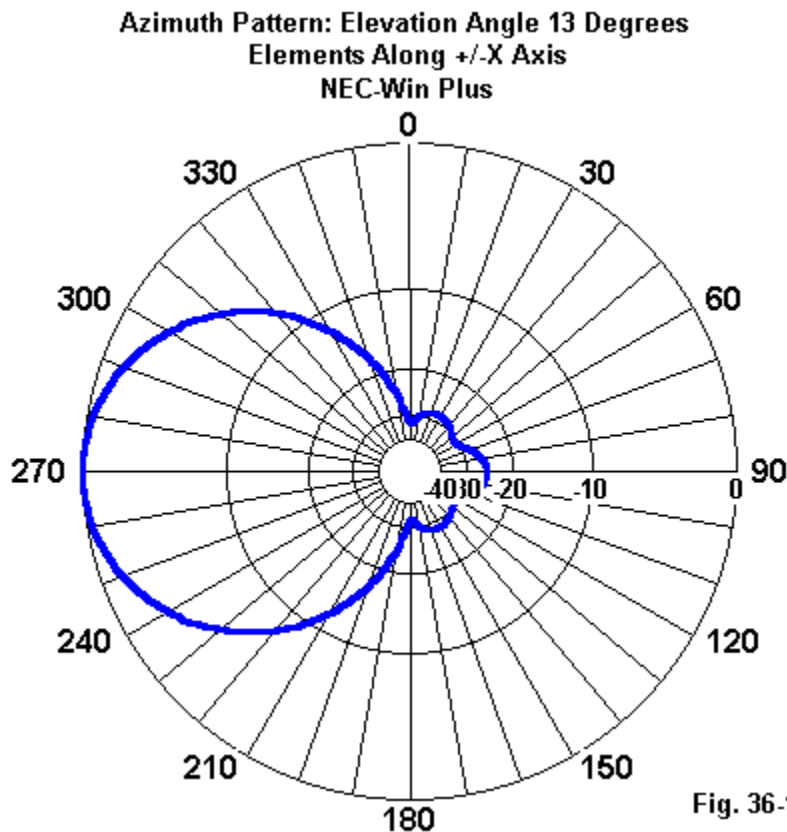


Fig. 36-9 shows the EZNEC version of the azimuth pattern. The forward lobe points toward 90 degrees, the heading of the Y-axis for positive values. However, contrary to azimuth conventions, the graphical heading is counterclockwise relative to the zero point. In short, we have a phi pattern.

**Fig. 36-10**

In **Fig. 36-10**, we have the NEC-Win Plus azimuth pattern. In this case, standard azimuth counting is employed in a clockwise direction. However, to place the pattern without converting the NEC table, the forward heading of the pattern now points to 270 degrees, the opposite direction of the positive forward Y-values (which would normally go to 90 degrees on a standard azimuth pattern).

My point in setting these items into print is not either to review the two software implementations of NEC or to be critical. Rather, the aim is to orient the user so the he or she understands how to read the data that appears on these patterns. Initially, the differences of each from standard azimuth patterns are negligible because the antennas for our test produce symmetrical patterns along their centerlines. Hence, left and right make no difference at all.

Not all antennas yield symmetrical patterns, and in some cases, left and right can make anywhere from a small to a large difference.

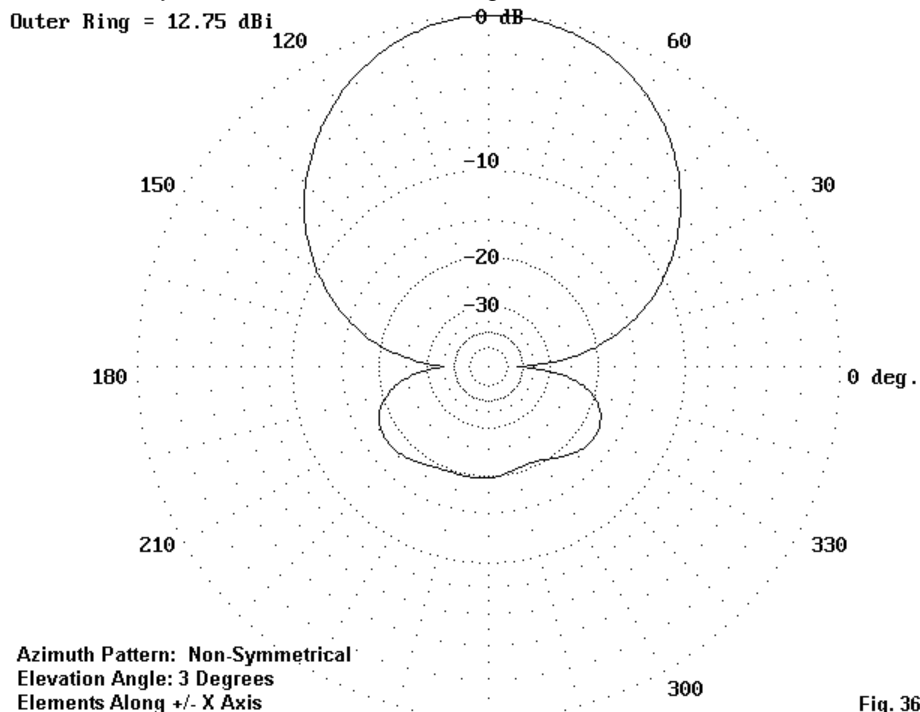
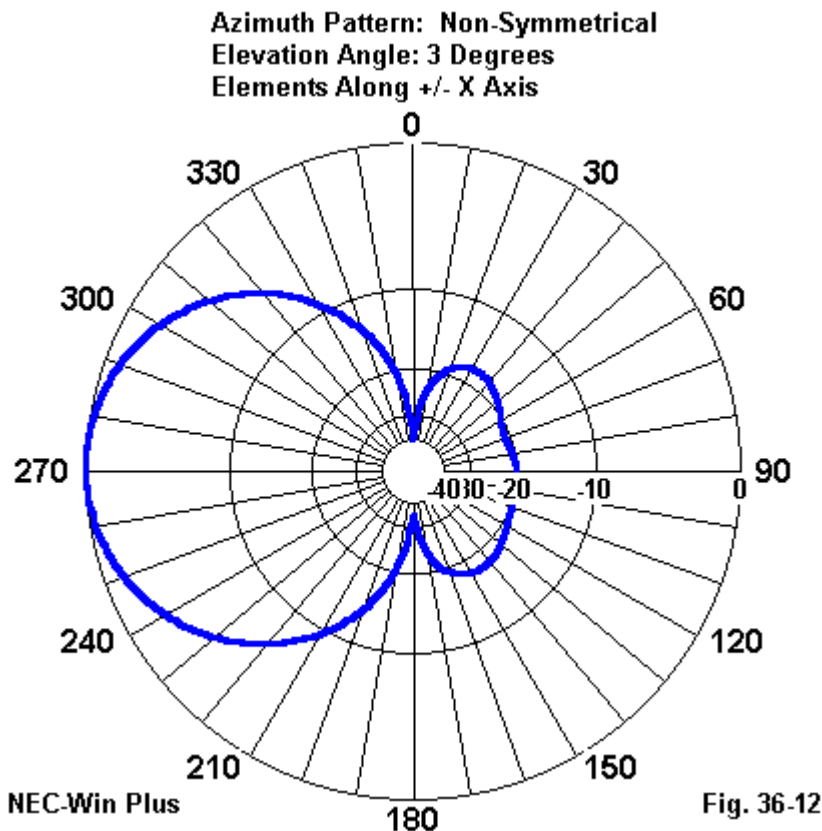


Fig. 36-11

To illustrate, let's use an antenna with only a small non-symmetry. It is a parasitic beam for 2-meters at a height of about 30' and modeled with the elements in the +/-X axis and the forward direction as a positive value of Y. **Fig. 36-11** is the azimuth pattern in EZNEC, with the forward direction at 90 degrees. However, notice the rear quadrants, where the pattern becomes obviously larger on one side than on the other. The pattern in this case shows the larger lump at about 215 degrees, about 125 degrees from the forward direction. The actual point in the rear where the signal strength is greatest is on the more diminutive rear lobe, about 125 degrees in the other direction from the forward lobe centerline. Note that we have to determine each differential by arithmetic. As well, the increasing values of the heading



as we moved left would be what we might expect had we been using a phi pattern rather than an azimuth pattern.

In **Fig. 36-12**, we see the NEC-Win Plus equivalent pattern. The bearing differentials are the same, but this time measured from a forward heading of 270 degrees—180 degrees in reverse of our expectations from having set the forward heading in the positive direction along the Y-axis. However, the increasing values to the right of the forward lobe are consistent with the standard azimuth conventions.

In each case, the exigencies of software development have created slight differences in the manner in which azimuth patterns are portrayed. For a symmetrical pattern, the differences make little or no difference and one can make few errors by virtue of the non-standard presentations. However, with non-symmetrical patterns, errors are possible. Although not likely to be significant in the case we are using as an illustration, the errors might well be important in other instances. Many off-center-fed multi-band antennas, for example, show a pattern that is very sharply stronger to one side of center than to the other. There are arrays that are directional by virtue of the element phasing relationships rather than by virtue of geometry. In all such cases, the critical question is this: which side is which?

The answer is fairly straightforward: ignore the heading numbers and place yourself as an ideal observer at the center of the pattern. Face in the direction that represents forward in the coordinate system within which you created the antenna structure. Non-symmetries will now be correctly identified in terms of left and right relative to your position. If you place a zero or north in the direction you are facing, then east will be to your right and west to your left. The pattern will be correct in either program for this way of looking at things.

Fig 36-13 is a graphic representation of the way to ensure that you are correctly oriented toward a non-symmetrical azimuth pattern, whatever its outer markings. Imagine yourself at the center of the antenna and the pattern. The antenna we are using here is a 2-element half-square—hence, the vertical elements at the ends of the horizontal phase lines. Since the horizontal members are parallel to the X-axis, the forward direction is in a positive direction in the Y-axis. Notice that the feedpoint is on the side of the antenna showing the larger rear lobe.

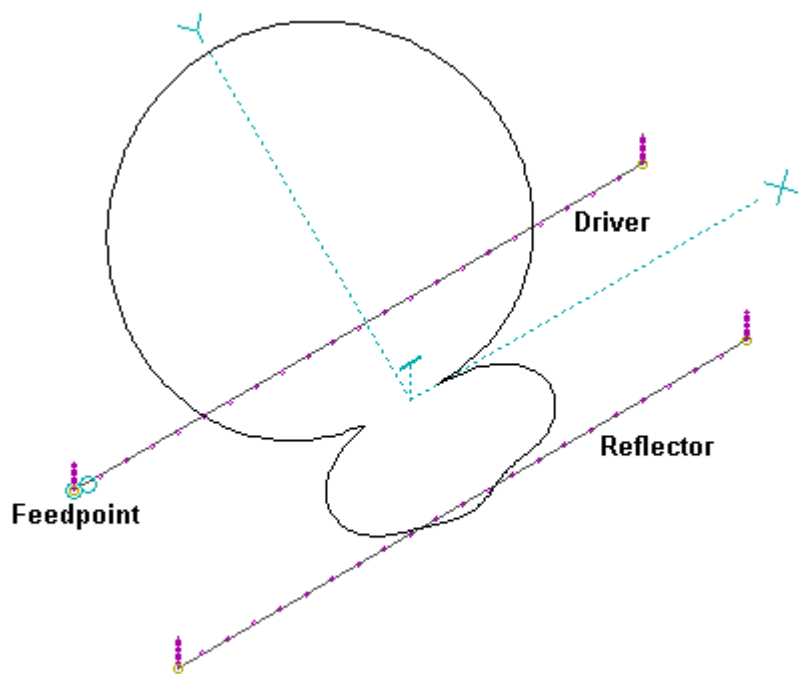


Fig. 36-13

**Half-Square Parasitic Beam
Elements Along +/-X Axis
Azimuth Pattern Superimposed**

We have noted that the latest version of EZNEC has an option to use compass bearings instead of counting counter-clockwise from the X-axis. The latter system is the one used in earlier versions of the program and shown in the illustrations so far. The new option is more than a way to count clockwise in the azimuth manner. It

changes, for some modeling exercises, the way we should model to have the antenna pattern register as facing north or to zero degrees.

Azimuth Pattern: Non-Symmetrical
Elevation Angle: 3 Degrees
Elements Along +/- X Axis

Fig. 36-14

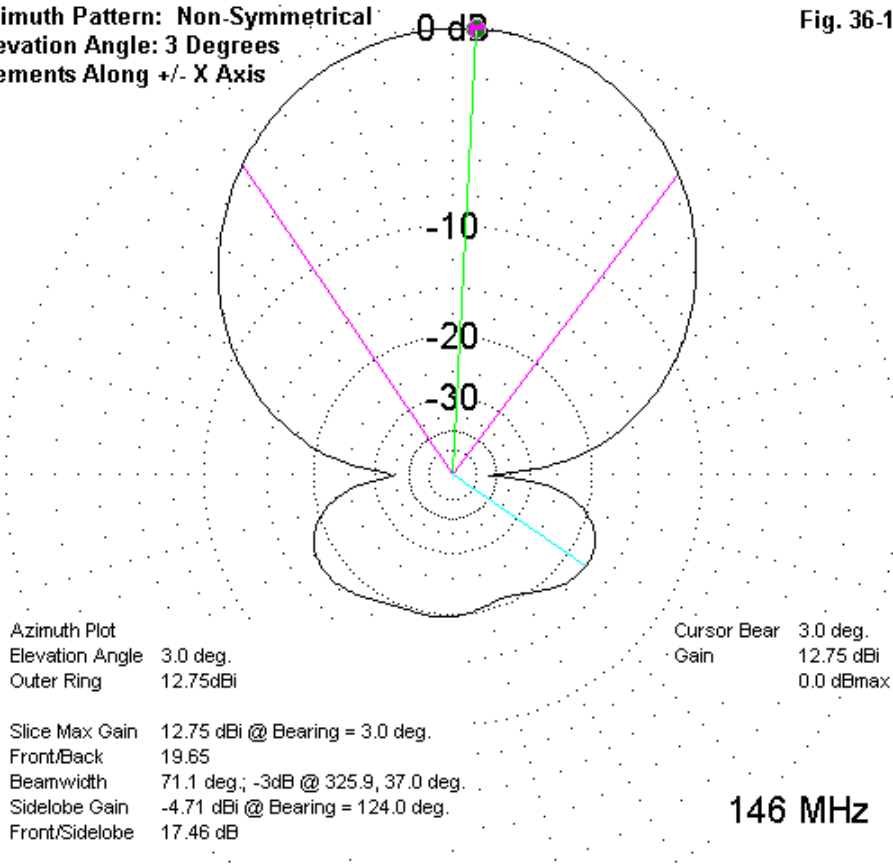


Fig. 14 illustrates an azimuth pattern in the new mode. As with the other patterns for the half-square beam, the horizontal portions of the elements are parallel to the X-axis, with the forward direction defined as a positive value of Y. The height requires a 3-degree elevation angle to record maximum radiation on the azimuth pattern. Because the antenna presents a slightly non-symmetrical pattern, the main lobe is offset 3 degrees from zero.

Note that to place the forward direction at zero-degrees on the pattern, one must model the antenna with the element extending parallel to the X-axis. This is the opposite convention from the one used in other implementations of either phi or azimuth patterns, where the elements must parallel the Y-axis to get a forward reading of zero degrees.

Although the pattern bears no heading labels, it does read correctly with respect to azimuth headings. Notice the line in the rear right quadrant, indicating the strongest side-lobe. The line, from the data series below the graphic, shows a bearing of 124 degrees, which is a correct number in azimuth terms relative to the zero heading directly up the page.

The purpose in surveying all of these options and variants of elevation/theta and azimuth/phi labels on graphics is to make you aware of the differences. By becoming aware of them, they will not take you by surprise when you develop and then interrogate a pattern. You will know in advance the conventions themselves and the particular ways in which they are implemented by at least some software. You should be able to adapt these notes to cover any other piece of modeling software that you may be using.

Since in all cases, the patterns are correct and correctly oriented to an ideal observer, the labels are simply ways to keep track of various facets of the pattern. Should absolutely correct azimuth labels be essential to some form of presentation, you can always run a screen grab of a pattern and then process it through a painting program. You need only change the labels to a set that is most suited to the presentation task.

However, over time, all software changes. So these notes may turn out to have only a short-term of direct relevance to the software packages from which I drew the examples. One of those changes likely to occur in the next few years is the incorpo-

ration of true azimuth inputs to one or more NEC programs, as an alternative to the present strict use of counterclockwise Cartesian coordinates. Since the NEC core requires Cartesian coordinates, the program will need to write a conversion table for the core's input file. The contexts within which compass bearing inputs are common include broadcast engineering and similar work. As well, those wishing to transfer modeling output files to propagation software in VOACAP format will also have use for this kind of input system when setting up complete fields of antennas. Compass-heading-input users will also want a true azimuth-elevation output plot that correctly reflects the input file. Hence, the likely implementation of the system will include a complete output conversion table from phi to azimuth or compass-rose headings. These NEC developments, however, lie in the future, although something similar is available in the proprietary program called Expert MININEC.

* * * * *

Models included: 36-1 through 36-2. (.NEC and .NWP model dimensions in meters; .EZ model dimensions in inches.)

37. Verticals: Using the MININEC Ground

Many vertical antennas and arrays use extensive ground radial systems. A model of the radial system very often requires many times the number of segments as the antenna wires themselves. Many modelers resort to the use of MININEC or a MININEC ground system attached to a version of NEC-2 (for example, EZNEC) to avoid modeling the radials system. The run times are shorter, for starters. Additionally, some popular programs in the low-end range do not have a sufficient number of segments available to fully model a radial system and the antenna atop it.

For reasons that are not altogether clear, the MININEC ground system with a $1/4$ wavelength monopole directly connected to ground has achieved a reputation for accuracy that is denied to NEC using the same modeling scheme and the Sommerfeld-Norton ground calculation system. If the intrinsic gain figures are not themselves useful, so the reasoning goes, the comparative figures for a baseline monopole and a more complex array will be useable using a consistent MININEC ground.

One disturbing tendency that has appeared in more than one volume containing otherwise impeccable technical information has been to combine or compare without caution the results of modeling using the simplified MININEC grounding system and modeling over Sommerfeld-Norton ground, with or without radials. In addition, a second disturbing tendency has emerged: to treat any predominantly vertical array as if it were purely vertical, even if some of the elements (driven or parasitic) slope.

The MININEC ground system becomes inaccurate for some wire antennas when some or all of the height of wires in the array is below about 0.2 wavelengths. The Sommerfeld-Norton ground calculation scheme, a part of the basic NEC core, can be accurate to within about 0.001 wavelength of the ground, so long as the wire surface does not go below that level. Some research indicates that a closer approach is possible. NEC-2 calls for a limit of about 30 wires for any one junction, although with relatively thin wires, that limitation can be pressed without inaccuracies arising. Therefore, a 32-radial system is well within NEC-2 capabilities. Some

low-end NEC programs (such as EZNEC and NEC-Win Plus) have facilities for automated radial system construction. With these abilities, it is surprising that few modelers actually model the radial systems, but opt instead to use a MININEC ground with a monopole directly connected to ground.

Therefore, it would appear to be useful if we return to basics and find out what the modeling results would be for various situations involving vertical antennas and arrays using a number of different ground systems for the modeling task. In the following exercises, all of which are conducted at 7.15 MHz, I shall use a 2" diameter copper main element. All radials (where used) and guy wires employed as parasitic elements will be 0.25" in diameter and also copper. I shall use a segment length of close to 1'/segment to assure convergence of the models. Since I shall be looking at antenna over various ground qualities, the following table summarizes the categories and their related conductivity and permittivity.

Ground Quality Label	Conductivity S/m	Permittivity (relative dielectric constant)
Very Poor	0.001	5
Poor	0.002	13
Good (Average)	0.005	13
Very Good	0.0303	20
Salt Water	5.0	81

With this data to ensure uniform treatment of each example, we can proceed. Most of the modeling data presented in these exercises will be in tabular form. One note of caution: the exercises will be wholly in the realm of comparing one type of model with another. No claims are made for the accuracy of the data with respect to test range measurements.

1. The 1/4 Wavelength Monopole

Fig. 37-1 illustrates the two forms of our first exercise. I begin with a 1/4-wavelength monopole directly connected to ground. The antenna is 32.9' long and uses 33 segments. The antenna model is tested using the categories of ground quality shown in the table above.

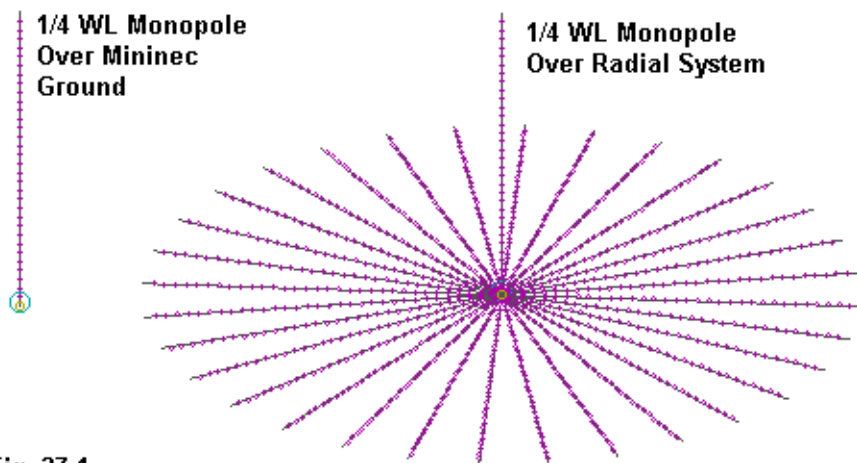


Fig. 37-1

In the first model test table, there are two columns of data. Column 1 represents the results of modeling within MININEC (3.13), which places the source directly at the ground connection point. The MININEC ground system always uses perfect ground as the basis of the source impedance report, so impedance is listed only for the “perfect” ground entry. Column 2 is the data from the use of the MININEC ground within a NEC-2 system (EZNEC). The numbers given represent the far field gain in dBi and the elevation angle of maximum radiation (TO angle). The slight differences, where they exist, result from the placement of the source in NEC within the lowest segment, rather than at its end, as is done in MININEC 3.13.

Ground	MININEC			NEC/w/MIN Gnd		
Perfect	5.14	0	35.9 - j 0.3	5.15	0	36.4 + j 1.7
Very Poor	-1.76	29		-1.76	29	
Poor	-0.28	27		-0.28	26	
Good/Average	-0.04	26		-0.04	26	
Very Good	1.94	21		1.94	21	
Salt Water	4.61	9		4.61	9	

In the following table, we have similar data in the first column, including the source impedance ($R \pm jX$ in Ohms), for the same antenna connected to ground using the Sommerfeld-Norton (S-N) ground calculation system. In the final column is data for the same antenna placed over a 32-radial ground plane that is 2" above ground. This height is close to, but not on, the conservative limit for minimum wire height above ground. The order of data is gain/TO angle/Source Z (if given). The "perfect" line is omitted. See model 37-1.

Ground	NEC/w/S-N Gnd			NEC/w/Radial System		
Very Poor	-2.20	29	40.1 + j 3.1	-1.15	29	30.7 - j 8.0
Poor	-1.29	27	45.8 + j 5.5	0.01	26	32.6 - j 5.4
Good/Average	-1.18	26	47.1 + j 4.9	0.14	26	34.2 - j 5.5
Very Good	0.89	21	46.3 + j 7.1	1.48	21	37.5 - j 2.8
Salt Water	4.57	9	36.7 + j 1.5	———		

NEC does not yield valid data for the "salt water" case for the ground plane system close to ground. Of interest in the tables are the following items.

1. With no ground plane, the NEC impedance entries are out of line with both the MININEC ground and the ground plane values. This variance represents one reason why some modelers prefer the MININEC ground for "no-radial" modeling.
2. The source impedance varies somewhat as the ground quality is changed, a feature that the MININEC ground modeling system cannot show.
3. There is no constant that one can use for all the systems to pre-estimate the change in gain value as one moves from one ground quality to another.
4. The value for the TO angle for any given ground quality is consistent for all of the ground systems examined.

The chief use of this data, however, will become apparent with the next exercise. The values shown here represent what a modeler might use as a baseline for estimating the advantages of a more complex array.

2. Two 1/4 Wavelength Monopoles Fed In-Phase

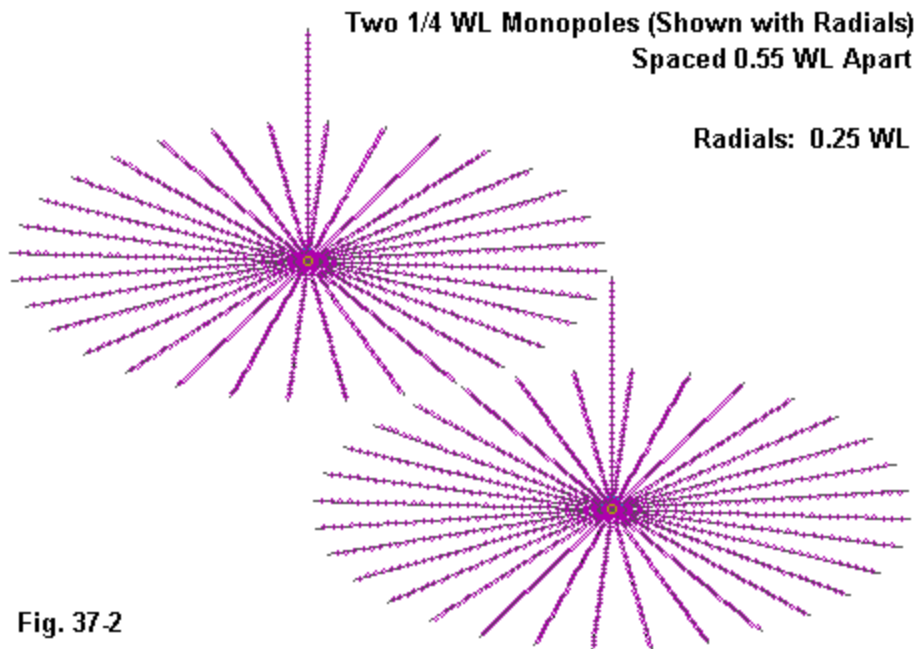


Fig. 37-2

In **Fig. 37-2**, we have 2 monopoles spaced just a bit more than 1/2 wavelength apart. For each case that we shall examine, we record the same data as in the first exercise, except that the impedance figures are understood as applying to each of the two sources, which are fed in phase with each other. Although **Fig. 37-2** shows the dual ground radial system, set up to avoid an intersection for this exercise, the first three data sets employ a direct connection of each monopole to ground. Not listed in the tables are horizontal -3 dB beam widths, which are completely consistent from one model to the next at any ground quality level. See model 37-2.

Ground	MININEC			NEC/w/MIN Gnd		
Perfect	9.06	0	27.8 - j13.4	9.06	0	28.3 - j11.7
Very Poor	2.15	29		2.15	29	
Poor	3.64	27		3.63	26	
Good/Average	3.88	26		3.88	26	
Very Good	5.85	21		5.85	21	
Salt Water	8.52	9		8.52	9	

Ground	NEC/w/S-N Gnd			NEC/w/Radial System		
Very Poor	1.77	29	31.4 - j 2.3	3.05	29	23.4 - j16.5
Poor	2.61	27	36.3 - j 2.2	4.22	27	24.7 - j15.1
Good/Average	2.80	26	36.6 - j 3.3	4.10	26	25.6 - j15.4
Very Good	4.87	21	35.8 - j 4.2	5.61	21	28.0 - j14.6
Salt Water	8.50	9	28.5 - j11.7	—		

Once more, salt water data for the ground plane system is not valid. However, the more important use that is made of numbers from this chart set is to estimate the advantage of the phase-fed system over a single monopole. Therefore, the next chart compares the gain advantage for each system (combining the MININEC direct ground systems into a single column).

Ground	NEC/w/MIN Gnd	NEC/w/S-N Gnd	NEC/w/Radial System
Very Poor	3.91	3.97	4.20
Poor	3.91	3.90	4.21
Good/Average	3.92	3.98	4.24
Very Good	3.91	3.98	4.13
Salt Water	3.91	3.93	—

The relative internal consistency of each system as we vary ground quality is interesting. The consistency between the use of the MININEC ground system and the S-N system suggests that for the purposes of gain comparisons, there is no reason to prefer the MININEC system.

However, the radial system provides an advantage figure that is 0.2 to 0.3 dB higher than those that emerged from the direct-ground connection systems. This difference is significant. A full analysis would need to survey many more complex arrays than the simple one used here before arriving at any general conclusions. However, the difference is notable. The initial conclusion is that gain advantage claims over a standard (such as the monopole used in this role) must always be given with the full particulars of the modeling conditions that produced them. More-

over, gain advantages produced by different ground systems for the models involved may not be directly comparable.

Once more the radial system provides a range of source impedance figures specific to the ground quality.

3. A Tilting 1/2 Wavelength Dipole

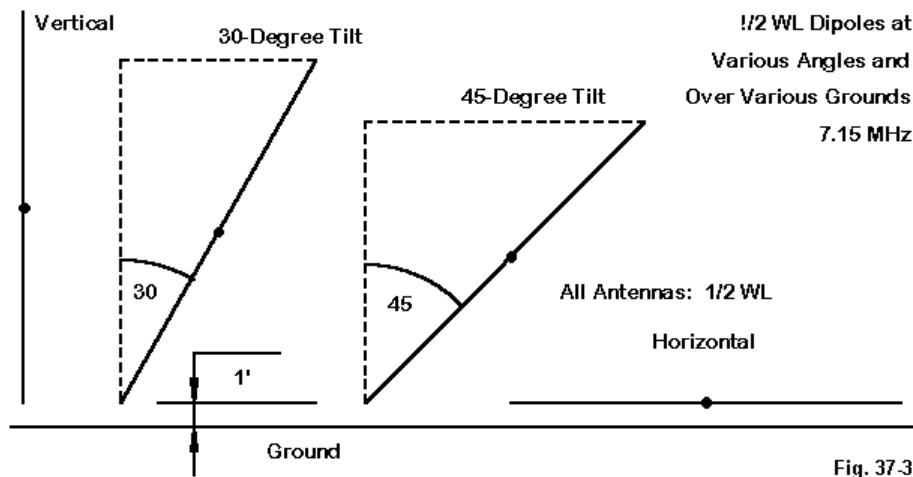


Fig. 37-3

Our third exercise is designed to serve as a reminder of the limitations inherent in the MININEC ground system. As suggested in **Fig. 37-3**, we shall use a 1/2-wavelength, 2" copper dipole. In successive steps, we shall tilt the vertical by 30, 45, 60, and 90 degrees. In each case, the left end of the dipole will be 1' off the ground. Thus, the final position will place the entire dipole at a height of 1'.

As before, we shall compare MININEC ground with S-N ground. We shall omit the separate columns for MININEC and NEC using the MININEC ground, since the results coincide almost exactly. The main differences that we shall examine lie between the MININEC and S-N ground systems in their handling of the tilting ele-

ment. In each case, we shall use a dipole length that has been resonated within the MININEC ground system and then record the source impedance that results from switching to the S-N system. See model 37-3, A-E. All gain and TO values are broadside to the wire (not in the direction of tilt).

A. Dipole Vertical: Length=64.9'; MIN Source Z: 99.8 - j 0.4

Ground	NEC/w/MIN	Gnd	NEC/w/S-N	Gnd
Very Poor	-1.20	22	-0.88	22 90.0 - j13.9
Poor	-0.03	20	0.13	20 94.4 - j 9.1
Good/Average	-0.21	19	-0.17	19 96.8 - j 9.3
Very Good	1.96	15	1.92	15 100.0 - j 4.9
Salt Water	5.91	7	5.91	7 99.9 - j 0.7

B. Dipole 30-Degrees Off Vertical: Length=64.0';
MIN Source Z: 93.0 - j 0.1

Ground	NEC/w/MIN	Gnd	NEC/w/S-N	Gnd
Very Poor	-0.44	29	-0.38	29 88.4 - j20.8
Poor	0.33	26	0.30	26 91.4 - j13.8
Good/Average	0.31	25	0.15	25 94.3 - j12.8
Very Good	1.83	20	1.66	20 96.0 - j 5.9
Salt Water	4.96	8	4.94	8 93.3 - j 0.5

To a small, but detectable, degree, the MININEC ground is beginning to overestimate the gain of the dipole, especially over better ground qualities.

C. Dipole 45-Degrees Off Vertical: Length=63.1';
MIN Source Z: 77.3 + j 0.4

Ground	NEC/w/MIN	Gnd	NEC/w/S-N	Gnd
Very Poor	0.74	42	0.18	42 84.1 - j26.1
Poor	1.15	40	0.66	40 84.1 - j17.2
Good/Average	1.38	43	0.77	43 86.9 - j14.6
Very Good	2.12	34	1.68	34 84.9 - j 5.3
Salt Water	4.02	10	3.98	10 78.0 + j 0.0

As we move to the 45-degree angle, the over-estimation of gain by the MININEC ground system becomes serious, averaging about a half dB. As well, the sensitivity of the element to the ground quality with respect to source impedance becomes apparent using the S-N ground system, but is invisible with a MININEC ground.

D. Dipole 60-Degrees Off Vertical: Length=62.6';
MIN Source Z: 49.2 - j 0.2

Ground	NEC/w/MIN	Gnd	NEC/w/S-N	Gnd
Very Poor	2.89	88	0.73	88 77.6 - j25.4
Poor	3.09	90	1.31	90 72.3 - j16.6
Good/Average	3.63	90	1.81	90 73.4 - j11.8
Very Good	4.27	90	3.12	90 63.9 - j 1.9
Salt Water	4.37	90	4.26	90 50.5 - j 0.1

As we tilt the element within 30 degrees of ground, almost the entire antenna lies below the so-called 0.2 wavelength limit for MININEC ground accuracy. The inaccuracies show up in two ways. First, the MININEC ground system gain is much too high. Second, the MININEC source impedance is much too low. The figures for the S-N ground for very good ground and better might well bear scrutiny as well.

E. Dipole 90-Degrees Off Vertical: Length=68.5';
MIN Source Z: 0.2 - j 0.3

Ground	NEC/w/MIN	Gnd	NEC/w/S-N	Gnd
Very Poor	24.26	90	-4.13	90 147.8 + j132.8
Poor	21.40	90	-6.76	90 141.5 + j134.6
Good/Average	20.91	90	-6.88	90 130.3 + j137.6
Very Good	16.95	90	-8.85	90 78.1 + j107.5
Salt Water	8.77	90	-9.38	90 11.4 + j 16.2

The MININEC values for the case of the dipole 1' off the ground clearly reveal the inadequacy of the ground system for wires very close to ground. In addition to the wholly unrealistic gain and source impedance values, the length of the required dipole is also a clue to the situation. Using the S-N ground system over very poor ground, the modeled dipole length for resonance is 58.3' and the source impedance is 104.3 - j 0.5 Ohms, with -4.88 dBi gain. Hence, the use of a MININEC ground does not even provide rudimentary guidance as to the required length of the element.

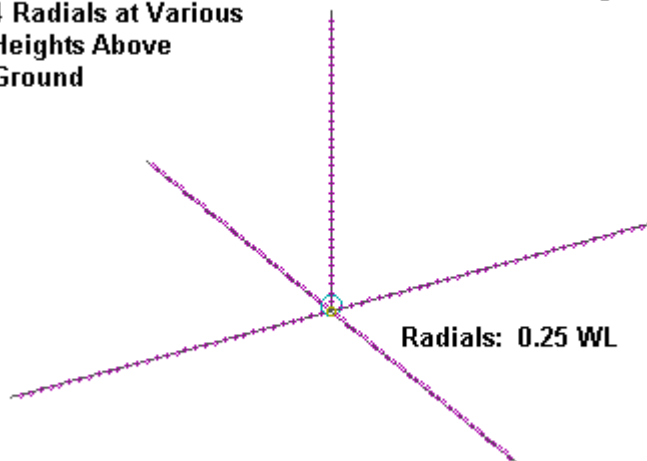
As the antenna becomes more horizontal and as more of its structure moves closer to the ground, the MININEC ground system creates increased errors and serves less and less as an adequate guide to the likely performance of the antenna modeled. Although this lesson is fundamental to almost any modeler when horizontal wires and arrays are in question, the message appears to dim when the antenna

bears the label “vertical array” or when sloping wires are part of the antenna structure, whether or not directly driven. Essentially, if any part of an antenna structure has a horizontal component to its radiation field and if that part falls below the threshold of accuracy for the MININEC ground system, then the use of the MININEC ground becomes untrustworthy.

4. A Vertical Monopole with a Simple Ground Radial System

**1/4 WL Monopole With
4 Radials at Various
Heights Above
Ground**

Fig. 37.4



There is one exception to the general rule just noted. Where a horizontal structure is symmetrical such that its radiation can be viewed as self-cancelling, the MININEC ground system remains quite reasonably accurate. Such an antenna appears in **Fig. 37-4**. The monopole with a 4-radial system, if elevated, shows quite similar results over a MININEC and a S-N ground calculation system.

The 7.15 MHz model has a set of 34.4' radials, 0.25" in diameter. The 2" diameter main element varies in length to establish resonance at each height. The test heights begin at 1/4 wavelength and halve in steps down to 1/32 wavelength. The following table compares NEC using a MININEC and a S-N ground. As well, figures are included for the same model directly handled in MININEC 3.13.

Height: 34.4' (1/4 WL)

Program	Monopole Length	Gain dBi	TO Angle degrees	Source Z R +/- jX Ohms
MININEC	34.6'	0.24	15	21.5 + j 0.7
NEC/w/MIN	34.2'	0.15	15	21.4 - j 0.4
NEC/w/S-N	34.2'	0.20	15	21.2 + j 1.0

Height: 17.2' (1/8 WL)

Program	Monopole Length	Gain dBi	TO Angle degrees	Source Z R +/- jX Ohms
MININEC	34.6'	-0.15	19	28.8 - j 1.0
NEC/w/MIN	34.3'	-0.23	19	28.9 - j 0.7
NEC/w/S-N	34.3'	0.22	19	26.1 - j 0.7

Height: 8.6' (1/16 WL)

Program	Monopole Length	Gain dBi	TO Angle degrees	Source Z R +/- jX Ohms
MININEC	34.4'	-0.27	22	34.4 - j 0.1
NEC/w/MIN	34.1'	-0.36	22	34.5 + j 0.4
NEC/w/S-N	34.3'	0.04	22	31.7 + j 0.4

Height: 4.3' (1/32 WL)

Program	Monopole Length	Gain dBi	TO Angle degrees	Source Z R +/- jX Ohms
MININEC	34.1'	-0.25	24	36.7 + j 0.4
NEC/w/MIN	33.7'	-0.34	24	36.5 - j 0.7
NEC/w/S-N	34.1'	-0.11	24	35.2 + j 0.9

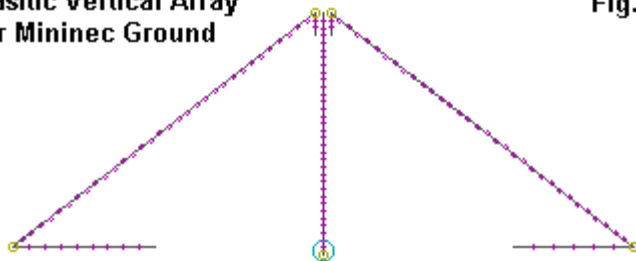
Despite the close approach to ground by the horizontal members of the monopole-plus-radials assembly, the figures comparing MININEC ground—used with either the NEC or MININEC algorithms—and the S-N ground are remarkably consistent. Field-canceling symmetrical structures are remarkably resistant to the error-producing aspects of the MININEC ground structure. See model 37-4.

5. A Parasitic Vertical Array with Sloping Parasitic Elements

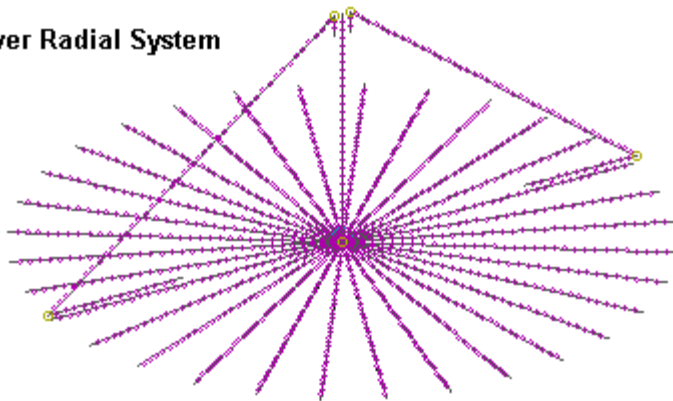
I found a parasitical array that has the general appearance of **Fig. 37-5** in a reputable handbook with the notation that it had been modeled using a MININEC ground because the NEC program lacked sufficient segment capacity to permit modeling the radial system. The present model is only like the original in appearance, since it is not a direct scaling of the MF array for 7.15 MHz. I have placed the lowest wires at the 1' level, corresponding to the lowest height in our third exercise. The parasitic element wires slope somewhat more than the originals. However, all that these modifications achieve is to make the results a bit more dramatic. See model 37-5.

**Parasitic Vertical Array
Over Mininec Ground**

Fig. 37-5



Over Radial System



The following table provides the dimensions of the array used in this example.

40-m vertical array

Frequency = 7.15 MHz.

Wire Loss: Copper – Resistivity = 1.74E-08 ohm-m, Rel. Perm. = 1

WIRES									
Wire Conn.	-End 1 (x,y,z : ft)			Conn.	-End 2 (x,y,z : ft)			Dia(in)	Segs
1		0.000,	0.000,	29.000	W2E1	0.000,	0.000,	0.167	2.00E+00 28
2	W3E1	0.000,	0.000,	0.167		34.400,	0.000,	0.167	2.50E-01 33
3	W4E1	0.000,	0.000,	0.167		33.739,	6.711,	0.167	2.50E-01 33
4	W5E1	0.000,	0.000,	0.167		31.781,	13.164,	0.167	2.50E-01 33
5	W6E1	0.000,	0.000,	0.167		28.603,	19.112,	0.167	2.50E-01 33
6	W7E1	0.000,	0.000,	0.167		24.324,	24.324,	0.167	2.50E-01 33
7	W8E1	0.000,	0.000,	0.167		19.112,	28.603,	0.167	2.50E-01 33
8	W9E1	0.000,	0.000,	0.167		13.164,	31.781,	0.167	2.50E-01 33
9	W10E1	0.000,	0.000,	0.167		6.711,	33.739,	0.167	2.50E-01 33
10	W11E1	0.000,	0.000,	0.167		2.6E-06,	34.400,	0.167	2.50E-01 33
11	W12E1	0.000,	0.000,	0.167		-6.711,	33.739,	0.167	2.50E-01 33
12	W13E1	0.000,	0.000,	0.167		-13.164,	31.781,	0.167	2.50E-01 33
13	W14E1	0.000,	0.000,	0.167		-19.112,	28.603,	0.167	2.50E-01 33
14	W15E1	0.000,	0.000,	0.167		-24.324,	24.324,	0.167	2.50E-01 33
15	W16E1	0.000,	0.000,	0.167		-28.603,	19.112,	0.167	2.50E-01 33
16	W17E1	0.000,	0.000,	0.167		-31.781,	13.164,	0.167	2.50E-01 33
17	W18E1	0.000,	0.000,	0.167		-33.739,	6.711,	0.167	2.50E-01 33
18	W19E1	0.000,	0.000,	0.167		-34.400,	5.2E-06,	0.167	2.50E-01 33
19	W20E1	0.000,	0.000,	0.167		-33.739,	-6.711,	0.167	2.50E-01 33
20	W21E1	0.000,	0.000,	0.167		-31.781,	-13.164,	0.167	2.50E-01 33
21	W22E1	0.000,	0.000,	0.167		-28.603,	-19.112,	0.167	2.50E-01 33
22	W23E1	0.000,	0.000,	0.167		-24.324,	-24.324,	0.167	2.50E-01 33
23	W24E1	0.000,	0.000,	0.167		-19.112,	-28.603,	0.167	2.50E-01 33
24	W25E1	0.000,	0.000,	0.167		-13.164,	-31.781,	0.167	2.50E-01 33
25	W26E1	0.000,	0.000,	0.167		-6.711,	-33.739,	0.167	2.50E-01 33
26	W27E1	0.000,	0.000,	0.167		4.1E-07,	-34.400,	0.167	2.50E-01 33
27	W28E1	0.000,	0.000,	0.167		6.711,	-33.739,	0.167	2.50E-01 33
28	W29E1	0.000,	0.000,	0.167		13.164,	-31.781,	0.167	2.50E-01 33
29	W30E1	0.000,	0.000,	0.167		19.112,	-28.603,	0.167	2.50E-01 33
30	W31E1	0.000,	0.000,	0.167		24.324,	-24.324,	0.167	2.50E-01 33
31	W32E1	0.000,	0.000,	0.167		28.603,	-19.112,	0.167	2.50E-01 33
32	W33E1	0.000,	0.000,	0.167		31.781,	-13.164,	0.167	2.50E-01 33
33	W1E2	0.000,	0.000,	0.167		33.739,	-6.711,	0.167	2.50E-01 33
34		0.853,	0.000,	26.448	W35E1	0.853,	0.000,	29.000	2.50E-01 33
35	W34E2	0.853,	0.000,	29.000	W36E1	35.000,	0.000,	1.000	2.50E-01 44
36	W35E2	35.000,	0.000,	1.000		21.500,	0.000,	1.000	2.50E-01 13
37		-0.853,	0.000,	26.448	W38E1	-0.853,	0.000,	29.000	2.50E-01 33
38	W37E2	-0.853,	0.000,	29.000	W39E1	-35.000,	0.000,	1.000	2.50E-01 44
39	W38E2	-35.000,	0.000,	1.000		-19.000,	0.000,	1.000	2.50E-01 15

SOURCES

Source	Wire Seg.	Wire #/Pct Actual	From End 1 (Specified)	Ampl.(V, A)	Phase(Deg.)	Type
1	28	1 / 98.21	(1 /100.00)	1.000	0.000	I

Ground type is Real, high-accuracy analysis
 Conductivity = .005 S/m Diel. Const. = 13

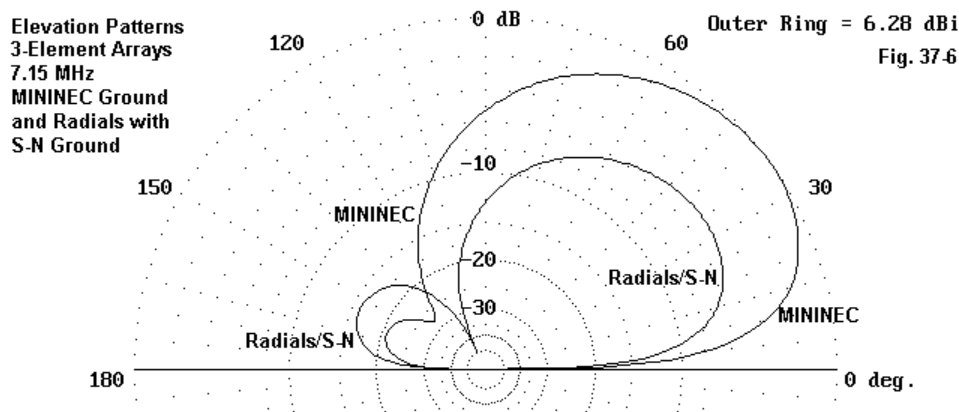
The following table lists the results for directly connecting the 1/4 wavelength driver to ground using the MININEC ground system. Direct connection using the S-N system is also shown for reference. The last entry shows the results of placing the monopole on a 32-radial system with the S-N ground. All models use average (good) ground.

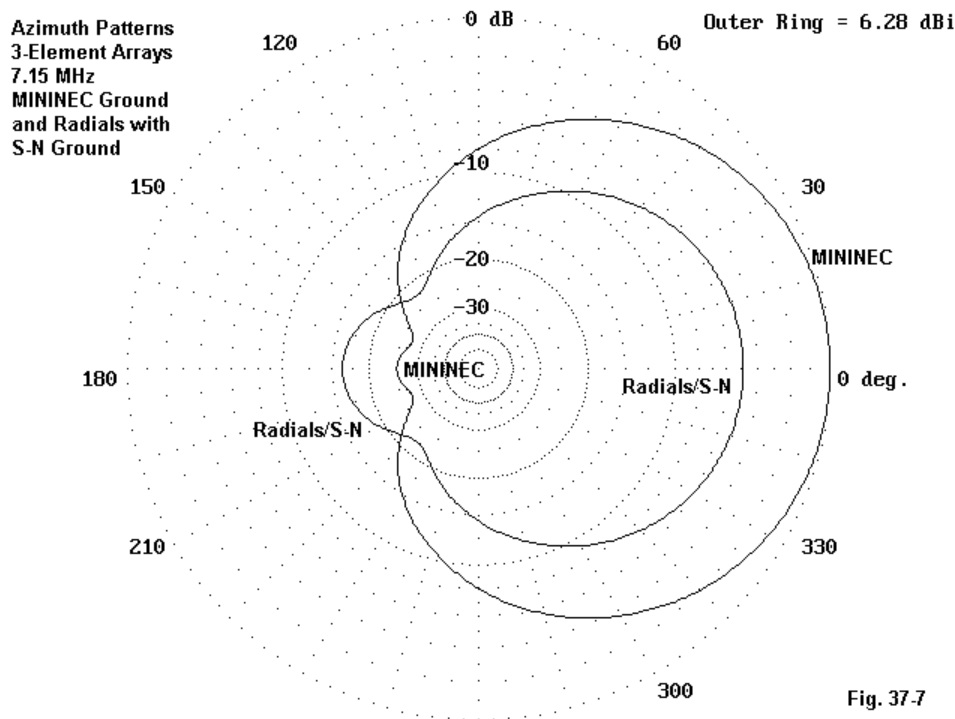
Ground System	Gain dBi	TO Angle degrees	Front-to-Back Ratio dB	Beamwidth degrees	Source Z R +/- jX Ohms
Direct Connection:					
MININEC	6.28	37	24.99	110.6	9.2 + j 9.1
S-N	-1.50	34	9.55	98.2	30.1 + j 21.6
Radial System:					
S-N	1.18	34	11.38	99.5	14.8 + j 3.8

Compared to a radial system over S-N ground, the MININEC system not only overestimates performance figures, but as well, provides dimensions that are at odds with those which might yield maximum gain and front-to-back ratio in the radial configuration. If optimization is performed, along with the use of additional radials, available in NEC-4, the performance of the array over radials might show better numbers, but still, nowhere near those provided by the MININEC ground analysis.

Fig. 37-6 provides a view of the MININEC and Radial system elevation patterns for comparison. **Fig. 37-7** provides a similar comparison of the azimuth patterns at the 34-degree elevation angle of maximum radiation.

The array uses near ground horizontal portions of the parasitic elements, along with sloping elements at about a 45-degree angle. Both of these conditions incur the typical MININEC ground errors. I have modeled the lowest wires very close to ground to accentuate the error potential of using the MININEC ground in arrays with the listed problematical structures. However, placing any part of the structure below 0.2 wavelengths and having a horizontal component to either driven or parasitic elements will leave the results equally untrustworthy.





Conclusion

The selection of a ground system for modeling vertical arrays requires considerable care. In general, any serious model—that is, one used for design, analysis, or publication—should employ a radial system as close as possible to the structure of the physical system to be used. If that requires borrowing or upgrading software and the structuring of models with well over 1000 segments, then that is the cost for internal consistency of modeling comparisons. (The largest models in these exercises used close to 2,200 segments.)

Models using different ground systems are not especially comparable, at least, not on a simple viewing of their report numbers. Even within the same system, there are differences in comparison numbers for larger arrays and whatever simpler standard might be used; hence, such comparisons should be made with reference to the actual ground quality of the antenna site.

The MININEC ground shortcut to vertical array modeling should generally be avoided or used sparingly and under very limited conditions. At the very least, the modeler should avoid using the MININEC ground system whenever any part of a radiating structure has a horizontal component and is below the 0.2-wavelength accuracy threshold. Better yet, the model should include the radial system that will be used at the site and employ the S-N ground calculation system. Although these measures would not guarantee the accuracy of performance figures from vertical array models relative to the actual installation, at the very least, they would ensure that internal consistency among modeled results is sustained.

* * * * *

Models included: 37-1 through 37-5 (with 37-3A through 37-3E). (.NEC and .NWP model dimensions in meters; .EZ model dimensions in feet.)

38. Radials: Segmentation and Convergence

Working with radial systems for vertical monopoles and arrays often puts modelers off, since the radials occupy far more wires and segments than the antenna elements themselves. Hence, there is a tendency to be satisfied with results of models that use directly grounded $1/4$ -wavelength monopoles without a radial system. As well, modelers rarely place radial systems beneath $1/2$ -wavelength antennas and arrays, especially if the elements make no connection to the ground.

In the preceding column, I noted some of the potential inaccuracies that may arise from using a simple MININEC ground with no radial system. The source impedance is calculated for a perfect ground only and hence does not show the range of variation that may be occasioned by placing the antenna system over different soil qualities. Comparisons between an array and a standard antenna, such as a $1/4$ -wavelength monopole yield different differentials when using the MININEC ground and when using a radial system. Moreover, if the array employs any element, driven or parasitic, with a horizontal component to its radiation field, and if the element has any part less than 0.2 wavelengths above ground, the use of the MININEC ground is subject to the known errors of that system for wires close to the ground.

Consequently, modelers who are serious about working with vertical antennas and arrays need to increase their familiarity with modeling radial systems using NEC and the attached Sommerfeld-Norton (S-N) ground calculation system. For NEC-2, which does not permit wires either on or below ground level, the radial system should be no closer to ground than about 0.001 wavelength. The use of very thin wires and length tapering is reported to permit placement of the radials even closer to the ground, but for most general modeling purposes, the 0.001 wavelength limit, rounded to a convenient number, should provide a self-consistent foundation for comparing arrays to some standard vertical antenna placed on the same radial system.

How Many Radials?

The rule of thumb governing the proximity of the radials to the ground in NEC-2 is not the only limitation the modeler should observe. Consider the radial systems in **Fig. 38-1**. The upper system uses 32 radials, each with 20 segments per radial. (The choice of 20 will become apparent later on; for now, it represents a relatively high segmentation density.) NEC-2 warns against using more than 30 wires at a single junction. As the angle between wires becomes smaller, the wire segments at the junction interpenetrate. At a certain angle that varies according to the wire diameter, the central portions of the segments will interpenetrate to a degree that introduces errors into the calculations. The NEC core does not specifically check for this limitation, as it does for wire intersections that occur at mid-segment points. Hence, it will not block the completion of the calculation. However, some programs check for this condition and will alert the user.

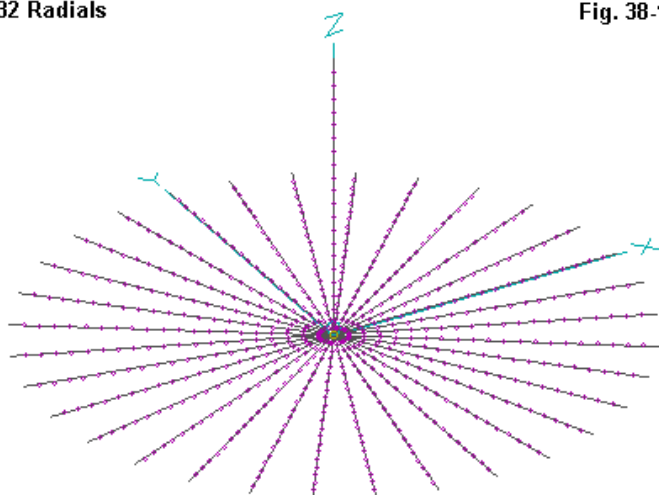
For radial systems, a 32-radial model does not press the limit significantly. However, we might check the results of using a 64-radial system, shown on the lower part of **Fig. 38-1**. As well, we might check both in both NEC-2 and NEC-4 to see if there is any difference of note. In both cases, we shall place a 40-meter copper vertical wire that is 0.25 m in diameter and also using 20 segments over a field of radials, each of which is copper and 2 mm in diameter. (2-mm wire falls between AWG #14 and AWG #12.) The frequency will be 1.83 MHz. The radial system is 0.164 m off the ground (0.001 wavelength). Beneath the radial system is “average ground” (conductivity: 0.005 S/m; dielectric constant: 13) in the S-N calculation system.

Core	No. of Radials	Gain dBi	TO Angle degrees	Source Impedance R +/- jX Ohms
NEC-2	32	1.02	22	39.3 + j 7.2
NEC-4	32	1.02	22	39.3 + j 7.7
NEC-2	64	1.01	22	38.8 + j 6.6
NEC-4	64	0.98	22	39.1 + j 7.0

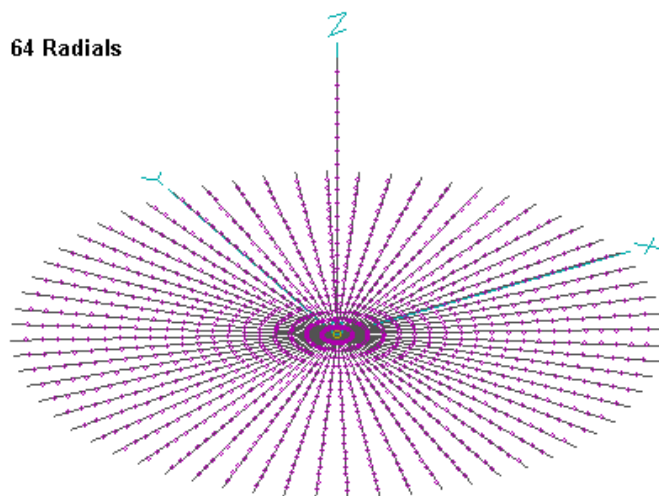
The 32-radial systems show excellent agreement between the two cores. However, as we double the radials, the results from the two cores begin to diverge. Normally, we would expect any gain difference between the cores to give the advantage to the system with the higher number of radials.

32 Radials

Fig. 38-1

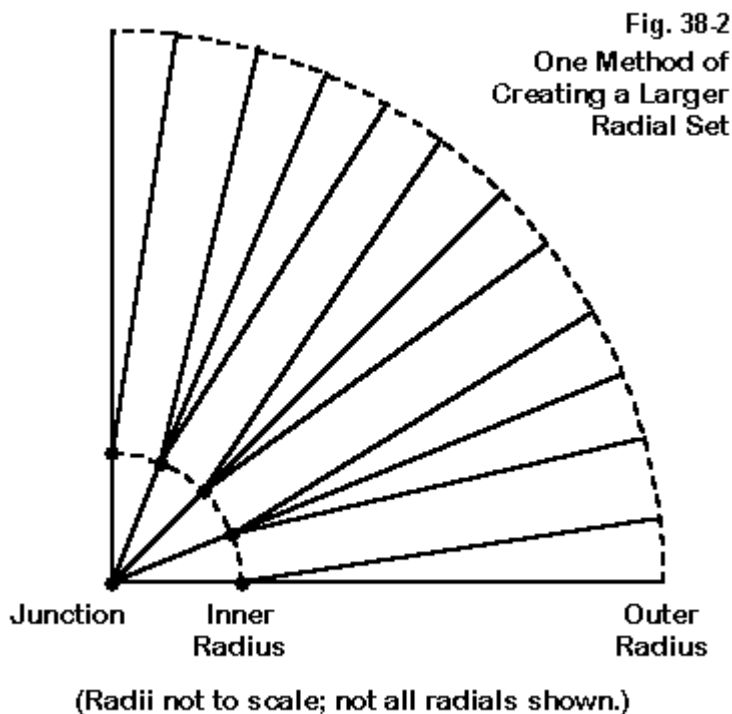


64 Radials



In fact, we obtain precisely the opposite results, although hardly to an operationally significant point. The source impedance in both cases decreases, as we might expect of a radial system with lower losses. However, the amount of decrease differs between the two cores.

For general purposes, then, the 32-radial system is a useful level. The model employed in the example required 33 wires and 660 segments. The 64-radial system required 65 wires and 1365 segments. Since run-time for a model increase with the number of segments and also with the number of wires, the smaller system is preferable for the additional reason of human impatience.



There are applications that call for exacting replication of radial systems that have more than 32 radials. **Fig. 38- 2** shows one scheme that can be used (and expanded as needed) for adding more radials without increasing the junction count. Although many versions are possible, the one in the figure uses a set of 16 inner radial wires, each of which connects to a set of outer radial wires. Creating such a system can be a tedious labor.

Simple radial sets can be created by automated radial makers that come with commercial implementations of NEC or by separate equation sets. To create the complex pattern shown in **Fig. 38-2**, we can make use of such facilities. First create a 16-radial set at the inner radius, ordinarily a set of 1-segment wires having the same length as the segments lengths in the outer wires. For the 20 segment wires of **Fig. 38-1**, a 5% of total length would suffice.

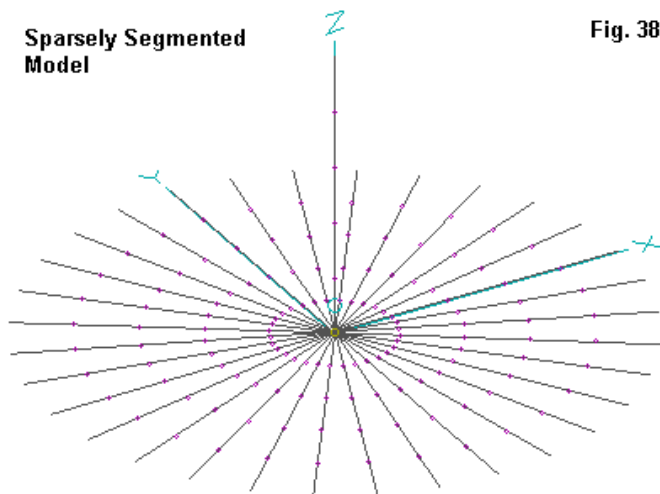
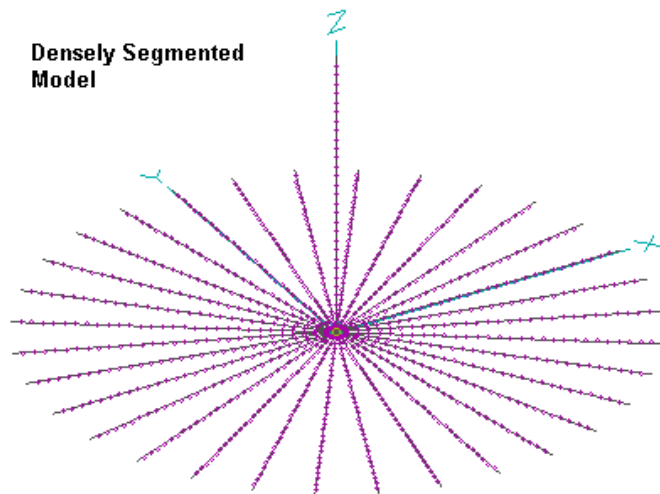
Next, create a 64-radial set (or whatever number is desired) using the outer radius for the wires. Then for each group of 4 outer wires, move their inner ends to the correct outer end of one of the set of 16. The result will be the configuration in **Fig. 38-2** with the minimal amount of independent calculation. Do not try to run the model until all of the outer radial wires are correctly placed at their inner ends. NEC will block the run with a message indicating mid-segment wire intersections.

Convergence

Complex geometries do not answer to the minimum segmentation rules for linear elements. And a radial system with a vertical antenna at right angles to the radials represents a complex geometry. Therefore, it is wise to perform a convergence test on radial systems with their antennas attached. **Fig. 38-3** shows two versions of the same antenna, one using a low segment density, the other a much higher level of segmentation. The question facing the modeler is at what level of segmentation he or she should declare convergence.

Sparsely Segmented
Model

Fig. 38-3

Densely Segmented
Model

Let's take the model that we used above. The antenna is a 40-meter long element, 0.25 m in diameter for 1.83 MHz. We shall use 32 radials of 2-mm diameter. Everything is copper. Once more, the radial system is 0.164 m or 0.001 wavelength off the ground for the benefit of NEC-2 restrictions. Hence, the tower top is at 40.164 m. Now let's uniformly segment each wire in steps of 5 from 5 segments per wire to 30 segments per wire. Each antenna model will be over average ground in the S-N system.

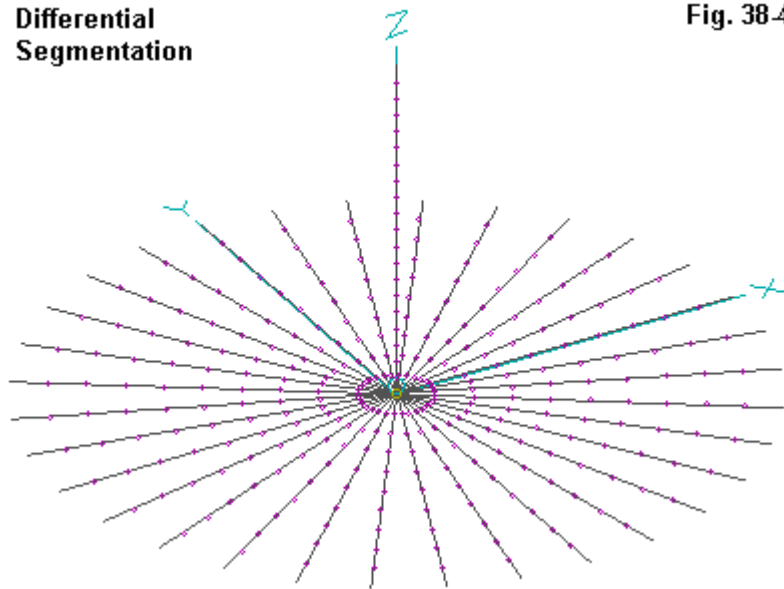
The results of the convergence test are as follows. The TO angle is omitted, since it is 22 degrees for all cases.

Segments/ Wire	Segment length wavelengths	Total Segments	Gain dBi	Source Impedance R +/- jX Ohms
5	0.0050	165	1.28	37.2 + j 9.4
10	0.0250	330	1.14	38.2 + j 8.5
15	0.0167	495	1.07	38.8 + j 8.0
20	0.0125	660	1.03	39.2 + j 7.7
25	0.0100	825	1.00	39.5 + j 7.6
30	0.0083	990	0.99	39.6 + j 7.5

Now comes the moment of decision—declaring the level of segmentation at which we arrive at convergence. In one sense, we have not arrived, since the progression of decreasing gain and source reactance, with an increasing source resistance, has not terminated. Ideally, we achieve convergence when the values noted simply vary around a central value with only small changes per increment of increased segmentation.

Obviously, holding out for the ideal can drive a modeler crazy. In practical terms, we achieve convergence when the differences between levels of segmentation make no operational difference relative to a real antenna whose properties we might measure after building. In these terms, 10 to 15 segments per wire would certainly suffice. More stringently, but still within the realm of realistic modeling, we can apply this standard: the differential between a given level of segmentation and the next lower level is not significantly larger than the difference between the given level and the next higher level. The 20-segment-per-wire level appears to meet this requirement easily.

In the end, however, it is up to the individual modeler to determine—relative to the overall task of which the model is a part—what is a suitable level of segmentation, that is, when convergence is obtained. Although I have shown the total number of segments in the 33-wire models used for the example, this factor should not be among the decision makers for any significant project. In all cases, where the information may be of use to those who might try to replicate the model, the segmentation data should be included in the model description.

**Differential
Segmentation****Fig. 38-4**

There is a tendency for newer modelers to assume that, because a radial system is largely self-canceling with respect to its radiation field, it is satisfactory to use fewer segments in radials than in the main radiator(s). The situation is illustrated in **Fig. 38-4**. Therefore, let's take our model and run it through some cases where there is a differential. Once more, the TO angle is a constant 22 degrees for all cases.

Segments/ Radial	Segments/ Radiator	Total Segments	Gain dBi	Source Impedance R +/- jX Ohms
5	10	170	1.23	37.4 + j 8.7
5	20	180	1.35	36.4 + j 9.5
10	20	340	1.14	38.3 + j 8.7
15	20	500	1.06	38.9 + j 8.1

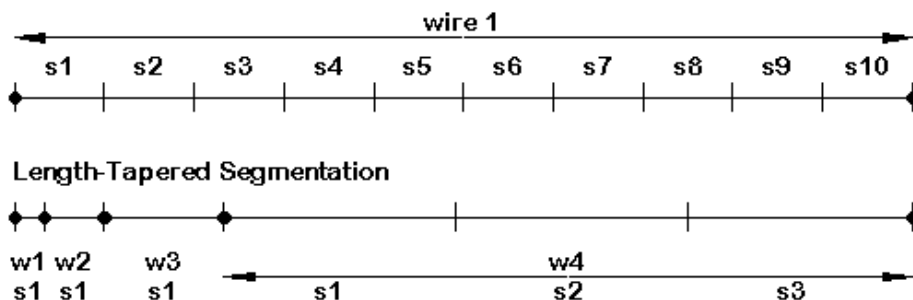
Notice that we do not approach the values of gain and source impedance that attach to the earlier table until we hit the 15-20 case. There is a reason for the variance. The segment lengths on either side of a source segment in NEC should be equal in order to obtain the greatest accuracy. Since the vertical is fed on its lowest segment, only the 15-20 case begins to approximate this condition. For this reason, the 5-20 case shows a higher deviance from the cases in the preceding table than does the 5-10 case, where we have a closer fit between the source segment and the innermost radial segments.

The upshot is that, for most purposes, using equal segment lengths for both radials and radiators is the most accurate route to follow.

Length Tapering

Standard Segmentation

Fig. 38-5



The 32-radial system using 20 segments per 1/4 wavelength wire remains a large model with respect to some low-end NEC modeling implementations. It requires 660 segments, which can overrun a 500-segment limitation. Although upgrading software to a professional package is wise for serious modeling, there is a

technique that the modeler can use to reduce the number of segments in the model without sacrificing accuracy. It is called length tapering and is illustrated in **Fig. 38-5**. Compare models 38-1 and 38-2.

The practice of tapering the length of segments progressively arose from necessity with the use of MININEC and its initial restriction to a maximum of 256 segments for the entire model. To handle angular junctions, the modeler had to either use very many segments or resort to length tapering. Because NEC cores are segment-limited only by the user's setting of a variable, length tapering is not widely used in NEC-2 or NEC-4 models. However, the technique remains a valid option for the modeler.

The principle of length tapering involves setting a lower and upper length limit. One commercial program uses a default lower limit of 0.0025 wavelength and an upper limit of 0.04 wavelength. The user can alter these values to suit a particular set of needs. However, for our example, let's use these values on each wire of the basic monopole model we have been using. We need to taper only the inner junction ends of each wire (although the user has the option to taper either or both ends). In the process of creating tapered-length elements, the program will replace each individual wire with a set of wires meeting the requirements. If we do this for the 32-radial monopole, we obtain a model using 165 wires and 330 segments—well within the program limitation of 500 segments per model. However, here are the results we obtain from the length-tapered model.

Total Wires	Total Segments	Gain dBi	Source Impedance R +/- jX Ohms
165	330	1.39	35.9 + j 5.6

The surprisingly high gain stems from an error we made in constructing the model. The tapered segment length increases when using a default system in a 2:1 ratio. Although the initial radial segments are the same length as the source segment, the segment on the monopole adjacent to the source segment is twice as long as the source segment. Let's go back and try again, using a bit of the data we obtained from our first try.

This time, we shall create a new wire that is .0025 wavelength long and running from 0.164 m to 0.574 m in the Z-axis. Now we shall finish the vertical portion of the

antenna with a second wire from the top of the first to the upper limit of the vertical. When we length taper the model, we shall skip the new wire. In this way, the first segment above the new wire will be the same length as the new wire, as will be the inner wires of the radials.

Because length-tapering may be unfamiliar to some readers, here is the model description in EZNEC format.

160-meter vertical w/radials: length tapered Frequency = 1.83 MHz.

Wire Loss: Copper - Resistivity = 1.74E-08 ohm-m, Rel. Perm. = 1

```

----- WIRES -----
Wire Conn.-- End 1 (x,y,z : m ) Conn.-- End 2 (x,y,z : m ) Dia(mm) Segs
1          0.000, 0.000, 40.164 W2E1 0.000, 0.000, 6.717 2.50E+02 6
2 W1E2 0.000, 0.000, 6.717 W3E1 0.000, 0.000, 3.440 2.50E+02 1
3 W2E2 0.000, 0.000, 3.440 W4E1 0.000, 0.000, 1.802 2.50E+02 1
4 W3E2 0.000, 0.000, 1.802 W5E1 0.000, 0.000, 0.983 2.50E+02 1
5 W4E2 0.000, 0.000, 0.983 W6E1 0.000, 0.000, 0.574 2.50E+02 1
6 W5E2 0.000, 0.000, 0.574 W7E1 0.000, 0.000, 0.164 2.50E+02 1
7 W12E1 0.000, 0.000, 0.164 W8E1 0.410, 0.000, 0.164 2.00E+00 1
8 W7E2 0.410, 0.000, 0.164 W9E1 1.229, 0.000, 0.164 2.00E+00 1
9 W8E2 1.229, 0.000, 0.164 W10E1 2.867, 0.000, 0.164 2.00E+00 1
10 W9E2 2.867, 0.000, 0.164 W11E1 6.143, 0.000, 0.164 2.00E+00 1
11 W10E2 6.143, 0.000, 0.164 40.966, 0.000, 0.164 2.00E+00 6
12 W17E1 0.000, 0.000, 0.164 W13E1 0.402, 0.080, 0.164 2.00E+00 1
13 W12E2 0.402, 0.080, 0.164 W14E1 1.205, 0.240, 0.164 2.00E+00 1
14 W13E2 1.205, 0.240, 0.164 W15E1 2.812, 0.559, 0.164 2.00E+00 1
15 W14E2 2.812, 0.559, 0.164 W16E1 6.025, 1.198, 0.164 2.00E+00 1
16 W15E2 6.025, 1.198, 0.164 40.179, 7.992, 0.164 2.00E+00 6
17 W22E1 0.000, 0.000, 0.164 W18E1 0.378, 0.157, 0.164 2.00E+00 1
18 W17E2 0.378, 0.157, 0.164 W19E1 1.135, 0.470, 0.164 2.00E+00 1
19 W18E2 1.135, 0.470, 0.164 W20E1 2.649, 1.097, 0.164 2.00E+00 1
20 W19E2 2.649, 1.097, 0.164 W21E1 5.676, 2.351, 0.164 2.00E+00 1
21 W20E2 5.676, 2.351, 0.164 37.848, 15.677, 0.164 2.00E+00 6
22 W27E1 0.000, 0.000, 0.164 W23E1 0.341, 0.228, 0.164 2.00E+00 1
23 W22E2 0.341, 0.228, 0.164 W24E1 1.022, 0.683, 0.164 2.00E+00 1
24 W23E2 1.022, 0.683, 0.164 W25E1 2.384, 1.593, 0.164 2.00E+00 1
25 W24E2 2.384, 1.593, 0.164 W26E1 5.108, 3.413, 0.164 2.00E+00 1

```

(Many radials omitted to compress the model description.)

```

141140E2 2.351, -5.676, 0.164 15.677, -37.848, 0.164 2.00E+00 6
142147E1 0.000, 0.000, 0.164 143E1 0.228, -0.341, 0.164 2.00E+00 1

```

143142E2	0.228,	-0.341,	0.164	144E1	0.683,	-1.022,	0.164	2.00E+00	1
144143E2	0.683,	-1.022,	0.164	145E1	1.593,	-2.384,	0.164	2.00E+00	1
145144E2	1.593,	-2.384,	0.164	146E1	3.413,	-5.108,	0.164	2.00E+00	1
146145E2	3.413,	-5.108,	0.164		22.760,	-34.062,	0.164	2.00E+00	6
147152E1	0.000,	0.000,	0.164	148E1	0.290,	-0.290,	0.164	2.00E+00	1
148147E2	0.290,	-0.290,	0.164	149E1	0.869,	-0.869,	0.164	2.00E+00	1
149148E2	0.869,	-0.869,	0.164	150E1	2.027,	-2.027,	0.164	2.00E+00	1
150149E2	2.027,	-2.027,	0.164	151E1	4.344,	-4.344,	0.164	2.00E+00	1
151150E2	4.344,	-4.344,	0.164		28.968,	-28.968,	0.164	2.00E+00	6
152157E1	0.000,	0.000,	0.164	153E1	0.341,	-0.228,	0.164	2.00E+00	1
153152E2	0.341,	-0.228,	0.164	154E1	1.022,	-0.683,	0.164	2.00E+00	1
154153E2	1.022,	-0.683,	0.164	155E1	2.384,	-1.593,	0.164	2.00E+00	1
155154E2	2.384,	-1.593,	0.164	156E1	5.108,	-3.413,	0.164	2.00E+00	1
156155E2	5.108,	-3.413,	0.164		34.062,	-22.760,	0.164	2.00E+00	6
157162E1	0.000,	0.000,	0.164	158E1	0.378,	-0.157,	0.164	2.00E+00	1
158157E2	0.378,	-0.157,	0.164	159E1	1.135,	-0.470,	0.164	2.00E+00	1
159158E2	1.135,	-0.470,	0.164	160E1	2.649,	-1.097,	0.164	2.00E+00	1
160159E2	2.649,	-1.097,	0.164	161E1	5.676,	-2.351,	0.164	2.00E+00	1
161160E2	5.676,	-2.351,	0.164		37.848,	-15.677,	0.164	2.00E+00	6
162 W6E2	0.000,	0.000,	0.164	163E1	0.402,	-0.080,	0.164	2.00E+00	1
163162E2	0.402,	-0.080,	0.164	164E1	1.205,	-0.240,	0.164	2.00E+00	1
164163E2	1.205,	-0.240,	0.164	165E1	2.812,	-0.559,	0.164	2.00E+00	1
165164E2	2.812,	-0.559,	0.164	166E1	6.025,	-1.198,	0.164	2.00E+00	1
166165E2	6.025,	-1.198,	0.164		40.179,	-7.992,	0.164	2.00E+00	6

———— SOURCES ————

Source	Wire Seg.	Wire #/Pct Actual	From End 1 (Specified)	Ampl.(V, A)	Phase(Deg.)	Type
1	1	6 / 50.00	(6 /100.00)	1.000	0.000	I

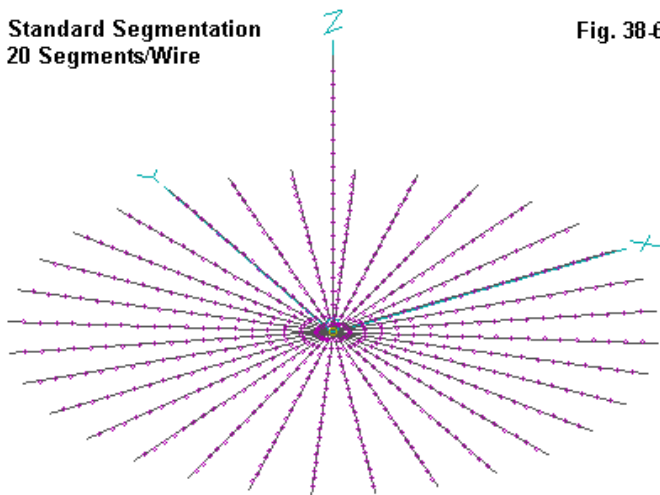
Ground type is Real, high-accuracy analysis

Conductivity = .005 S/m Diel. Const. = 13

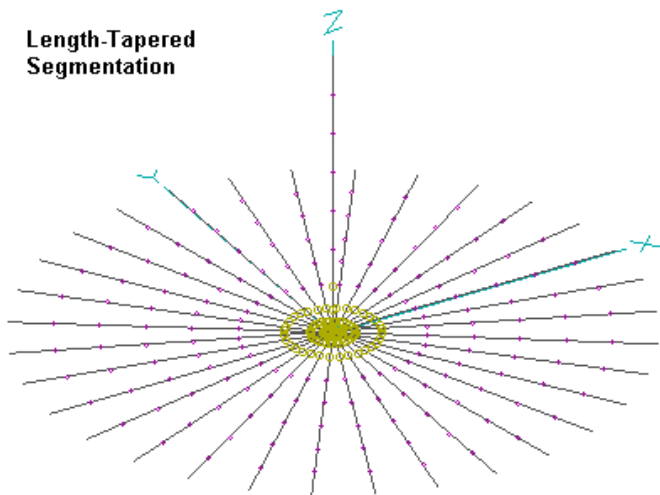
Fig. 38-6 is a view of the length-tapered model above. Since the model begins with the upper end of the vertical element, the new wire is Wire 6, as also indicated by the source entry. The radials were developed by first creating and tapering one radial. Then the radial maker was applied to the substitute wire group to yield the remaining 31.

**Standard Segmentation
20 Segments/Wire**

Fig. 38-6



**Length-Tapered
Segmentation**



The new model returns the following reports.

Total Wires	Total Segments	Gain dBi	Source Impedance R +/- jX Ohms
Correctly length-tapered model			
166	331	0.93	39.9 + j 6.2
20-segment per wire model			
33	660	1.03	39.2 + j 7.7
10-segment per wire model			
33	330	1.14	38.2 + j 8.5

The reports from the length-tapered segment model better approaches the reports for the 20-segment/wire model than does the reported data for the 330-segment (10 segments per wire) model. Moreover, the length-tapered model produces a gain figure in the direction that the progression toward convergence was taking when terminated at 30 segments per wire. Hence, it is, in general, a better model-type to use than simply reducing the segmentation density to a level deemed to be within program limitations.

These notes cover only a few of the elements of adequate radial system modeling. The escape from large models that we effected by length tapering each long wire may be adequate for simple vertical monopole systems. However, there are many larger radial systems used by multi-element vertical arrays. We cannot evade large models with vertical arrays. Nonetheless, we need to look at their construction, our project for next time.

* * * * *

Models included: 38-1 through 38-2. (All model dimensions in meters.)



39. Radials: Complex Radial Systems

In the past two columns, we examined some of the modeling issues surrounding vertical antennas using radials systems. These columns, like all those in this series, were predicated on using a version of NEC-2 as the basic modeling core. We were left with some questions of modeling complex radial systems, which we shall examine in this column. However, it may be useful to begin by reviewing the limitations of NEC-2 with respect to radial systems.

Elevated vs. Buried Radials

NEC-2 does not permit wires either on or below ground. Therefore, radial systems must be constructed above ground, usually at a minimum height of about 0.001 wavelength. NEC-2 also recommends limiting the number of wires at a junction to about 30, making a 32-radial system about the largest that is practical. As noted in previous columns, there are some work-arounds, but these parameters generally set the limits for vertical antenna radial systems. Length-tapering techniques can reduce model size, and that technique allows many 32-radial systems to be modeled within the 500-segment limit of some commercial implementations of NEC-2.

However, modelers should be aware that there are significant differences in reports from above ground radial system models—even when pressed to the limit of proximity to the ground—and buried radial system models. Of course, buried radials are only feasible in NEC versions above NEC-2. However, without some sense of what NEC-4 might report for a buried radial system, the NEC-2 modeler might uncritically accept a report from the NEC-2 above ground system model as reflecting accurately what occurs with a buried radial system.

Therefore, consider the following simple model: a 40-m element for 1.83 MHz with a diameter of 25-mm (nearly 1"). The diameter for the model was chosen to simplify the modeling of the radial systems, since the length-to-diameter ratio would be better than 4:1 throughout. The radials will consist of 2-mm diameter wires.

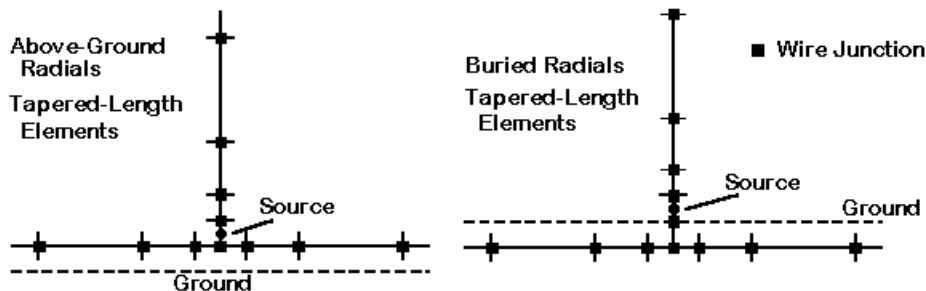


Fig. 39-1

Above-Ground and Buried Radial System Models

The ground treatment for separate above ground and buried radial systems is indicated in **Fig. 39-1**. The radials in the above ground system will be 0.001 wavelength above ground (0.164 m or about 6.5"). A fixed-length 1-segment source wire that is 0.001 wavelength long is at the base of the vertical. The radials and the main element above the source segment are length-tapered from 0.001 wavelength to 0.04 wavelength, which ensures that segments adjacent to the source segment are the same length as the source segment itself.

The buried radial system requires a wire junction at ground, so we shall add a 1-segment wire below ground. It is 0.001 wavelength long to match the depth of the radials. The radials and main element above the source wire are length-tapered as in the above ground model. Compare the modeling details of models 39-1 and 39-2 to more clearly see the differences between above ground and below ground monopole + radial structures.

I constructed radial systems using 4, 8, 16, 32, 64, and 128 radials for the models using NEC-4. The 128-radial system approaches the practical limit of small angles between wires and may result in somewhat dubious results for radial systems of that size. However, the trends in the two types of radial systems are fascinating, as the following tables reveal.

Table 1. 40-m vertical monopole, 25 mm diameter; 40.96-m (0.25 wavelength) radials, 2 mm diameter, tapered segmentation: 0.001 to 0.04 wavelength per wire; radials 0.001 wavelength above ground; NEC-4.

Soil Type	Gain dBi	TO Angle degrees	Source Impedance R +/- j X Ohms
4-radials: 31 wires; 61 segments			
Very Poor	-1.90	27	41.91 + j 18.38
Poor	-0.33	25	40.27 + j 22.38
Good	0.66	22	41.28 + j 23.89
Very Good	2.45	17	42.26 + j 21.04
8-radials: 55 wires; 109 segments			
Very Poor	-1.47	27	37.49 + j 3.69
Poor	0.03	25	36.84 + j 6.82
Good	1.01	22	37.99 + j 8.78
Very Good	2.81	17	38.89 + j 9.56
16-radials: 103 wires; 205 segments			
Very Poor	-1.34	27	35.91 - j 1.80
Poor	0.09	25	36.08 + j 0.89
Good	1.06	22	37.37 + j 2.61
Very Good	2.92	16	37.91 + j 4.36
32-radials: 199 wires; 397 segments			
Very Poor	-1.29	27	35.09 - j 3.55
Poor	0.09	25	35.69 - j 1.05
Good	1.04	22	37.24 + j 0.48
Very Good	2.92	16	37.83 + j 2.46
64-radials: 391 wires; 781 segments			
Very Poor	-1.23	27	34.36 - j 3.63
Poor	0.10	25	35.24 - j 1.36
Good	1.02	22	36.97 - j 0.10
Very Good	2.91	16	37.91 + j 1.99
128-radials: 775 wires; 1549 segments			
Very Poor	-1.12	27	33.81 - j 3.04
Poor	0.17	25	34.80 - j 0.95
Good	1.03	22	36.51 + j 0.04
Very Good	2.87	16	37.97 + j 1.89

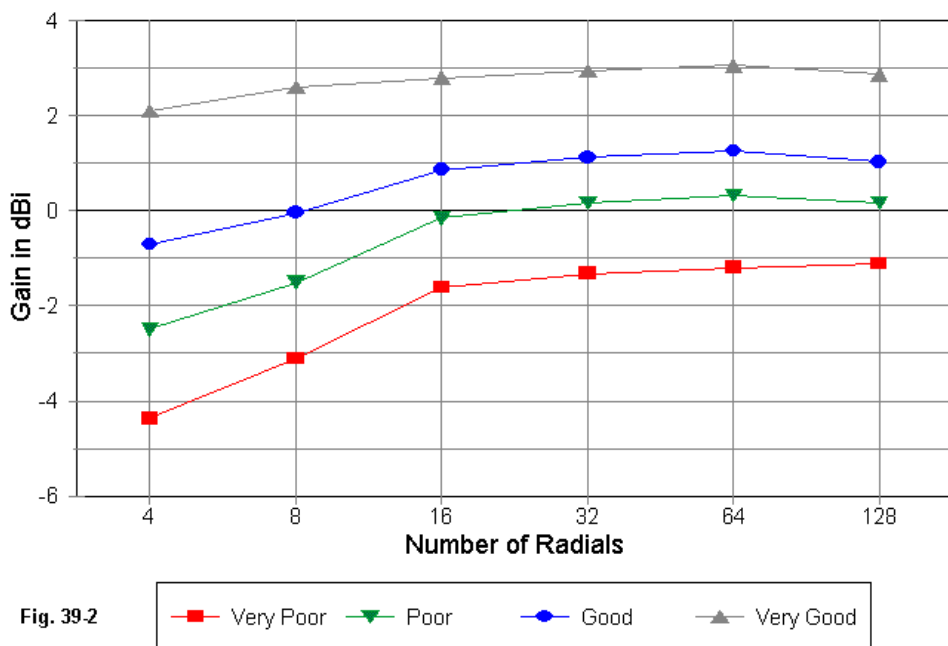
Table 2. 40-m vertical monopole, 25 mm diameter; 40.96-m (0.25 wavelength) radials, 2 mm diameter, tapered segmentation: 0.001 to 0.04 wavelength per wire; radials 0.001 wavelength below ground; NEC-4.

Soil Type	Gain dBi	TO Angle degrees	Source Impedance R +/- j X Ohms
4-radials: 32 wires; 62 segments			
Very Poor	-4.37	27	87.04 + j 25.31
Poor	-2.49	25	72.45 + j 19.47
Good	-0.71	23	60.96 + j 20.42
Very Good	2.10	17	47.34 + j 14.52
8-radials: 56 wires; 110 segments			
Very Poor	-3.11	28	65.90 + j 18.09
Poor	-1.51	25	58.63 + j 15.18
Good	-0.04	23	52.43 + j 15.94
Very Good	2.60	17	44.34 + j 12.60
16-radials: 104 wires; 206 segments			
Very Poor	-1.61	28	52.71 + j 12.43
Poor	-0.16	25	49.71 + j 12.18
Good	0.86	23	46.79 + j 12.83
Very Good	2.79	16	42.20 + j 11.18
32-radials: 200 wires; 398 segments			
Very Poor	-1.32	27	44.89 + j 7.54
Poor	0.17	25	43.44 + j 9.55
Good	1.12	22	42.67 + j 10.46
Very Good	2.94	17	40.48 + j 10.03
64-radials: 392 wires; 782 segments			
Very Poor	-1.19	27	40.68 + j 4.11
Poor	0.32	25	39.43 + j 7.08
Good	1.26	22	39.73 + j 8.50
Very Good	3.05	17	39.06 + j 9.07
128-radials: 776 wires; 1550 segments			
Very Poor	-1.12	28	38.60 + j 2.18
Poor	0.17	25	37.32 + j 5.29
Good	1.03	23	37.91 + j 6.99
Very Good	2.87	17	37.94 + j 8.27

With better soil quality, the differences between the above ground and buried radial models are not severe. However, with very poor soil, the 4-radial systems

show a great disparity: nearly 2.5 dB. As the graph in **Fig. 39-2** shows, buried radial systems show a rapid rise in gain as radials increase from 4 to 16, but the curves are much shallower after that point. Although the curve for very poor soil continues to rise through 128 radials, the curves for better soils actually decrease in gain from 64 radials upward. Hence, my trepidation over the 128-radial models.

160-m 1/4-WL, .25-m dia.; 2-mm radials
GP: tapered; .164-m below ground



Perhaps the most telling differences between above ground and buried radial system models lie in the source impedance reports. **Fig. 39-3** graphs the source resistance of above ground and buried radial systems for very poor and very good soil through the range of radials used. Note that there is no aberration in the curves, with a steady descent in all cases. Hence, there is also a reservation in my trepidation about the 128-radial models. The above ground and buried radial models for very good soil are quite parallel and not very far apart. However, for very poor soil, the buried radial system model reports much higher values of source resistance with lower numbers of radials.

Radials 0.001 WL Above & Below Ground Source R: VP and VG Soil

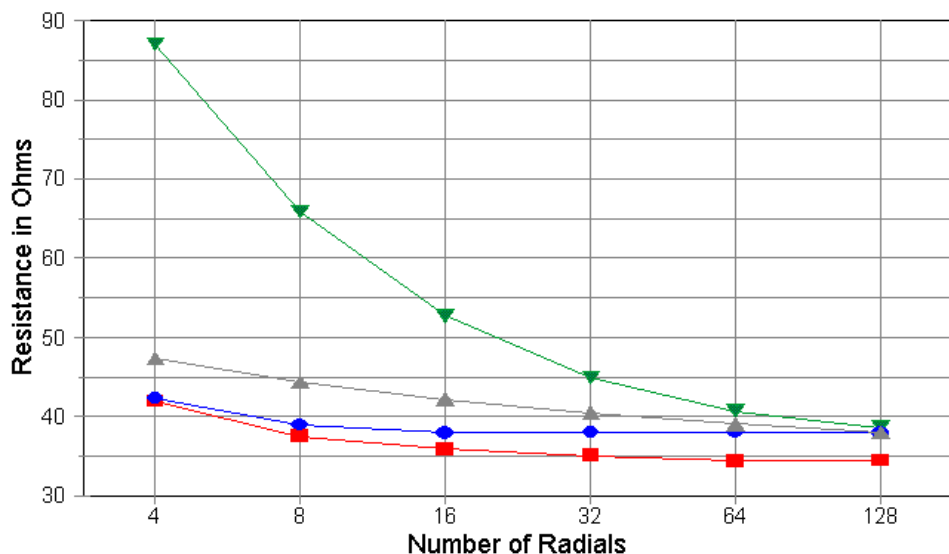


Fig. 39.3

—■— VP-Above —▼— VP-Below —●— VG-Above —▲— VG-Below

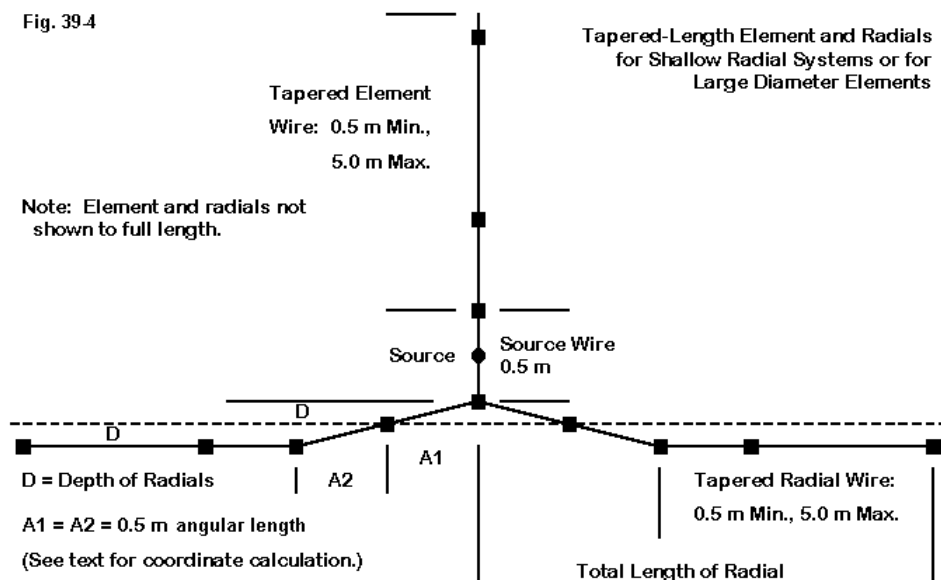
The upshot is that above ground radial systems have severe limitations in their role as substitutes for buried radial systems. If one plans to seriously model buried radial systems, then an investment in NEC-4 is likely the best course.

We have examined some data derived from models of 160-meter monopoles and radials systems in order to compare some modeling techniques. The data, however, is not necessarily transferable to other frequency ranges without some significant adjustment—in the data, not in the general modeling techniques. Indeed, as an exercise of instruction concerning what the modeling software yields by way of data on monopoles above buried radial sets of different sizes, you may wish to replicate the modeling experiment on each of the harmonically related amateur bands on which such antennas are common—for example, 160 meters through 40 meters.

Sloping Buried Radials

The model that we just used limited the diameter of the main element to an unnaturally low size for 160 meters, and the radials were purposely buried over 6" deep so that a relatively simple model might be used. However, there are many cases of shallower radials and fatter main elements. Either of these cases can press the NEC limits for a good length-to-diameter ratio for the segments.

Fig. 39.4



The problem has a fairly straightforward solution—and likely not the only one feasible. **Fig. 39-4** sets up a radial system for a main element that is 0.125 m (about 4.92") in diameter, along with a radial system buried only 0.082 m (0.0005 wavelength or 3.3") deep, the dimension D on the sketch. If we use our rule of thumb of keeping the wire lengths in models with complex geometry at a 4:1 length-to-diameter ratio, then the minimum wire or segment length will be 0.5 m, the lengths of A1 and A2 on the sketch.

We can start the main element (relative to ground) 0.082 m above ground and use a 1-segment source wire followed by a tapered-length remainder of the element, with the tapering having a 0.5-m minimum length and perhaps a 5-m maximum length for the segments. The first sloping portion of each radial will be from a height of 0.082 m to zero, with the second going from zero to -0.082 m. Since the sine of the angle is 0.082 over 0.5, the angle is 9.44 degrees. The cosine of this angle is .986, so the dimension along the ground is 0.493 m. Little harm would be done in using a round number like 0.5 for this dimension with shallow angles. However, for angles above 30 degrees—which are common in such models—the sloping wire length requires the use of this excursion from dimension to sine to angle to cosine to dimension. Hence, using the full progression of calculations is recommended for all cases.

The following table contains partial descriptions (3 of 32 radials in each case) of two models: one is a simple buried radial system like the one used with the 25-mm main element; the other is a sloping radial model used with a 250-mm main element. The contrast in modeling may reinforce the technique just described. Compare models 39-2 and 39-3.

Simple Junction Between Main Element and Radials

160-m 1/4 wl vertical, tapered radials Frequency = 1.83 MHz.

Wire Loss: Copper — Resistivity = 1.74E-08 ohm-m, Rel. Perm. = 1

WIRES									
Wire Conn.	--	End 1 (x,y,z : m)	Conn.	--	End 2 (x,y,z : m)	Dia(mm)	Segs		
1		0.000, 0.000, 40.000	W2E1		0.000, 0.000, 5.242	2.50E+01	7		
2	W1E2	0.000, 0.000, 5.242	W3E1		0.000, 0.000, 2.621	2.50E+01	1		
3	W2E2	0.000, 0.000, 2.621	W4E1		0.000, 0.000, 1.311	2.50E+01	1		
4	W3E2	0.000, 0.000, 1.311	W5E1		0.000, 0.000, 0.655	2.50E+01	1		
5	W4E2	0.000, 0.000, 0.655	W6E1		0.000, 0.000, 0.328	2.50E+01	1		

```

6   W5E2   0.000, 0.000, 0.328 W7E1   0.000, 0.000, 0.164 2.50E+01  1
    Tapered-length portion of main element
7   W6E2   0.000, 0.000, 0.164 W8E1   0.000, 0.000, 0.000 2.50E+01  1
8   W7E2   0.000, 0.000, 0.000 W9E1   0.000, 0.000, -0.164 2.50E+01  1
    Fixed wires of main element
9   W15E1  0.000, 0.000, -0.164 W10E1  0.164, 0.000, -0.164 2.00E+00  1
10  W9E2   0.164, 0.000, -0.164 W11E1  0.491, 0.000, -0.164 2.00E+00  1
11  W10E2  0.491, 0.000, -0.164 W12E1  1.147, 0.000, -0.164 2.00E+00  1
12  W11E2  1.147, 0.000, -0.164 W13E1  2.457, 0.000, -0.164 2.00E+00  1
13  W12E2  2.457, 0.000, -0.164 W14E1  5.078, 0.000, -0.164 2.00E+00  1
14  W13E2  5.078, 0.000, -0.164      40.955, 0.000, -0.164 2.00E+00  7
    First tapered-length radial
15  W21E1  0.000, 0.000, -0.164 W16E1  0.161, 0.032, -0.164 2.00E+00  1
16  W15E2  0.161, 0.032, -0.164 W17E1  0.482, 0.096, -0.164 2.00E+00  1
17  W16E2  0.482, 0.096, -0.164 W18E1  1.125, 0.224, -0.164 2.00E+00  1
18  W17E2  1.125, 0.224, -0.164 W19E1  2.410, 0.479, -0.164 2.00E+00  1
19  W18E2  2.410, 0.479, -0.164 W20E1  4.981, 0.991, -0.164 2.00E+00  1
20  W19E2  4.981, 0.991, -0.164      40.168, 7.990, -0.164 2.00E+00  7
    Second tapered-length radial
21  W27E1  0.000, 0.000, -0.164 W22E1  0.151, 0.063, -0.164 2.00E+00  1
22  W21E2  0.151, 0.063, -0.164 W23E1  0.454, 0.188, -0.164 2.00E+00  1
23  W22E2  0.454, 0.188, -0.164 W24E1  1.059, 0.439, -0.164 2.00E+00  1
24  W23E2  1.059, 0.439, -0.164 W25E1  2.270, 0.940, -0.164 2.00E+00  1
25  W24E2  2.270, 0.940, -0.164 W26E1  4.692, 1.943, -0.164 2.00E+00  1
26  W25E2  4.692, 1.943, -0.164      37.838, 15.673, -0.164 2.00E+00  7
    Third tapered-length radial (or 32 total radials)

```

———— SOURCES ————

Source	Wire Seg.	Wire #/Pct Actual	From End 1 (Specified)	Ampl.(V, A)	Phase(Deg.)	Type
1	1	7 / 50.00	(7 / 50.00)	1.000	0.000	V

Ground type is Real, high-accuracy analysis
 Conductivity = .005 S/m Diel. Const. = 13

Angular-Wire Junction of Main Element and Radials

160-m 1/4 wl vertical, buried radials Frequency = 1.83 MHz.

Wire Loss: Copper — Resistivity = 1.74E-08 ohm-m, Rel. Perm. = 1

———— WIRES ————

Wire Conn.	— End 1 (x,y,z : m)	Conn. —	End 2 (x,y,z : m)	Dia(mm)	Segs
1	0.000, 0.000, 40.000	W2E1	0.000, 0.000, 4.328	2.50E+02	9
2	W1E2 0.000, 0.000, 4.328	W3E1	0.000, 0.000, 2.328	2.50E+02	1
3	W2E2 0.000, 0.000, 2.328	W4E1	0.000, 0.000, 1.328	2.50E+02	1

Tapered-length portion of main element

4	W3E2	0.000,	0.000,	1.328	W5E1	0.000,	0.000,	0.328	2.50E+02	1
Fixed length section of main element										
5	W10E1	0.000,	0.000,	0.328	W6E1	0.945,	0.000,	0.000	2.00E+00	1
6	W5E2	0.945,	0.000,	0.000	W7E1	1.890,	0.000,	-0.328	2.00E+00	1
Two sloping wires of first radial										
7	W6E2	1.890,	0.000,	-0.328	W8E1	2.890,	0.000,	-0.328	2.00E+00	1
8	W7E2	2.890,	0.000,	-0.328	W9E1	4.890,	0.000,	-0.328	2.00E+00	1
9	W8E2	4.890,	0.000,	-0.328		40.960,	0.000,	-0.328	2.00E+00	10
Tapered-length portion of first radial										
10	W15E1	0.000,	0.000,	0.328	W11E1	0.927,	0.184,	0.000	2.00E+00	1
11	W10E2	0.927,	0.184,	0.000	W12E1	1.854,	0.369,	-0.328	2.00E+00	1
Two sloping wires of second radial										
12	W11E2	1.854,	0.369,	-0.328	W13E1	2.834,	0.564,	-0.328	2.00E+00	1
13	W12E2	2.834,	0.564,	-0.328	W14E1	4.796,	0.954,	-0.328	2.00E+00	1
14	W13E2	4.796,	0.954,	-0.328		40.173,	7.991,	-0.328	2.00E+00	10
Tapered-length portion of second radial										
15	W20E1	0.000,	0.000,	0.328	W16E1	0.873,	0.362,	0.000	2.00E+00	1
16	W15E2	0.873,	0.362,	0.000	W17E1	1.746,	0.723,	-0.328	2.00E+00	1
Two sloping wires of third radial										
17	W16E2	1.746,	0.723,	-0.328	W18E1	2.670,	1.106,	-0.328	2.00E+00	1
18	W17E2	2.670,	1.106,	-0.328	W19E1	4.518,	1.871,	-0.328	2.00E+00	1
19	W18E2	4.518,	1.871,	-0.328		37.842,	15.675,	-0.328	2.00E+00	10
Tapered-length portion of third radial (of 32 total radials)										
SOURCES										
Source	Wire Seg.	Wire #/Pct Actual	From End 1 (Specified)	Ampl.(V, A)	Phase(Deg.)	Type				
1	1	4 / 50.00	(4 / 50.00)	1.000	0.000	V				

Ground type is Real, high-accuracy analysis

Conductivity = .005 S/m Diel. Const. = 13

Intersecting Radial Fields

Sloping radials are not the only complexity that we may encounter when working with radial systems for vertical arrays. **Fig. 39-5** shows two intersecting radial systems for a 2-element array. Only a few wires have been shown in the sketch to preserve some clarity. See model 39-4 for a sample of this type of radial system. Between the two radial systems, there is a line of intersection, which for most purposes can be taken as being defined by the midpoint between the two radial systems. Actual radials might well pass over and under each other, as indicated by the dashed extensions in the figure. However, it is also common to join electrically the ends of relevant radials so that the junctions form a line corresponding to the verti-

cal dashed line in the sketch. The junctions along the line of intersection may be connected by wires or simply left open.

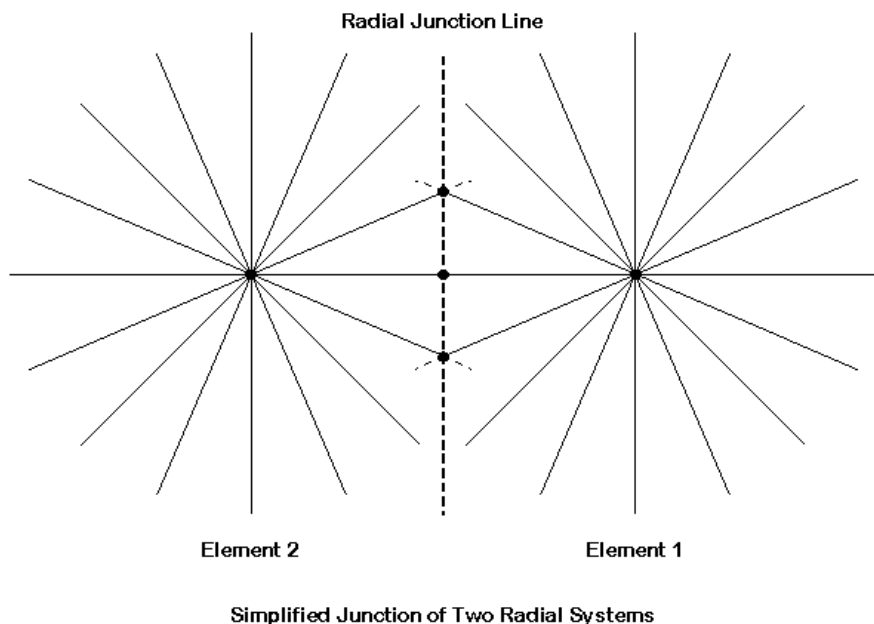


Fig. 39.5

Fig. 39-6 shows a 3-system set of intersections. The principles are the same for any number of intersecting radial systems. The key problem in constructing a model is getting rid of overlapping wires, since the NEC core will reject any model with wires that intersect at other than segment junctions. Instead, we need to calculate the coordinates of each intersecting radial so that we end up with true wire junctions. Model 39-5 provides a sample of a triple radial system.

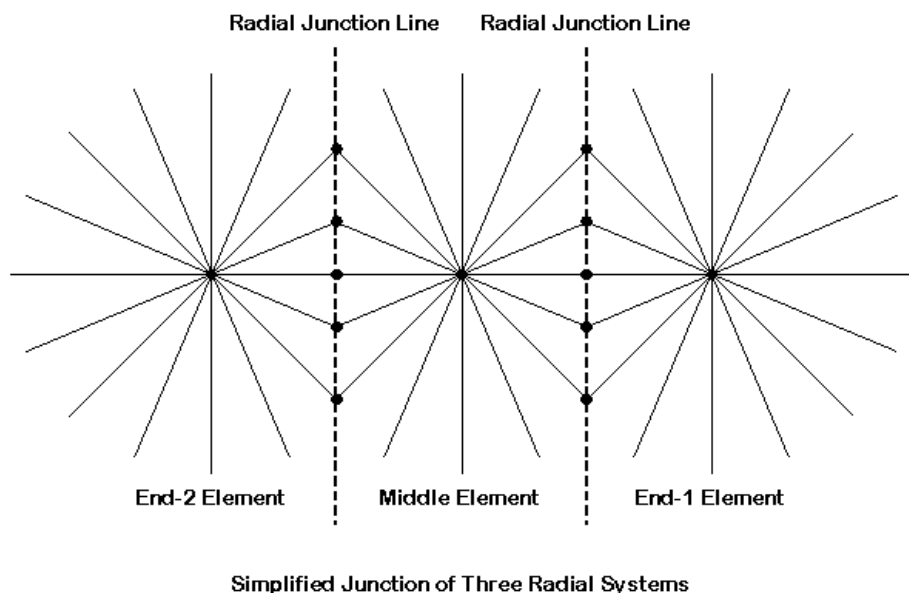
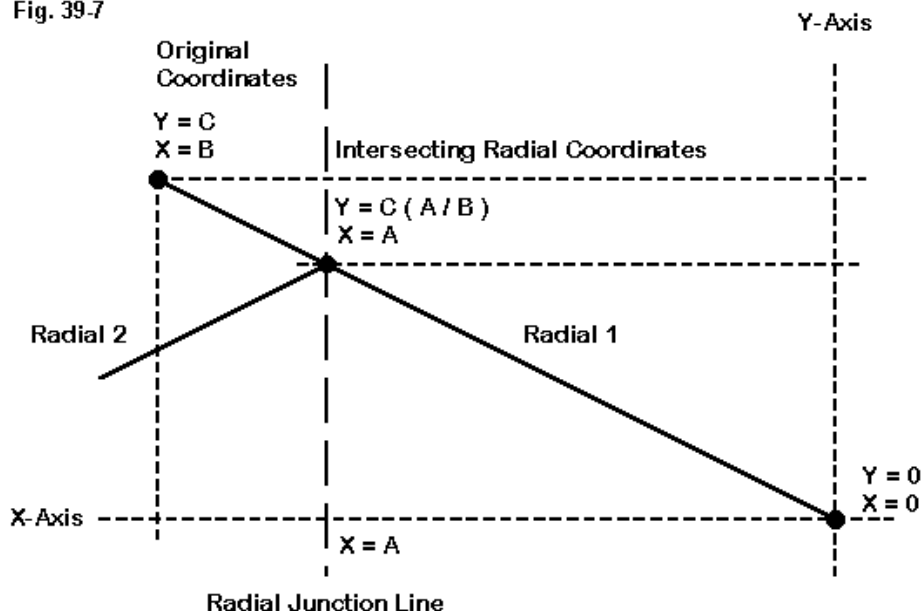


Fig. 39-6

The calculation technique is very straight forward, although its execution can be tedious for very large radial systems. Refer to **Fig. 39-7** for guidance. We can find the line of intersection along (let us say) the X-axis. Hence, we know the X coordinate of any radial to be shortened for a junction along this line. Since the original and the shortened radial coordinates define a pair of congruent triangles, the ratio of the new (shorter) X-axis coordinate to the original is also the ratio of the new Y-axis coordinate to the original. Of course, both of these numbers are most easily obtained if the origin of the radial system on which we do the original shortening is $X=0$ and $Y=0$. (We can always displace the entire system once our calculations and modifications are complete.)

Fig. 39-7



Calculating Coordinates for Intersecting Radials

If we are using uniform segmentation of the radial wires, then the same ratio that we used to determine the coordinates also tells us the number of segments to use in the shorter radial. The total number of calculations will actually be smaller than we might expect, since we can simply use the values that we get for the positive Y direction in the negative direction with a sign change (assuming an evenly symmetrical radial model). These new radial terminations also become the terminating coordinates for the second radial system where it intersects the first. If a multiple radial system is used and if the junction lines are equally spaced from the center element, the numerical values—with sign adjustments—are applicable to both junction sets. Only the process of entering the values on the wire chart is somewhat tedious and error-prone.

The techniques of generating complex radial fields apply equally to those we place above ground and to those we bury. From the notes developed here and using whatever automated facilities may exist within your particular NEC software, you can generate quite reasonable models for virtually any vertical antenna or array that uses a radial system. As we have seen from the preceding columns, such models are much preferable to the all-to-common over-simplifications that we have used in the past.

* * * * *

Models included: 39-1 through 39-5. (All model dimensions in meters.)



40. Resolution

Modelers often seek the shortest run times, the smallest tables, and the least resolution that they can get by with. This somewhat careless practice often begets errors of various sorts. So let's spend a little time looking at the areas of modeling where resolution makes a difference—or at least a potential difference—to the outcome of a modeling session.

1. Segmentation: Every segment adds more time to each run of the NEC core. Hence, modelers tend to use the least number of segments that they think will do a minimal but adequate job. Of course, the test of whether a model is sufficiently segmented is the convergence test, which we noted in detail in the very first episode of this series.

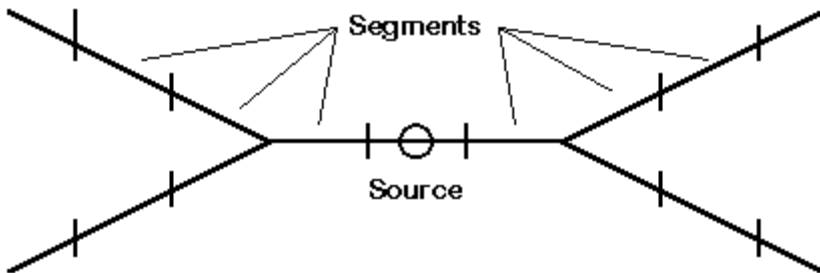
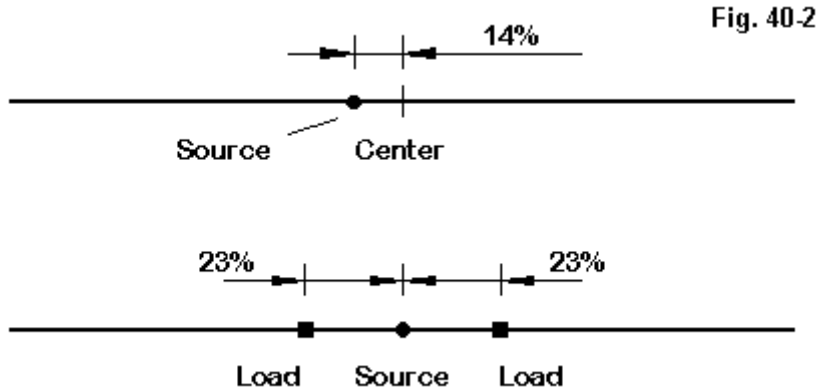


Fig. 40-1

There are a number of areas in which we dare not use too few segments. **Fig. 40-1** shows just one sample that should suffice as a reminder for virtually all other cases. In this partial sketch of a common feed for two antenna elements, a single source segment may lead to inaccurate results. Hence, we normally employ at least 3 segments for the common section, and this action may result in quite short

segments. The wires moving off from the junctions also require short section, close to a match for the segment lengths in the common wire. With uniform segmentation of the remainder of the antenna, we may end up with a very large model in terms of the number of segments. The modeler can length-taper the elements so that the far ends have longer segments. However, the test of whether a particular scheme of length-tapering (described in discussions of radial is recent episodes) is adequate is a comparison of the results with a uniformly segmented model. Hence, for at least part of our work, very large models for seemingly simple antennas may not be avoidable. See model 40-1 for a sample.

In some projects, we may be interested in the trends in the current magnitude and phase along elements, for example, in comparing long elements to very short ones or in comparing linear elements to loops of various shapes. Here again, a highly segmented set of elements—with attention to the relative equality of segment length among the items compared—can better reveal the finer details of the trends than truncated versions of the same models.



Adequate segmentation is also required for precise placement of off-center sources and loads, as suggested in **Fig. 40-2**. A dipole that may yield very accurate results with only 11 segments does not provide the modeler with the ability to place

an off-center source at exactly 14% of the distance from the element center toward one end. Likewise, a high number of segments are required to place loading inductors 23% of the distance from the element center outward towards the element ends. If one is analyzing an existing antenna that uses such placements, segmentation shortcuts will yield unreliable results.

Of course, the ultimate model-size cutting exercise occurs with vertical antennas when we attempt to avoid the construction of a radial system. See the last three columns in this series for ways to develop adequate radial systems.

Segmentation issues affect most of the tabular outputs available from NEC, including the values for currents and far-field strength. Near field and ground wave results are also affected. So it is impossible to over-stress the use of adequate segmentation—both in terms of numbers and in terms of other constraints that we have noted from time to time—in the development of an adequate model. The longer core run-times will result in longer output tables of values. The tables of currents on each segment may be especially important in some applications. The following lines are only a sample, drawn from a random model.

CURRENTS AND LOCATION

DISTANCES IN WAVELENGTHS

SEG. (AMPS)	TAG - - -	COORD. OF X	SEG. CENTER Y	Z	SEG. LENGTH	- - - REAL	CURRENT IMAG.
NO.	NO.	PHASE					
1	1	-0.2363	0.0000	0.0000	0.00508	5.0770E-04	-1.6493E-04
5.3382E-04		-17.997					
2	1	-0.2312	0.0000	0.0000	0.00508	1.3834E-03	-4.4791E-04
1.4541E-03		-17.940					
3	1	-0.2261	0.0000	0.0000	0.00508	2.1974E-03	-7.0900E-04
2.3089E-03		-17.883					
4	1	-0.2210	0.0000	0.0000	0.00508	2.9845E-03	-9.5965E-04
3.1350E-03		-17.825					
5	1	-0.2160	0.0000	0.0000	0.00508	3.7529E-03	-1.2025E-03
3.9408E-03		-17.766					
6	1	-0.2109	0.0000	0.0000	0.00508	4.5061E-03	-1.4387E-03
4.7302E-03		-17.708					
7	1	-0.2058	0.0000	0.0000	0.00508	5.2460E-03	-1.6690E-03
5.5051E-03		-17.648					

8	1	-0.2007	0.0000	0.0000	0.00508	5.9734E-03	-1.8936E-03
6.2664E-03	-17.589						
9	1	-0.1957	0.0000	0.0000	0.00508	6.6889E-03	-2.1127E-03
7.0146E-03	-17.528						
10	1	-0.1906	0.0000	0.0000	0.00508	7.3926E-03	-2.3263E-03
7.7500E-03	-17.468						
11	1	-0.1855	0.0000	0.0000	0.00508	8.0844E-03	-2.5344E-03
8.4724E-03	-17.406						
12	1	-0.1804	0.0000	0.0000	0.00508	8.7642E-03	-2.7371E-03
9.1816E-03	-17.344						

The output file gives too much data per line to contain each data line to 1 line in this format. However, the 12 lines shown bear some examination. Notice the rate of change of current per segment. (The NEC output report uses absolute segment numbers rather than a listing by wire and segment. The EZNEC current table translates this data back into the wire and segment numbers that apply to the wires specified by the user.) The greater the number of segments for a wire of a given length, the slower will be the rate of change of current per segment, since the rate of change along the entire wire will be the same in both cases. Higher segment density often allows one to locate better the effects of element loads and other phenomena that may cause significant shifts in current.

Perhaps the one limitation of some entry-level software is that they place segmentation restrictions on the modeler who takes these notes seriously. Other entry-level software (such as NEC-Win Plus) and upgrades from the entry level, provide more than enough segments for the largest model one might imagine well into one's career.

2. Pattern Resolution: A second arena in which resolution can make a large difference involves the far-field radiation patterns that we specify. **Fig. 40-3** is a screen grab (from NEC-Win Plus) of an azimuth pattern specification box. Among the matters that we can as users determine is the resolution of the pattern, that is, at what angular increments NEC will produce a table of values out of which the interface program creates a graph of the pattern.

Three-dimensional patterns, available in some implementations of NEC (for example, NEC-Win Plus and EZNEC 3.0) require a relatively high value for the increment, somewhere between 3 and 5 degrees as the lowest value. Since the program must calculate all values for all bearings in the free-space sphere or the

hemisphere over ground, excessive resolution encounters two problems. First, the higher the resolution, the longer the core run time. Second, because the result is presented as a single graphic, the result of maximum resolution would be a solid mass of dots and connecting lines that would obscure the view of useful detail.

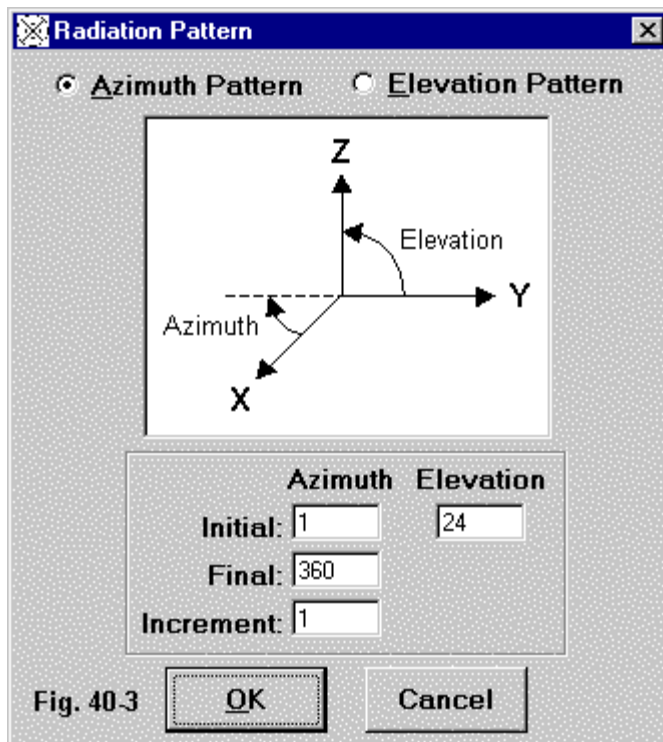


Fig. 40-4 shows a pair of 3-D patterns of a quad beam over ground, taken from NEC-Win Plus. The 10-degree resolution graphic provides more widely spaced lines for easier identification of portions of the pattern, especially those parts on the far side of the pattern. However, notice the level of distortion to the pattern relative to the 5-degree resolution version. Entire segments of the major lobes appear to be missing from the graphic. In contrast, the 5-degree version show much more detail, but at the expense of blurring the details, especially of the concentrated lobe structure to the rear of the pattern.

Resolution Level: Detail vs. Readability

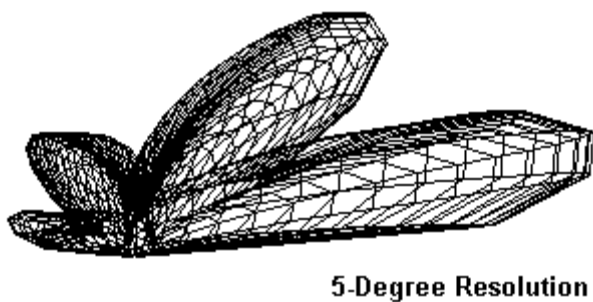
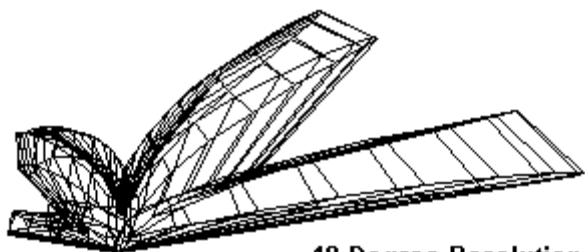


Fig. 40-4

Even the 5-degree 3-D graphic shows strong signs of distortion relative to the actual pattern. The sharp corners taken by lines at intersections are unnatural to normal radiation patterns.

3-D patterns are both a convenience and often a useful way to cross check our identification of the strongest lobe or the deepest null of a pattern. In addition, we can rapidly survey a pattern for various oddities, such as lobes that increase in strength upward or downward, but which also change the azimuth bearing of maximum strength as we change the elevation angle as well.

However, the main work of far-field pattern analysis is usually a function of 2-dimension elevation and azimuth patterns. For these patterns, unless we have a special function in mind, we resort to the maximum resolution (or minimum increment) made available to us by a program. For many programs, this is 1 degree. However, some implementations of NEC, such as EZNEC, provide resolutions as fine as 0.1 degree. This degree of fineness requires a table with ten times the number of values as needed with 1-degree resolution, and the graphic calculations naturally take longer. However, the chief question for the modeler is this: when are they useful?

For most azimuth patterns, a resolution of 1 degree is more than adequate. For very regular patterns with few lobes and nulls, even a 5-degree resolution will yield a satisfactory azimuth pattern. Typical of the antennas able to use lower resolutions in azimuth patterns are the dipole, Yagi, and quad beam.

Until a wire reaches 10 to 15 wavelengths, a 1-degree resolution captures all of the relevant detail. Non-integer wavelength values (for example, 19.6 wavelengths) that show both emergent and declining lobes and nulls may require a slightly higher resolution to capture every detail of note. As well, complex wire arrays with equally complex phasing conditions among the wires may yield patterns with side and rear structures that benefit from resolutions less than 1 degree. However, these instances are fairly rare.

More commonly, the modeler requires better than 1-degree resolution with elevation patterns as the antenna height exceeds several wavelengths above ground. Let's look at some elevation patterns at different resolution levels and different heights to get a feel for what occurs. We shall use the EZNEC 0.1-degree level, along with

the more universal 1.0-degree level. Our subject antenna will be a simple horizontally polarized Yagi set for 299.7925 MHz, so that each wavelength is also 1 meter. See model 40-2 and vary its height.

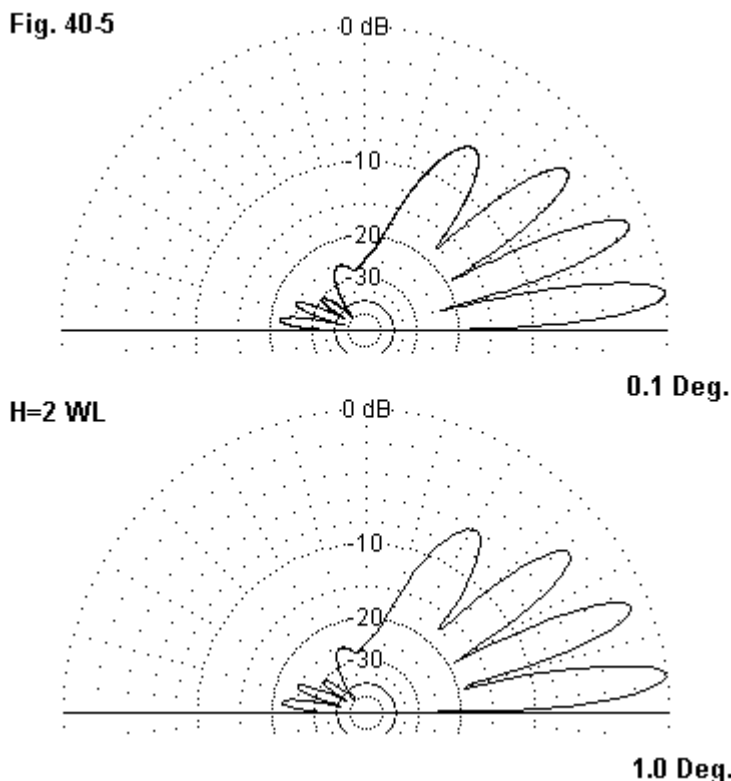


Fig. 40-5 shows the elevation patterns for both degrees of resolution at an antenna height of 2 wavelengths. The patterns are indistinguishable to the eye. In fact, both patterns show an elevation angle of maximum radiation (TO angle) of 7 degrees (7.0 in the 0.1-degree system).

Let's elevate the antenna to 8 wavelengths. For those who are familiar only with HF antennas, an 8-wavelength height is virtually unthinkable. At 20 meters, we are speaking of 525' or so. However, at 300 MHz, the height is simply 8 meters or about

26' up. As we scan **Fig. 6**, there appears at first sight to be little difference between the patterns, and the TO angles (2 vs. 1.8 degrees) seem to confirm that the two patterns are virtually identical. However, look closely at the second lobe in the 1-degree resolution pattern. It should be stronger than the third—as shown by the 0.1-degree resolution pattern—but it is not. Slight irregularities in the lobe structure have begun to appear as a result of insufficient pattern resolution.

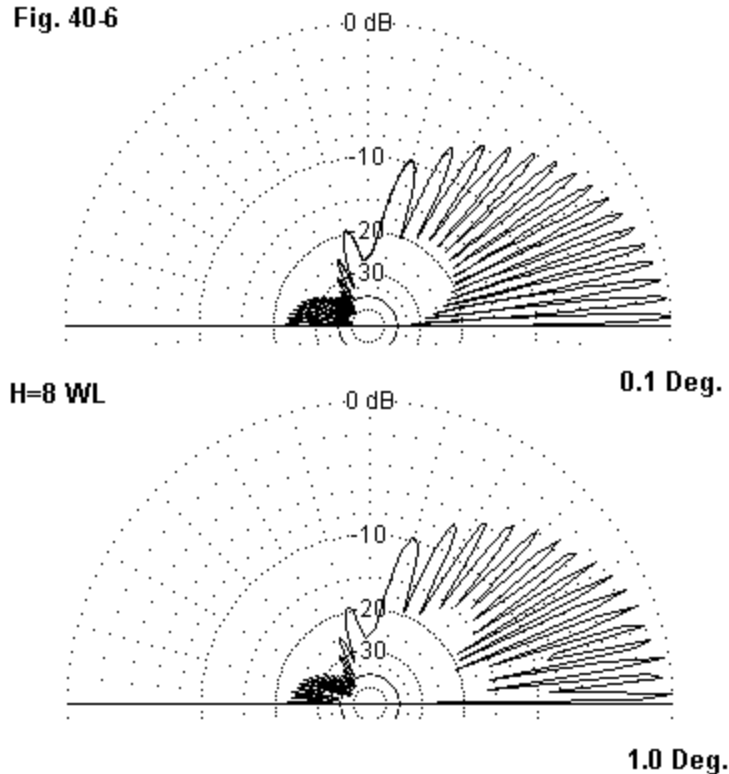
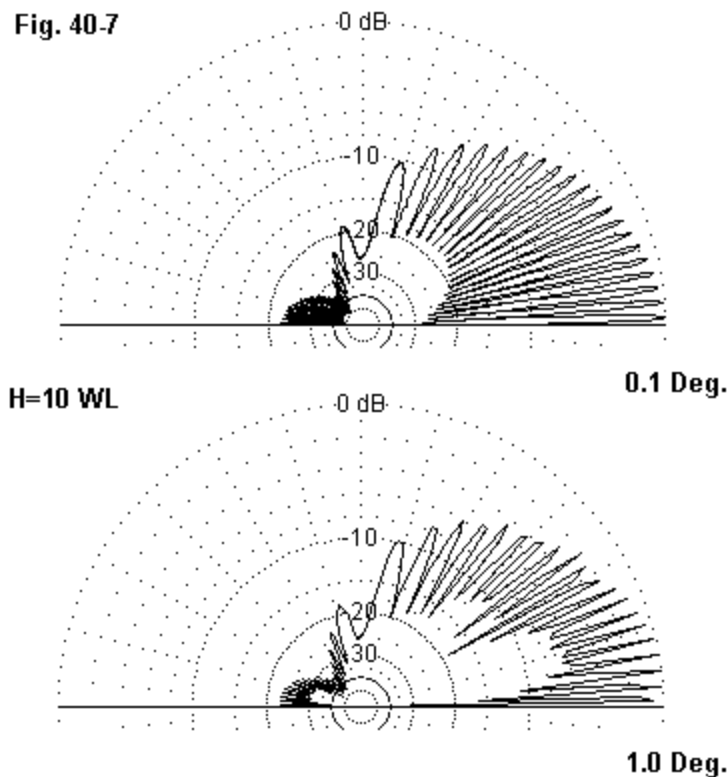
Fig. 40-6

Fig. 40-7



If we further elevate the antenna to 10 wavelengths (10 m or 33' at 300 MHz), the irregularities become serious, as shown in **Fig. 40-7**. Note that in the 1-degree resolution version of the pattern, many lobes appear as straight-line to points rather than as rounded lobes. Note also that the lowest lobe, which should be the strongest and is the strongest in the 0.1-degree resolution pattern, is weaker than the

lobes above it in the 1-degree resolution pattern. In fact, the pattern identifies the TO angle as 7 degrees rather than as the more nearly correct 1.4 degrees.

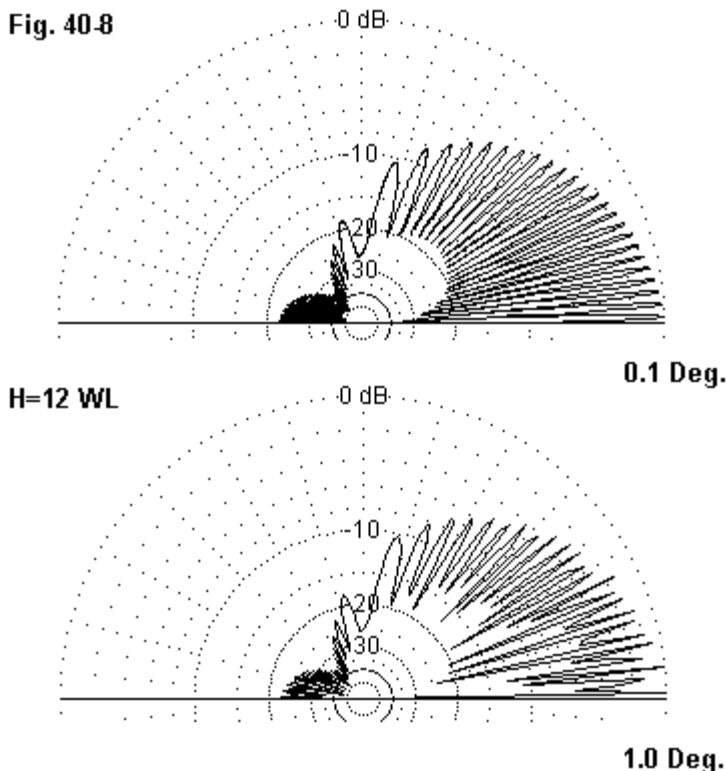
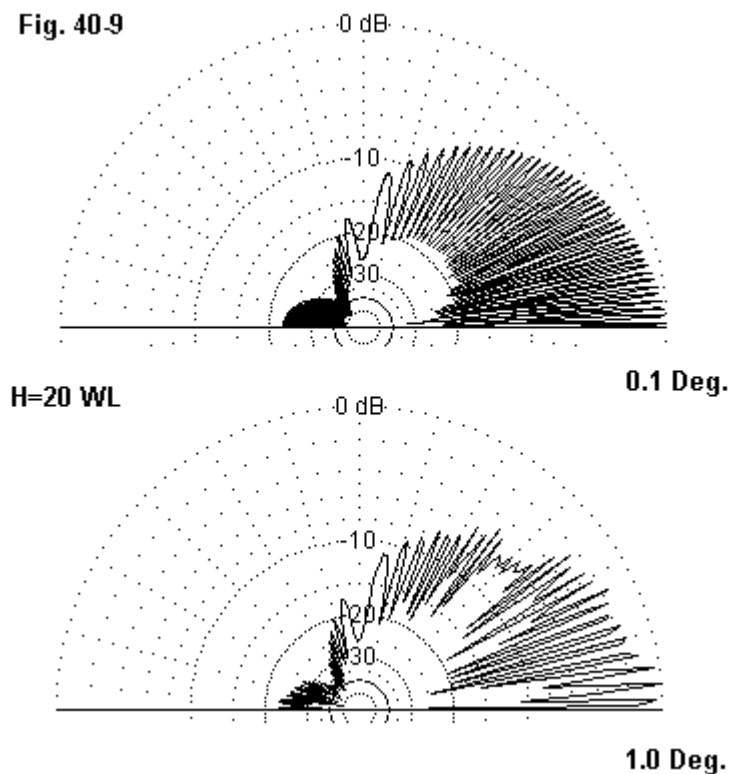


Fig. 40-8 carries the problem still further as we elevate the antenna to 12 wavelengths (12 m or 39'). The 1-degree pattern identifies the strongest lobe at 6 degrees up, whereas the 0.1-degree version places it at 1.2-degrees elevation. Note also that, although all 24 lobes from the ground up to 90 degrees (zenith) are present, the null structure has deteriorated significantly. Compare the two graphics with respect to the interior that shows the depth of nulls. Very often, this structure reveals inadequacies of resolution more evidently than tracing the outer perimeter of

the lobes. An adequate pattern for an antenna producing a quite regular far field should show the relatively smooth curve of nulls displayed by the 0.1-degree resolution pattern. If this smooth curve is absent without other known cause, then suspect that the pattern resolution may be inadequate.

Fig. 40-9

Let's jump to an antenna height of 20 wavelengths (20 m or about 66' at 300 MHz). We can count lobes in **Fig. 40-9** and see that the 1-degree resolution pattern shows only 28 of the 40 total lobes in the 0.1-degree version. Considerable portions of the fine structure of the pattern are missing, and the lower resolution pattern identifies the TO angle as 5 degrees. The more nearly correct value is 0.7 degrees.

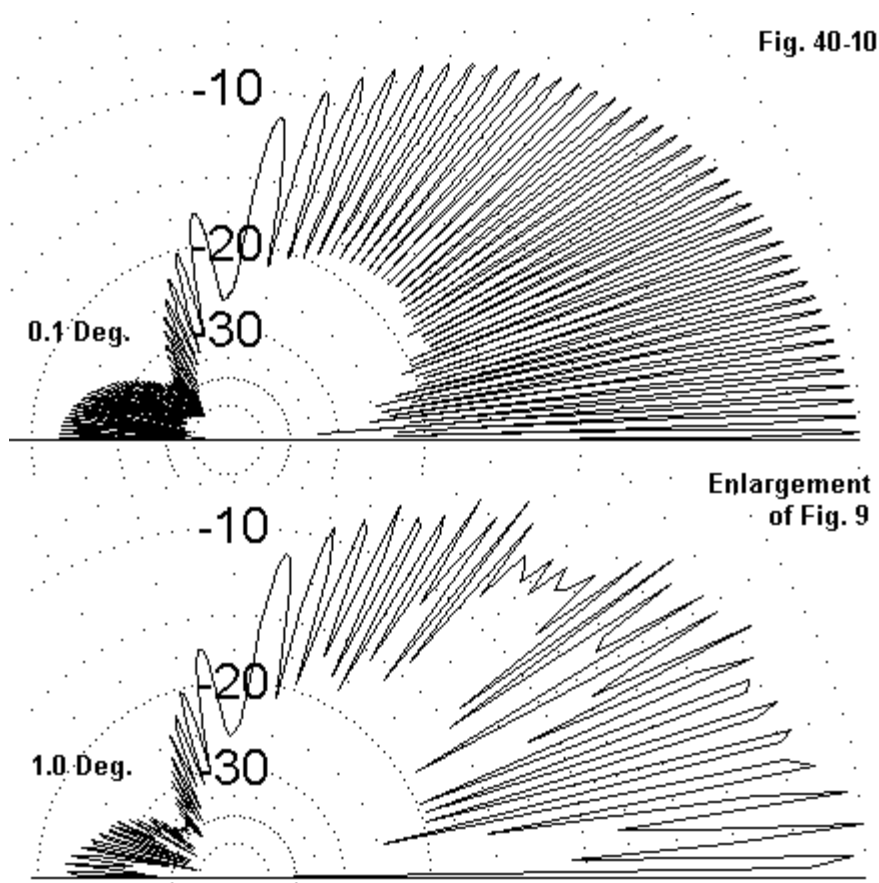
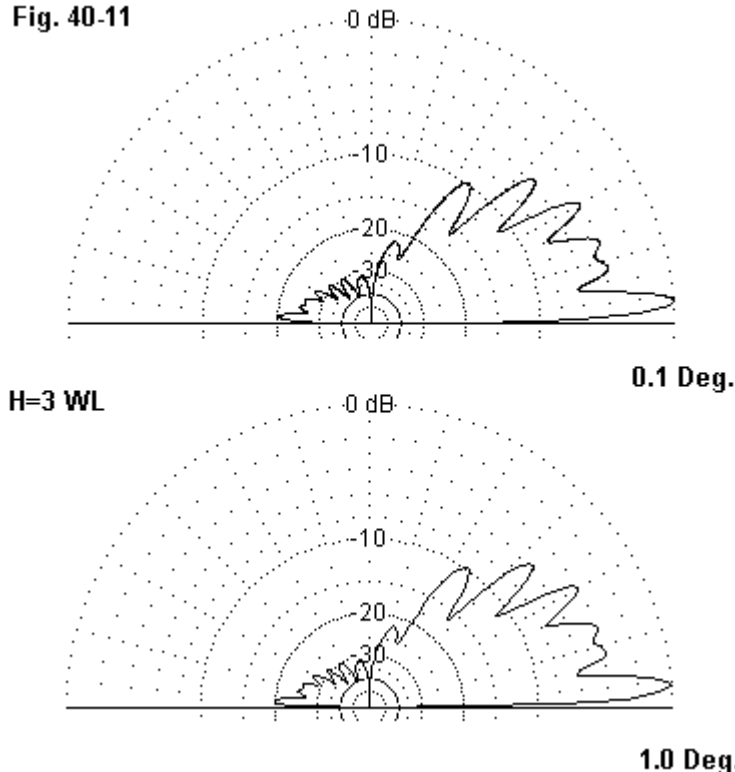


Fig. 40-10 enlarges the patterns to reveal just how much of the pattern detail has been lost by the 1-degree resolution pattern. Entire sections of the pattern show almost no nulls, and the lobes are irregularly spaced in many areas. Some wider lobes are actually two lobes with the null between having been missed by the lower resolution.

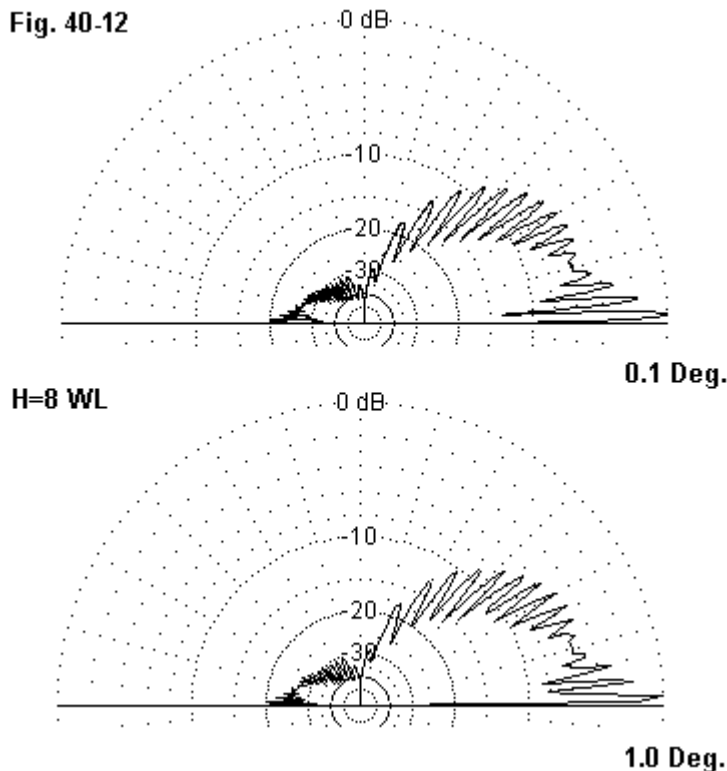
However, **Fig. 40-10** has a second message for the perceptive viewer. Although the outer limit of the lobe structure appears to form a smooth curve, just as we might

expect, the inner structure of nulls is showing the first signs of deterioration. Nothing is seriously amiss yet, and the pattern is perfectly usable for all normal purposes. However, a mere 20-wavelengths up is a fairly low height for many UHF antenna installations. Hence, even the 0.1-degree resolution pattern table promises to reach a limit of usefulness at frequencies lower than the limit for the remainder of NEC calculations.

Fig. 40-11

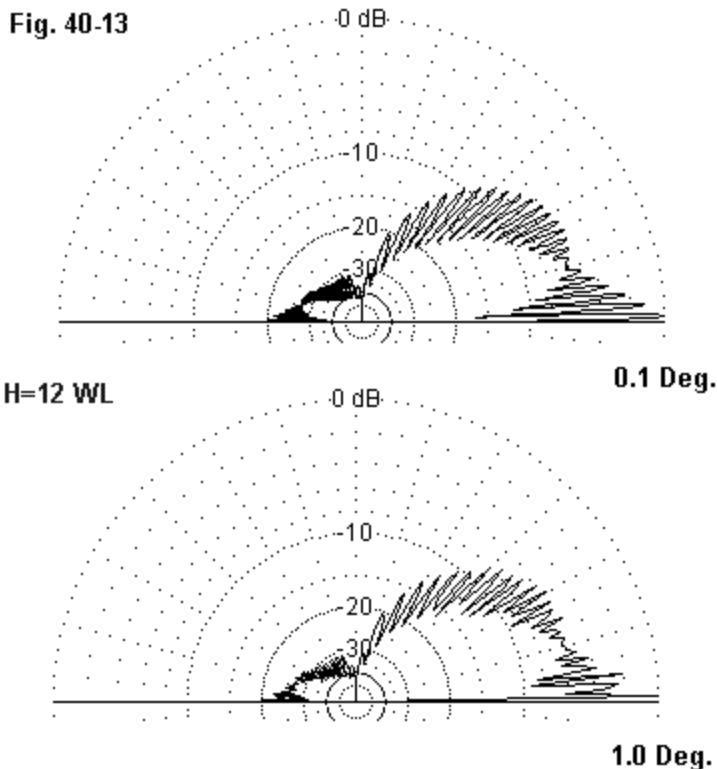
Vertically polarized antennas tend to show the same signs of inadequate pattern resolution, but in ways whose appearance varies from their horizontally polarized brethren. Therefore, let's look at a 3-element Yagi for 299.7925 MHz that is turned to be vertical. We shall be looking for signs of pattern deterioration that are similar to those we have thus far observed. See model 40-3.

Fig. 40-11 forms our baseline, with the antenna 3 wavelengths in the air over average ground. Essentially, there is no difference between the two elevation patterns, and the lower (1-degree) resolution version is perfectly adequate for all normal purposes.



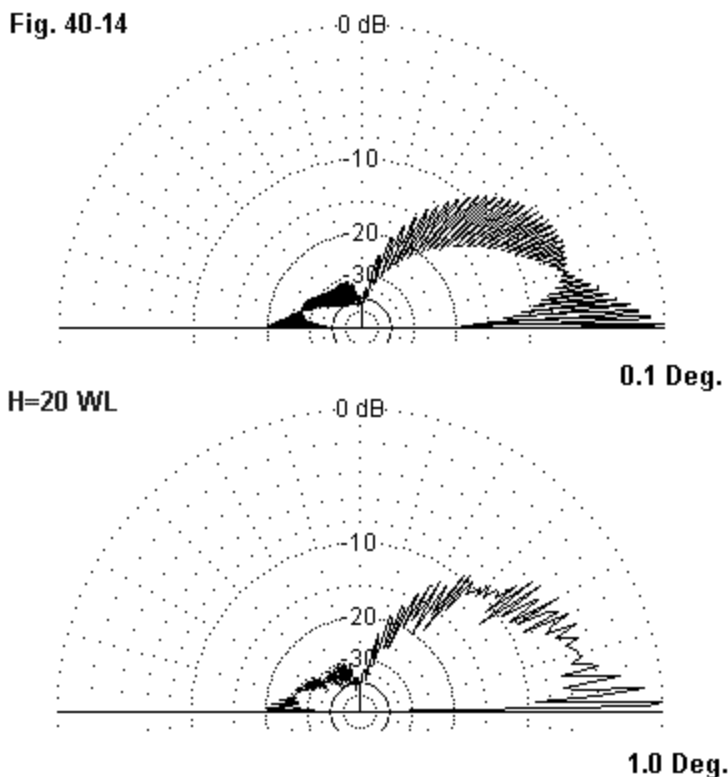
As we raise the antenna to 8 wavelengths (8 m or 26' at 300 MHz), the signs of inadequacy in the 1-degree pattern might elude us, especially if we focus upon the outer edge of the lobes in **Fig. 40-12**. However, in the 1-degree resolution pattern, notice the absence of a deep null between the first and second lobes, a sign that the degree of resolution is inadequate to pick up values close to the deepest null. By way of contrast, the interior structure of the 0.1-degree resolution pattern forms a smooth curve. The pattern of lobes and nulls for a vertically polarized antenna is

different from that of a horizontally polarized antenna of the same general type. Hence, each polarization will show different outer and inner curves formed by the tips of the lobes and of the nulls.



By the time we reach an antenna height of 12 wavelengths (12 m or 39'), the 1-degree resolution pattern in **Fig. 40-13** has severely deteriorated to the point of yielding inaccurate information. The higher resolution plot shows the TO angle at 1.2 degrees, with the next major lobe at 3.5 degrees. However, the 1-degree plot—

while giving us an accurate 1 degree for the TO angle—reports the next major lobe at 6 degrees. Our last pattern, **Fig. 14**, taken at an antenna height of 20 wavelengths, shows severe deterioration of both the interior and exterior curves. Contrasting the 0.1 and 1 degree resolution plots should provide ample guidance in detecting when pattern resolution is severely inadequate.

Fig. 40-14

Conclusion

The adequacy and accuracy of the information that we derive from NEC models depends to a great degree upon our selections as users. In this episode, we have noted two general areas in which we are prone to use inadequate resolution: segmentation and pattern resolution. Both tendencies can yield unrecognized inaccurate results and should be avoided—without going to the wasteful extreme of using uninformative excess resolution.

We are also limited to some extent by extant implementations of NEC, only some of which provide either or both the pattern resolution needed for high UHF antennas or the number of segments adequate for large models. Therefore, if we are not going to develop our own interface systems for the available NEC cores, we must use care in selecting the software we buy. As in all such matters, we must match up the software capabilities to the set of anticipated tasks. If entry-level software fails to meet user needs, upgrading is certainly in order.

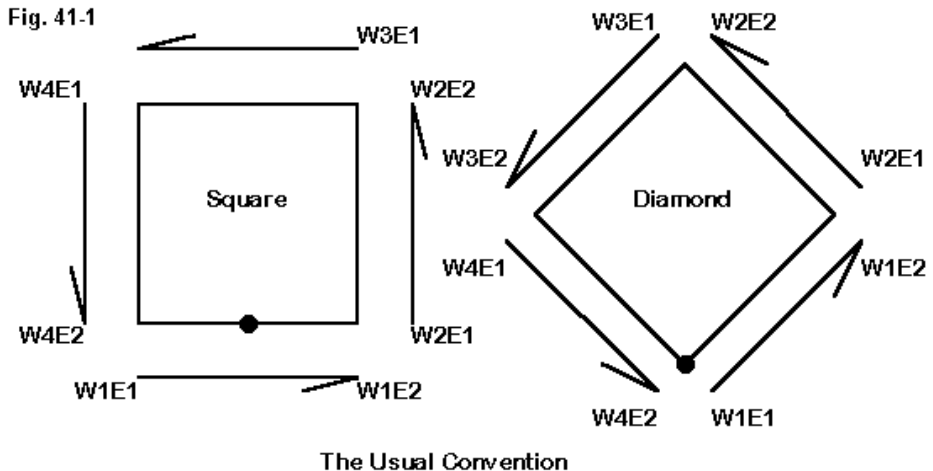
* * * * *

Models included: 40-1 through 40-3. (All model dimensions in meters.)



41. Multiple-Feedpoint Loop Modeling

There are a number of questions that often arise surrounding quad loop modeling. Some of the answers to these question also apply to other antenna models, so it may be worthwhile to spend an inordinate amount of time with the simple quad loop.



For a single quad loop with a single feedpoint, the conventions of modeling shown in **Fig. 41-1** are very convenient. Essentially, we model “around the horn,” taking one wire after the other so that End-2 of the preceding wire matches End-1 of the succeeding wire. We can apply the technique to either square or diamond quad loops—or to any other closed polygon.

The technique is orderly, giving us a systematic way of keeping track of the wires in complex arrays of which this loop may be one of many. However, the technique has more to recommend it than simple orderliness.

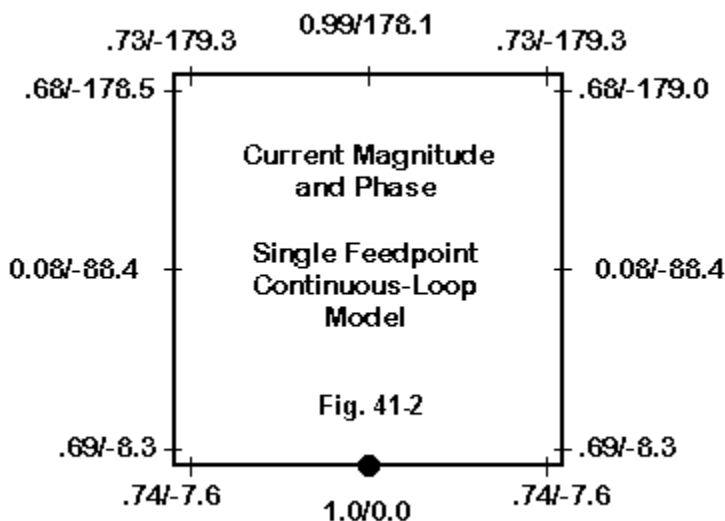


Fig. 41-2 shows the current magnitudes and phase angles at selected points around the loop. Each loop side (21.876") for the sample model has 21 segments (in case you want to replicate the exercise). Copper wire and an arbitrary but resonant (+/- j1 Ohm reactance) frequency of 144.4 MHz with #18 wire complete the essential ingredients for the model used here. See model 41-1.

Note that as we begin at the source (the dot in the figure) and move in either direction, we have an orderly progression of current magnitudes and phase angles. Because we have a single feedpoint and a wire that is not perfectly conductive, the midpoints of the vertical wires do not show a relative current magnitude of zero or a phase of exactly -90 degrees. At the upper corners, current magnitude is very

slightly less than at the lower corners—not enough to affect antenna operation, but enough to prove that copper has a small amount of resistive loss.

The figure that may seem oddest to the beginning modeler is the phase angle at the point directly opposite the feed point. However, in most implementations of NEC, phase angle values are run from -179.99 to +179.99. The sudden shift in the phase angle value to +178.1 degrees is the equivalent of having a phase angle of -181.9 degrees. With that mental adjustment, then, we have a seemingly smooth transition of current levels along the quad wires.

However, appearances—especially when developed by showing only selected values—can be deceiving. Well over half of the current phase transition occurs in the small region around the vertical wire mid-points, where the current magnitude also approaches zero and rises again. This set of transitions is similar to that for a dipole end, except that the dipole end is open.

In fact, one way to think about a quad loop is as two dipoles with the ends bent toward each other until they touch. The touching ends eliminate the shortening of the so-called end-effect, and a quad loop will have a circumference that is longer than the sum of two dipoles. As well, the effects of changing the wire diameter are opposite each other. For resonance, the fatter the wire of a dipole, the shorter its length must be. For a closed loop, the fatter the wire, the larger the loop circumference for resonance. Despite these behavioral differences, it is often useful to look at a 1-wavelength loop with a single feed as two dipoles with touching ends.

One result of this orientation to the loop is to think of the halves of the overall quad as being in phase and hence additive in their pattern production. In fact, a quad loop of the specifications used in this exercise has a free-space gain of about 3.3 dBi in contrast to the 2.1-dBi gain of a dipole in free space.

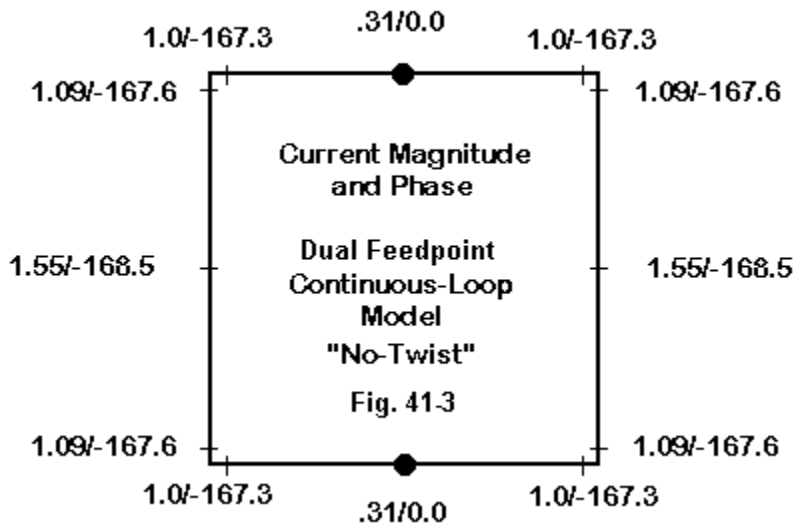
However, if the two halves of the loop, counting from the left side mid-point to the right side mid-point are two dipoles in phase, why does the upper horizontal mid-point show a phase angle about 180 degrees out of phase with the feedpoint? The answer lies partially in the modeling convention we chose and partially in data that we do not see in **Fig. 41-2** (or in any of the usual tables produced by NEC). The wire direction of our continuous loop model is opposite for the upper and lower horizontal wires. Since current values are functions of the End-1 to End-2 orientation of the

wires, we find a -180 -degree phase angle at the top relative to the zero-degree phase angle at the bottom. What we do not see is that the voltage at the upper mid-point would have a phase angle that is also 180 degrees out of phase with the voltage at the feedpoint. Hence, the combination yields a power that is in phase for the two positions on the wire loop.

A similar phenomenon occurs with a number of other antennas, some of which are not closed loops. For example, a half square fed at one corner can be thought of as two right angle Vees, each with a quarter wavelength leg vertical. The horizontal quarter wavelength sections join at their ends. The standard and correct way of treating the half square is as two quarter wavelength verticals in phase spaced just about $1/2$ wavelength apart. The $1/2$ wavelength horizontal wire is often called a phasing line because most of the radiation from it cancels.

However, if we model two $1/4$ -wavelength verticals independently, we must provide two sources, each of which has the same current magnitude and phase angle. Only in this way can we obtain a pattern similar to that of the half square. However, if we look at the current tables for the half square, then we find that the current at the corner away from the feedpoint has a phase angle about 180 degrees different from that of the source. Once again, the voltage phase angle at the far corner would also be 180 degrees different from that of the source, establishing an in-phase relationship between the two points.

For single feed systems, these small mental adjustments make almost no difference in the ways in which we handle loops and half squares in the design or analysis efforts to construct arrays with them. However, the adjustments required begin to make a larger difference—with more room for unseen errors—whenever we begin to look at multiple feedpoints on a single wire structure. For example, we can feed a quad loop at both the upper and lower wire center-points. We might use equal lengths of parallel feedline with a junction to the main feedline directly between the upper and lower loop wires. To feed the loop wires in phase, we would physically run the wires in straight lines, with no twist to either the upper or the lower section from the junction.

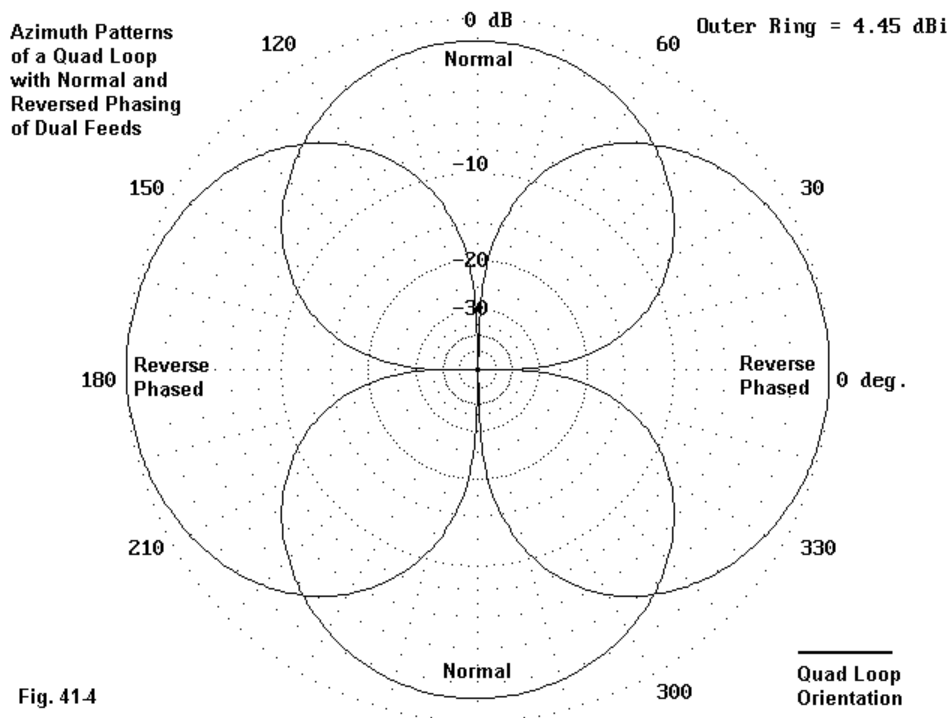


However, our model—if it uses the convention of wire structuring that we started with—will not reflect reality if we feed it as we would when building the physical antenna. **Fig. 41-3** shows two source points, one at the center of each horizontal wire. Both sources are specified for a current magnitude of 1 and a phase angle of 0, as revealed by the designation “No-Twist” on the figure. Relative current magnitude and phase angle values are shown for the same points as in **Fig. 41-2**. See model 41-2.

The current magnitude and phase angle values are very much different from those in **Fig. 41-2**. In fact, the no-twist sourcing of this model has in fact placed two sources that are 180 degrees out of phase on the model, since a source is in series with its wire. Moreover, the source follows the End-1 to End-2 orientation of the model. Hence, the source on the upper wire is set in the opposite direction as the

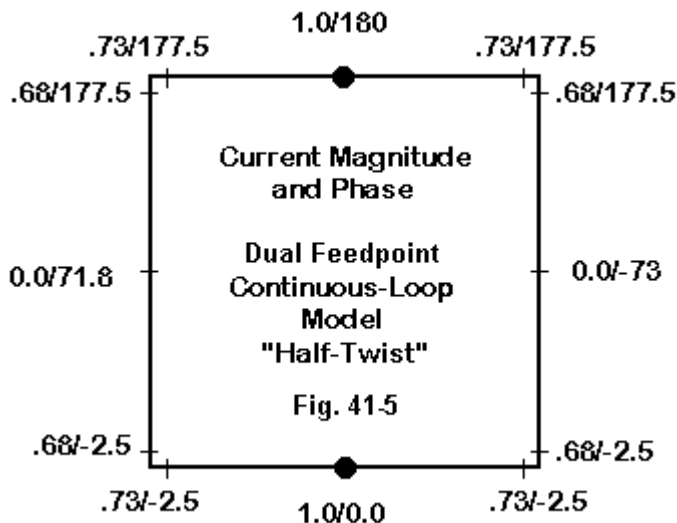
source on the lower wire. However, we cannot change the voltage phasing, so that the two feedpoints are now out of phase relative to each other.

A similar situation would occur if we simply placed a second source on the half square at the “other” corner of the array. (In fact, if one draws the open wire ends of a half square together, letting the horizontal wire bend at its center, the result would be a diamond-shaped quad loop.)



Note that there is no error within NEC in this regard—only an error caused by our not keeping track of the wire directions and making the sources coincide with those directions. Physically, the difference between feeding the two wires in phase and out of phase makes a big difference to the resulting pattern. **Fig. 41-4** shows the patterns for a normal quad with an in-phase dual feed and one that is dual fed out of phase. The “normal” in-phase feed results in pattern lobes broadside to the plane of the loop. In contrast, out-of-phase feeding results in lobes off the edges of the loop—a situation not designed to bring out the best in a multi-element quad beam.

If we adhere to the modeling convention with which we started—remembering that it is most useful for single feedpoint loops—then our model only (and not the physical antenna) will have to place a half twist in one (but not both) of the two sections of feedline from the junction to the antenna wire. Now the model will yield a correct radiation pattern and a set of correct feedpoint values for a dual in-phase feed quad loop. See model 41-3.



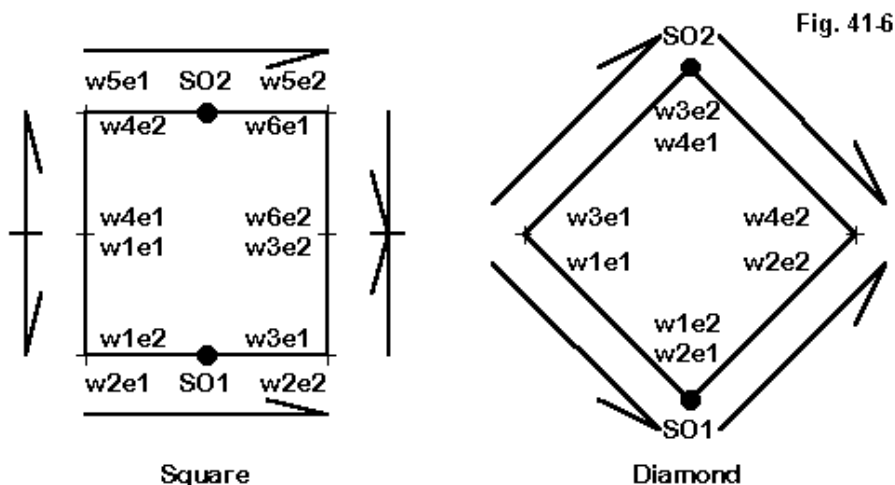
However, not everything regarding the model will be in best order. Our artifice, while correcting certain elements of the modeling—the ones of highest interest to most casual modelers—has still left some data out of good order. **Fig. 41-5** sketches the dual feed situation with one source set at 0 degrees and the other set at 180 degrees. Around the perimeter are the relative current magnitude and phase angle readouts yielded by NEC for the model. Note initially that each outer corner has a phase angle that is -2.5 degrees relative to the source phase angle. However, their values are very different.

We may also wish to look at the side mid-point values. Although the current magnitude has gone so close to zero as to not record in limited decimal places, the phase angle is not an anticipated ± 90 degrees. The values differ and depart from 90 degrees by what seems to be a significant amount. However, remember that the closer to the exact mid-point we get, the more rapid is the change of current magnitude and phase angle. At these point—as well as at the open ends of a dipole, NEC calculations may depart by considerable amounts from what we presume (rather than calculate) from theoretical considerations. For the model at hand, the spatial displacement between the calculated ± 70 degree angles and a true 90 degrees would amount to a very small fraction of an inch at the frequency in question.

You may establish the correctness of the in-phase feeding as requiring no half twist in reality. Simply construct a small quad loop within the frequency range of whatever antenna analyzer you may have. Use equal lengths of parallel feedline from the two source points to a common junction—and then a length of line about 1 wavelength long to the meter. If you give one section of line a half twist, your source impedance will have a very low resistive component—a few Ohms. With correct in-phase feeding, the resistive component will be moderate to high, depending the length of the two sections of line and where you draw the line between “moderate” and “high.”

If we wish all of our values to be correctly aligned and thus to require no mental adjustments from the modeler, then multiple feed quad loops must employ a different convention from the one with which we started. In short, we must model them as two bent in-phase dipoles. **Fig. 41-6** provides some guidance. For a diamond-shaped quad loop, we need add no wires to the model. Instead, we simple model both the upper and lower Vees from left to right, with junctions at the far left and at the far right. (Of course, we might as easily have gone from right to left in both

cases, but these notes follow the western convention of reading from left-to-right in most matters.) Now both source points will follow suit and be in phase. However, remember that for highest accuracy, sources at model corners or junctions of wires should use either a short 3-segment wire on which to place the source or use a split source. See model 42-4.



A Better Convention for Dual Feeds

What the square loop gains in simplicity of feeding, it loses in the need to add wires relative to the standard way in which we model quad loops. We must start at the far left mid-point at a junction of two wires, one of which goes down, the other of which goes up. The horizontal wires can be single wires with an odd number of segments in order to center each of the two sources. At the right, we again need two wires, one from the bottom horizontal and the other from the top horizontal—with a junction at the exact center point between the horizontals. Thus has our 4-wire model of a quad loop grown into 6 wires.

Segmenting the model also calls for attention. If our horizontal wires have 21 segments apiece, then each of the verticals should use either 10 or 11 segments so that segment lengths will be approximately equal throughout the model. Unfortunately, I still encounter many models that simply give every wire the same number of segments, regardless of the wire length. Sometimes, this practice causes no harm; sometimes it yields significantly flawed modeling results. So I have simply tucked in this reminder.

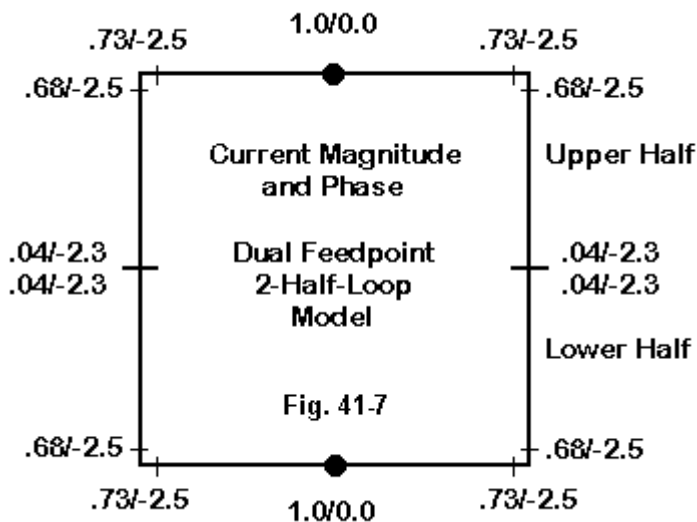


Fig. 41-7 shows the current magnitudes and phase angles that result from the revised model. All four corners of the model are now synchronized. However, do not be fooled by the nicely balanced current values at the mid-points of the sides. The region at the very center of the sides—corresponding roughly to the ends of a dipole—undergoes a very rapid change in current magnitude and phase. You can see this in action by using 100 segments for each of the vertical wires and 201 segments for the horizontals—or as close to this as a software limitation in total

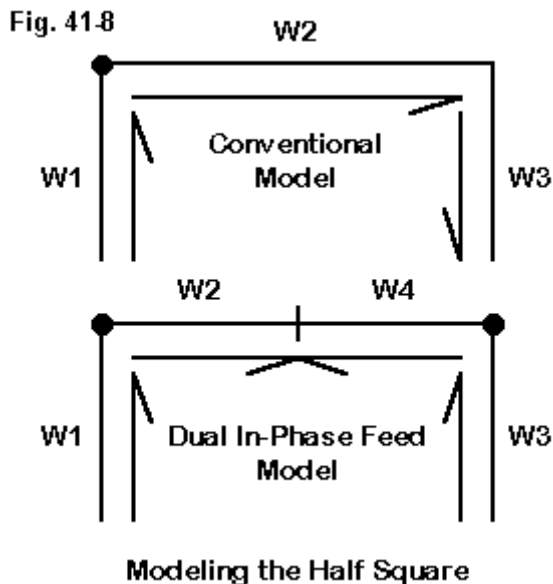
segments may permit. Explore especially the current magnitudes and phases for the segments at End 1 of wires 1 and 4 and at End 2 of wires 3 and 6.

Getting into the habit of modeling dual-feed quad loops (and similar closed polygons) in the way suggested here may not be easy. Of course, since square quad arrays and diamond quad arrays do not differ significantly in performance, you can always simply use diamond-shaped elements and avoid having the 2 extra wires per loop. Or, you can simply model in the old way and make mental adjustments as you go. Or you can simply tell yourself that the current magnitude and phase angle data makes no difference to anything and model in any old way that gets all of the wires roughly in place. None of these options is advisable, although reality tells us that some modelers will use them.

One way to get into the habit of using better conventions in modeling is to annotate models thoroughly. Virtually all software allows for the use of the CM entry—the comment card in the Fortran deck. Besides using this facility to give basic information about the antenna that the model replicates, you should also give yourself a record of any features of the modeling process that might be subject to memory loss later.

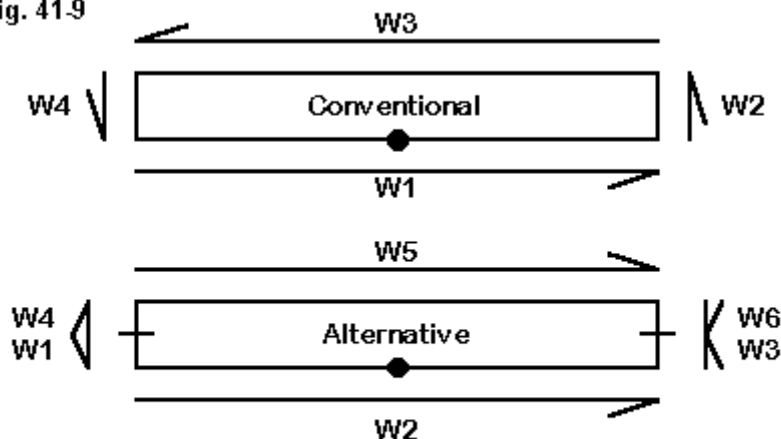
In addition, if the dual fed quad loop is to be used in an array of loops, it is useful to model each other loop in the same manner as the driven element. This practice will ensure that current magnitude and phase values on the parasitic elements track those on the driver in accurate ways.

What applies to the quad loop also applies to other types of antennas. **Fig. 41-8** shows the conventional single-feed half square, modeled in typical fashion. However, for a dual feed model that establishes an in-phase feed system, something like the alternative convention should be followed. The vertical wires, as radiators, should be parallel with respect to their End-1 to End-2 orientations. This creates horizontal legs that project toward each other and meet in the middle. Now, when we place separate but in-phase sources at the two corners, the model will perform as it would in reality (apart from the field of sappy pine trees in which we were forced to erect the actual antenna and which is not part of the model).



Less likely to be done is the alternative method of modeling a folded dipole, as shown in **Fig. 9**. Note that even with a single feedpoint, the current magnitudes and phases will read differently according to the convention of modeling that we select. The currents on a modeled folded dipole are a combination of “radiating” and “transmission-line” currents. For an accurate correlation between a single-wire dipole and a folded dipole, you must separate the two types of currents. The resulting radiating currents will be virtually identical to those in the single-wire dipole. At every point along the antenna structure the transmission-line currents will show a $\pm 90^\circ$ -degree phase angle relative to the source current. As one widens the spacing between the wires and adjusts the length for a return to near-resonance, the transmission line currents disappear. By the time we reach the square shape of a quad loop, they do not show up on the model.

Fig. 41.9



Modeling the Folded Dipole

A correct analysis of a folded dipole that goes beyond simply recording its gain and pattern features requires that we set up the model with the wires correctly oriented to track the current magnitudes and phase angles along the wires. The folded dipole and the quad loop have a common feature: we may model them in the simplest fashion when our modeling task is equally simple. However, more complete analysis places additional modeling demands on us. The utility and sensibleness of the resulting data will depend to a great degree on the manner in which we construct our models.

From the examples that we have examined, you should have acquired an appreciation for the differences that modeling conventions can make in the data—and sometimes, the pattern—outputs from NEC. In all cases, models should avoid shortcuts. Instead, the conventions adopted for a kind of antenna or array should be those which yield the most correct outputs across the board, whether we intend

initially to use some of the data or not. We may often later find occasion to look into the tabular data, and their usefulness without mental or paper conversions—or re-making the initial model—will depend upon the care we use in constructing the initial model.

* * * * *

Models included: 41-1 through 41-4. (.NEC and .NWP model dimensions in meters; .EZ model dimensions in inches.)



42. Moving and Rotating

Windows-based facilities make available to the programmer, and the programmer sometimes makes available to the user, the ability to move and manipulate blocks of numbers. Of greatest interest to this series is the ability to move and rotate wires in an antenna model. It is a very handy feature that is often overlooked by users of programs that have it. I tend to use it considerably—even to the point of moving models from one program to another with the facility and back again—if the other program has a feature that I need there.

3-Element Yagi: Reflector at 0, Boom = Y-Axis

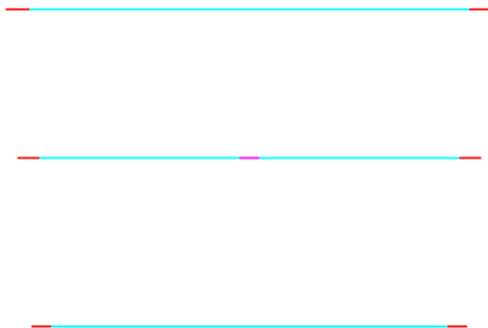
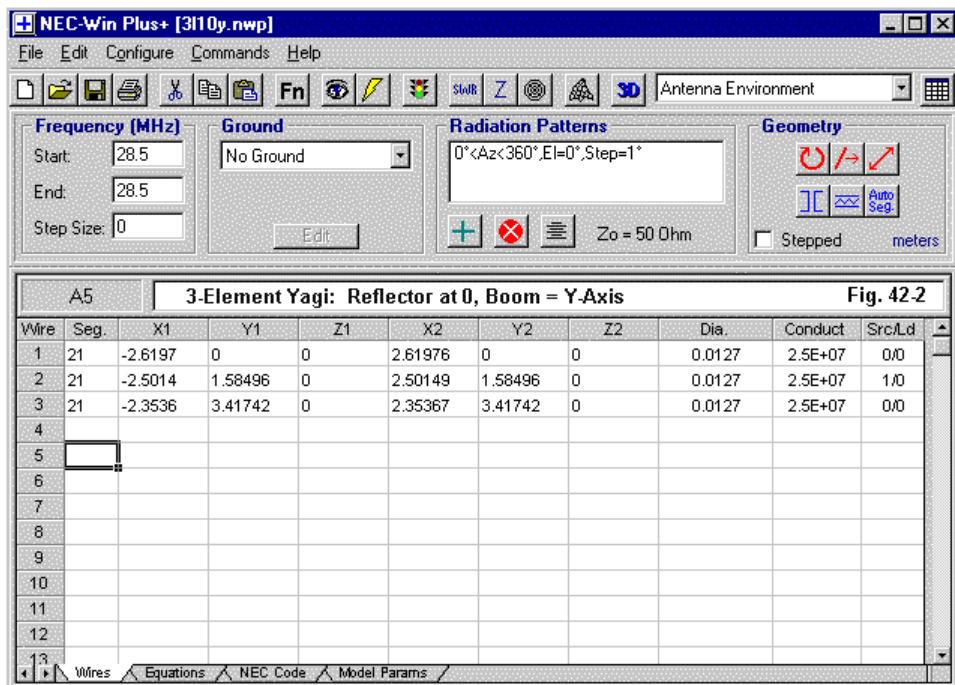


Fig. 42-1

So let's tell a short story with lots of pictures to get a handle on moving and rotating the wires of a model. **Fig. 42-1** is the outline of a simple 3-element Yagi that happens to be cut for 10 meters. My habitual conventions result in two features of note here. First, I tend to model with the reflector at zero and all other elements

having positive spacing values ahead of the reflector. Second, I tend to model element length from $-X$ to $+X$, which aligns the boom along the Y -axis. Not everybody uses these conventions, so we may wish to translate the model to something in accord with other conventions. See model 42-1.

Fig. 42-2 shows the main screen of NEC-Win Plus, which happens to have the necessary facilities. Version 4 of EZNEC will have full wire movement and rotation facilities, but is not generally available at the time of writing. The dimensions of the elements appear in the X1 and X2 boxes, with the spacing in the Y1-Y2 boxes. Note the longest element—the reflector—is at $Y=0$.



Now move to the “Geometry” box in the upper right corner of the screen. We shall play with only two buttons on the top row. The left button is for rotation, which we shall look at shortly. The middle button is for moving one or more wires, which we shall examine immediately.

Suppose that we wanted to shift all three wires so that the beam’s boom is centered on $Y=0$. Since the Yagi is 3.41742 m long, we need to move the beam to the rear by -1.70871 m. We can do this by subtracting the movement number from each Y value. However, let’s block the entire set of 3 rows and then click on the “Move” button.

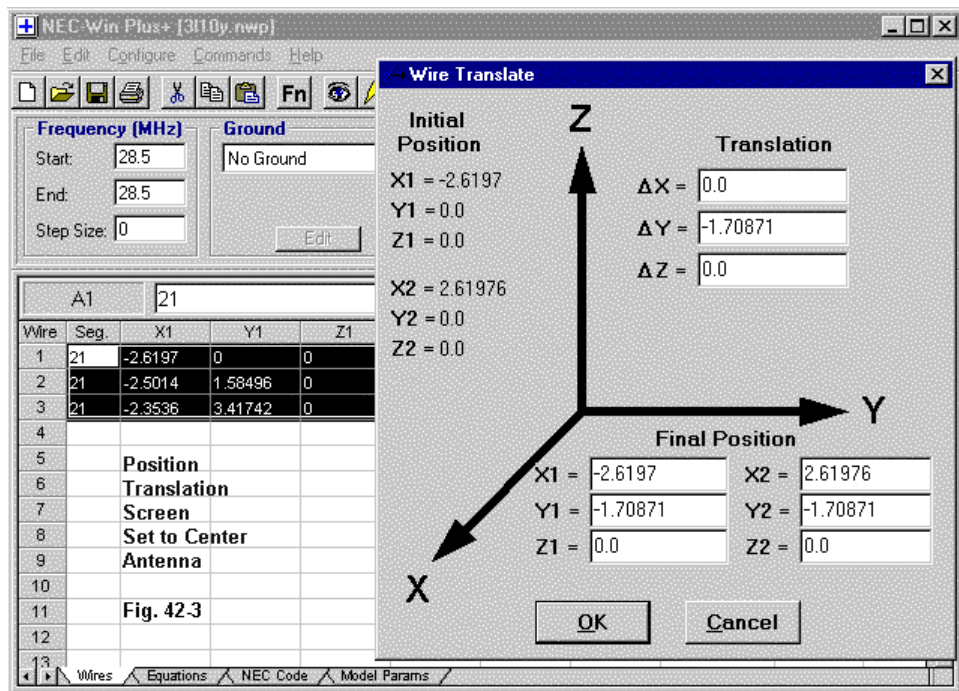
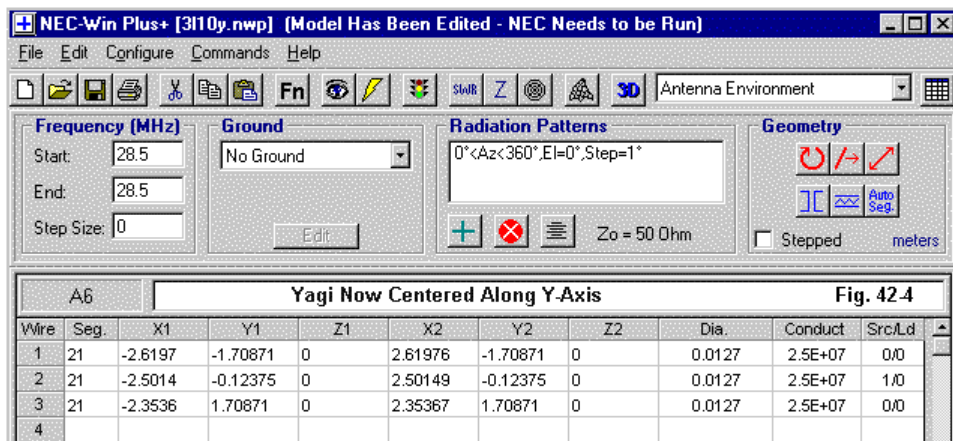


Fig. 42-3 gives us the resulting screen. The “Move” box is overlaid on the main screen, but you can see the blocking of the relevant wire entries that will allow us to move all three wires at once. In the translation entry area, -1.70871 has been entered for delta-Y. The initial and final positions of the first wire is shown, but the action will affect all of the wires that we have placed in the block.

Fig. 42-4 shows the main screen for the finished product. The Y-axis values are now +/-1.70871 m. Note that the driven element for this array is not centered on the boom, but is slightly to the rear of center. See model 42-2.



There are many good reasons for wanting to center a Yagi in this way. For example, if we are modeling a stack of antennas for different bands, we would want the antennas to line up with the mast as the center spot for the array. In some cases, the center of weight will not coincide exactly with the center of the boom, so adjustments may be needed. Nonetheless, the ability to move numerous elements at once by the same precise amount is handy to shorten the work—and to eliminate errors with respect to individual elements.

Side-by-side stacks are also common. We can use the blocking facility to copy a set of elements from the basic antenna. Then we can move the new elements to

their final position by translation in any one or more of the axes. When making up VHF squares of Yagis, for instance, I tend to copy one Yagi. Next, I position each Yagi equal distances on each side of a chosen axis. Then I copy both wire sets to create two more Yagis. These two can be moved together along a single axis to complete the square array.

Although these actions have been illustrated with NEC-Win Plus, similar movement facilities are available in EZNEC using the “Group” change facilities in that program.

Now let's suppose that someone prefers to have the Yagi elements extended along the Y-axis, with the boom along the X-axis. In NEC-Win Plus, we may make the maneuver by going into each wire end entry set and swapping the X1 and Y1—as well as the X2 and Y2—values, wire by wire. However, there is a quicker way using the “Wire Rotate” routine.

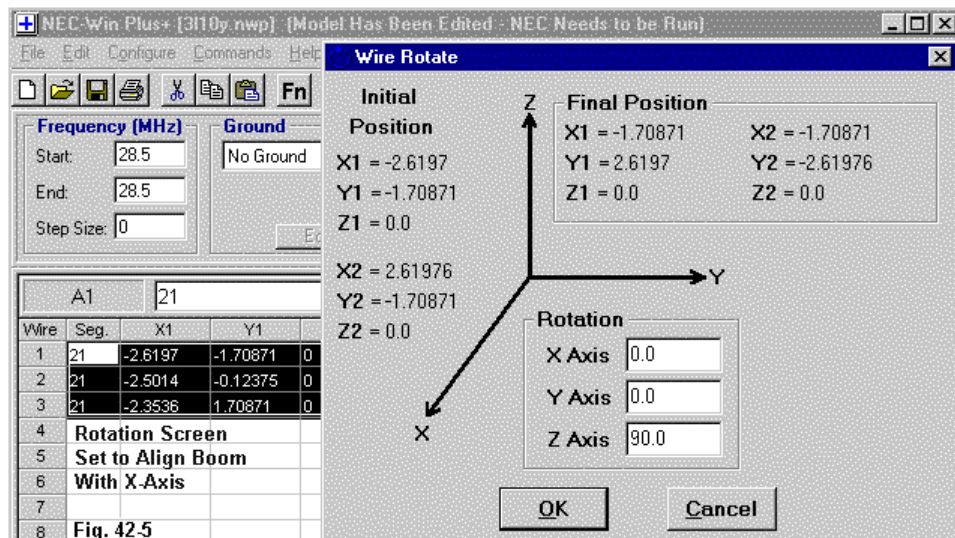
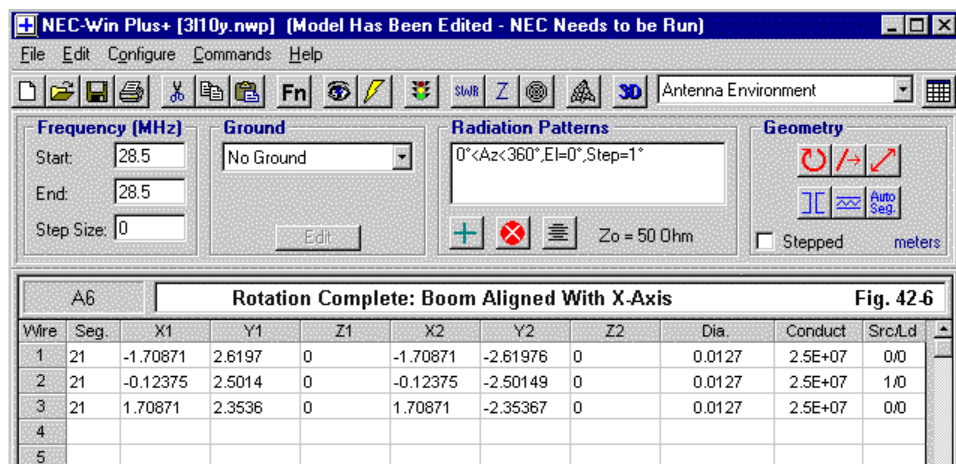


Fig. 42-5 shows our centered Yagi with all wires within a block. Also in the picture is the rotation box. Since we wish to change the X-Y orientation of the antenna, the rotation will be around the Z-axis. Note the entry of 90 degrees in the “Rotation” area, with the initial and final values for the first wire shown as a check on the work before we commit to it. See model 42-3.

By now, sharp-eyed readers will have noticed that the elements are not perfectly symmetrical relative to the boom axis. As I noted, I often move models from one program to another, and this model originated in another program. Translation from one format to another often requires a bit of clean-up, which has not been performed yet. However, before finalizing a model “for the record,” it is important to do the clean-up—not so much because it will change antenna performance reports, but because these small inexactitudes often distract and sometimes confuse others who may examine the model.



In **Fig.42-6**, we have the rotated antenna wire table—complete with its not-quite-symmetrical elements. However, compare **Fig. 42-6** and **Fig. 42-4** to note the 90-degree reorientation of the beam.

We could have performed the same rotation on the initial model, which placed that reflector at zero. By rotating the antenna around the Z-axis, the reflector would have remained at zero, but on the X rather than the Y-axis. The Z-axis is always presumed to have X and Y values of zero. If we had placed the reflector at Y=10 m initially, under rotation, the reflector would end up at X=10 m.

One convenient use of the rotation facility is to test stacks of Yagis. A common configuration is a stack of 2 Yagis, with one fixed toward a target region. (U. S. contesters use Europe as a common target for such arrays.) The top beam rotates. Now suppose that we feed both arrays in phase. What happens to the composite pattern as we rotate the upper antenna some angular distance out of perfect alignment. Begin with model 42-4, an aligned stack.

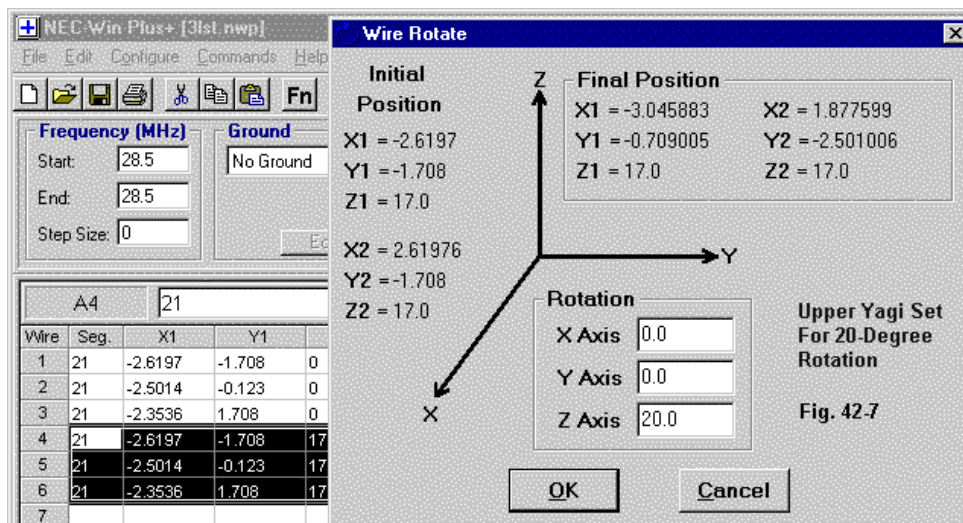


Fig. 42-7 shows the situation. Wires 1-3 represent the lower beam that is fixed. Wires 4-6 represent the upper beam that we intended to rotate. 17 m is a very large spacing for 10-meter arrays, but it will serve for the example. Let's rotate the upper beam 20 degrees and see what happens to the composite pattern.

The rotation box shows the 20-degree rotation of the blocked wires—the upper Yagi—around the Y-axis. Both beams are otherwise identical. The final position listings in the rotation box may not seem informative at first sight, but they can assist in the prevention of errors before we alter the model itself.

Fig. 42-8 gives the final result for the tire upper beam in Wires 4-6. If the coordinates do not seem to let us know that the rotation is correctly done, we can always turn to the antenna view screen. See model 42-5.

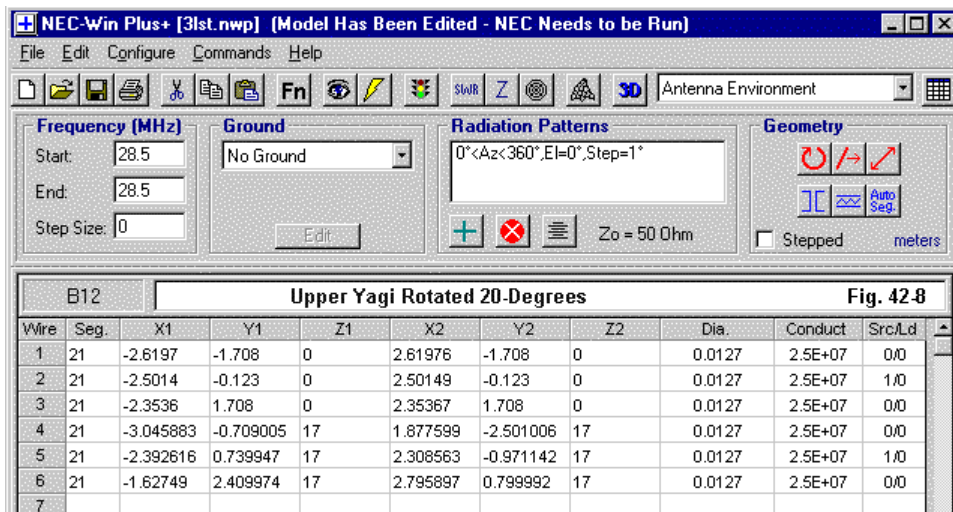


Fig. 42-9 shows the antennas. I have drawn the two arrays closer to each other to reduce the size of the image. However, we can see that the rotated upper array has elements that preserve their alignment with each other. A protractor will confirm that the rotation angle is 20 degrees.

What we can learn from the exercise may surprise some and be old hat to others. We would want to keep a record for various angular intervals relevant to our concerns—perhaps data and patterns every 20 degrees from in-line to out-of-line (remembering that we will get mirror images as we return from out-of-line back to in-line). Recording gain and front-to-back ratio, and checking the elevation patterns as

well as the azimuth patterns will give us a rather complete picture of what happens as we rotate the top beam only.

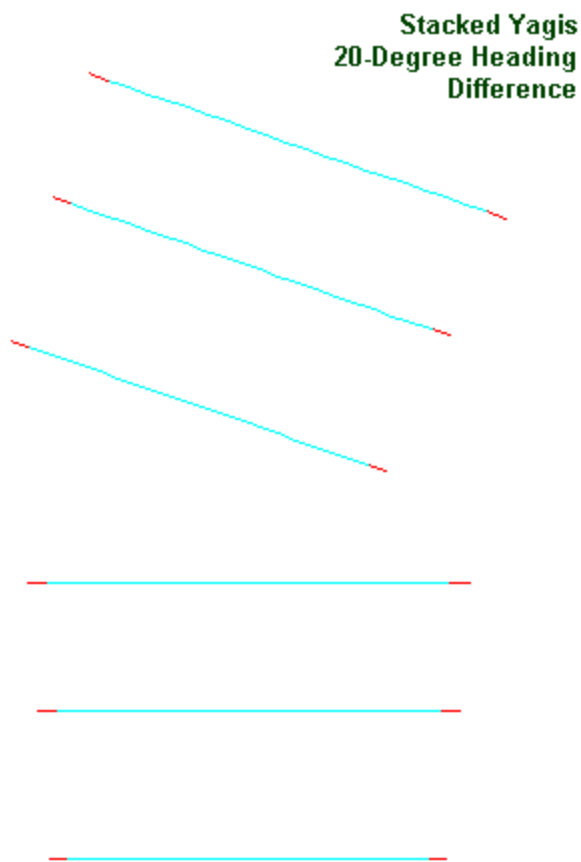


Fig. 42-9

In **Fig. 42-10**, we can see the pattern for the example. The in-line case would have placed the pattern on a heading of 270 degrees in the plot. With the top beam rotated clockwise by 20 degrees, the maximum forward gain bearing is shifted by only 10-11 degrees. Since this is only a hypothetical exercise, I shall do the unforgivable and leave the remainder of what happens to the gain and front-to-back ratio—as well as to the vertical pattern—to the reader as an exercise well worth doing.

Stacked Yagis: 20-Degree Heading Difference

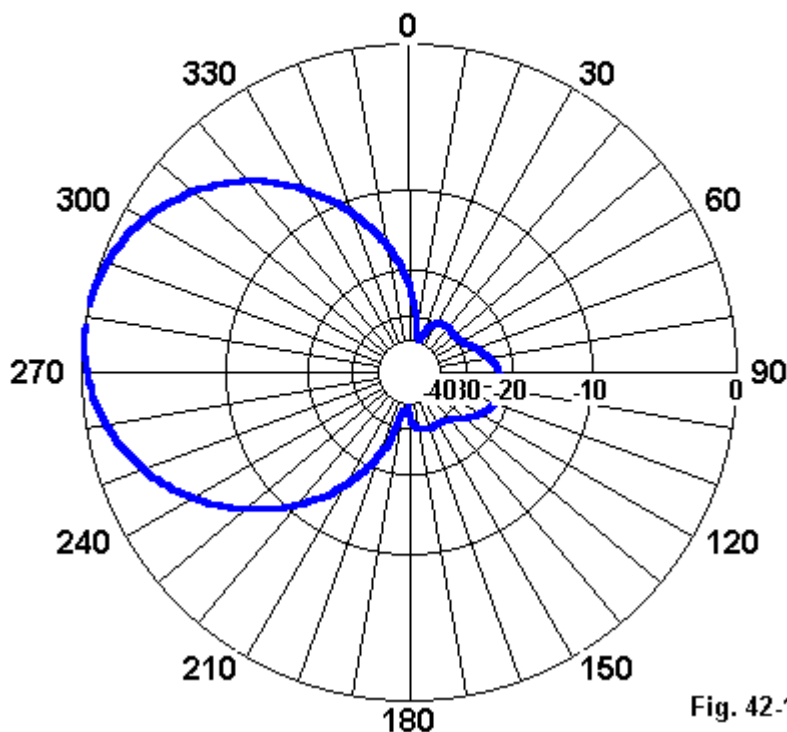


Fig. 42-10

The ability to rotate several wires at a time in a complex set of wires representing a large stack has further utility. In planning stacks, hams often combine 40-meter beams with multi-band antennas for 20-10 meters. One common technique is to place the 40-meter antenna at right angles to the multi-band array in order to minimize interactions and to permit closer spacing. Assume that the 40-meter array is above the multi-band antenna. Just how much separation is enough for in-line and for 90-degree orientations? A single model with some rotation of one of the two arrays will tell us much.

We can, of course, combine rotations with movements to try to find the very best position for one array relative to another to minimize unwanted interactions. A similar problem occurs with multi-band quads, but here, the desire is often to place one or more VHF quads in the center region of the larger collection of HF loops. With the rotation facility, we can check performance potential with the VHF quads facing forwards or backwards. Likewise, with the movement facility, we can run the VHF quads forwards and backwards in the quest for perfect, non-interactive placement.

We can perform similar tests with relative ease for arrays of Yagis or quads formed into squares, triangles, rhombi, etc. Changing separation, forward-rearward alignment, and angular relative positions is made fairly simple by the facilities we have been exploring.

Let's take a simple example. Suppose we model a square quad for 20 meters. Face-on, it will have the appearance of **Fig. 42-11** and model 42-6. Now suppose that we wish to convert the square quad into a model of a diamond-shaped quad. One way to do this is to note the length of any one side of each loop in the square quad. From the center of the quad, each unseen support arm will be 0.707 times the length of a side, and this value will determine the plus and minus Z values and the plus and minus X values (or the Y values, if one uses that convention) for the new model. Then we create 8 new wires using these coordinates.

2-Element Quad: Square Configuration

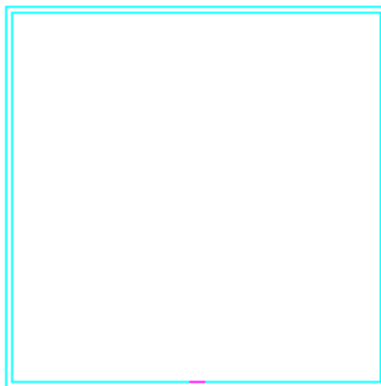
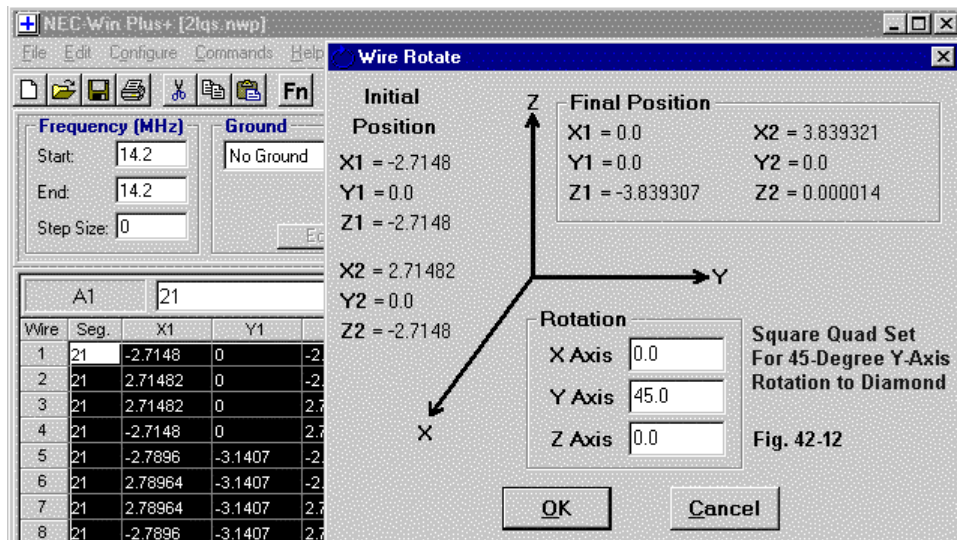


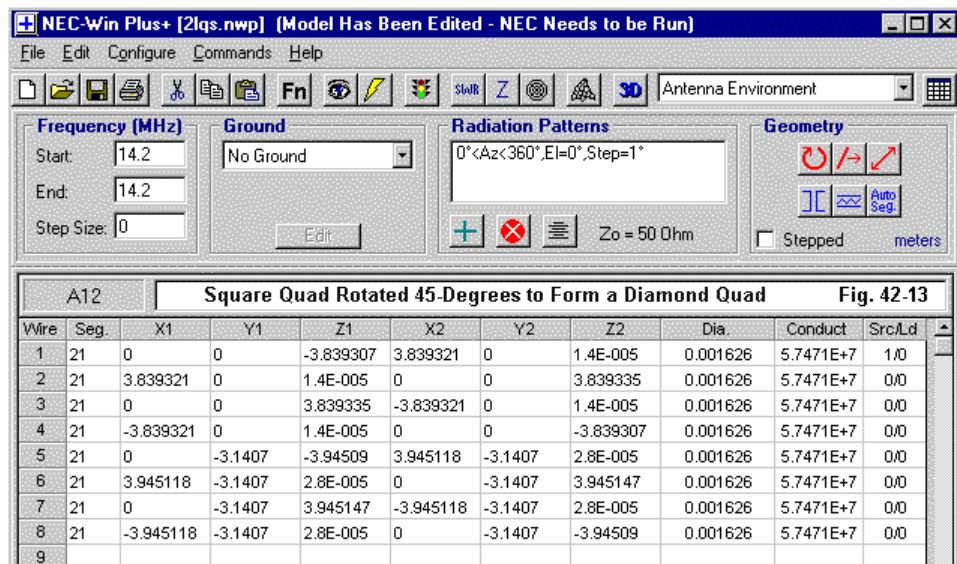
Fig. 42-11

As the old saying goes, “Stop. There must be an easier way.” There is.

In **Fig. 42-12**, we can see the block that encloses the values for the initial square quad. To the right is the rotation box. Our use of it this time will not involve the Z-axis. Instead, we shall use the Y-axis as the axis of rotation. The result will be to turn the elements in terms of the values of X by the amount specified—45 degrees.

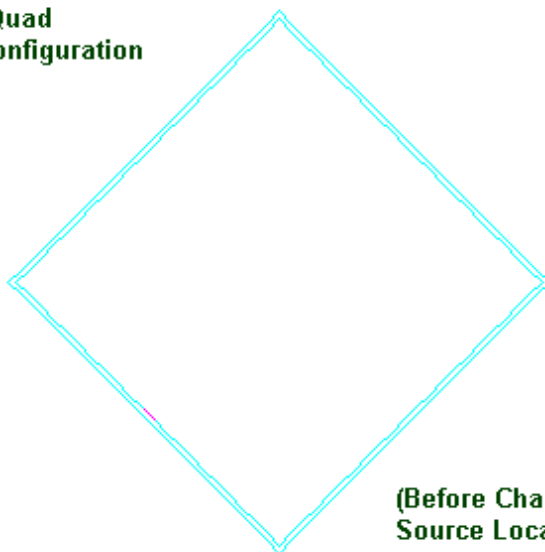


The finished product appears in **Fig. 42-13**. Note that the initial quad model had some trailing extra decimal place entries, suggesting once more that I pulled a model from elsewhere and have not cleaned it up yet. Note also that some of the Z values that ought to be zero are calculated to be very tiny numbers (E-5). We certainly should clean up these numbers. See model 42-7.



However, except for a little messiness in the fifth decimal place and beyond, the quad has converted to a diamond shape in perfect order, as revealed by **Fig. 42-14**. The conversion was much faster than the recalculation of each wire end and reentry from scratch.

Our work, however, is not finished. Note that the source segment is located along one leg of the driven loop. We need to move the source to one corner. We can implement the source using a split source technique, or we can create a short 3-segment wire at the corner and place the source on the center segment. We connect the ends to each of the adjacent legs of the driven loop that we opened up to make room for the feedpoint wire.

**2-Element Quad
Diamond Configuration****Fig. 42-14****(Before Change of
Source Location)**

Rotation in the X- and Y-axes has many applications beyond the simple case we used as an illustration here. For example, one question raised by operators at both HF and VHF is the effect on skip communications of changing the angle of the antenna relative to the terrain. The ability to rotate the antenna along its boom can provide some provisional answers to these questions—and rotating the entire antenna at once to various angles makes the data gathering process fairly efficient.

How high must a VHF/UHF beam be to permit its main lobe to accurately track a satellite without undue influence on the elevation of the lobe by ground reflections? Once more, changing both the angle and the elevation of the antenna by rotation and movement actions provides relatively speedy answers.

How will antennas on separate towers affect each other at various distances and various aiming bearings? The antennas may be at the same or different heights and operate on the same or different frequencies. It is possible to check the current levels of each antenna when one is left unfed while the other is fed. The exercise is never a short one, but the ability to change directions for each antenna, as well as moving them about the hypothetical antenna farm yard, will yield a large batch of data much faster than making changes to the antennas wire by wire.

Similar analyses can be performed between antennas and wire-grid models of buildings, vehicles, and other objects in the antenna's area. The move and rotation facilities allow the modeler to push buildings around with far greater ease than reinstalling a tower or reconstructing a home or utility building.

These are only some ways in which the move and rotation facilities in some programs can be used to expedite the gathering of useful data from antenna models. If we master them well, then we may well become interested in tackling larger, more informative projects with our modeling software. I hope these small exercises make you more aware of what is available to you and why it is worthy to become familiar with how to use it.

I have not focused on scaling elements in this episode largely because we devoted an entire installment to the subject (No. 26). However, it might be useful to note that scaling facilities—whether based on frequency or simple multipliers—add another tool to the collection that can be speed our work and enable us to do more work than we might have initially imagined possible.

* * * * *

Models included: 42-1 through 42-7. (All model dimensions in meters.)



43. Modeling Element Substitutes

An under-appreciated property of arrays of many types is the fact that double (and more complex) thin-wire elements can serve as substitutes for impractical fat elements. As we reduce the diameter of an element, the mutual coupling between elements within arrays—both phased and parasitic—decreases, with a consequent decrease in array gain and an offset in frequency of other array properties. Much, but not all, of an array's properties can be fully restored by the substitution for the impractical fat element and the single thin wire element of a double-wire element. For most standard arrays, only the gain will suffer. The double-wire element will restore a good portion of the gain. However, the higher losses of the double wire elements relative to the original fat element will limit the degree of restoration. The larger the number of $1/2$ wavelength elements or their equivalents, the lower the percentage of gain restoration. Nonetheless, the use of double-wire elements to preserve such operating parameters as the pattern shape, the front-to-back ratio, and the feedpoint impedance often suffices to make the use of double-wire elements preferable to single thin-wire elements.

The key question for these notes is how effectively to model double-wire elements so that we meet two criteria:

1. The substitute element is an effective substitute for the original fat element; and
2. The substitute double-wire element is adequately modeled to assure accurate modeling results.

The first step in the process is sketched in **Fig. 43-1**. We take one representative element from the original array and find its self-resonant frequency. Then we construct a double-thin-wire element model of the same length and place it at the same frequency. We next vary the spacing between the wires each side of a centerline until the new element is resonant. Resonance technically means having a purely resistive source impedance with no reactance. There are no task-independent standards for what counts as resonance, but my experience suggests that resonating an antenna within $\pm j1$ Ohm of reactance is not a difficult task.

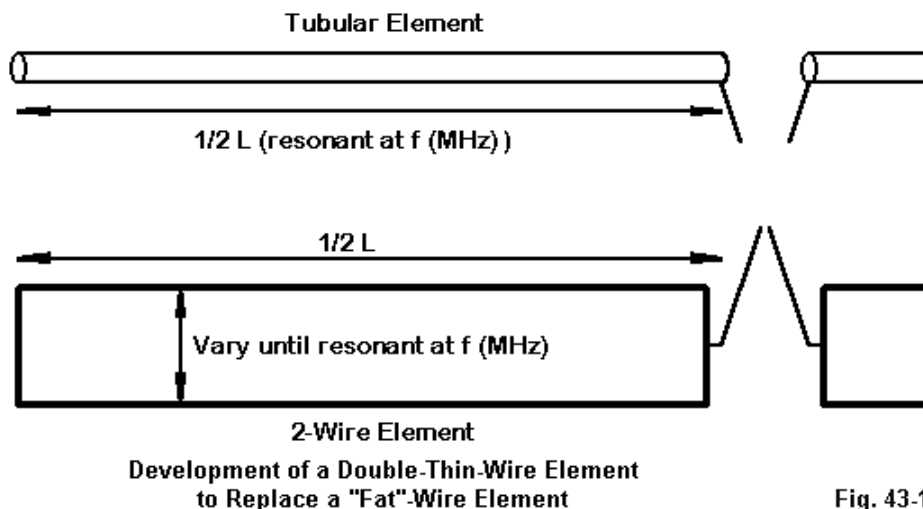
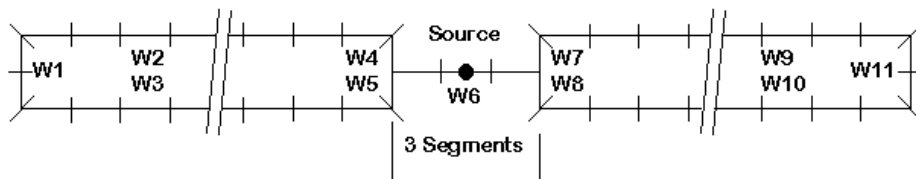


Fig. 43-1

To be exact, we should perform the same exercise with each element within any array. However, unless there are oddities to the array, modeling a single representative element normally suffices to provide a usable uniform wire spacing for double-wire elements throughout the substitute array.

Critical to the first step and to rebuilding the subject array with double-wire elements is figuring out how to model the substitute elements. **Fig. 43-2** provides one useful technique.



Modeling a Double-Wire Substitute Element

Fig. 43-2

Assuming a driven element, we need a source wire. For most modeling, the segment with the source should be the same length as the immediately adjacent segments. Hence, the first task is to model a source wire (designated W6 in the sketch) at the element center (assuming for simplicity a symmetrical set of elements in the array). How long we should make the wire and its segments is a function of the wires labeled W4, W5, W7, and W8. The length of each of these wires is one-half the spacing of the double wires in the ultimate substitute element. Hence, the length of the source wire should be close to 1.5 times the spacing of the wires. Arriving at the final number will, of course, require some trial-and-revision modeling in pursuit of the double wire spacing figure in the first step in the process.

The end wires (W1 and W11) ideally should be composed of 2 segments each. Equally ideal would be the case of keeping all of the segments in the model the very same length. This practice is the most accurate, but can result in large models even of single elements. The minimum requirement is that the segmentation for each of the 4 long wires (W2, W3, W9, and W10) should be identical to ensure that the segment junctions in parallel wires align with each other. Otherwise, NEC may show some inaccuracies. The level of segmentation along these wires can be determined by experimenting with levels of segmentation on a single element. As the segmentation is reduced from the ideal level, the element reactance will increase. The user must determine at what level the reactance is too high for us to use the element-as-modeled as a substitute for the original fat-wire element. A few Ohms reactance relative to a resistive value of 70 Ohms is normally acceptable for most design exercises. However, the lower the resistive source impedance values encountered in the array, the higher the need to use more adequate segmentation on the substitute elements.

These practices are sufficient for modeling double wire substitute elements for common parasitic arrays, such as Yagis. A 3-element 80-meter Yagi modeled with 4" diameter elements will show considerably more gain than a version made from #12 or #14 AWG wire, even when both are optimized for their wire sizes. Most of the gain—within a few tenths of a dB—can be restored using double-wire equivalents for the 4" elements.

A More Complex Case: the Quad Loop

Quad beams show relatively narrow operating bandwidth with respect to some parameters, largely because we conventionally construct them from thin wire elements. For most installations, the use of fatter aluminum tubing is impractical. Therefore, the double-wire substitute for a better-performing fat-element version of the quad becomes a desirable alternative.

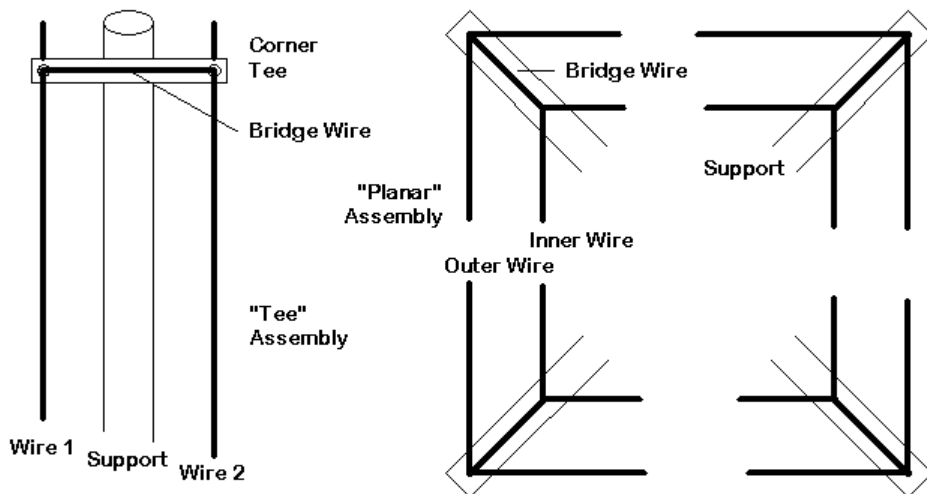


Fig. 43-3

Fig. 3 shows two ways of creating double-wire elements for quads. On the left is the Tee assembly, which places one wire ahead of the original element position and one wire behind the original element position, using a cross or Tee bar attached to the normal quad arm support to hold the wires at a constant distance. Note the use of a shorting wire between the elements at each corner. An alternative to the Tee assembly is the planar arrangement of loops in a double-wire substitute element. The planar assembly places both loops at the same distance from other elements in the array, but one loop must be larger than the other. A good starting point in developing such a loop is to place each loop the same amount larger and smaller than the original element. Extensive modeling with each type of double wire element has shown that in every normal parasitic array tested, there is no performance difference between the two double-loop arrangements so long as the wire spacing is the same within each element.

How we then handle the double-wire elements follows the same procedure as for linear elements. See **Fig. 43-4** for the outline of a 2-element quad beam using the Tee arrangement. Of course, the sketch does not show the support structure, which we shall assume is invisible to RF. See model 43-1.

Especially notable in **Fig. 43-4** is the feedpoint arrangement, which follows the same rules that we used for the linear elements that we examined. The source is on a 3-segment wire at the center of the lower portion of the driven element. The double wire arrangement begins and ends in the same way as the linear element. The only difference is that the elements do not have ends, but form loops. The corner shorting wires are necessary to ensure that each loop in an element has virtually the same current at each corresponding point of each wire. In practice, adding further shorting wires at mid-side points would likely be good building practice.

**Outline Sketch of a 2-Element Quad
Using 2 #14 AWG Wires Spaced
Front-to-Back (Tee Corners)**

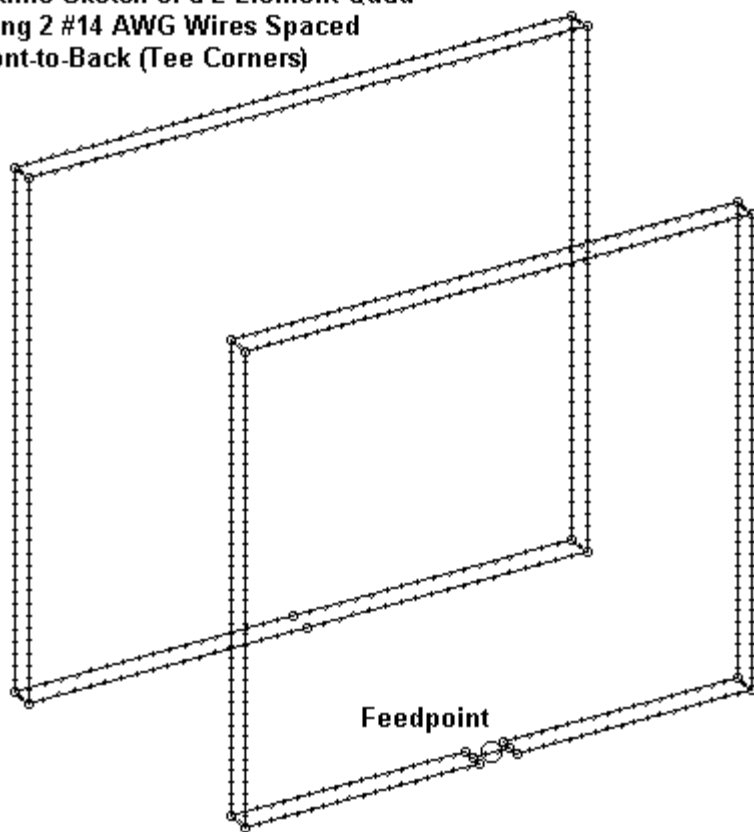


Fig. 43.4

The planar loop structure appears in **Fig. 43-5**, a version of the very same quad using the alternative form of loop construction. See model 43-2. For many installations, planar loops would be simpler to construct, since they require no additional attachments to the support arms except as necessary to hold the loop corners in place. Likewise, the source treatment for the planar loop driver is the same as for the Tee-assembly. With the planar loop model, it is important to use a level of segmentation that is dictated by the wire spacing in order to keep the segment junctions well aligned. Note at the corners that the outer loop has exactly 2 more

segments than the inner loop, which is a function of setting the segment length equal to half the wire spacing. That value is initially dictated by the length of the wires from the source wire to each of the longer loop wires.

**Outline Sketch of a 2-Element Quad
Using 2 #14 AWG Wires in
Planar Configuration**

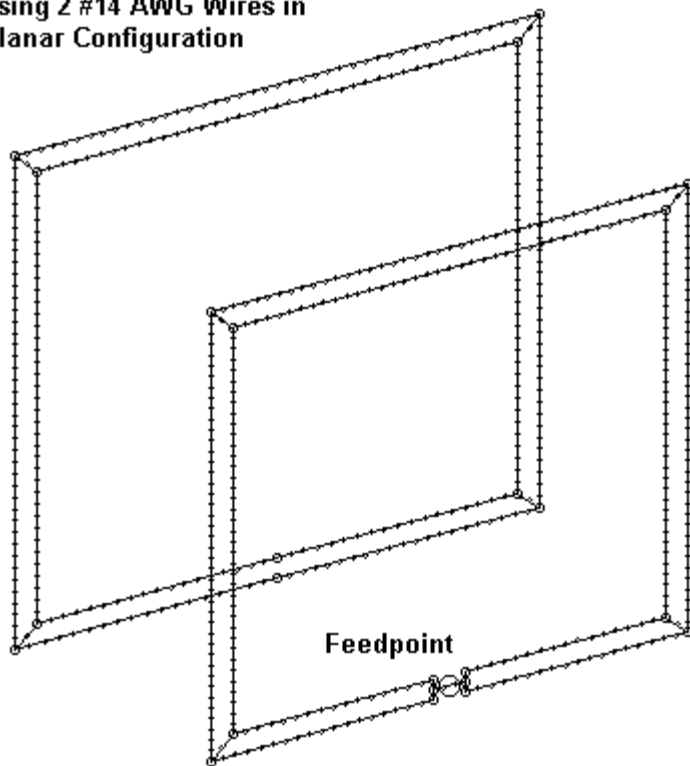


Fig. 43-5

Although linear double-wire elements are quite straightforward to model, loop structures can be sufficiently complex to make it difficult for the modeler to keep his place. Hence, utilizing every available modeling aid, including a good plan on paper

before model construction, is always sound advice. However, access to a model-by-equation facility can go a long ways toward making the process very easy.

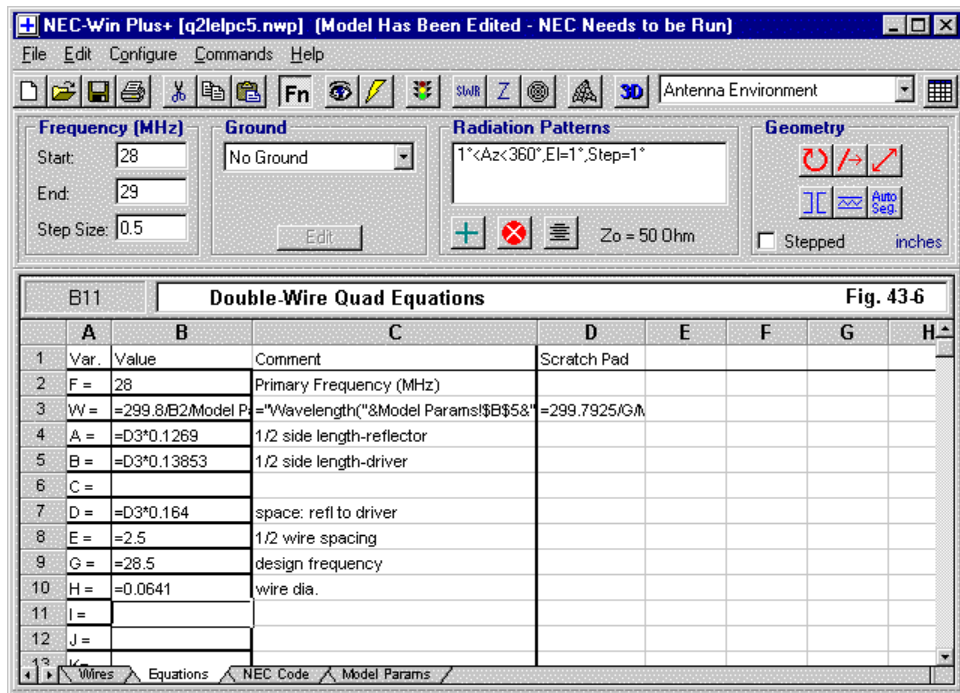


Fig. 43-6 shows the equations page of a NEC-Win Plus model of a 2-element quad. In this simplified version, each of the loop half-sides is defined by a simple equation referenced to the length of a wave at the design frequency (variables A and B). D defines the driver-reflector spacing. H is the user input wire size, corresponding here to #14 AWG wire. We can change the design for other wire sizes by entering the new size and changing the constants in the equations for A, B, and D. We can also change the design frequency in variable G.

The essential loop-creation variable is E, which specifies half the distance between #14 wires. The total spacing will be 5"—the selected substitute for the original 0.5" elements upon which the model is based. The rest of the task is simply to set up the wires for the model to make use of these variables.

Fig. 43-7 shows the wire page in symbolic form for the 2-element quad. Wires 1-19 represent the driven element, with the source wire shown in the top place in the listing. Wires 20-33 list the reflector loop, which lacks the need for a source wire and hence uses fewer entries on the wires page. Out of view below the bottom of the figure are the last 4 wires (30-33) which form the corner connectors for the reflector double loop.

The length of the source wire is defined in numerical terms so that it is 1.5 times the spacing between wires. Otherwise, the entire structure is set up in terms of variables. The inner and outer loops of each element are set by using the baseline dimensional variable (A or B) and adding to it or subtracting from it half the spacing distance, as represented by variable E. Although the wire page may look complex to newer modelers, consider the ease of introducing errors—if only by transposing digits here and there—should every wire spreadsheet cell need a numeric entry. For example, in the present model, the values of A and B are 51.90357 and 57.3246, which are in fact not used directly on the wire page. Instead, for each entry, we add 2.5 or subtract 2.5 to obtain each of the loop corners.

Still, there must be a somewhat easier way to model double-wire elements to arrive at models with fewer segments and even fewer wire entries.

NEC-Win Plus+ [q2lelpc3.nwp] (NEC Needs to be Run)

File Edit Configure Commands Help

Antenna Environment

Frequency [MHz]
 Start: 28.5
 End: 28.5
 Step Size: 0.1

Ground
 No Ground

Radiation Patterns
 1°<Az<360°,E=1°,Step=90°
 Zo = 50 Ohm

Geometry
 Stepped inches

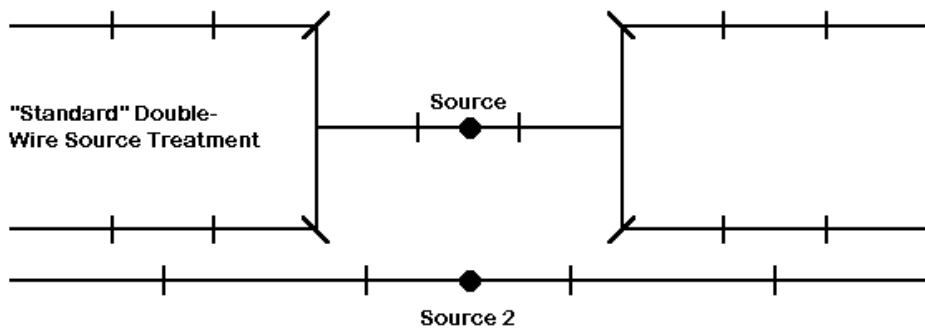
Double-Wire Quad Wire Set-Up **Fig. 43-7**

Wire	Seg.	X1	Y1	Z1	X2	Y2	Z2	Dia.	Conduct	Src/Ld
1	3	-3.75	0	=-A	3.75	0	=-A	=H	Copper	1/0
2	1	3.75	0	=-A	3.75	0	=-A-E	=H	Copper	0/0
3	18	3.75	0	=-A-E	=A+E	0	=-A-E	=H	Copper	0/0
4	42	=A+E	0	=-A-E	=A+E	0	=A+E	=H	Copper	0/0
5	42	=A+E	0	=A+E	=-A-E	0	=A+E	=H	Copper	0/0
6	42	=-A-E	0	=A+E	=-A-E	0	=-A-E	=H	Copper	0/0
7	18	=-A-E	0	=-A-E	-3.75	0	=-A-E	=H	Copper	0/0
8	1	-3.75	0	=-A-E	-3.75	0	=-A	=H	Copper	0/0
9	1	3.75	0	=-A	3.75	0	=-A-E	=H	Copper	0/0
10	16	3.75	0	=-A-E	=A-E	0	=-A-E	=H	Copper	0/0
11	38	=A-E	0	=-A-E	=A-E	0	=A-E	=H	Copper	0/0
12	38	=A-E	0	=A-E	=-A-E	0	=A-E	=H	Copper	0/0
13	38	=-A+E	0	=A-E	=-A+E	0	=-A+E	=H	Copper	0/0
14	16	=-A+E	0	=-A-E	-3.75	0	=-A+E	=H	Copper	0/0
15	1	-3.75	0	=-A-E	-3.75	0	=-A	=H	Copper	0/0
16	2	=A+E	0	=A+E	=A-E	0	=A-E	=H	Copper	0/0
17	2	=A+E	0	=-A-E	=A-E	0	=-A+E	=H	Copper	0/0
18	2	=-A-E	0	=-A-E	=-A+E	0	=-A+E	=H	Copper	0/0
19	2	=-A-E	0	=A+E	=-A+E	0	=A-E	=H	Copper	0/0
20	21	0	=D	=-B-E	=B+E	=D	=-B-E	=H	Copper	0/0
21	42	=B+E	=D	=-B-E	=B+E	=D	=B+E	=H	Copper	0/0
22	42	=B+E	=D	=B+E	=-B-E	=D	=B+E	=H	Copper	0/0
23	42	=-B-E	=D	=B+E	=-B-E	=D	=-B-E	=H	Copper	0/0
24	18	=-B-E	=D	=-B-E	0	=D	=-B-E	=H	Copper	0/0
25	18	0	=D	=-B+E	=B-E	=D	=-B+E	=H	Copper	0/0
26	38	=B-E	=D	=-B+E	=B-E	=D	=B-E	=H	Copper	0/0
27	38	=B-E	=D	=B-E	=-B+E	=D	=B-E	=H	Copper	0/0
28	38	=-B+E	=D	=B-E	=-B+E	=D	=-B+E	=H	Copper	0/0
29	18	=-B+E	=D	=-B+E	0	=D	=-B+E	=H	Copper	0/0

Wires Equations NEC Code Model Params

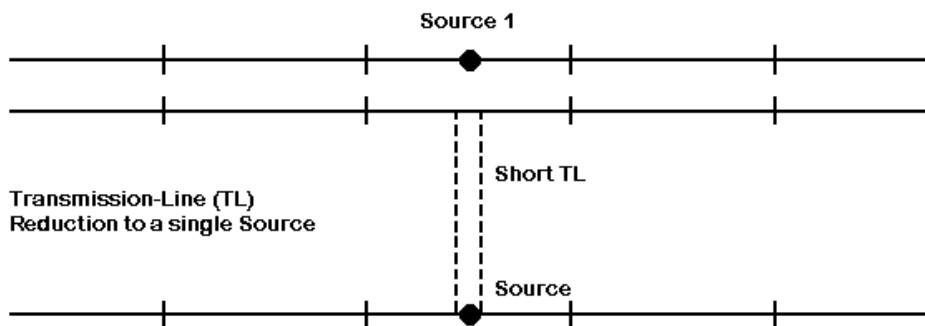
Some Simplifications and Cautions

We can significantly reduce the level of segmentation if we can do away with the source wire as a separate single wire. There are two ways to accomplish this, as shown in **Fig. 43-8**.



Parallel Sources for
Double Wire Elements

Fig. 43-8



Below the “standard” treatment of a double-wire assembly, we see an element having two wires and two sources. This wire set might be the center of a linear

element or the feedpoint area of a quad loop. By using two sources, we not only eliminate the separate source wire assembly, but as well, we increase the ideal segment length to the actual spacing between the two wires. Once more, we might judiciously reduce segmentation further by sampling a single element as a means of discovering how using few and long segments affects the self-resonant impedance of the element. Once more, the limits of allowable variation depend on the task at hand and are a user-responsibility. For loops, corner shorting wires are required to ensure similar current patterns on the two wires.

Calculating the actual source impedance from this virtual parallel feed system requires only a bit of hand-calculator work. Suppose that a quad loop returned values of $165 + j2$ Ohms for Source 1 and $138 - j3$ Ohms for Source 2. We need not do any fancy vector work to arrive at the final single source value. Instead, use the hand calculator to add the inverses of the two resistances and then take the inverse of the result (75.1). Do the same for the reactance values, taking into account their signs (+j6).

Perhaps the only thing that the hand calculation robs us of is using program facilities to determine the SWR and to plot such values over a sweep of frequencies. Only if we can reduce the parallel impedance to a single value within the program can we use these conveniences.

The lower portion of **Fig. 43-8** shows one technique that works with good accuracy. We select one of the two wires in the driven double-wire element to be the source wire. From the source segment to the corresponding segment on the other wire within the element, we create a transmission line using the TL facility within NEC. Since the TL line is strictly mathematical, we may choose for it any value of characteristic impedance and any length. The characteristic impedance should be close to the median resistive value between those that would appear on each of the two lines in a parallel source model. Using the figures that we just examined, a characteristic impedance of 150 Ohms would be quite reasonable. Precision is not too critical, since we shall make the line almost impossibly short. Any transmission line effects an impedance transformation continuously down its length. Thus, an extremely short line is needed so that the impedance placed in parallel with the source is as close as possible to that occurring on the second wire of the pair. I have used lines as short as 0.001' with success, although that practice may be a bit fussy. The sample problem return a source impedance of $75.2 + j5.6$ Ohms, which

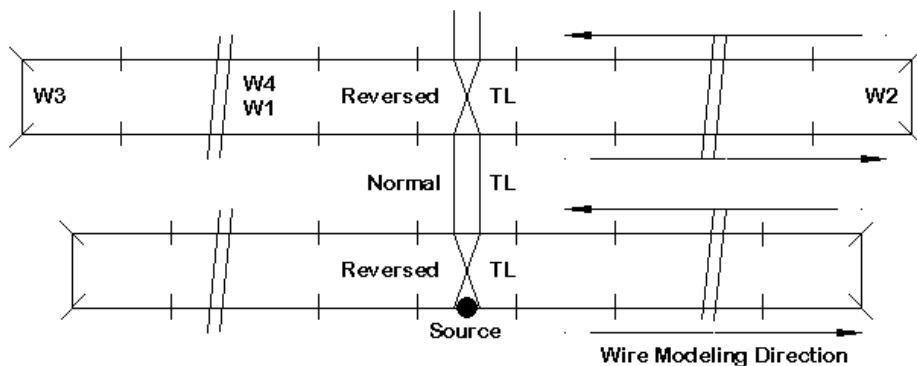
is certainly as close as one needs to the calculated parallel values. See model 43-3 for a sample of this technique.

There are some cautions that must be observed if the TL substitute for a double source is to provide reasonable results—not only in terms of the source impedance, but as well, in terms of the reported far-field pattern. The orientation of the TL line—that is, whether it is “Normal” or “Reversed”—will be a function of how we construct the double wire elements. For example, the portions of the planar quad loops that we connected with a TL line for a single feed both proceeded from -X to +X. Hence, the current direction was the same for both wires. Therefore, we employed the TL as Normal.

One convention for constructing continuous loop double wire linear elements is to go around the horn, that is, to let the bottom wire move from -X to +X, then to create the end wire, next to make the other long wire move from +X to -X, and finally to close the loop with the other end wire. In this situation, the current direction on the two wires is in opposition. For a single wire element or even such a wire within a parasitic array, there are no negative consequences for the far-field pattern. However, if we had applied the TL line to achieve a simulated parallel source, we would need to use the “Reverse” option, which in fact places a half twist on the line and reorients the sources in parallel.

Observing this requirements becomes especially important if we choose to model certain types of driven arrays using double-wire elements as substitutes for single fat elements. The LPDA makes a fine example. It consists of a sequence of linear elements, each of which is connected to the next, both fore and aft, by a phasing line. The line is reversed between each pair of elements.

Fig. 43-9 sketches the forward-most 2 elements of an LPDA array. Assume for the moment that we model each substitute double-wire element as a continuous loop, so that the direction of modeling is reversed for each long wire of each element loop. In order to capture the action of the LPDA, we must parallel the two wires into a virtual single feed point for the phasing line and then we must have a phase reversal between the first element and the second.



An Alternative Method of Modeling
2-Wire Elements in LPDAs

Fig. 43-9

Using the modeling convention chosen, each element contains within it a phase reversal relative to a parallel feed. Hence, the very short TL we create to connect the two wires within an element must be reversed.

We shall connect the “rear” wire of one element to the “forward” wire of the next element. How do we effect the required phase reversal from one element to the next? We do so by making use of the fact that the connected wires already have a reversed phase relative to each other. Hence, we use a phase-line section in its normal mode.

It is possible to use an alternative convention in creating the double-wire elements. We can let each wire in the element pair have the same modeling direction, say, from -X to +X. In this case, we would use a normal very short phase line between wires within an element and a reversed phase line to connect one element to the next.

Either system will return the same results in terms of array source impedance and far-field pattern values. With careful model construction, both are capable of very useful and accurate results. However, mixing systems tends to yield a bewildering array of meaningless results.

Properly and carefully used, the techniques we have explored can allow the modeler to create full models that once seemed too complex to tackle. Often, models use simplified fat-element models for double-wire elements and simply presume that they are “accurate enough.” That presumption is wholly unnecessary, since there are a host of techniques, not only to fully model double-wire elements, but as well to do so in reasonably compact models. Therefore, even those having segment-limited NEC modeling programs should be able to handle most of the cases that arise. Moreover, the results obtained—when compared to both fat-wire and single thin-wire models—can be edifying. In fact, they can go a long way toward helping to make design and construction decisions.

Perhaps I can summarize the most significant findings from my use of the technique with Yagi, quad, and LPDA designs that use two thinner wires (AWG 12 to AWG #14) to replace a single fat element, when both are brought to the same self-resonant frequency.

1. The source impedance characteristics of a well-designed double-wire substitute for a single fat element will be virtually identical to the original design. The more complex the geometry of the antenna, the more difficult it may be to obtain these characteristics, including the desired SWR curve, on the first try.

2. The front-to-back characteristics of a directional array, such as a Yagi or a quad beam will also be virtually unchanged when moving from the fat element to the pair of thinner wires. The higher the number of elements, the more likely it will be that you may have to make slight adjustments to position the frequency of the maximum 180-degree front-to-back ratio exactly where it was in the original design. The slight movement in maximum front-to-back ratio frequency suggests that the mutual coupling between the substitute elements may not be identical to that of the original fat elements, although the difference is often too small to require any redesign. In some cases, the peak front-to-back ratio may exceed the value obtained from the original elements. The reason for this effect is also an influence on the forward gain.

3. The forward gain of an array using wire pairs to replace a single fat element may be slightly less than the original. Although the wire pair has the same self-resonant frequency as the original element, it does not have the same surface area. The smaller surface area and the resulting skin-effect resistance are sufficient to

increase losses—especially in the lower HF range—even if the original element is aluminum and the substitutes are copper. Gain losses (and improved peak front-to-back ratio) tend to increase with the number of elements. However, these losses rarely exceed a few tenths of a dB. Given the reduction in weight of the array using two thinner wires—especially in quad designs, the reduction in forward gain is normally tolerable.

4. A pair of thinner wires yields significant performance improvements over single thin-wire designs in terms of both gain and source impedance performance (that is, a wider SWR curve), that it is a worth-while design alternative to consider, despite the increased complexity of the design models.

* * * * *

Models included: 43-1 through 43-3. (All model dimensions in inches.)



44. Designing With NEC: A Case Study Part 1: The 4 Ss

Recently, I had occasion to design a 4+-element, 5-band quad array. The exercise brought to mind a number of questions that have been sent to me over the last few months, many of which involved ideas that came into play during the process of generating the antenna design. Hence, I thought that making a case study of the design effort might be useful to others who wish to use NEC (or MININEC) to design one or more antennas of the garden variety. By garden variety, I mean antennas of conventional HF and VHF design and structure.

The effort begins far from the software itself. Before we are done, we shall be thoroughly involved with NEC, but initially, we start with pencil and paper (or word processor and screen). The first step is deciding and defining what we wish to design.

Specifications

In any design process, if you do not know what you want to achieve, you will never know when you have achieved it—or why you may be falling short of the goal. Therefore, the first “S” on our list is a set of specifications that gives a detailed picture of the antenna you wish to design. All such lists involve familiarity with the antenna type so that the specifications are realistic. For the case in hand, the antenna is a 5-band quad on a 26' boom. There will be at least 4 elements per band, arranged in the standard way: a 10' separation of the reflector from the driver, with directors at 8' intervals ahead of the driver.

Starting Point

Before we complete the list of specifications, let's introduce another “S.” Since we do not need to reinvent the large multi-band quad array, we might as well begin with an existing antenna that comes closest to what we wish to design. In this case, it is the “3.5-element” quad array designed by Danny Mees, ON7NQ, and described in some detail in *Quad Notes*, Vol. 1. For 20, 17, and 15 meters, the antenna has 3 elements that use the 10'-8' spacing. For 12 and 10 meters, Danny inserted an

extra element 5' ahead of the reflector (and hence, 5' behind the lower-band drivers). These elements are the drivers for the higher bands, and the remaining two elements become directors. **Fig. 44-1** shows the general outline of the array.

ON7NQ 3.5-Element, 5-Band Quad Outline Sketch

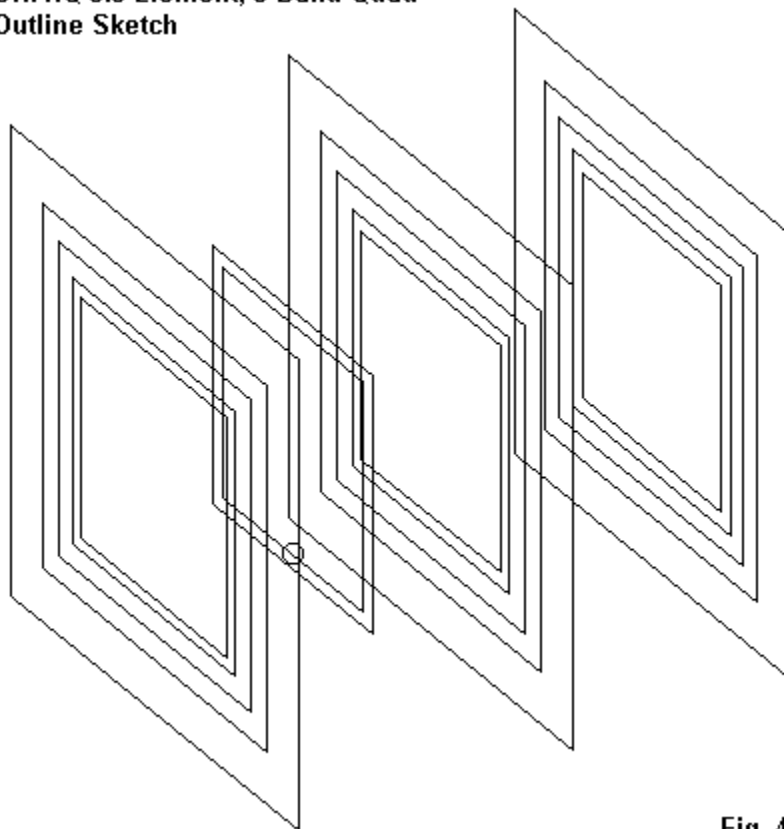


Fig. 44-1

By analyzing the ON7NQ array, we can get a fairly good idea of 3+-element performance potentials and put ourselves in a better position to set specifications for the 4+-element array. The following table lists the dimensions of the elements,

band-by-band. For the moment, we may ignore the first two columns and focus solely on the side-length and circumference of each element. See model 44-1.

ON7NQ 3.5-element 5-Band Quad Dimensions (Inches)

Modeling Variable	Antenna Part	1/2 Side Length	Side Length	Loop Circumference
A	20 Refl	108.5	217.0	868.0
B	20 Dri	106.85	213.7	854.8
C	20 Dir 1	102.5	205.0	820.0
D	—			
E	17 Refl	84.25	168.5	674.0
(F)	(Reserved for Start Frequency)			
G	17 Dri	83.15	166.3	665.2
H	17 Dir 1	79.9	159.8	639.2
I	—			
J	15 Refl	72.4	144.8	579.2
K	15 Dri	71	142.0	568.0
L	15 Dir 1	69	138.0	552.0
M	—			
N	12 Refl	61.2	122.4	489.6
O	12 Dri	59.95	119.9	479.6
P	12 Dir 1	59.1	118.2	472.8
Q	12 Dir 2	59.35	118.7	474.8
R	—			
S	10 Refl	55.34	110.68	442.7
T	10 Dri	52.9	105.8	423.2
U	10 Dir 1	52.3	104.6	418.4
V	10 Dir 2	51.995	103.99	416.0
(W)	(Reserved for Start Wavelength)			
X	—			

Note: To convert to meters, divide inches by 39.37.

These elements were converted into numbers for a NEC-4 model, the details of which we shall shortly address. For now, our main interest lies in the band-by-band performance reports.

Modeled Performance: ON7NQ 3.5-element, 5-Band Quad
NEC-4; Full Segmentation

Freq. MHz	Gain dBi	Front/Back dB	Impedance R +/- jX	50-Ohm SWR
14.0	8.42	11.83	37.6 - j 18.5	1.66

14.175	8.29	15.06	44.3 + j	4.4	1.17
14.35	8.06	9.76	34.8 + j	36.5	2.50
18.068	8.47	21.80	42.7 - j	5.1	1.21
18.118	8.42	25.52	43.5 - j	0.3	1.15
18.168	8.36	20.90	43.2 + j	4.6	1.19
21.0	8.43	15.28	49.7 - j	20.1	1.49
21.225	8.52	20.98	46.4 - j	0.0	1.08
21.45	8.47	10.24	36.2 + j	30.7	2.16
24.89	9.26	22.72	35.1 - j	2.1	1.43
24.94	9.22	18.92	41.1 + j	2.3	1.27
24.99	9.18	16.70	47.6 + j	4.8	1.12
28.0	9.01	18.40	43.8 - j	31.6	1.96
28.2	9.35	25.89	45.3 - j	11.0	1.29
28.4	9.62	30.72	51.3 + j	6.8	1.15
28.6	9.85	22.80	58.7 + j	9.6	1.27
28.8	9.73	12.38	31.1 + j	8.1	1.68

The array is a quite good performer of its type, although there are a few areas on which we might like to make improvements as we work toward the larger design. The 20- and 15-meter bands are limited to the lower ends. Whole band coverage would be desirable if possible. It is unlikely that a wire quad array of this order can be made to cover the entire first MHz of 10 meters at the level of performance reported.

The antenna also makes evident certain other limits of wire quad arrays. Although monoband Yagis can be designed with better than a 20 dB front-to-back ratio across the band of interest, wire quads have much narrower bandwidth limits. Therefore, a 15 dB front-to-back figure is more likely to be achieved. As well, thin-wire quad arrays are subject to rapid changes in performance characteristics with relatively small changes in frequency. Therefore, it pays to scan the edges as well as the middle of even the narrowest amateur bands to assure adequate performance. Notice, for example, the 6-dB drop in the front-to-back ratio on 12 meters from one edge of the band to the other.

Specifications—Again

The object of the design process will be an enlarged version of the ON7NQ array, with an extra director 8' in front of the current forward director. The array will retain the extra elements for 12 and 10 meters and place them as in the original. Now we can set some goals derived from the array we have just examined.

Gain: at least 0.7 dB greater than the existing array

Front-to-Back Ratio: at least 15 dB across each band—if possible

Source Impedance: less than 2:1 50-Ohm SWR for direct feed (individually)
on each band with a standard 50-Ohm coaxial cable

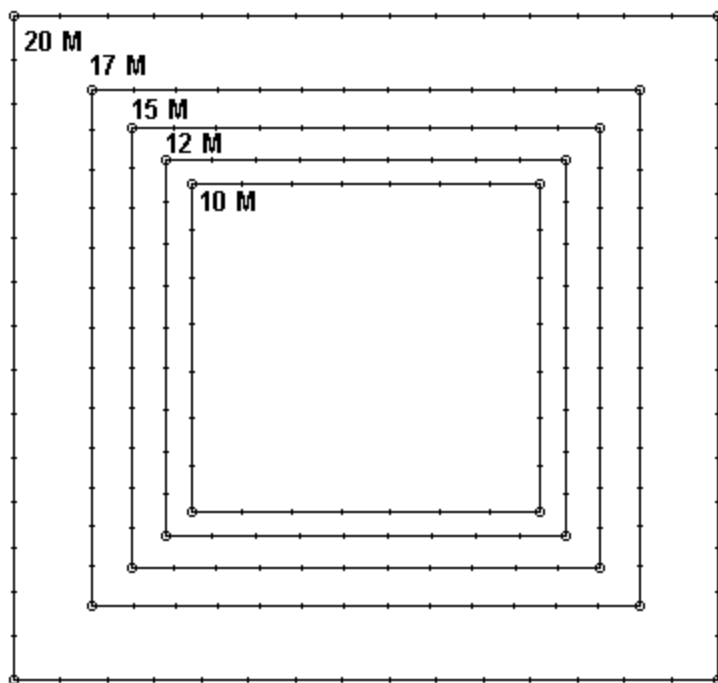
Coverage: Full band coverage of all bands, with 800 kHz coverage of 10 meters

Let's see how completely we can realize these goals.

Strategy

To develop a model with which we can easily work while designing takes some forethought. First, the model will be large—22 elements to be exact, with each element consisting of 4 wires. To meet the general recommendation that segment junctions be aligned as closely as is reasonable possible, the wires for each band will require different levels of segmentation. If 10 meters receives 7 segments per side-wire for each elements, then we should increase the number of segments per side by 2 for each lower band. The 20 meter elements will use 15 segments per side, about twice the number as those in each side of the 10-meter elements. **Fig. 44-2** sketches the segmentation of the reflector elements from the array.

The basic model for the array consists of 88 wires and 944 segments. We shall look at the model-size issue momentarily.

Full Segmentation Scheme: 7 to 15 Segments per Wire**Fig. 44-2**

First, let's examine how design work will proceed. We have the ON7NQ dimensions, but we must allow for the possibility that a larger array will require at least small changes in any of the dimension figures. As well, we must begin with an

educated guess at the proper size for the new directors that we shall add. Then, the process will be to optimize the dimensions to achieve the performance specifications.

The model will be set in free space so that its dimensions can be set out in terms of both +/-Y and +/-Z. This limits the key dimensional number to one per element. However, manually changing the dimensions of any single element requires up to 16 numerical entries into a wire table, with considerable chance for the usual embarrassing lot of split-key entries and transposed numbers.

To simplify the process, I used the model-by-equation facility. The first column of the ON7NQ dimension table lists the variable to which each element dimension is assigned. (Note that the software used, NEC-Win Plus, reserves F for the start frequency and W for the corresponding wavelength.) The variables carry us up through X in the alphabet of available variables. To avoid using up variables on the fixed spacing between elements, these values were entered numerically on the Wires page. **Fig. 44-3** shows a partial page of values.

Although not clearly evident from the wires-page graphic, I arranged the wires according to the spacing from the reflector, with all 5 reflectors listed first, from the lowest band to the highest. Then come the two high band drivers, followed by the 5 elements spaced 10' from the reflectors. However, on the equations page, each band's elements are grouped together and labeled, since the optimizing process would proceed one band at a time. **Fig. 44-4** shows the equations page.

Segmentation

Hand optimizing a design requires many small changes in one or more dimension, followed by a sweep of the band in question to check performance at the band edges and at mid-band. (Of course, more detailed sweeps are occasionally useful to watch the progression of performance characteristics over smaller frequency spreads.) The time required for a NEC run increases with the square of the increase in the number of segments. Anything that might be done to shorten the waiting time would prove useful so long as it did not introduce unacceptable errors in the results.

NEC-Win Plus+ [on7nq5.nwp]

File Edit Configure Commands Help

Antenna Environment

Frequency [MHz]
 Start: 28
 End: 29
 Step Size: 0.2

Ground
 No Ground

Radiation Patterns
 0°<Az<359°,El=1°,Step=1°
 Zo = 50 Ohm

Geometry
 Stepped inches

Partial View: Wires Page With Variables Fig. 44-3

Wire	Seg.	X1	Y1	Z1	X2	Y2	Z2	Dia.	Conduct	Src/Ld
11	11	0	=J	=J	0	=J	=J	12 AWG	Copper	0/0
12	11	0	=J	=J	0	=J	=J	12 AWG	Copper	0/0
13	9	0	=N	=N	0	=N	=N	12 AWG	Copper	0/0
14	9	0	=N	=N	0	=N	=N	12 AWG	Copper	0/0
15	9	0	=N	=N	0	=N	=N	12 AWG	Copper	0/0
16	9	0	=N	=N	0	=N	=N	12 AWG	Copper	0/0
17	7	0	=S	=S	0	=S	=S	12 AWG	Copper	0/0
18	7	0	=S	=S	0	=S	=S	12 AWG	Copper	0/0
19	7	0	=S	=S	0	=S	=S	12 AWG	Copper	0/0
20	7	0	=S	=S	0	=S	=S	12 AWG	Copper	0/0
21	9	60	=O	=O	60	=O	=O	12 AWG	Copper	0/0
22	9	60	=O	=O	60	=O	=O	12 AWG	Copper	0/0
23	9	60	=O	=O	60	=O	=O	12 AWG	Copper	0/0
24	9	60	=O	=O	60	=O	=O	12 AWG	Copper	0/0
25	7	60	=T	=T	60	=T	=T	12 AWG	Copper	1/0
26	7	60	=T	=T	60	=T	=T	12 AWG	Copper	0/0
27	7	60	=T	=T	60	=T	=T	12 AWG	Copper	0/0
28	7	60	=T	=T	60	=T	=T	12 AWG	Copper	0/0
29	15	120	=B	=B	120	=B	=B	12 AWG	Copper	0/0
30	15	120	=B	=B	120	=B	=B	12 AWG	Copper	0/0
31	15	120	=B	=B	120	=B	=B	12 AWG	Copper	0/0
32	15	120	=B	=B	120	=B	=B	12 AWG	Copper	0/0
33	13	120	=G	=G	120	=G	=G	12 AWG	Copper	0/0
34	13	120	=G	=G	120	=G	=G	12 AWG	Copper	0/0
35	13	120	=G	=G	120	=G	=G	12 AWG	Copper	0/0
36	13	120	=G	=G	120	=G	=G	12 AWG	Copper	0/0
37	11	120	=K	=K	120	=K	=K	12 AWG	Copper	0/0
38	11	120	=K	=K	120	=K	=K	12 AWG	Copper	0/0
39	11	120	=K	=K	120	=K	=K	12 AWG	Copper	0/0

Wires Equations NEC Code Model Params

NEC-Win Plus+ [on7nq5.nwp]

File Edit Configure Commands Help

Antenna Environment

Frequency [MHz]
 Start: 28
 End: 29
 Step Size: 0.2

Ground
 No Ground

Radiation Patterns
 0°<Az<359°,El=1°,Step=1°
 Zo = 50 Ohm

Geometry
 Stepped inches

Equations Page With Variables Fig. 44.4

A1	Var.							
A	B	C	D	E	F	G	H	
1	Var. Value	Comment	Scratch Pad					
2	F = 28	Primary Frequency (MHz)						
3	W = =299.8/B2/Model P	= "Wavelength(" & Model Params!\$B\$5"						
4	A = =108.5	20 ref						
5	B = =106.5	20 dri Wire 29						
6	C = =97.5	20 D1						
7	D = =98	20 D2						
8	E = =84.25	17 ref						
9	G = =82.8	17 dri Wire 33						
10	H = =79.9	17 D1						
11	I = =79.9	17 D2						
12	J = =72.7	15 ref						
13	K = =70.7	15 dri Wire 37						
14	L = =69.75	15 D1						
15	M = =69.65	15 D2						
16	N = =61.2	12 ref						
17	O = =60.3	12 dri Wire 21						
18	P = =59.1	12 D1						
19	Q = =59.9	12 D2						
20	R = =59.3	12 D3						
21	S = =55	10 ref						
22	T = =52.9	10 dri Wire 25						
23	U = =52.2	10 D1						
24	V = =52.5	10 D2						
25	X = =52	10 D3						
26	Y =							
27	Z =							
28								
29								

Wires Equations NEC Code Model Params

To reduce the size of the model, I reduced the segmentation for each element wire in the following way. 20-, 17-, and 15-meter elements used 7 segments per side, while 12- and 10-meter elements used 5 segments per side. I reached this decision after checking the performance of the ON7NQ array on each band with full segmentation and with the reduced segmentation scheme. Although the numbers did not exactly coincide, the progression of values for each model was sufficiently close to permit initial modeling via the smaller model. However, these results would be considered provisional, pending a recheck using the full segmentation scheme. In that way, only final tweaking—if any should be needed—would require the larger, slower model.

The process of hand-optimizing even a complex model like a multi-element, multi-band quad is not completely random. **Fig. 44-5** shows the outline of the new array. The starting point might be anywhere. However, in the development of such arrays, one of the most stable bands turns out to be 15 meters. That is, it tends to be least affected by changes to the other bands. So optimizing 15 meters first is a good way to proceed. Then work outward through 17 meters to 20 meters and inward through 12 meters to 10 meters. As we shall have occasion to note in detail when we evaluate the design, the bands that are not bound by other band elements on both sides tend to be more difficult to set.

The development of a design is made easier by attending to details as we proceed. First, although we need to change the source location with every change in band, we can remember where to place the source by annotations on the equations page, as is evident in **Fig. 44-4**. Second, we can be alert to patterns that develop on one band and apply them to related bands.

A case in point is the fact that for each of the 2 highest bands, the middle director needs to be larger than either the first or the third director. The second director on 20 meters was also larger than the first, although this pattern did not hold for 17 and 15 meters.

**W4RNL 4.5-Element, 5-Band Quad
Outline Sketch**

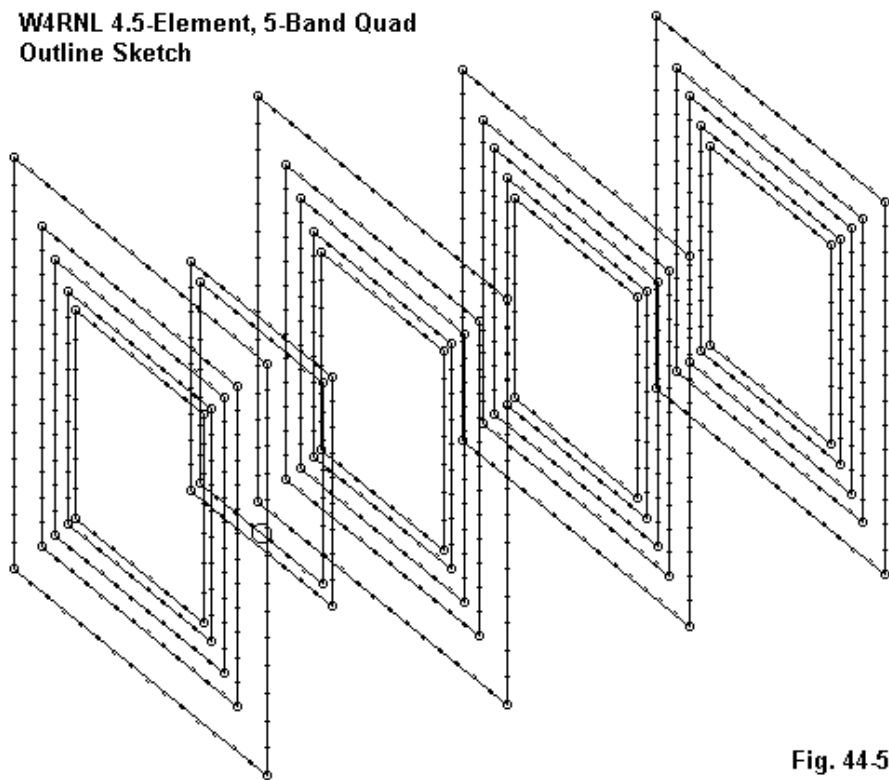


Fig. 44.5

A second case in point concerns which method to use to arrive at a desired feedpoint impedance. One method involves making changes to the reflector; the other involves work with the directors. In the optimizing process for this array, I quickly learned that enlarging the reflector to increase the feedpoint impedance

resulted in more rapid reductions in gain and front-to-back ratio than did the manipulation of the director dimensions.

Many of these points are evident in the table of dimensions and variables used for the final version of the design exercise.

W4RNL 4.5-element 5-Band Quad Dimensions (Inches)

Modeling Variable	Antenna Part	1/2 Side Length	Side Length	Loop Circumference
A	20 Refl	108.5	217.0	868.0
B	20 Dri	106.5	213.0	852.0
C	20 Dir 1	97.5	195.0	780.0
D	20 Dir 2	98.0	196.0	784.0
E	17 Refl	84.25	168.5	674.0
(F)	(Reserved for Start Frequency)			
G	17 Dri	82.8	165.6	662.4
H	17 Dir 1	79.9	159.8	639.2
I	17 Dir 2	79.9	159.8	639.2
J	15 Refl	72.7	145.4	581.6
K	15 Dri	70.7	141.4	565.6
L	15 Dir 1	69.75	139.5	558.0
M	15 Dir 2	69.65	139.3	557.2
N	12 Refl	61.2	122.4	489.6
O	12 Dri	60.3	120.6	482.4
P	12 Dir 1	59.1	118.2	472.8
Q	12 Dir 2	59.9	119.8	479.2
R	12 Dir 3	59.3	118.6	474.4
S	10 Refl	55.0	110.0	440.0
T	10 Dri	52.9	105.8	423.2
U	10 Dir 1	52.2	104.4	417.6
V	10 Dir 2	52.5	105.0	420.0
(W)	(Reserved for Start Wavelength)			
X	10 Dir 3	52.0	104.0	416.0

Note: To convert to meters, divide inches by 39.37.

The performance figures reported by the small model used to manipulate dimensions are as follows.

Modeled Performance: W4RNL 4.5-element, 5-Band Quad
NEC-2; Reduced Segmentation

Freq.	Gain	Front/Back Impedance	50-Ohm
-------	------	----------------------	--------

MHz	dBi	dB	R +/- jX	SWR
14.0	8.81	15.13	33.9 - j 20.3	1.86
14.175	8.57	16.66	52.0 + j 10.3	1.23
14.35	8.13	9.92	57.7 + j 34.1	1.89
18.068	9.21	21.09	35.6 - j 2.6	1.41
18.118	9.17	21.91	38.8 + j 5.0	1.32
18.168	9.09	18.22	41.9 + j 11.9	1.37
21.0	9.41	15.09	41.0 - j 16.6	1.51
21.225	9.42	17.06	56.3 + j 7.6	1.20
21.45	9.53	20.97	34.5 + j 8.1	1.52
24.89	10.19	21.88	40.7 + j 4.1	1.25
24.94	10.21	19.60	42.2 + j 7.3	1.26
24.99	10.18	16.57	43.5 + j 12.0	1.34
28.0	9.51	12.01	39.7 - j 27.9	1.92
28.2	10.08	16.81	48.6 - j 12.4	1.29
28.4	10.54	20.44	47.2 - j 2.8	1.08
28.6	10.81	19.69	42.2 + j 17.2	1.50
28.8	10.53	32.57	64.7 + j 15.4	1.45

Before we comment on the success or failure of the design exercise, let's look at the numbers that emerged from the use of the fully segmented model on NEC-2.

Modeled Performance: W4RNL 4.5-element, 5-Band Quad
NEC-2; Full Segmentation

Freq. MHz	Gain dBi	Front/Back dB	Impedance R +/- jX	50-Ohm SWR
14.0	8.81	15.02	33.6 - j 20.5	1.88
14.175	8.58	16.76	51.9 + j 10.0	1.22
14.35	8.14	9.96	57.8 + j 33.8	1.89
18.068	9.24	22.03	36.0 - j 1.7	1.39
18.118	9.18	21.26	39.3 + j 5.7	1.31
18.168	9.10	17.39	42.3 + j 12.5	1.37
21.0	9.49	15.33	41.4 - j 15.6	1.47
21.225	9.47	17.04	57.0 + j 7.5	1.21
21.45	9.55	19.16	31.3 + j 9.9	1.70

24.89	10.27	21.77	38.6 + j 5.2	1.33
24.94	10.29	19.80	40.2 + j 9.1	1.34
24.99	10.25	16.77	41.9 + j 14.3	1.43
28.0	9.59	12.15	40.7 - j 27.4	1.88
28.2	10.15	17.00	49.3 - j 12.7	1.29
28.4	10.60	20.50	47.1 - j 2.8	1.09
28.6	10.85	19.76	42.6 + j 18.0	1.52
28.8	10.51	29.74	64.9 + j 12.1	1.40

The deviations between the two sets of numbers are noticeable, but not large. Perhaps the greatest difference occurs on 12 meters, where the segmentation on the small model shifted to 5 segments per wire from the higher value of 7 used for 20-15 meters. Nonetheless, nothing in the sweeps of the larger model suggested that any modifications to the design were necessary.

On occasion, NEC-2 and NEC-4 may differ slightly in values reported for quad arrays. This difference is most noticeable in monoband arrays where an array is set to a precise resonance (less than 1 Ohm reactance) and/or a precise front-to-back peak value at the design frequency. The differences are usually a matter of +/-10 kHz or so in the frequency of resonance or front-to-back peak. Although the differences are small—perhaps less than operationally significant—a sweep of the design using NEC-4 seemed in order to be certain that some of the more rapidly changing operational characteristics did not yield odd results.

Modeled Performance: W4RNL 4.5-element, 5-Band Quad
NEC-4; Full Segmentation

Freq. MHz	Gain dBi	Front/Back dB	Impedance R +/- jX	50-Ohm SWR
14.0	8.81	15.02	33.7 - j 20.8	1.88
14.175	8.58	16.76	51.9 + j 10.0	1.22
14.35	8.14	9.95	57.8 + j 34.0	1.89
18.068	9.23	22.01	36.1 - j 1.8	1.39
18.118	9.18	21.24	39.2 + j 5.7	1.32
18.168	9.10	17.38	42.3 + j 12.5	1.38
21.0	9.49	15.33	41.5 - j 15.6	1.47
21.225	9.47	17.04	57.0 + j 7.5	1.21
21.45	9.54	19.13	31.3 + j 10.0	1.70

24.89	10.27	21.79	38.6 + j 5.3	1.33
24.94	10.28	19.82	40.3 + j 9.1	1.35
24.99	10.24	16.77	41.9 + j 14.4	1.43
28.0	9.59	12.15	40.8 - j 27.4	1.88
28.2	10.15	17.00	49.3 - j 12.7	1.29
28.4	10.60	20.51	47.1 - j 2.8	1.09
28.6	10.85	19.77	42.6 + j 18.1	1.52
28.8	10.51	29.75	64.9 + j 12.1	1.40

Happily, the NEC-2 and NEC-4 results are coincident to the n th degree. I list them here simply to note that, where the software is available, such checks are useful and advisable. The check is especially applicable in this case, where the model-by-equation facility was not available in a NEC-4 version for use from the beginning of the process of design.

So now we have a design for a 4.5-element quad on a 26' boom. However, we still have two major question areas left over. First, is the design—as a design—successful relative to the specifications that we set up originally? Second, what relationship does this design—as a model—have to an eventual physical antenna? We shall look at both questions and the collection of data that forms some kind of a set of answers to them next time.

* * * * *

Models included: 44-1 through 44-2. (All model dimensions in inches.)



45. Designing With NEC: A Case Study Part 2: Evaluation & Reality

In the first part of the case study, we looked at the 4 Ss of designing by modeling: Starting Point, Specifications, Strategy, and Segmentation. Essentially, we began with a design by ON7NQ and built upon it on the way to developing the following antenna model, shown as a wire assembly. See model 44-2 from the preceding column.

W4RNL 4.5-Element, 5-Band Quad Model

Wire Loss: Copper – Resistivity = $1.74\text{E-}08$ ohm-m, Rel. Perm. = 1

WIRES									
Wire Conn.—		End 1 (x,y,z : in)		Conn.— End 2 (x,y,z : in)		Dia(in)		Segs	
1	W4E2	0.000,-108.50,-108.50	W2E1	0.000,108.500,-108.50	8.09E-02	15			
2	W1E2	0.000,108.500,-108.50	W3E1	0.000,108.500,108.500	8.09E-02	15			
3	W2E2	0.000,108.500,108.500	W4E1	0.000,-108.50,108.500	8.09E-02	15			
4	W3E2	0.000,-108.50,108.500	W1E1	0.000,-108.50,-108.50	8.09E-02	15			
5	W8E2	0.000,-84.250,-84.250	W6E1	0.000, 84.250,-84.250	8.09E-02	13			
6	W5E2	0.000, 84.250,-84.250	W7E1	0.000, 84.250, 84.250	8.09E-02	13			
7	W6E2	0.000, 84.250, 84.250	W8E1	0.000,-84.250, 84.250	8.09E-02	13			
8	W7E2	0.000,-84.250, 84.250	W5E1	0.000,-84.250,-84.250	8.09E-02	13			
9	W12E2	0.000,-72.700,-72.700	W10E1	0.000, 72.700,-72.700	8.09E-02	11			
10	W9E2	0.000, 72.700,-72.700	W11E1	0.000, 72.700, 72.700	8.09E-02	11			
11	W10E2	0.000, 72.700, 72.700	W12E1	0.000,-72.700, 72.700	8.09E-02	11			
12	W11E2	0.000,-72.700, 72.700	W9E1	0.000,-72.700,-72.700	8.09E-02	11			
13	W16E2	0.000,-61.200,-61.200	W14E1	0.000, 61.200,-61.200	8.09E-02	9			
14	W13E2	0.000, 61.200,-61.200	W15E1	0.000, 61.200, 61.200	8.09E-02	9			
15	W14E2	0.000, 61.200, 61.200	W16E1	0.000,-61.200, 61.200	8.09E-02	9			
16	W15E2	0.000,-61.200, 61.200	W13E1	0.000,-61.200,-61.200	8.09E-02	9			
17	W20E2	0.000,-55.000,-55.000	W18E1	0.000, 55.000,-55.000	8.09E-02	7			
18	W17E2	0.000, 55.000,-55.000	W19E1	0.000, 55.000, 55.000	8.09E-02	7			
19	W18E2	0.000, 55.000, 55.000	W20E1	0.000,-55.000, 55.000	8.09E-02	7			
20	W19E2	0.000,-55.000, 55.000	W17E1	0.000,-55.000,-55.000	8.09E-02	7			
21	W24E2	60.000,-60.300,-60.300	W22E1	60.000, 60.300,-60.300	8.09E-02	9			
22	W21E2	60.000, 60.300,-60.300	W23E1	60.000, 60.300, 60.300	8.09E-02	9			
23	W22E2	60.000, 60.300, 60.300	W24E1	60.000,-60.300, 60.300	8.09E-02	9			
24	W23E2	60.000,-60.300, 60.300	W21E1	60.000,-60.300,-60.300	8.09E-02	9			
25	W28E2	60.000,-52.900,-52.900	W26E1	60.000, 52.900,-52.900	8.09E-02	7			

26	W25E2	60.000, 52.900, -52.900	W27E1	60.000, 52.900, 52.900	8.09E-02	7
27	W26E2	60.000, 52.900, 52.900	W28E1	60.000, -52.900, 52.900	8.09E-02	7
28	W27E2	60.000, -52.900, 52.900	W25E1	60.000, -52.900, -52.900	8.09E-02	7
29	W32E2	120.000, -106.50, -106.50	W30E1	120.000, 106.500, -106.50	8.09E-02	15
30	W29E2	120.000, 106.500, -106.50	W31E1	120.000, 106.500, 106.500	8.09E-02	15
31	W30E2	120.000, 106.500, 106.500	W32E1	120.000, -106.50, 106.500	8.09E-02	15
32	W31E2	120.000, -106.50, 106.500	W29E1	120.000, -106.50, -106.50	8.09E-02	15
33	W36E2	120.000, -82.800, -82.800	W34E1	120.000, 82.800, -82.800	8.09E-02	13
34	W33E2	120.000, 82.800, -82.800	W35E1	120.000, 82.800, 82.800	8.09E-02	13
35	W34E2	120.000, 82.800, 82.800	W36E1	120.000, -82.800, 82.800	8.09E-02	13
36	W35E2	120.000, -82.800, 82.800	W33E1	120.000, -82.800, -82.800	8.09E-02	13
37	W40E2	120.000, -70.700, -70.700	W38E1	120.000, 70.700, -70.700	8.09E-02	11
38	W37E2	120.000, 70.700, -70.700	W39E1	120.000, 70.700, 70.700	8.09E-02	11
39	W38E2	120.000, 70.700, 70.700	W40E1	120.000, -70.700, 70.700	8.09E-02	11
40	W39E2	120.000, -70.700, 70.700	W37E1	120.000, -70.700, -70.700	8.09E-02	11
41	W44E2	120.000, -59.100, -59.100	W42E1	120.000, 59.100, -59.100	8.09E-02	9
42	W41E2	120.000, 59.100, -59.100	W43E1	120.000, 59.100, 59.100	8.09E-02	9
43	W42E2	120.000, 59.100, 59.100	W44E1	120.000, -59.100, 59.100	8.09E-02	9
44	W43E2	120.000, -59.100, 59.100	W41E1	120.000, -59.100, -59.100	8.09E-02	9
45	W48E2	120.000, -52.200, -52.200	W46E1	120.000, 52.200, -52.200	8.09E-02	7
46	W45E2	120.000, 52.200, -52.200	W47E1	120.000, 52.200, 52.200	8.09E-02	7
47	W46E2	120.000, 52.200, 52.200	W48E1	120.000, -52.200, 52.200	8.09E-02	7
48	W47E2	120.000, -52.200, 52.200	W45E1	120.000, -52.200, -52.200	8.09E-02	7
49	W52E2	216.000, -97.500, -97.500	W50E1	216.000, 97.500, -97.500	8.09E-02	15
50	W49E2	216.000, 97.500, -97.500	W51E1	216.000, 97.500, 97.500	8.09E-02	15
51	W50E2	216.000, 97.500, 97.500	W52E1	216.000, -97.500, 97.500	8.09E-02	15
52	W51E2	216.000, -97.500, 97.500	W49E1	216.000, -97.500, -97.500	8.09E-02	15
53	W56E2	216.000, -79.900, -79.900	W54E1	216.000, 79.900, -79.900	8.09E-02	13
54	W53E2	216.000, 79.900, -79.900	W55E1	216.000, 79.900, 79.900	8.09E-02	13
55	W54E2	216.000, 79.900, 79.900	W56E1	216.000, -79.900, 79.900	8.09E-02	13
56	W55E2	216.000, -79.900, 79.900	W53E1	216.000, -79.900, -79.900	8.09E-02	13
57	W60E2	216.000, -69.750, -69.750	W58E1	216.000, 69.750, -69.750	8.09E-02	11
58	W57E2	216.000, 69.750, -69.750	W59E1	216.000, 69.750, 69.750	8.09E-02	11
59	W58E2	216.000, 69.750, 69.750	W60E1	216.000, -69.750, 69.750	8.09E-02	11
60	W59E2	216.000, -69.750, 69.750	W57E1	216.000, -69.750, -69.750	8.09E-02	11
61	W64E2	216.000, -59.900, -59.900	W62E1	216.000, 59.900, -59.900	8.09E-02	9
62	W61E2	216.000, 59.900, -59.900	W63E1	216.000, 59.900, 59.900	8.09E-02	9
63	W62E2	216.000, 59.900, 59.900	W64E1	216.000, -59.900, 59.900	8.09E-02	9
64	W63E2	216.000, -59.900, 59.900	W61E1	216.000, -59.900, -59.900	8.09E-02	9
65	W68E2	216.000, -52.500, -52.500	W66E1	216.000, 52.500, -52.500	8.09E-02	7
66	W65E2	216.000, 52.500, -52.500	W67E1	216.000, 52.500, 52.500	8.09E-02	7
67	W66E2	216.000, 52.500, 52.500	W68E1	216.000, -52.500, 52.500	8.09E-02	7
68	W67E2	216.000, -52.500, 52.500	W65E1	216.000, -52.500, -52.500	8.09E-02	7
69	W72E2	312.000, -98.000, -98.000	W70E1	312.000, 98.000, -98.000	8.09E-02	15
70	W69E2	312.000, 98.000, -98.000	W71E1	312.000, 98.000, 98.000	8.09E-02	15
71	W70E2	312.000, 98.000, 98.000	W72E1	312.000, -98.000, 98.000	8.09E-02	15

72	W71E2	312.000,-98.000, 98.000	W69E1	312.000,-98.000,-98.000	8.09E-02	15
73	W76E2	312.000,-79.900,-79.900	W74E1	312.000, 79.900,-79.900	8.09E-02	13
74	W73E2	312.000, 79.900,-79.900	W75E1	312.000, 79.900, 79.900	8.09E-02	13
75	W74E2	312.000, 79.900, 79.900	W76E1	312.000,-79.900, 79.900	8.09E-02	13
76	W75E2	312.000,-79.900, 79.900	W73E1	312.000,-79.900,-79.900	8.09E-02	13
77	W80E2	312.000,-69.650,-69.650	W78E1	312.000, 69.650,-69.650	8.09E-02	11
78	W77E2	312.000, 69.650,-69.650	W79E1	312.000, 69.650, 69.650	8.09E-02	11
79	W78E2	312.000, 69.650, 69.650	W80E1	312.000,-69.650, 69.650	8.09E-02	11
80	W79E2	312.000,-69.650, 69.650	W77E1	312.000,-69.650,-69.650	8.09E-02	11
81	W84E2	312.000,-59.300,-59.300	W82E1	312.000, 59.300,-59.300	8.09E-02	9
82	W81E2	312.000, 59.300,-59.300	W83E1	312.000, 59.300, 59.300	8.09E-02	9
83	W82E2	312.000, 59.300, 59.300	W84E1	312.000,-59.300, 59.300	8.09E-02	9
84	W83E2	312.000,-59.300, 59.300	W81E1	312.000,-59.300,-59.300	8.09E-02	9
85	W88E2	312.000,-52.000,-52.000	W86E1	312.000, 52.000,-52.000	8.09E-02	7
86	W85E2	312.000, 52.000,-52.000	W87E1	312.000, 52.000, 52.000	8.09E-02	7
87	W86E2	312.000, 52.000, 52.000	W88E1	312.000,-52.000, 52.000	8.09E-02	7
88	W87E2	312.000,-52.000, 52.000	W85E1	312.000,-52.000,-52.000	8.09E-02	7

In order to evaluate the design—while still in its modeling stage—let's review the performance of the smaller ON7NQ design.

Modeled Performance: ON7NQ 3.5-element, 5-Band Quad
NEC-4; Full Segmentation

Freq. MHz	Gain dBi	Front/Back dB	Impedance R +/- jX	50-Ohm SWR
14.0	8.42	11.83	37.6 - j 18.5	1.66
14.175	8.29	15.06	44.3 + j 4.4	1.17
14.35	8.06	9.76	34.8 + j 36.5	2.50
18.068	8.47	21.80	42.7 - j 5.1	1.21
18.118	8.42	25.52	43.5 - j 0.3	1.15
18.168	8.36	20.90	43.2 + j 4.6	1.19
21.0	8.43	15.28	49.7 - j 20.1	1.49
21.225	8.52	20.98	46.4 - j 0.0	1.08
21.45	8.47	10.24	36.2 + j 30.7	2.16
24.89	9.26	22.72	35.1 - j 2.1	1.43
24.94	9.22	18.92	41.1 + j 2.3	1.27
24.99	9.18	16.70	47.6 + j 4.8	1.12
28.0	9.01	18.40	43.8 - j 31.6	1.96

28.2	9.35	25.89	45.3 - j	11.0	1.29
28.4	9.62	30.72	51.3 + j	6.8	1.15
28.6	9.85	22.80	58.7 + j	9.6	1.27
28.8	9.73	12.38	31.1 + j	8.1	1.68

For comparison, here are the modeled performance figures for the larger design.

Modeled Performance: W4RNL 4.5-element, 5-Band Quad
NEC-4; Full Segmentation

Freq. MHz	Gain dBi	Front/Back dB	Impedance R +/- jX	50-Ohm SWR
14.0	8.81	15.02	33.7 - j	20.8
14.175	8.58	16.76	51.9 + j	10.0
14.35	8.14	9.95	57.8 + j	34.0
18.068	9.23	22.01	36.1 - j	1.8
18.118	9.18	21.24	39.2 + j	5.7
18.168	9.10	17.38	42.3 + j	12.5
21.0	9.49	15.33	41.5 - j	15.6
21.225	9.47	17.04	57.0 + j	7.5
21.45	9.54	19.13	31.3 + j	10.0
24.89	10.27	21.79	38.6 + j	5.3
24.94	10.28	19.82	40.3 + j	9.1
24.99	10.24	16.77	41.9 + j	14.4
28.0	9.59	12.15	40.8 - j	27.4
28.2	10.15	17.00	49.3 - j	12.7
28.4	10.60	20.51	47.1 - j	2.8
28.6	10.85	19.77	42.6 + j	18.1
28.8	10.51	29.75	64.9 + j	12.1

Design Evaluation

In this morass of data are some significant figures. First, note that, to a very large degree, the performance curves of the larger array on each band tend to replicate the curves of the smaller array, but with a higher gain. The replication strongly suggests that—with a few exceptions—the array has yielded about all of the performance of which it is capable. But how well did it meet its specifications?

1. Gain: at least 0.7 dB greater than the existing array

Although the improvement in gain is not a constant for any individual band, the following average-gain-advantage/band list does suggest the performance improvement provided by the extra set of directors.

Performance Improvement: 3.5 Elements vs. 4.5 Elements

Band	Gain Improvement
20 Meters	0.25 dB
17	0.75
15	1.03
12	1.04
10	0.90

Only 20 meters fails to show a considerable gain increase. The reasons will be explained in the discussion of “Coverage.”

2. Front-to-Back Ratio: at least 15 dB across each band—if possible

Only the upper end of 20 meters and the lowest end of 10 meters fail to reach the 15-dB front-to-back ratio. The 10-meter low-end failure stems from the fundamental narrow-band nature of wire quads. The SWR curve is wider than the front-to-back curve in virtually all cases, even when the front-to-back limit is lowered to 15 dB.

3. Source Impedance: less than 2:1 50-Ohm SWR for direct feed (individually) on each band with a standard 50-Ohm coaxial cable

The 4.5-element array, unlike the 3.5-element quad, achieves the SWR goal on all bands, with the restriction of 10 meters to the first 800 kHz of the band. The failure of the 3.5-element quad to achieve the SWR goal on 15 meters is correctable with slight shortening of the driven element. The SWR at the low end of the band (1.49:1) suggests that considerably more capacitive reactance can be tolerated at 21 MHz, with a consequent lowering of inductive reactance at the high end of the band. However, this approach does not work on 20 meters, since the low-end resistive component is well below 40 Ohms, indicating a limit to the capacitive reac-

tance increase that might be tolerated. One or the other end of the band ends up with an SWR in excess of 2:1

4. Coverage: Full band coverage of all bands, with 800 kHz coverage of 10 meters

This criterion essentially is a replication of the SWR specification. The breadth of 10 meters has already been noted as the source of the cut-off at 28.8 MHz and the low front-to-back ratio and gain in the first 100 kHz of the band. However, 20 meters also calls for comment.

On a normal (20-10-meter) quad, 20-meters is unbounded on the outside. Moreover, the boom length for 4 elements is exceptionally short. 26' would be about the normal boom length for a 3-element monoband 20-meter quad, although the gain would be similar to the peak value for the large array on 20. To achieve full band coverage with the 4.5-element antenna, considerable changes to the director sizes were needed compared to the 3.5-element array director. As well, the forward director is larger than the inner director.

It is possible with larger directors to achieve higher gain over part of the 20-meter band. Free-space gain values up to 9.25 dBi were achieved in some versions. However, the higher the gain, the narrower the available operating region, as defined by the 2:1 SWR figure. As well, the checkpoint numbers recorded to indicate array behavior tend to gloss over many facets of both gain and front-to-back ratio. For example, on 20 meters, maximum gain occurs just above the lower end of the band, with maximum front-to-back occurring at about 14.1 MHz. Hence, it pays to use checkpoint data with caution and to perform detailed frequency sweeps for each band to assess the performance more thoroughly.

To achieve an acceptable SWR value for the entire band, it was necessary to accept as well a lower gain value. The performance tapers off at the high end of the band, although operation on that portion of the band is possible. By accepting a bandwidth restriction on 20 meters, the smaller 3.5-element array was able to achieve somewhat higher gain at the low end of the band relative to its size. Therefore, the small average gain increase on 20 for the 4.5-element array results in part from differences in the design specifications for the two different antennas.

If we were to increase the boom length to 30 feet, changing the forward director spacing from 8' to 12' from the preceding element set, we might be able to elevate 20-meter performance by about 0.2 dB, with a very slight decrease in the gain slope, and to obtain a very slightly shallower front-to-back curve with small rises in the band edge performance. However, the cost in terms of a longer boom, with consequential loading considerations, may make this small gain somewhat gratuitous. In any event, the potential is there for anyone who wishes to re-tweak the array on all other bands.

Reality 1: Pattern Shapes

Some designers expect multi-band arrays to achieve patterns similar to those of monoband directional antennas. The forward lobe will be a single large oval, while the rearward radiation will consist of from 1 to 3 small lobes, each at least 20 dB under the forward gain. Unfortunately, multi-band arrays (with the possible exception of large LPDAs) tend to have patterns that are often far from well behaved. The interaction among the elements—even supposedly inactive elements—remains considerable, as would be evident from an exploration of the current tables produced by NEC. This condition is not exclusively a quad problem, but also attends to large multi-band Yagis as well.

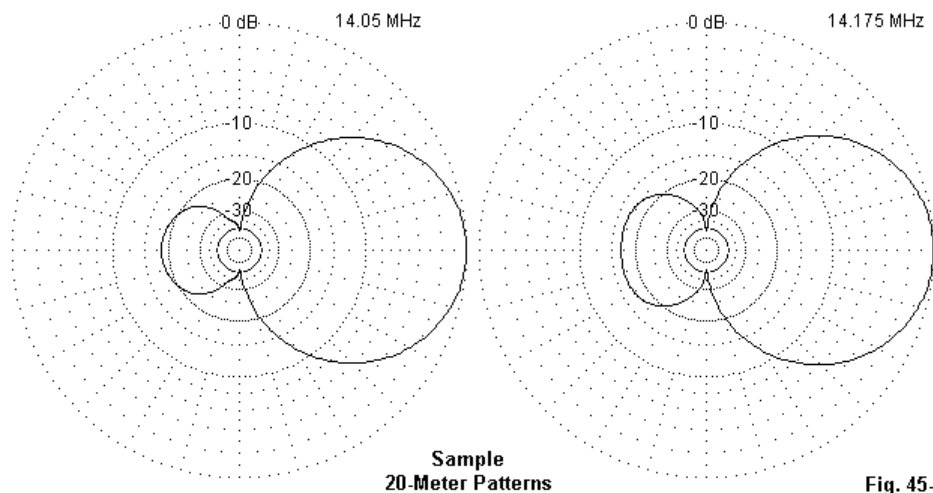
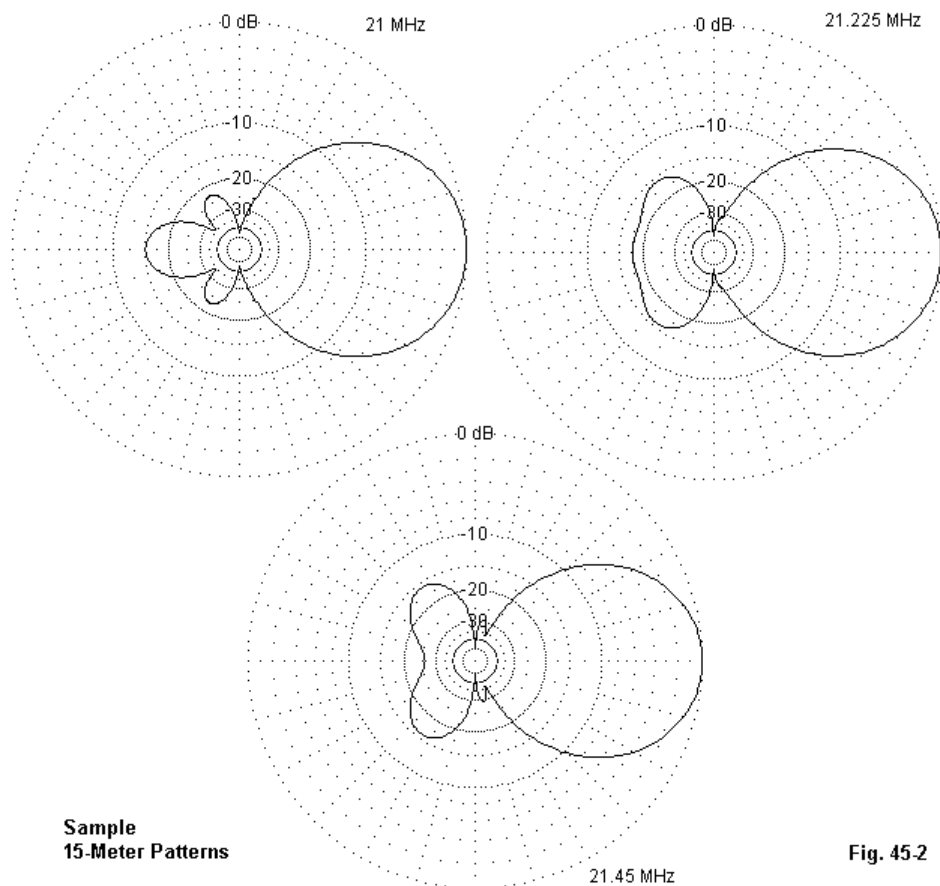


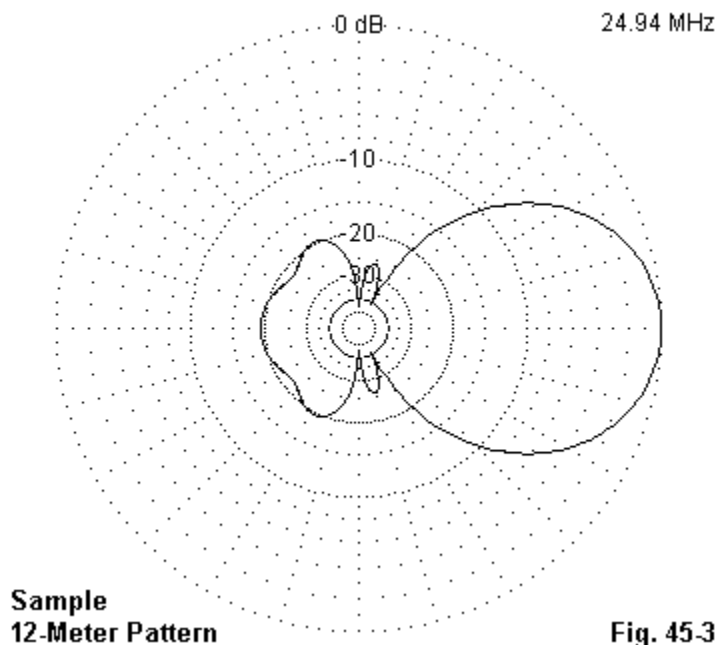
Fig. 45-1

Not all bands suffer from ill-behaved patterns. As the 20-meter samples in **Fig. 45-1** show, the patterns are quite ordinary. However, as the outside loop set, the 20-meter elements interact least with other elements in the array.



The sample 15-meter patterns in **Fig. 45-2** show a truer picture of the effects of interactions between the active and inactive elements in the array—where “inactive” means elements for a band other than the one in use. One casualty of the interac-

tion is the front-to-rear ratio, as rearward side lobes grow to considerable proportions. A number of design decisions were made in the process of modeling and optimizing this band. The gain was sacrificed to a small degree in order to obtain the best possible progression of rear lobe formation across the band.



The single 12-meter pattern in **Fig. 45-3** frames another common element interaction problem—the formation of side lobes. The small side lobes appear from 15 meters on upward in frequency and are likely the result of harmonic operation of larger elements. Under these conditions, currents in the vertical side wires can yield radiation to the array sides in the form of minor side lobes.

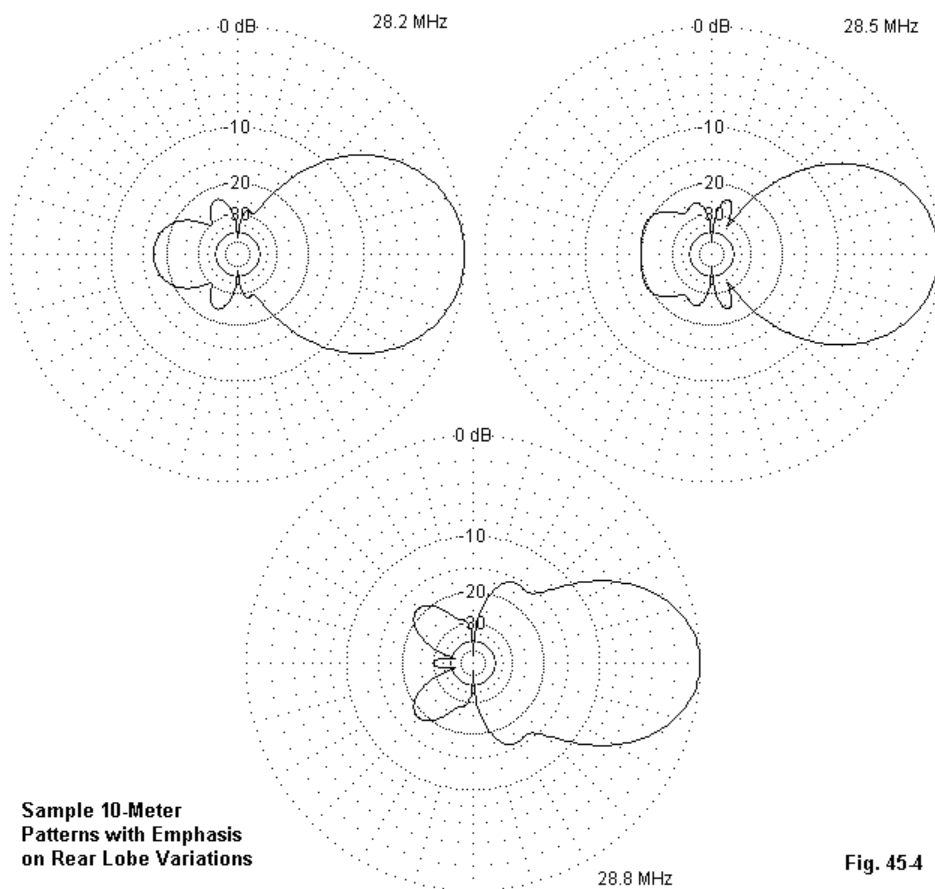


Fig. 45-4 provides a progression of 10-meter patterns to display how radically a pattern may change across a wide band. The changes to the rear pattern are most

evident. However, in the forward direction, note that the minor side lobes develop into considerable bulges with increases in frequency. Of all bands, 10 meter may be the most sensitive to excitation of inactive elements. The 12-meter elements are within the range of reflector size, and the 20-meter elements may operate in a harmonic mode, even though isolated from the 10-meter elements by Intervening elements for other bands.

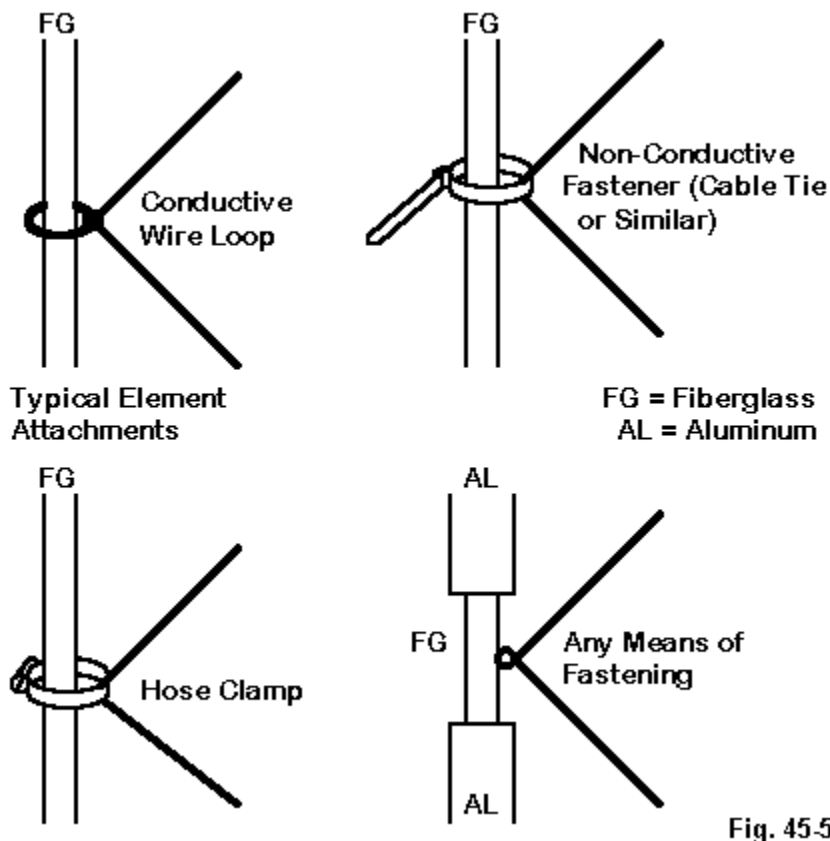
By no means does less-than-perfection in the array patterns count against the use of multi-band, multi-element quads. Rather, they are a simple fact of life that one must take into account both in the design and utilization phases of the antenna.

Reality 2: Quad Construction

We have noted the relationship between the design-by-modeling process and the ultimate use of the quad array. Omitted to this point is the relationship between antenna design and modeling on the one hand and antenna construction on the other. Ordinarily, we have passed over this aspect of activity with simple cautions that the model applies accurately within the limitations of the construction process.

For the present array design, we should add something a little more concrete. Antenna models using bare wire do not take into account construction variables unless the modeler specifically simulates them. The present design is no exception. However, quad construction practices are highly variable, as illustrated simply in **Fig. 45-5**.

The sketch illustrates only 4 among a large number of conditions that may exist at the attachment point between the support arms and the wire elements. Two common methods of attachment are the use of hose clamps and the use of wire loops to fix the position of the element corner. It does not matter whether the element is connected electrically to the metal device that pins the element to the arm. The fixture acts as a simple closed loop connected or coupled to the element at the corner. A quad element has considerable current magnitude at its corners, and such a loop can alter the resonant frequency of the loop when compared to the system in the upper right of the figure, where attachment is made via a wholly non-conductive set of components.



Metal attachment fixtures can act as loads on the wire loop. For most cases, the loop size can be adjusted to accommodate the fixture. Perhaps the simplest way to

do this with any accuracy is to model only the set of driven elements to obtain their independent resonant frequencies, but using the dimensions prescribed by the overall array model. Then construct the drive element set using the proposed construction technique. Measure the resonant frequency of each loop. For a given construction technique, any shift in frequency relative to the model should be consistent for both driven and parasitic elements, although the amount may vary from one band to the next.

One may then create reactive loads at each corner of the modeled element until it has the same resonant frequency as the measured drivers. The same load values for each band can be inserted into each corner of each element in the full array. Then, the loop dimensions are adjusted in the model until design performance is restored. The resulting dimensions should prove to be an accurate guide to final construction. For an array of this size and potential performance, the extra modeling and test effort should not be considered excessive.

Some quads use aluminum arms with fiberglass or similar non-conductive sections for element attachment. The proximity of the aluminum sections of the arms to the elements suggests that the same test procedure is in order as we used for metal clamps to wholly insulated arms.

The quad array described here as a design project for NEC software also reveals another feature that impinges on construction. Many of the performance-improving increments of element adjustment involved changes of a tenth of an inch at a time, especially on the higher bands. Since the change was made to a variable representing $1/8$ the loop circumference, some elements of the array may be sensitive to changes as small as an inch in overall wire length for a loop. The designer should flag extra-sensitive elements for special care during construction. Sensitivities of this order are natural to a 5-band array with 22 elements in an elongated cube that is only 18' per side by 26' in length.

Apart from this specific antenna, the general principle to be observed is that one cannot simply take modeled dimensions and create a physical antenna. One must first correlate the model to the physical conditions of the construction methods used. In some cases, the selection of materials will permit the modeled dimensions to be used as given. I have constructed both wire and tubular element antennas on 10

meters where the modeled dimensions and the physical antenna were under 1" apart.

However, wherever the physical antenna may have some potential for placing metal within the immediate field of the elements, either the modeler must simulate those objects in the model or he must develop a test regimen to establish a correlation between the design model and the physical prototype. We have illustrated only one of many possible correlation methods. The transition from model to physical antenna should be undertaken with as much care as is put into the modeling design process and into the construction process. Carelessness in any of the three phases of work can yield mediocre communications results.

The primary subject of these columns is antenna modeling. However, I hope that this foray into a specific design project not only provides some awareness of the modeling work involved, but as well helps one to integrate modeling into the overall process that runs from antenna idea to antenna reality.

* * * * *

See model 44-2 from the preceding column.



46. A Load in Parallel With a Source

One of the examples in my text, *Basic Antenna Modeling: A Hands-On Tutorial*, involves applying a beta match to a 3-element Yagi. The challenge is to place a reactive load in parallel with the source. Since several of the techniques require a rather high level of segmentation, we shall use a model already set up for the job. **Fig. 46-1** shows the evolution through which we shall go before departing from it.

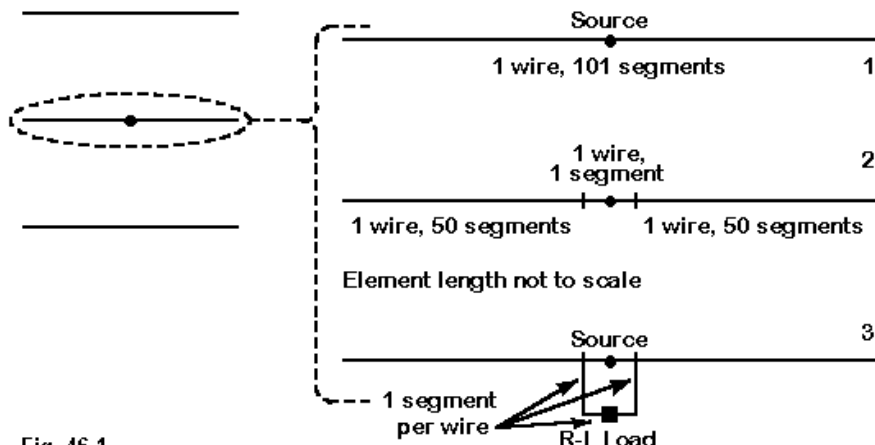


Fig. 46-1

The reflector and the director of the Yagi, set up for 14.175 MHz, follow the segmentation pattern in the top driver option. However, the actual driver uses a 3-wire set-up, with the 1-segment wire in the center having the same length as the remaining segments in the driver. In this way, we assure a correct source imped-

ance calculation regardless of what we do in order to place the load in parallel with the source.

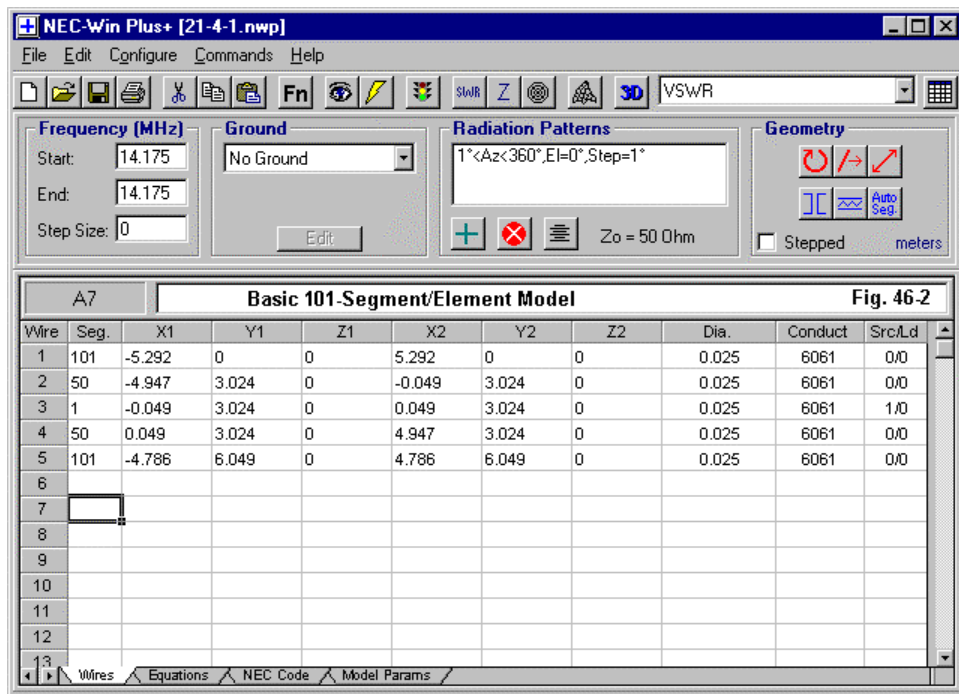


Fig. 46-2 shows the basic Yagi model in its present form. If we place the source on wire 3 with no matching system, then the impedance will be about $23.4 - j 24.6$ Ohms. The impedance is ripe for matching to a 50-Ohm coax line with a beta match. A beta match is made up of an L-network with a reactance in series with the load and a shunt reactance across the source—the coax in this case. The series reactance is already present in the antenna driver source impedance. Hence, the

beta match physically consists of the deceptively simple placement of a reactance across the terminals to which the coax connects with the driver.

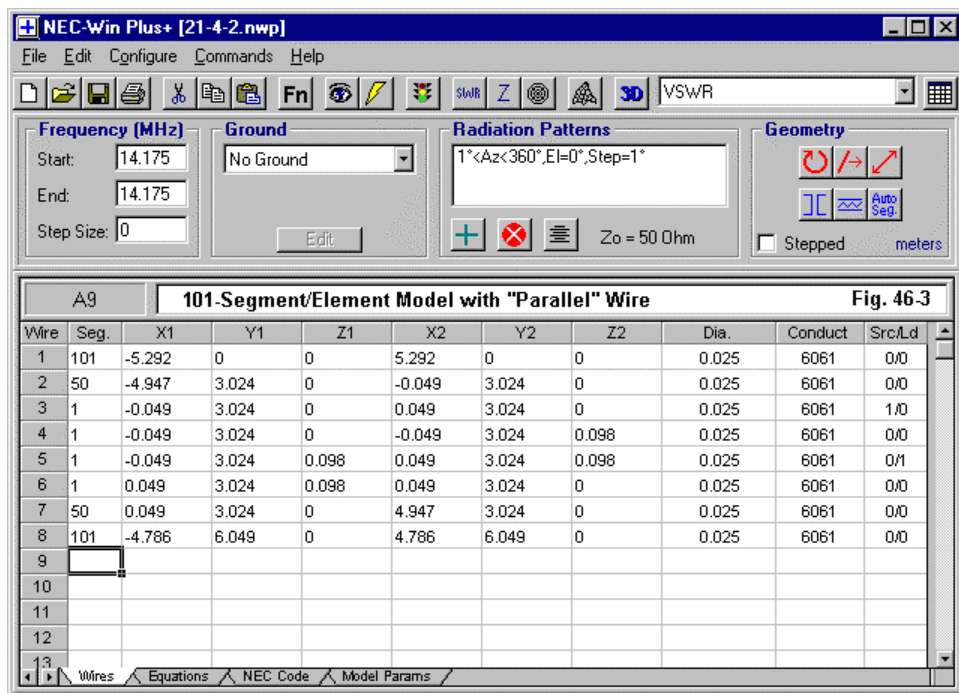
$$\delta = \sqrt{\frac{R_{High}}{R_{Low}} - 1} \quad X_S = \delta R_{Low} \quad X_P = \frac{R_{High}}{\delta} \quad (1)$$

Standard L-network calculations, summarized in the equation set (1), provide the level of reactance necessary to effect a good 50-Ohm match. For the case at hand we need just about 50 Ohms (46.9 Ohms, to be more and perhaps spuriously precise) of inductive reactance for the parallel component to go with the nearly 25 Ohms of series capacitance. Indeed, the transformation of 23.4 Ohms to 50 Ohms calls for a series capacitive reactance of 24.95 Ohms, and we have 24.6 Ohms in place—a very close setting of the driver length.

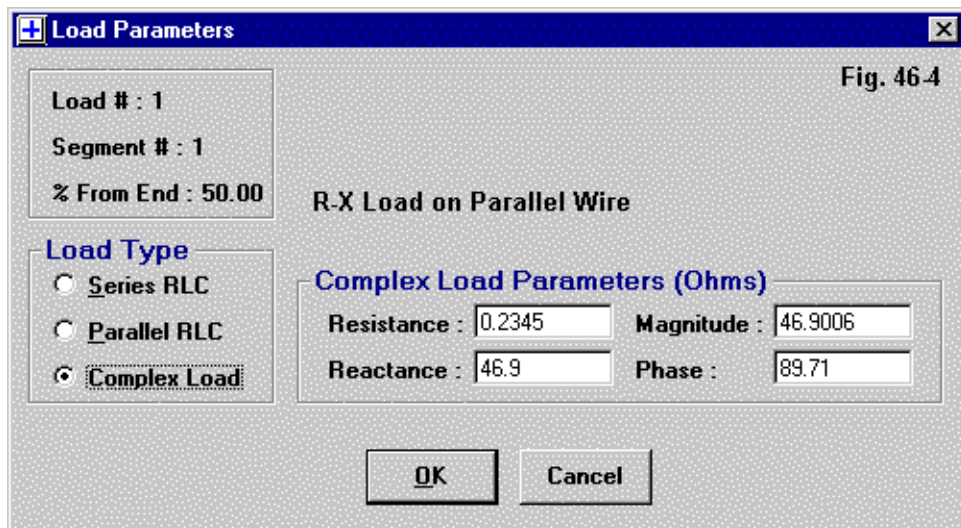
Essentially, we have two ways to achieve the inductive reactance: a standard inductor or a shorted length of transmission line. Before we finish, we shall look at both methods, but let's start with the coil. It will involve the more complex modeling.

We cannot simply place a reactive load on the source segment. Every such load will wind up in series with the source, when our goal is to place it in parallel with the source. If we wish to place a reactive load in parallel with the source, one technique is to model the antenna so that there is a physical place for the load to be. To make a place, we must model a set of wires such that they are in parallel with the source segment.

The lowest portion of **Fig. 46-1** shows the physical arrangement. We simply add three wires to form a square with the 1-segment source wire. The high level of segmentation is designed—well within the limits of NEC's segment length to wire radius limitations—to keep the assembly as small as feasible so that it does not contribute significantly to the radiation pattern of the antenna, thereby distorting the performance reports. **Fig. 46-3** shows the resulting model with its new square.



To Wire 5, the one that is physically parallel to the source wire, we shall add a load. The next questions are “what kind?” and “how much?” Spot-frequency modeling can use a simple R-X load in which we specify the resistance and reactance of the load. Let’s assume a coil Q of 200. With a 46.9-Ohm reactance, the resistance will be 0.2345 Ohms at the specified Q. **Fig. 46-4** shows the entry of the 2 values on the load set-up screen, along with added data on the load magnitude and phase angle. See model 46-1.



With the load specified, the new source impedance is $57.6 + j 1.5$ Ohms. This value is correct for 14.175 MHz. However, R-X loads have a limitation. A coil will change reactance for every change in frequency. An R-X load will hold the reactance at the same value for every frequency we might check. Hence, an R-X load will not give a true picture of the source impedance across the 20-meter band.

$$X_L = 2\pi fL \qquad L = \frac{X_L}{2\pi f} \qquad (2)$$

We have an easy alternative. On wire 5, instead of using an R-X load, we can employ an R-L-C load. Since there is no capacitance in the load we are applying, we shall leave its value at zero. The resistance remains 0.2345 Ohms. From fundamental equations that appear in every handbook and that are repeated in equation set (2), we can calculate the inductance that provides a reactance of 46.9 Ohms at 14.175 MHz: 0.5266 uH. See model 46-2.

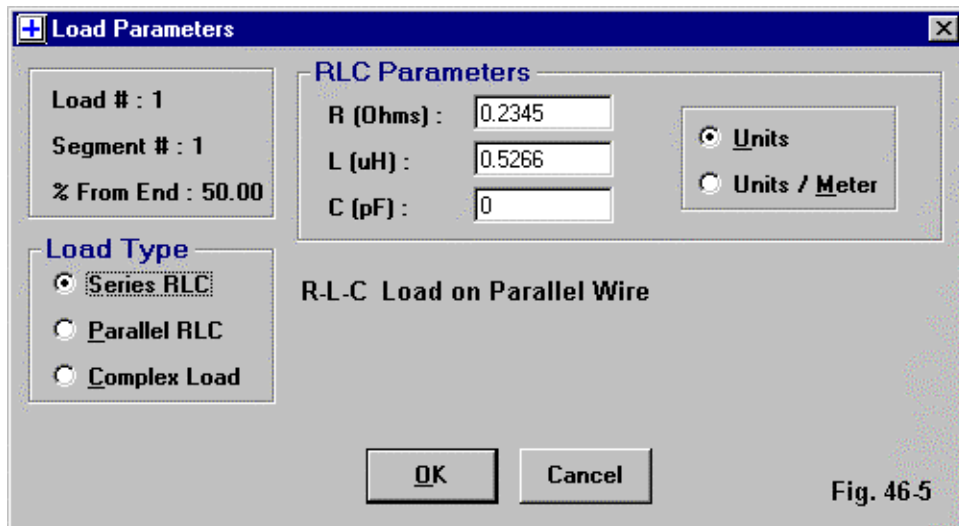


Fig. 46-5

Fig. 46-5 shows the entry screen for R-L-C loads, with the resistance and inductance properly entered. When we run the model, it shows a feedpoint impedance of $57.6 + j 1.4$ Ohms, the same as with the R-X load. Where differences will appear is in source impedance reports at a distance from the design frequency. In general, an R-X load will provide too optimistic a portrait of the source impedance and resulting 50-Ohm SWR. A resistance-inductance load is necessary to arrive at a more conservative but more correct set of curves.

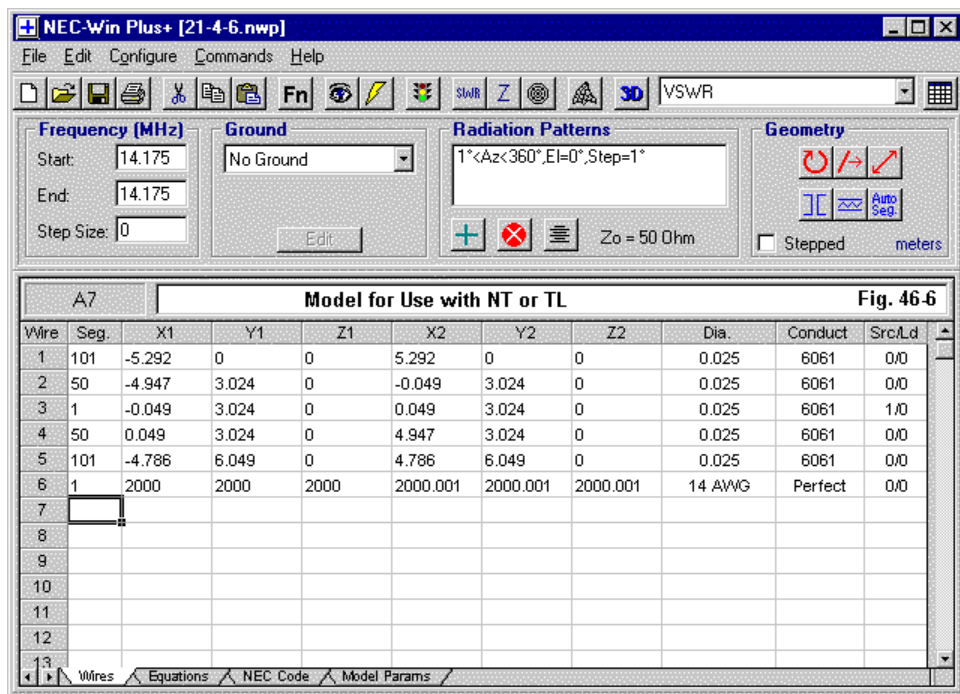
Incidentally, throughout this sequence of models, both the ones covered so far and those yet to be examined, the free-space gain of the Yagi varied by only 0.06 dB and the front-to-back ratio varied by less than 0.1 dB. Since the feedpoint impedance reported so far coincides with L-network calculations within a few Ohms, the techniques are accurate and harmless to the model.

If we are dissatisfied with the 7-Ohm deviation of the matched model from the calculated nearly perfect 50-Ohm value—perhaps due to some task-driven requirement—then we can check the original model with the addition of the square to see if the square in fact changed the source impedance significantly. To do this, we need only return to version with the R-X load. We can change the values for R and X to 1E10 to simulate an open circuit. With the present driver dimensions (+/-4.947 m), the source impedance in our check model reports as 23.3 - j 24.6 Ohms. The added structure does not significantly affect the source impedance (originally 23.4 - j 24.6 Ohms).

Nonetheless, the structure is composed of “fat” wire (25 mm or about 1”) in order to avoid NEC difficulties with angular junctions of wires having dissimilar diameters. As well, the beta shunt component is placed at a slight distance from the actual source. In order to arrive at a value of source impedance within about 1 Ohm of calculations, it is necessary to juggle two aspects of the model: the driver length and the reactance (or inductance) of the shunted load. For the model that we have been using, I arrived at a source impedance of 50.6 + j 0.3 Ohms with a reactance of 48.5 Ohms and a driver length of +/-4.963 m. The actual values do not necessarily reflect what the physical antenna would require, but the juggling is typical of the adjustment procedure used with beta matches to arrive at an acceptable, if not perfect, match. Modeling does have more than numerical analogs to antenna construction, if we are alert to identify them.

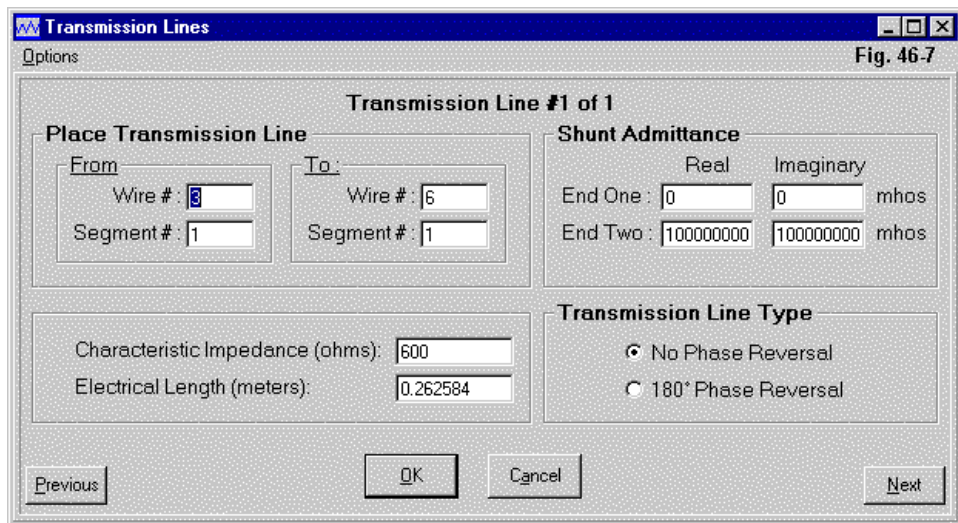
One limitation of the “added-square” system of putting a load in parallel with the source is that it will disable the use of Leeson corrections, if our model uses a tapered-diameter schedule of tubing. However, the uniform diameter model can be used for analytical purposes, with the tapered diameter version later developed to determine the exact element lengths required for the physical antenna.

If we wish to avoid the use of a square of wires at the feedpoint, we can still arrive at a model of a beta match. The techniques will employ either a transmission line or a network. Either modeling option requires that we create an “arbitrary” wire at a distance from the antenna. The wire should be far enough away to create no detectable effects on the model. As well, the wire can be perfect or lossless, be a single segment, and be so short and thin that it is virtually invisible to radiated RF energy. **Fig. 6** shows the revised model with the square missing but with the arbitrary wire added into the wire set.



The required shunt or parallel beta inductive reactance can be obtained not only from an actual inductor, but as well from a shorted transmission line stub, the proverbial beta “hairpin.” Transmission lines connected to the same segment as a source appear in parallel with the source. Therefore, we can simply create a transmission line using the “TL” facility built into NEC.

Fig. 46-7 shows the required transmission line screen. The transmission line goes from the source wire (3) to the new distant wire (6). To make sure that the transmission line appears as a short, we enter very high values of admittance, the equivalent of entering exceptionally low values of impedance. The real and imaginary components are the conductance and the susceptance, the inverse of resistance and reactance. We enter values such as 1E10 in both places. Some programs automate this feature so that the user only needs to enter the request for a shorted (or open) stub. See model 46-3.



Every beta hairpin or stub will have a characteristic impedance based upon the diameter of the wires making up the line and the distance between them. For this exercise, we have arbitrarily set the characteristic impedance at 600 Ohms, indicating a fairly wide spacing between wires. The length is determined from the fact that the inductive reactance of a shorted stub is the product of the line characteristic impedance and the tangent of the line's length in electrical degrees. The ratio of the inductive reactance to the line impedance gives us the tangent of the line length in degrees, which we can then convert into a fraction of a wavelength and from there into a physical length (assuming a velocity factor of 1.0). For this case, the required line length is 0.262584 meters (since the entire dimension set for the model has been in meters). With this length, we obtain a source impedance of $49.2 - j 0.0$ Ohms. This value is a few Ohms different from the values using the load applied to the parallel wire square and is likely more accurate, since it involves the addition of nothing physical to the antenna.

Like the R-L-C type load, the transmission line stub will yield correct results on a frequency sweep. Since the stub is specified as a set of physical dimensions (including the characteristic impedance, which is derived from physical properties of the line), it will correctly modify the source impedance over a wide frequency range. In addition, even if the ultimate antenna will employ a beta shunt inductor rather than a hairpin stub, the transmission line stub can be used with a tapered diameter element set as a substitute for the coil for design purposes. The SWR curves for the stub may not exactly coincide with those for the coil. Use of the coil to determine the operating SWR bandwidth can be done with the uniform-diameter model. The two significant items that a TL line will not reveal are a. any losses in the line (not usually a problem with short stubs) and b. the effects of the physical line on the radiation pattern.

Networks [X]

Options Fig. 46-8

Network #1 of 1

Place Network

<p>From</p> <p>Wire #: <input type="text" value="3"/></p> <p>Segment #: <input type="text" value="1"/></p>	<p>To:</p> <p>Wire #: <input type="text" value="6"/></p> <p>Segment #: <input type="text" value="1"/></p>
---	--

Short-Circuit Admittance Matrix

	Real	Imaginary	
Y_{11}	<input type="text" value="0.0001066"/>	<input type="text" value="-0.0213214"/>	mhos
Y_{12}	<input type="text" value="0"/>	<input type="text" value="0"/>	mhos
Y_{22}	<input type="text" value="100000000"/>	<input type="text" value="100000000"/>	mhos

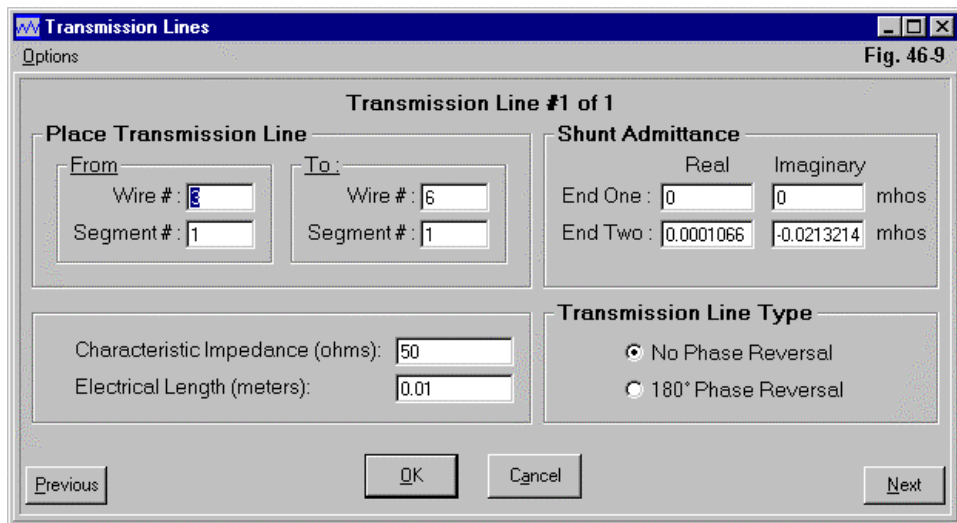
We have not yet exhausted the ways in which we can add a parallel load to a source segment. For example, we have not yet employed a “network,” the NT function of NEC. We can convert the required values of series resistance and reactance to their equivalents for use in a short-circuited admittance matrix. An example of the network screen appears in **Fig. 46-8**.

The source wire (3) represents the first port, while the “arbitrary” wire (6) represents the second port. Into the Y11 boxes we insert the real and imaginary values required for a parallel or shunt admittance. We leave Y12’s values as zeroes. We create a short circuit at the Y22 entry place by using very high values (1E10) for both the real and imaginary components. All we need to do now is determine the real and imaginary components for Y11.

$$G_P = \frac{R_s}{R_s^2 + X_s^2} \qquad B_P = -\frac{X_s}{R_s^2 + X_s^2} \qquad (3)$$

The equations in set (3) provide us with the conversion formulas to apply to the series resistance (0.2345 Ohms) and reactive (46.9 Ohms) in order to arrive at usable numbers. The resulting values appear in **Fig. 46-8**. The result, when the model is run, is a source impedance of 49.0 - j 0.0 Ohms, which is in very close agreement with the transmission stub result we just finished examining. However, the network result is as limited as the R-X load technique: it is correct for only the single frequency for which it is specified. See model 46-4.

Some programs do not provide the user with ready access to the network (NT) facility, but they do permit use of the transmission line (TL) facility. In such as case, we can simulate the network load across the source. Let’s examine **Fig. 46-9**, the same transmission line screen that we used for the shorted stub. However, we shall approach it from a different angle.



The line runs from wire (3) to wire (6). Let's set the characteristic impedance at the value of the line to which we wish to effect a match, that is, to 50 Ohms, the value of the coax that we want matched to the antenna. The length of a transmission is independent of the distance between wires (3) and (6) and can be set into the TL call. We do not want the line to create any significant impedance transformation, so we shall make the line very short. The arbitrary length used in this exercise is 0.01 meters.

Next, let's place the (overly precise) shunt admittance values that we calculated into the real and imaginary (conductance and susceptance) boxes at the "far" end of the very short line. We now have the load across the source. The source impedance that NEC reports from this model is $49.0 - j 0.3$ Ohms, almost precisely the value obtained by using the network. However, like the network technique, this application of the transmission line facility is limited to a single test frequency. See model 46-5.

Of the 5 techniques that we have shown for modeling a beta match, the beta inductor on the extra wire square and the transmission line stub are certainly the most useful. Both are responsive to changes in frequency and therefore produce relative accurate impedance and SWR curves for estimating the operating bandwidth of the loaded source antenna. One can change the value of the inductor's Q and develop sets of curves for the operating bandwidth using different values of Q . However, the "added-square" technique is not applicable if tapered-diameter elements are used with the Leeson corrections enabled.

In spite of this judgment, this exercise has had something of an ulterior motive. The network facility available within NEC (-2 or -4) is rarely used by modelers, especially modelers with less experience in handling shunt admittance networks. Indeed, most amateurs are far more familiar with the concepts of resistance, reactance, and impedance than with their very useful inverse concepts of conductance, susceptance, and admittance. For such reasons as these, some implementations of NEC omit the network facility altogether (along with many other lesser-used facilities) from basic software packages. Other implementations include the facility, but pass over it in silence in manuals. Indeed, the NEC user manual itself is somewhat opaque on the subject for anyone not having significant previous experience with networks

The examples that I have contrived for this exercise are in many ways unnecessary for effectively modeling a load across a source. However, they do call attention to two facts: 1. the network facility is available and can be put to service, and 2. the transmission line facility is a special case of the network facility.

Networks can place loads of various orders across any segment. For very large models, an added advantage of the network is that the load can be changed without causing a recalculation of the structure matrix, as is required when using standard loads (the LD facility). As well, networks are in parallel with sources on the same segment, unlike loads (LD), which are in series with sources on the same segment. To offset this advantage, we may note once more that the network value does not automatically scale with frequency changes, as does an R-L-C load.

It may be the case that the increasing speed of desk-top computers and the ease with which one may form a work-around for paralleling a source and a load have largely obviated the advantages of using networks for small to fairly large size

models. In any event, we have at least made a passing acquaintance with networks, and that may be enough for one exercise.

* * * * *

Models included: 46-1 through 46-5. 46-4 and 46-5 not available in .EZ format. (All model dimensions in meters.)



47. So You Want to Read a NEC-Deck

Those who develop implementations of NEC for newer users often create “user-friendly” interfaces between the data that the NEC core requires and what the user sees on screen. The result is very often a more effective first use of the program. However, the interface can obscure the basic structure of the NEC core and its potentials.

Many users of ELNEC and EZNEC are wholly unfamiliar with the basic elements of a standard .NEC input file, since the program uses a proprietary model file system. The model description bears a close but unclear relationship to a comparable .NEC file. Users of NEC-Win Plus may also be unfamiliar with the terms and layout of an EZNEC antenna description file (called a PD file for the abbreviated keystrokes used to generate it). Some users of Plus may never even look at the available spreadsheet screen that gives the file listing in ASCII .NEC-format terms. As an exercise in correlating user formats and .NEC files, let’s compare the data of an EZNEC model description file and the corresponding lines of a standard .NEC file. The exercise will acquaint us with the basic terms of the NEC deck.

In most advanced implementations, NEC uses a card-deck input file whose format goes back to the early days of FORTRAN, when punch cards provided computational inputs. Nowadays, we simply type in a single line of input-file text as a replacement for the old punch cards—and many current FORTRAN users simply do not make a connection between the line format and the old punch card requirements. For brevity, each card contains a labeled sequence of information, the individual parts separated by a delimiter. Since we Americans use “.” as our decimal indicator, we use commas or spaces to separate information. European formats may vary.

To get us started, let’s compare the antenna description file for a simple 2-element Yagi with the corresponding card deck. Then we can explain each type of card we encounter. If you wish, you can try your hand at correlating each element in the NEC deck to elements in the EZNEC antenna description file before reading beyond them.

EZNEC Antenna Description File

2el Yagi 12M

Frequency = 24.95 MHz.

Wire Loss: Aluminum - Resistivity = 4E-08 ohm-m, Rel. Perm. = 1

WIRES

Wire Conn.-	End 1 (x,y,z : ft)	Conn.-	End 2 (x,y,z : ft)	Dia(in)	Segs
1	-9.100, 0.000, 40.000	9.100, 0.000, 40.000	1.00E+00	11	
2	-8.800, -4.800, 40.000	8.800, -4.800, 40.000	1.00E+00	11	
3	-0.200, 0.000, 1.000	0.200, 0.000, 1.000	# 14	1	

SOURCES

Source	Wire Seg.	Wire #/Pct Actual	From End 1 (Specified)	Ampl.(V, A)	Phase(Deg.)	Type
1	1	3 / 50.00	(3 / 50.00)	1.000	0.000	V

LOADS

Load	Wire Seg.	Wire #/Pct Actual	From End 1 (Specified)	R (Ohms)	X(Ohms)
1	6	2 / 50.00	(2 / 50.00)	1.000	100.000

TRANSMISSION LINES

Line	Wire #/% Actual	From End 1 (Specified)	Wire #/% Actual	From End 1 (Specified)	Length	Z0 Ohms	Vel Fact	Rev/ Norm
1	1/50.0	(1/50.0)	3/50.0	(3/50.0)	Actual dist	50.0	0.66	N

Ground type is Real, high-accuracy analysis

Conductivity = .005 S/m Diel. Const. = 13

MEDIA

Medium	Conductivity(S/m)	Dielectric Const.	Ht(ft)	R Coord(ft)
1	5.000E-03	13.00	0 (def)	0 (def)

.NEC Input File

CM 2el Yagi 12M

CE

GW 1 11 -9.1 0 40 9.1 0 40 .04165

GW 2 11 -8.8 -4.8 40 8.8 -4.8 40 .04165

GW 3 1 -.2 0 1 .2 0 1 2.6706E-03

GS 0 0 .3048


```

GE 1
GN 2 0 0 0 13 .005 0 0 0 0
EX 0 3 1 0 1 0
LD 4 2 6 6 1 100 0
LD 5 1 1 11 2.4938E7
LD 5 2 1 11 2.4938E7
LD 5 3 1 1 2.4938E7
TL 1 6 3 1 50 18.01 0 0 0 0
FR 0 1 0 0 24.95 0
RP 0 1 361 1000 76 0 1 1
EN

```

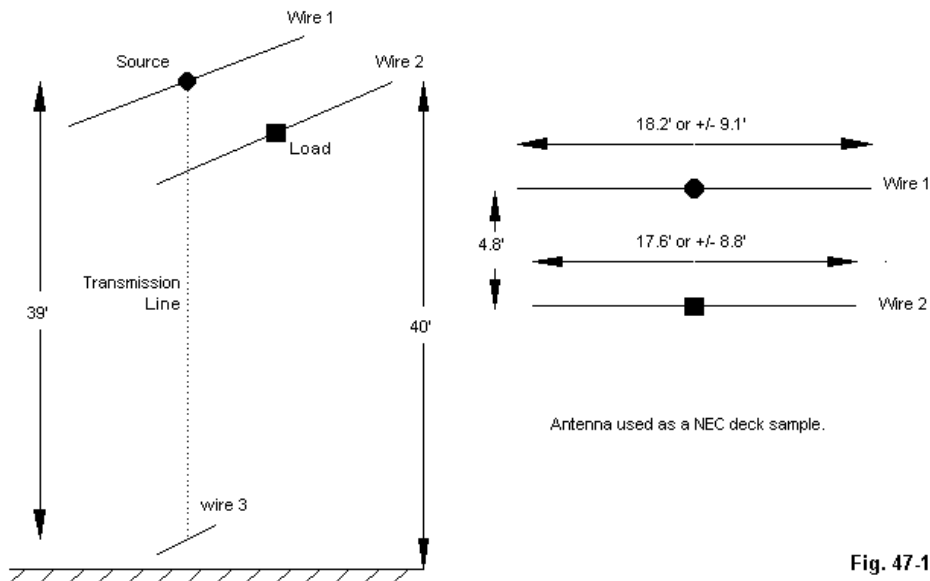
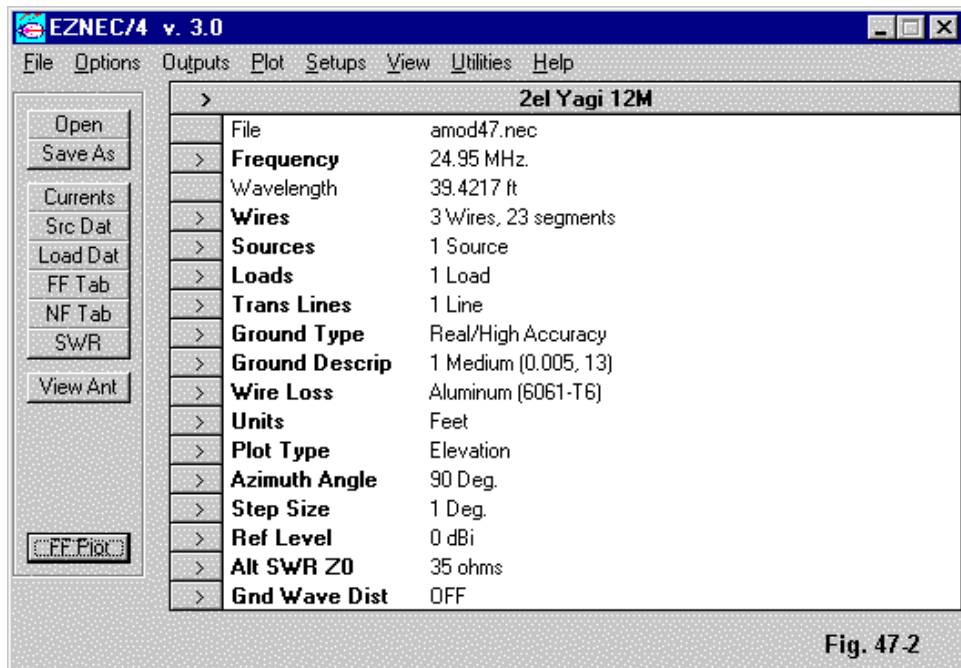
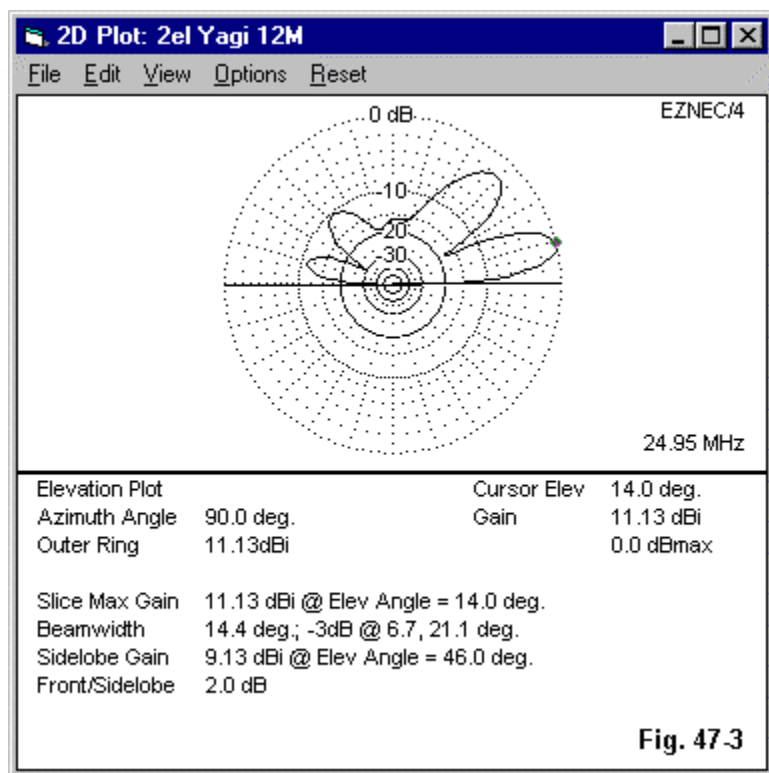


Fig. 47-1

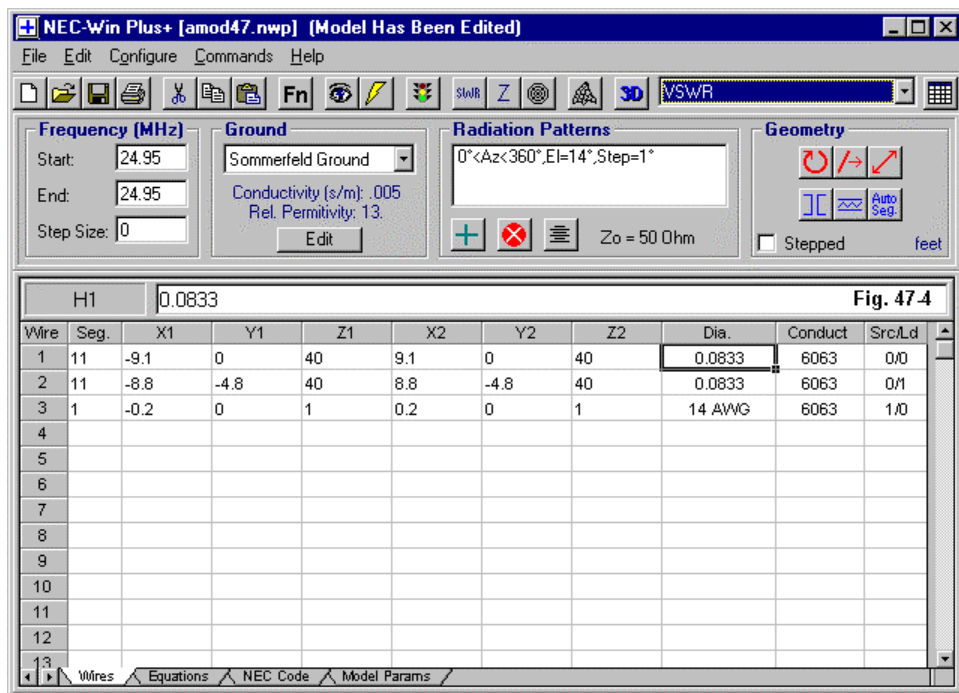
The antenna described by these two files is shown in **Fig. 47-1**. It is a simple 2-element Yagi of relatively modest performance.

The main screen of EZNEC 3.0 shows us the basic modeling data in the form illustrated in **Fig. 47-2**. Most of the detail resides in sub-screens that the user accesses by mouse-clicking on the entry line in the main screen. The results appear in **Fig. 47-3**, which I have shown as an elevation plot, even though the model specifies an azimuth plot.





NEC-Win Plus uses a different type of main screen, with considerable, but far from total, data entry up front. Frequency, wires, element diameter, and material all may be done from the lead page, although the specifics of the pattern request, ground, source, load, and transmission line require sub-screens. **Fig. 47-4** illustrates the situation. A full readout of the .NEC file, like the one shown below the EZNEC model description file, is available from the “NEC Code” tab of the spreadsheet.



Whatever the program, the performance results are the same: Gain: 11.1 dBi; 180-degree front-to-back ratio: 11.1 dB; feedpoint impedance: $42 + j5$ ohms. The general azimuth pattern at the take-off angle of 14 degrees appears in **Fig. 47-5**. NEC-Win Plus has a data ("Analysis") screen attached to its polar plot, but it has been omitted here.

Azimuth Pattern: Elevation Angle 14 Degrees

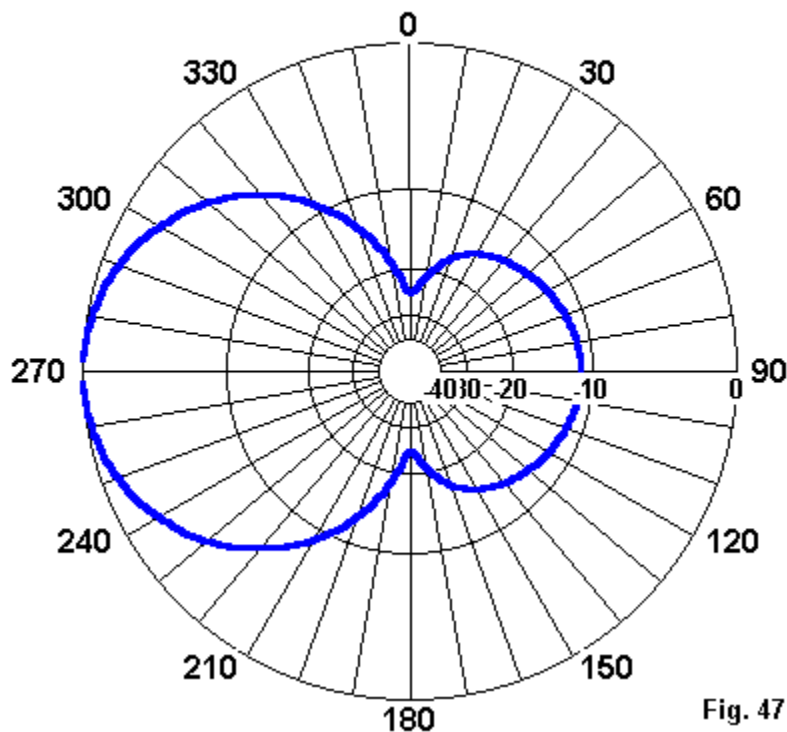


Fig. 47-5

I have purposely modified a simple antenna to include an inductive load in the reflector, thus making it physically shorter than the driven element. I have also run a 50-ohm transmission line straight down to within 1' of the ground and created a source wire there. If we had only the simple 2-element Yagi with which to work, our NEC deck would be pretty skimpy.

Let's look at each card in the deck and read out the information, cross checking it against the EZNEC file. In most cases, I have spread the data units out and labeled them beneath.

1. CM 2el Yagi 12M

This is a comment card for storing information about the file in ASCII text. It does not enter into the calculations. You may have any number of comment cards, although some implementations limit them. In EZNEC, you may have only one CM card, called the "title." (However, EZNEC 3.0 permits the user to generate a text file to accompany the model with any number of ASCII text comments added. This replaces the CM cards of a standard NEC file.)

2. CE

This card is the "comment end" card, signaling that data for calculation follows.

3.	GW	1	11	-9.1	0	40	9.1	0	40	.04165
	GW	2	11	-8.8	-4.8	40	8.8	-4.8	40	.04165
	GW	3	1	-.2	0	1	.2	0	1	2.6706E-03
	Type	Tag	Segs	E1 X	E1 Y	E1 Z	E2 X	E2 Y	E2 Z	Radius

Type GW cards describe the antenna geometry. Each antenna wire, or "Tag," has a separate numbered card or line (1, 2, and 3). The Segs (segmentation) entry tells how many segments the wire is divided into (11 each for Tags 1 and 2, 1 segment for Tag 3). Then come the Cartesian coordinates for End 1 and End 2 of each straight wire. Here, as in the EZNEC file, they are given in feet. Finally, the wire size is given as a radius. (It is 1/2 the diameter given in the EZNEC file. However, the EZNEC file lists the diameter in inches. The NEC deck must use the same units throughout the GW cards, so a 1" diameter becomes a 0.04165' radius. See also the NEC-Win Plus entry for diameter—also in feet and hence 0.0833. The wire size figure for Tag 3 is the radius of #14 wire, in feet.)

4.	GS	0	0	.3048
	Type			Multiplier

Although most implementations of NEC, such as NEC-Win and EZNEC, give the user a choice of common units of measure for setting up the antenna geometry,

NEC itself calculates only in meters. In the last of its 4 columns, the “geometry scaling” card gives the multiplier needed to convert to meters.

```
5.  GE      1
    Type  End
```

The “geometry end” type card signals the end of the wire set-up and prepares the way for other data that enter into the calculations.

```
6.  GN      2      0      0      0      13      .005      0      0      0      0
    Type  G-type          Die-C.  Cond.
```

The ground parameter card specifies the type of ground calculation system and the necessary parameters to make the calculation. Here, we show a single medium, although a second medium can be set.

There are 4 types of ground systems used with NEC: -1 = free space; 0 = a finite ground with a reflection coefficient approximation (the “fast” ground in EZNEC); 1 = a perfectly conducting ground; and 2 (used here) specifies a finite ground using the Sommerfeld-Norton method of calculation for greatest accuracy. (In addition, EZNEC implements the MININEC ground calculation system for users who may find it convenient for some vertical antenna models.)

Finite ground conditions (cases 0, 1, and 2) require two numbers to implement calculations. The first is a relative dielectric constant, usually given as an integer. Second is the conductivity in Siemens/meter (mhos/meter in older terminology). Both are generally derived from tables. The values shown represent a default presumption of medium earth conditions. Both numbers are omitted for perfect ground.

As with many cards in the NEC deck, there are unlabeled “0” fields. Some of these represent fields simply left blank; others represent input positions for more specialized conditions not relevant to most common ham HF antennas. (Some may be relevant to VHF and UHF antennas.)

```
7.  EX      0      3      1      0          1      0
    Type  S-type Tag      Seg          Voltage:  Real  Imaginary
```

The “exitation” or source information card allows for many types of exitation, of which only voltage sourcing is usual in HF ham use. Hence, the source-type is “0”. The next two columns specify the placement of the source in terms of tag number and segment number in that wire. Here, the remote wire has only one segment, and the source is placed at its center. Many programs allow specification of the source at some distance from End-1 of the designated wire, and will then place the source as close to that point as segmentation permits.

For most ham uses, sources are either voltage or current. The latter is useful for scanning current levels along a wire, since a voltage source of “1” yields small fractions of an amp current, making scanning more difficult. Current sources may also be necessary for some advanced applications.

Nonetheless, both types of sources are voltage sources ultimately. The current source is generated by a voltage source set on a remote wire and transformed into a current source by a phase-shifting network. The NEC deck for a NEC-Win Plus model will show the wire and line, while EZNEC stores this information internally.

Voltages are given in terms of X and Y (“real” and “imaginary”) coordinates derived from inputs that can be given as a voltage and its phase angle. User current magnitude and phase angle inputs are converted to appropriate voltage values at the remote source wire.

In general, when converting among programs (for example, between EZNEC Pro and NEC-Win Pro), it is best to use a voltage source to avoid the possibility that one program cannot read the other’s remote wire current source technique. Changing back to a current source can be done after file conversion is complete.

8.	LD	4	2	6	6	1	100	0
	Type	L-type	Tag	Start Seg	End Seg	R	L or X	C

There are two types of loads to consider: concentrated element-loading quantities and distributed element material loads. This card illustrates an inductive load added to the center of the reflector. Load types 0 through 3 represent categories of R-L-C combinations that can make up a load. This card shows a type 4 load, which is specified in terms of a series resistance and reactance in Ohms.

The “tag” and “segment” items locate the load at the midpoint of wire 2. Since there are start and end segment numbers, some loads may be distributed for more than a single section, but most ham antennas employ concentrated loading located within a single segment.

The final two values (1 and 100) specify the resistance and reactance of the load in ohms. Capacitive reactance, of course, would be entered as a negative number.

9.	LD	5	1	1	11	2.4938E7
	LD	5	2	1	11	2.4938E7
	LD	5	3	1	1	2.4938E7
	Type	L-type	Tag	Start	Seg End	Seg Conductivity

Material losses are type-5 loads. As with other loads, the wire (tag) must be identified, along with the first and last segments to which the load applies. Note that these loads apply in addition to any lumped-constant loading of types 0 through 4.

To avoid confusion by newer modelers, EZNEC only refers to lumped constants as loads, preferring instead to call material loads “wire losses.” EZNEC also expresses these losses as a function of resistivity and relative permittivity. However, the value of resistivity in this case, 4.0E-08 ohms, is simply the reciprocal of the NEC deck conductivity value of 2.4938E7 mhos or Siemens. Additionally, EZNEC restricts antennas to one type of material per model, although the NEC deck permits a specification of a different conductivity value for each wire. Note the NEC-Win Plus entry space for a conductivity value for each wire in the antenna model.

10.	TL	1	6	3	1	50	18.01	0	0	0	0
	Type	Start	tag/seg	End	tag/seg	Zo	Length				

Transmission lines are not physical models in NEC, but non-radiating mathematical constructs. Hence, they can have any length, regardless of the actual distance between their start and end points on wires. Special techniques are used for shorted and open stubs, but the example here runs a common coax line from the antenna proper to a short segment used a. to terminate the transmission line and b. to serve as the overall source point for the antenna system.

By now, the start and end wire and segment numbers are obvious. As in the EZNEC PD file, the next two columns specify the characteristic impedance of the line and its length. In EZNEC, this can be done in several ways, all of which translate into a final characteristic impedance and definite length in meters. In the PD file, the length was given as the actual distance between wires, 39', modified by the velocity factor of the line, .66. This results in an electrical length of 59.1' or 18.01 meters. In NEC-Win Plus and Pro, one must enter the total electrical length and hence pre-calculate the value from the physical length and the velocity factor of the line used.

11.	FR	0	1	0	0	24.95	0
	Type	Stepping	No. of FQs			Start FQ	Increment

Antennas are modeled at one or more frequencies. If a single frequency is used, as in this example, the information needed is limited. "Frequency sweeping" requires more information.

Stepping can be non-linear (stepping = 1), but normal ham frequency sweeps are linear, changing frequency by the same amount each time. For sweeps, the user specifies the number of frequency steps, the start frequency, and the increment by which to step. For this single frequency model, the number of frequency steps is 1, and the increment is 0, while the modeled frequency is 24.95 MHz.

12.	RP	0	1	361	1000	76	0	1	1
	Type	Mode	No. Theta	No. Phi	Special	Theta	Phi	Th Inc	Ph Inc

The report card specifies what output data is desired from the calculations. Mode "0" is the normal mode for far-field data.

Horizontal angular changes are measured as "phi" degrees. Elevation angular changes are measured as "theta" degrees. Although most hams are used to counting elevation from the ground up, NEC counts theta angles from the zenith down.

This example specifies a report for one theta (elevation) angle, but a full circle of azimuth (phi) angles. Skipping the "Special" column for a moment, the theta angle is 76 (or 90 - 76 for a 14 elevation angle). The figure is a start figure, although only one theta angle has been specified. The azimuth or phi start angle is 0, but will pass

through 361 (to ensure a complete circle with a common value at each end of the progression). Both theta and phi are specified for increments of 1 for good resolution.

The “Special” column contains 4 values that direct the calculations to produce certain types of outputs. 1000 is normally used for vertical, horizontal, and total non-normalized power gains with no averaging. Other outputs are available, and the user is usually interrogated in plain language for the desired output data and form by each program.

Users of NEC will sometimes be surprised to find that a symmetrical antenna, such as a Yagi, produces a main lobe identified by as much as 2 to 3 less than the expected bearing. Implementations of NEC may identify either the first instance of the maximum power gain as the main lobe or may sample the subsequent headings and center the identified main lobe heading among equal maximum readings. If a program uses the first of these options, then increasing the phi increment will often return the main lobe to its expected position.

13. EN

EN signals the end of the .NEC file. The line is not necessary with some output requests, but never hurts.

Hopefully, this brief trip through a short NEC deck will orient you to how the input files are constructed for use with NEC. Remember that the card explanations have not covered all the ways in which one may place data on a card of a given type. Only the most common kinds of data inputs for typical ham antenna installations have been illustrated.

The low-end implementations of NEC-2 omit many of the features and functions available with core in order to create the user-friendly interface that covers the features most needed by the average user. However, high-end programs designed with less “friendliness” and more calculating potential (such as NEC-Win Pro and—for NEC-4—GNEC) tend to make the entire deck available to the user. As a reference, here is a list of NEC-2 cards, some of which we have reviewed and some of which will seem odd. In addition, cards like the RP request have far more options than we have covered, including not only far field patterns, but ground wave pat-

terns as well. EX allows not only for definite voltage sources, but as well for plane-wave excitation for receiving analysis.

Structure Geometry Input Cards

CM, CE	Comment Cards
GA	Wire Arc Specification
GE	End Geometry Input
GF	Read Num. Greens Function
GH	Helix-Spiral Specification
GM	Coordinate Transformation
GR	Generate Cylindrical Structure
GS	Scale Structure Dimensions
GW	Wire Specification
GX	Reflection in Coordinate Planes
SP	Surface Patch

Program Control Cards

CP	Maximum Coupling Calculation
EK	Extended Thin-Wire Kernel
EN	End of Run
EX	Excitation
FR	Frequency
GN, GD	Ground Parameters
KH	Interaction Approximation Range
LD	Loading
NE, NH	Near Fields
NT	Networks
NX	Next Structure
PQ	Print Control for Charge on Wires
PT	Print Control for Current on Wires
RP	Radiation Pattern
TL	Transmission Lines
WG	Write Num. Greens Function File
XQ	Execute

Some programs, like EZNEC, do not generate a NEC deck, but instead communicate with the NEC-2 calculating engine via a number of binary files. (A NEC deck output is available in EZNEC Pro with the NEC-4 calculating engine.) Some programs, like NEC-Win Plus, use alternative formatting methods—a spreadsheet file in this case, but also make available the option of saving the model as a .NEC file. Others, like NEC-Win Pro or GNEC, make the deck an integral part of the

modeling process. Getting used to the NEC deck can increase your ability to glean more from whatever program you choose as your basic modeling vehicle. Familiarity may also aid you in interpreting articles that present antenna modeling data in .NEC input file format. Patches, Green's functions, networks, and wire grids are beyond the scope of this introduction, but may be found in NOSC Technical Document 116, Volume 2, *Numerical Electromagnetics Code (NEC)—Method of Moments, Part III: User's Guide* (1981), which is the source of most of this data.

* * * * *

Model included: 47-1. (All model dimensions in feet.)



48. Radiation Plots: Polar or Rectangular; Log or Linear

The user of NEC or MININEC often has choices in how to graphically portray data. The choices (not all of which may be available within a particular program) generally consist of the following.

1. Polar Plot: Logarithmic Scale
2. Polar Plot: Linear Scale
3. Rectangular Plot: Linear Scale
4. Rectangular Plot: Logarithmic Scale

I have heard numerous arguments for and against each type of presentation. I shall forego all of them. Instead, let's pick an antenna whose plot has some relatively fine detail (in terms of secondary lobes of interest). Then, let's look at the free-space plots under each of the options listed above.

Fig. 48-1 presents the .NEC file of a 12-element Yagi with a test frequency of 148 MHz. The linear elements extend from -X to +X, with the boom extending from a value of zero on the Y- axis to positive Y-values. The dimensions are in meters. The boom length is 6.045 m long (about 19.8'). The 4.76-mm diameter (0.00238-m radius) elements are 0.1875" (3/16") rod. The material is standard aluminum (read from the LD lines), and the elements are presumed to be well insulated and isolated from any conductive materials in the boom that supports them. The environment is free space. As is usual for Yagis, the source or feedpoint is at the center of the second element from the rear. **Fig. 48-2** presents an outline sketch of the antenna. See model 48-1.

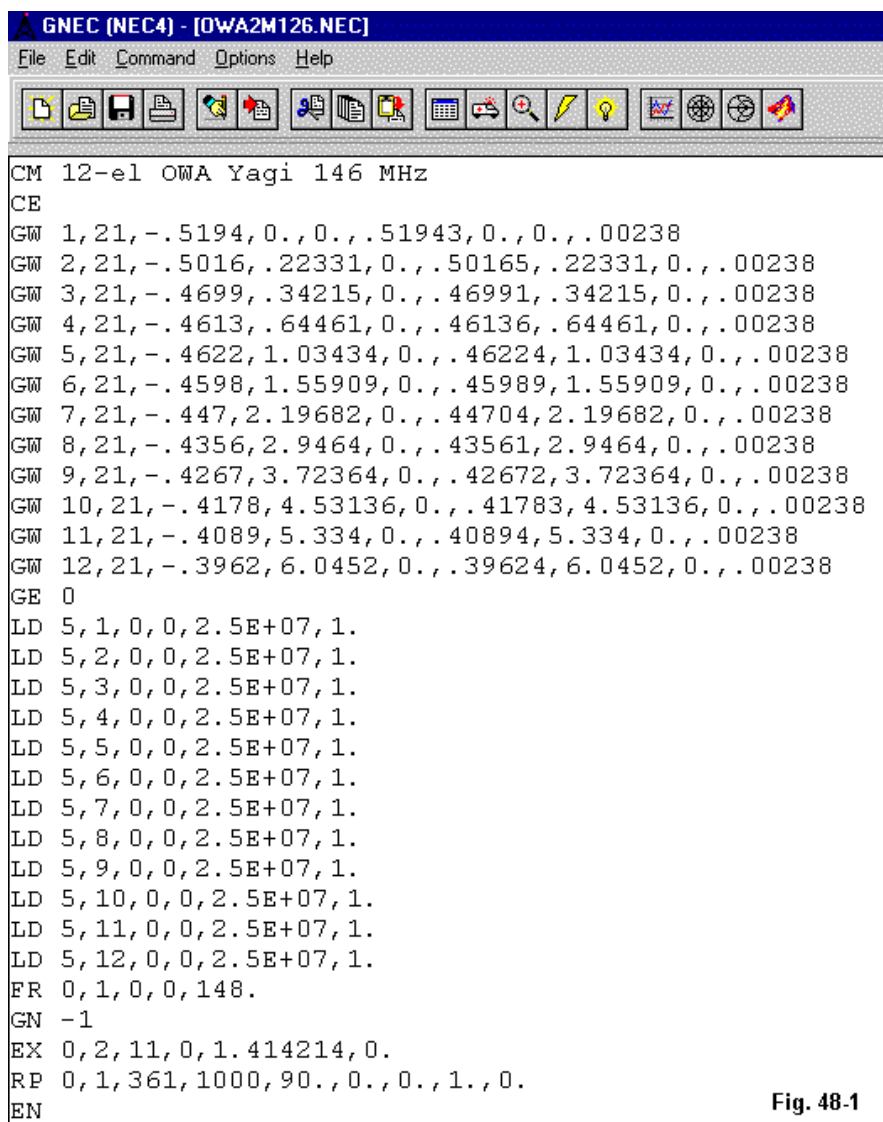


Fig. 48-1

Outline Sketch of the 12-Element Yagi Subject Antenna

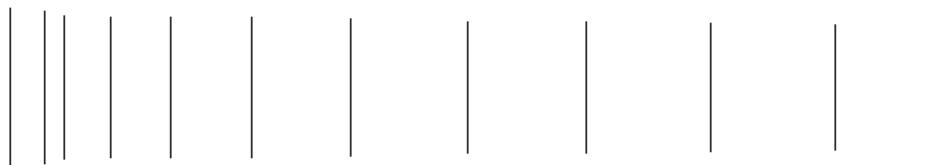


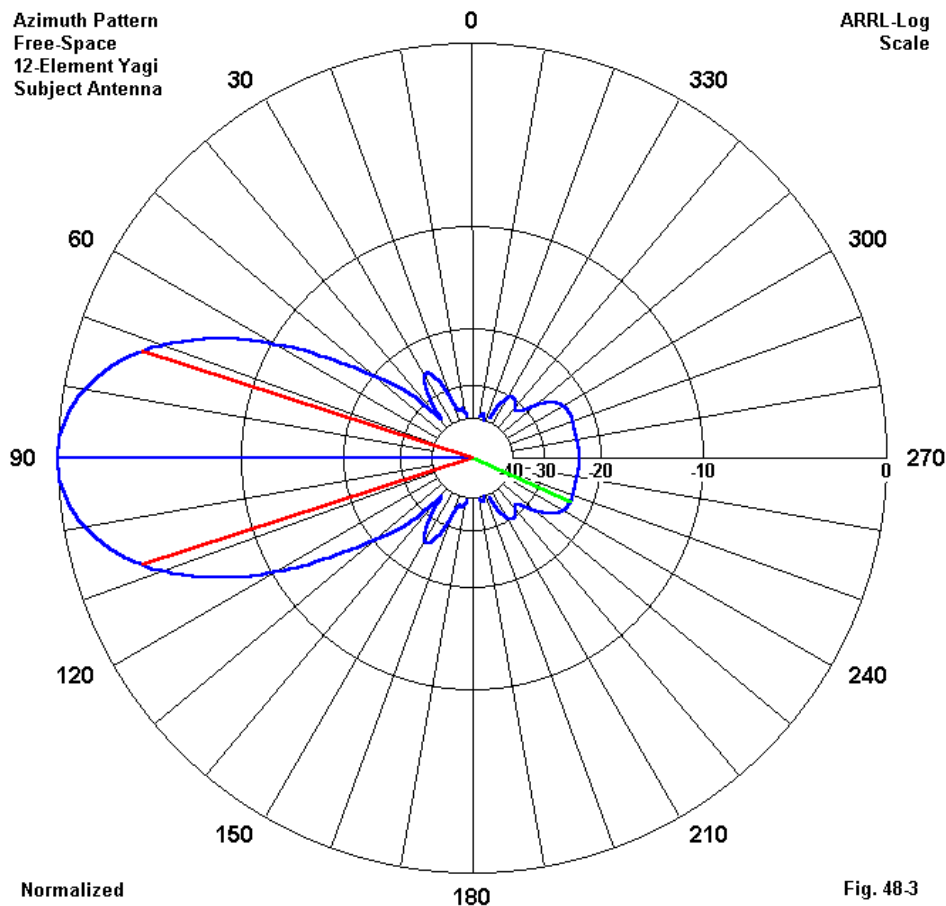
Fig. 48-2

For the record, when modeled in NEC-4, the array has a free-space gain of 14.27 dBi, a worst-case front-to-back ratio of 23.14 dB, a source impedance of $43.9 - j 4.0$ Ohms, and a 50-Ohm SWR of 1.17:1. The -3dB beamwidth is about 36 degrees. However, these figures do not tell us anything of the pattern shape: whether it has very significant secondary forward or rearward lobes or whether the pattern is clean and well controlled. To determine these matters, we can examine the tabular data provided by NEC or we can examine graphical plots of the data. The NEC core yields only the tables. All graphics are added by the programmer.

In the following notes, all patterns will be products GNEC by Nittany Scientific. My program choice for this exercise was simple: GNEC has both polar and rectangular plot capabilities. For linear plots, the user has the option of selecting maximum and minimum values for the plotting space.

The Logarithmic Polar Plot

The logarithmic polar plot shown in **Fig. 48-3** was a creation of the American Radio Relay League somewhere in the distant past. This type of logarithmic plot is perhaps the most familiar of the common polar plotting styles used. In some software, plotting beyond the -40 dB point is shown, although in this GNEC plot, the line is cut off at this point. In principle, graphing can go on down to an infinitesimal value.



Every polar plot scheme is subject to a set of equations that determines the placement of the data points that make up the curve. The angle at which they occur

is fixed by the data itself, but the distance from the plot center is a function of the equations used. The equations may be simple—as they are in linear plots—or complex, as in the present log plot. Note that plotting radiation strength in dB on a log scale results in a form—but not the only possible form—of a double log plot.

First, the plot in **Fig. 48-3** is normalized, which is to say that its outer ring is given a value of 1.0 for plot point calculation purposes. The maximum gain of the array is set equal to this value. Hence, the pattern just touches the outer ring. In normalized plots of radiation patterns recorded in dB, the outer ring is usually set to zero dB with inner rings set of -X dB each, where X is another matter of choice—usually of the software writer. Non-normalized plots are possible and often used, although the normalized plot permits the largest pattern that will fit within the outer ring of the graphic.

Second, we need to determine the point positions for any heading in terms of their distance from the plot center to the outer ring. Since the plot shows the headings of the -3 dB points for the pattern, we can illustrate the process used to generate the plot in **Fig. 48-3** with good simplicity. By using the -3 dB points, we have already made the first step. Let MG = the maximum gain of the pattern and GH = the gain at some new heading—in this case either 72 or 108 degrees.

$$EX = MG - GH \quad (1)$$

EX is simply the difference between the maximum gain and the gain at the new heading. For our example, the gain at 72 and 108 degrees is close to 11.27 dBi.

The position of the dots for 72 and 108 degrees are determined by the next equation, in which VP = the value point as a decimal value relative to 1 and hence the distance away from the center of the plot toward the outer ring.

$$VP = 0.89 \sqrt{\frac{EX}{2}} \quad (2)$$

The -3 dB points will be about 0.84 of the way from the center toward the outer circle. In a similar manner, we calculate that the worst case front-to-back ratio point,

23.14 dB, will be at about 0.26 of the way from the center to the outer ring. Relative to the outer ring distance on the plot in **Fig. 48-3**, you can measure these distances with a ruler. The particular equation shown applies only to values of radiation strength given in terms of dB and requires modification for values given in terms of measured or calculated signal voltage.

Although the plots on most antenna modeling software mark the reference rings in 10 dB increments, there is nothing fixed about this practice. In fact, ARRL publications use 3 dB increments down through -12 dB with further -18 and -24 dB markers. Moreover, there is nothing fixed (except by tradition) about the equation itself. In non-normalized plots, the user may have a choice of selecting the value of the outer ring. In such cases, the adjustment of the pattern to the selection is simple arithmetic. The gain at every heading is calculated against the value set for the outer ring instead of against the maximum gain of the pattern.

The logarithmic scale is perhaps the most familiar of the many options for plotting a radiation pattern. It tends to enhance the forward lobe and to emphasize the beamwidth, especially of narrow-beamwidth arrays such as the subject 12-element Yagi. At the same time, it also tends to reduce the resolution of fine detail of weaker portions of the pattern.

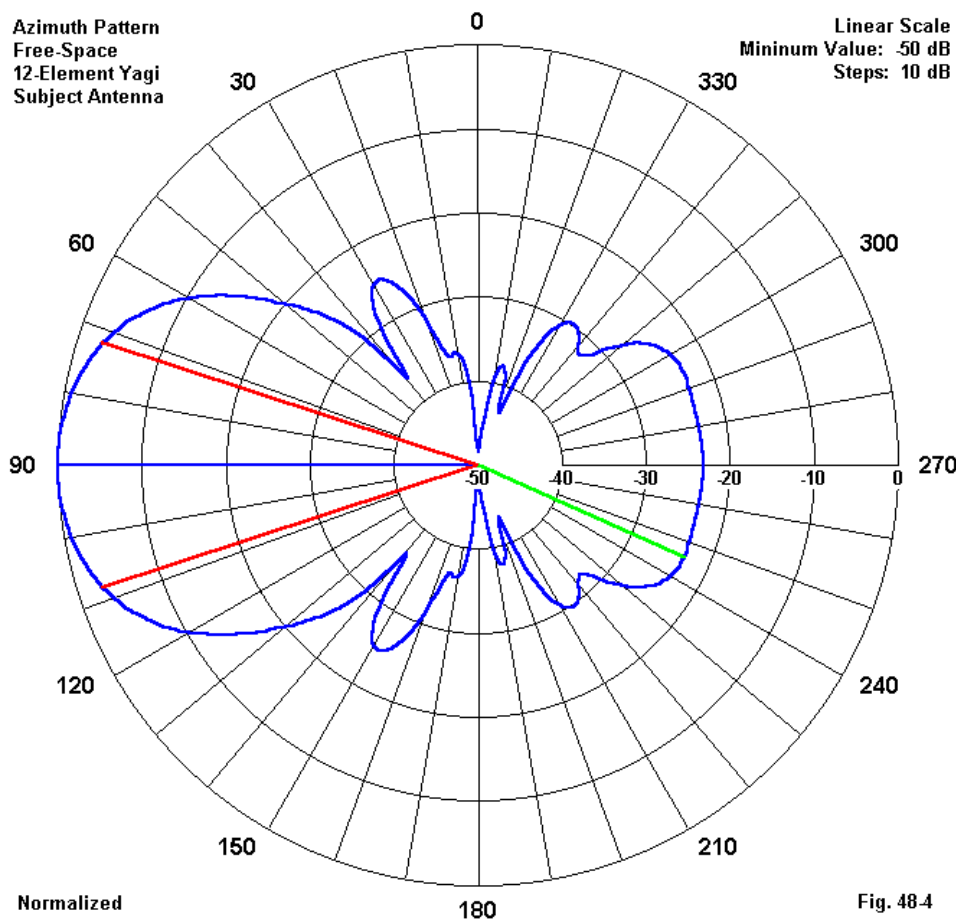
The Linear Polar Plot

An alternative to the log polar plot is the linear polar plot, shown for our subject antenna in **Fig. 48-4**. Note that in this context, “linear” refers to a linear counting of decibels, which is already a logarithmic function relative to power or to voltage and/or current.

Because the plot steps from the center of the graphic toward the outer ring are linear, the -10-dB ring in **Fig. 48-4** is much closer to the outer ring than with the log plot in **Fig. 48-3**. The effect is to broaden the visual pattern and to enhance the detail of the plot with respect to weaker portions of the pattern. Compare the rearward portion of the plots in **Fig. 48-3** and **Fig. 48-4**, as well as the secondary lobes. Remember that both plots present the same data. The difference lies in the manner of presentation.

Azimuth Pattern
Free-Space
12-Element Yagi
Subject Antenna

Linear Scale
Minimum Value: -50 dB
Steps: 10 dB



The plot in **Fig. 48-4** uses a scale that runs from 0 dB for the outer ring to -50 dB at the center. Unlike the log plot, a linear plot must specify both the outer ring and the center values. For a normalized pattern, the outer ring equals the maximum gain of the antenna under study. The minimum or plot-center value is a user choice. In this case, -50 dB provided a good visualization of the secondary lobe structure—and that fact determined the choice. As a point of comparison with the log plot, the -3 dB points on the 50-dB scale are .94 of the way toward the outer ring, while the worst-case front-to-back ratio point is .54 of the way from the center.

Azimuth Pattern
Free-Space
12-Element Yagi
Subject Antenna

Linear Scale
Minimum Value: -185 dB
Steps: 35 dB

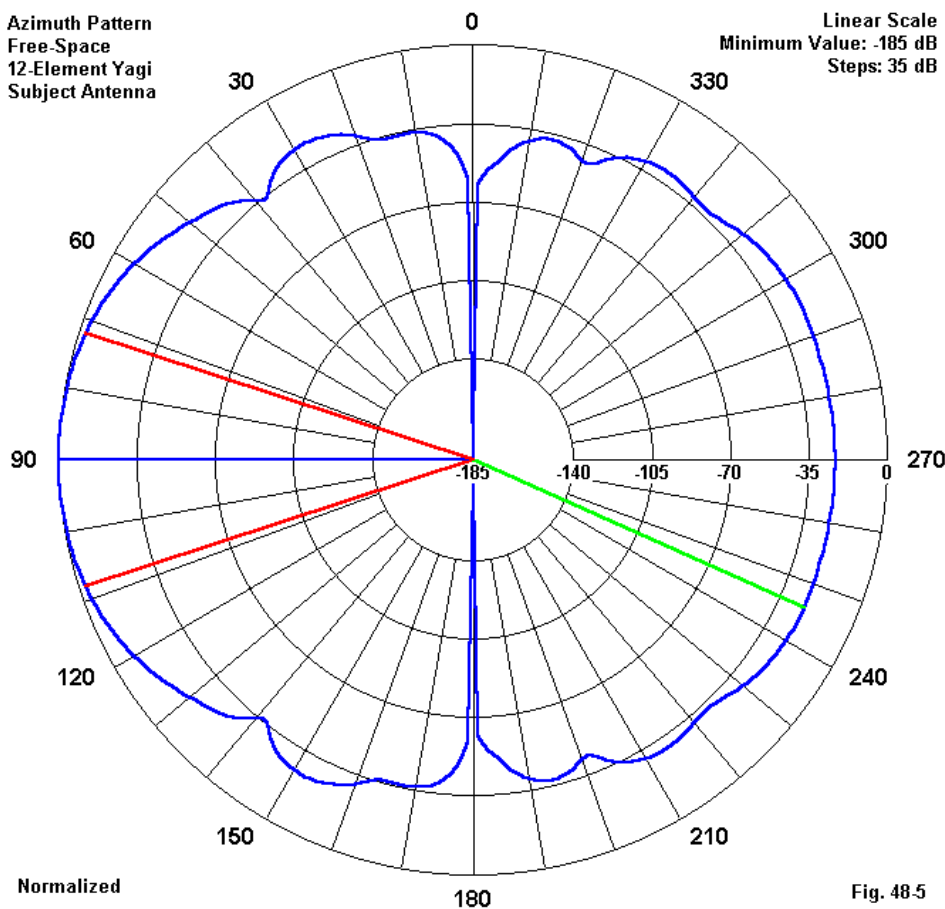


Fig. 48.5

Linear polar plots are not automatically superior to log plots. Indeed, since the center point value is user selected (or in some cases, software selected without user choice), the utility of a linear polar plot depends upon the center value selected. It is possible to create virtually useless linear polar plots.

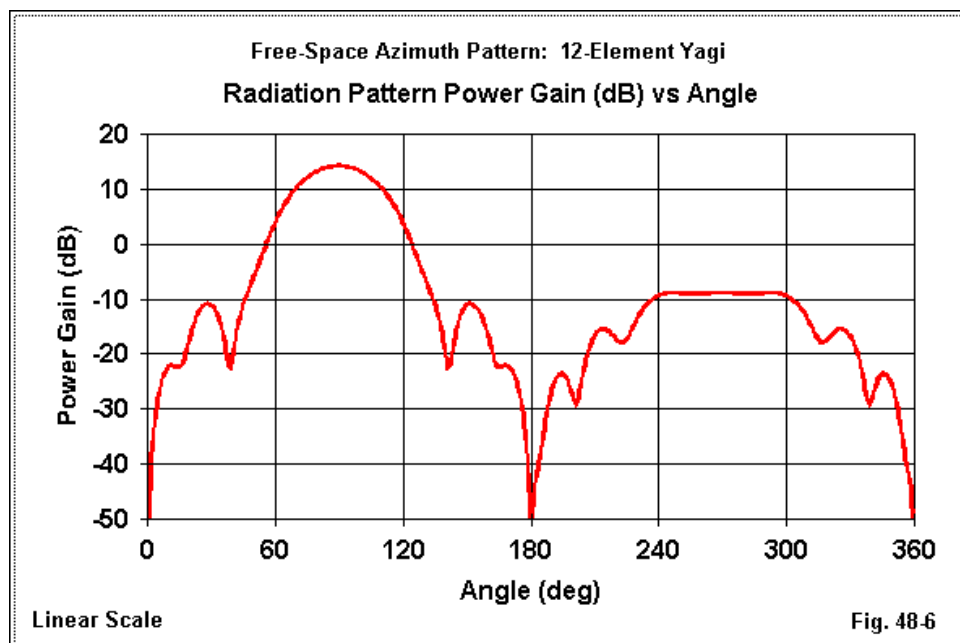
Fig. 48-5 shows a worthless linear polar plot of the subject antenna. It uses a center value of -185 dB and 35-dB steps in the rings. Since the free-space pattern of a horizontally polarized directional antenna with linear elements very often results in very high values of front-to-side ratio, an automated program can make unwise choices for the user. In **Fig. 48-5**, the selected values spread the pattern to such extremes that differentiation of any detail is almost impossible. In short, the linear polar plot is not intrinsically better or worse than a log plot in showing any particular features of a pattern's shape or features.

Selecting a linear polar plot value set, then, is the most crucial step in generating a plot that does useful work in demonstrating salient points of the radiation pattern. Since the center point is user or software selected, its value must always be made accessible to the plot reader, either by a legend or by a plot-line label. Otherwise, the plot may become seriously misleading.

In non-normalized plots, the user once more selects the gain value assigned to the outer ring. Then the gain of the pattern at every heading becomes a percentage of the distance from the center to the gain value set into the outer ring. Since computer graphics programs tend to separate the setting of the polar plot space and rings from the assignment of data points within the rings, the value of the outer ring will usually be recorded in a separate alphanumeric entry. The plot rings usually retain the same labels, regardless of the outer ring value.

The Linear Rectangular Plot

Fig. 48-6 shows a rectangular plot of the radiation pattern data using a linear scale for the Y-axis. Many analysts prefer the rectangular plot because it allows a comparison of signal strength (whatever the units happen to be) at every heading with only a glance at the reference lines across the plot from the Y-axis. The plot in **Fig. 48-6** has not been normalized. Indeed, normalization is more the exception than the rule with rectangular plots, because the practice often creates odd increments between values on the Y-axis. Odd numbering of the Y-axis markers tends to defeat the easy determination of gain values for every heading.



The generation of a linear rectangular graph requires close attention by the user, especially to the Y-axis minimum and maximum value. Indeed, in some cases, the user may have to experiment with the selection of values to reveal all of the relevant data in sufficient detail. The selected value captures the low-level variations in strength near the front-to-side bearings without going to extremes. There are no further lobes to be revealed by carrying the 0, 180, and 260 degree values below the -50 dB point.

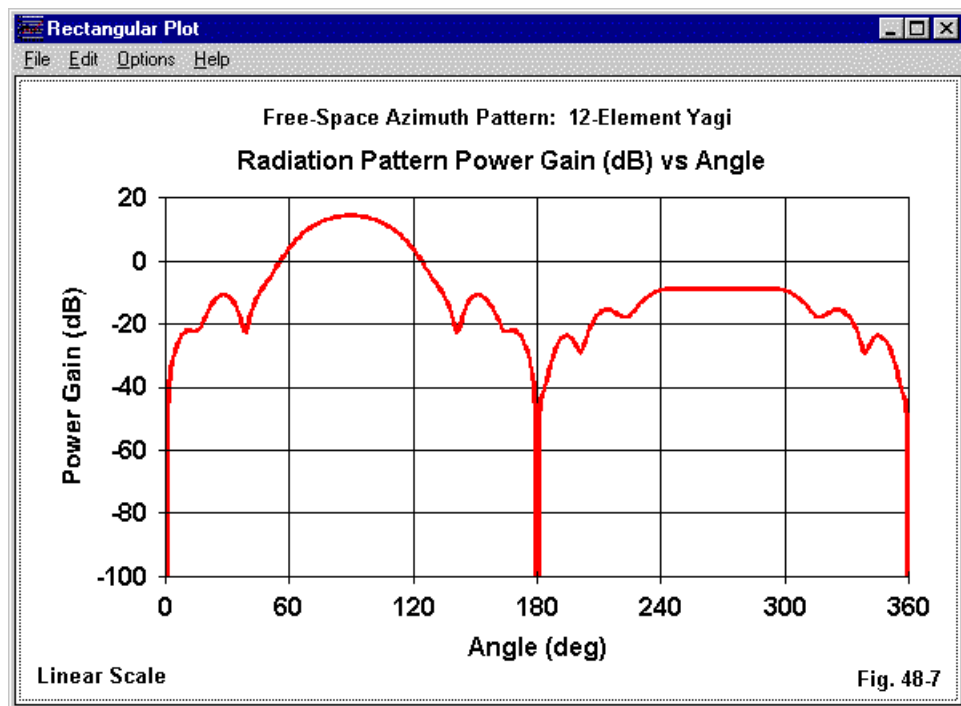


Fig. 48-7

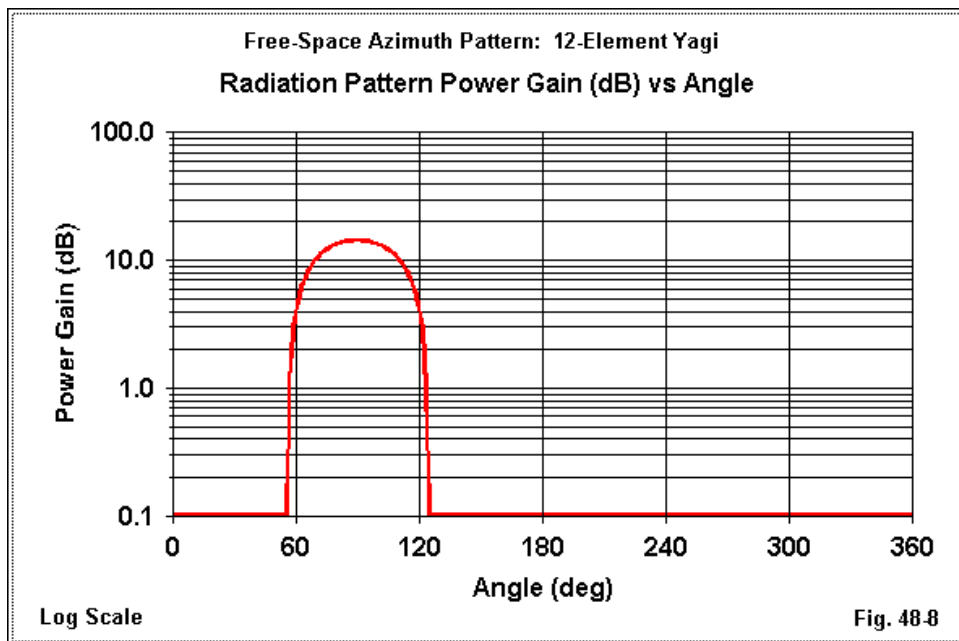
In the graph shown in **Fig. 48-6**, the minimum value could have been carried to -100 dB, as it was in **Fig. 48-7**. However, the detail of the pattern for values between -30 and +20 dB would have been obscured by unneeded “scrunching.” For example, in **Fig. 48-7**, it is not easy to tell if the smallest side lobes of the forward pattern (between 0 and 180 degrees) show a peak or are simply level. The determination is easy to make in **Fig. 48-6**.

The rectangular graph also provides the rationale for setting up the original model with the linear elements set on the +/-X axis. The result is to place the main lobe of the array on the Y-axis in the wire set-up screen, that is, at a 90-degree heading. Although the other convention of laying elements on the +/-Y-axis is often convenient for polar plots, the set-up used here presents the forward and rearward pattern

details as complete lobe structures. In **Fig. 48-6**, one might have added the labels “forward” and “rear” to the left and right portions of the graph, respectively.

In short, creating a rectangular plot requires forethought that goes all the way back to the initial model set-up. Of course, this caution applies mostly to cases where one uses the graphic capabilities built into a given piece of software. If one exports the radiation pattern data to a spreadsheet, one can then manipulate either the plotting facility or the angular data. Thus, the resulting rectangular plot can have the appearance of **Fig. 48-6** (or any other that may fit a given antenna pattern), whatever the orientation of the initial model.

The Logarithmic Rectangular Plot



The Y-axis of a rectangular plot can be given a log scale. But the results may become “the plot that failed,” as in **Fig. 48-8**. If you compare **Fig. 48-8** with **Fig. 48-6**, you will discover that only the portion of the graph in which gain values exceed 0 dB appear on the new plot. That is a problem with logarithms—they work with positive numbers. Such a problem would not exist if we were plotting signal strength in volts.

To achieve a proper logarithmic scale for the Y-axis of a rectangular plot would require exportation of the radiation pattern data, followed by a conversion of the entire lot of it into positive numbers. Then one might use that converted data with a log Y-axis, although the labels might be reconverted to values corresponding to those on the original data table.

These last notes have made a small case for exporting data from the NEC output file to programs within which the data may be manipulated for the most effective presentation and study. Even the most competent antenna modeling software will have limitations and cannot anticipate all possible user needs or interesting results that call for special presentation. If it could anticipate all needs, we might simply set up a data bank of results and forget the modeling process itself.

In the end, the modeler should be prepared to go beyond the modeling software itself to develop effective graphics—whether for radiation patterns or any other facet of the data generated by the core. The forethought required for setting up a model in anticipation of graphing the results carries over into appropriate levels of afterthoughts to apply the best graphing techniques for data that will not fit prescribed patterns.

In the end, there is more to antenna modeling than can be written into the modeling software itself.

However, we began our work as a short dash through the various radiation pattern-plotting options that we most use. Throughout, we have avoided arguments for or against any one of the many possibilities, since most of those arguments presume sets of well-chosen user options for graphic minimum and maximum values. Instead, we have focused on two functions. One is the potential of each plotting scheme for presenting data in a form that is most easily read and most fruitfully

studied. The other is the responsibility of the user to select plotting scale values that will achieve the goal of easy reading and useful examination.

There is no universal best plotting method for radiation patterns. However, for any given plotting goal, one may determine the best way among available methods for achieving a set of goals.

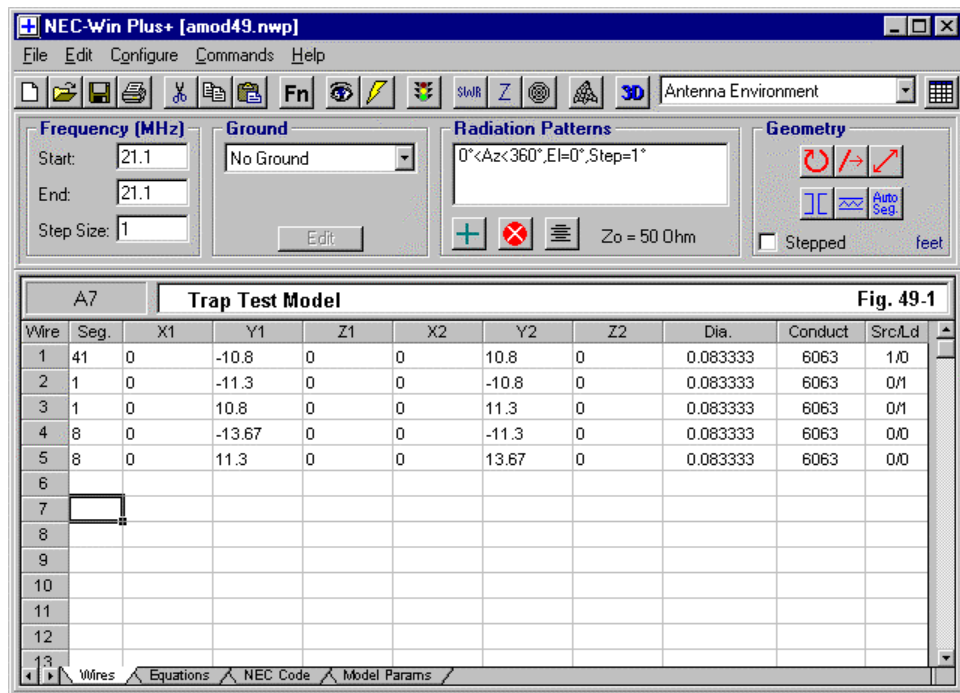
* * * * *

Model included: 48-1. (All model dimensions in meters.)

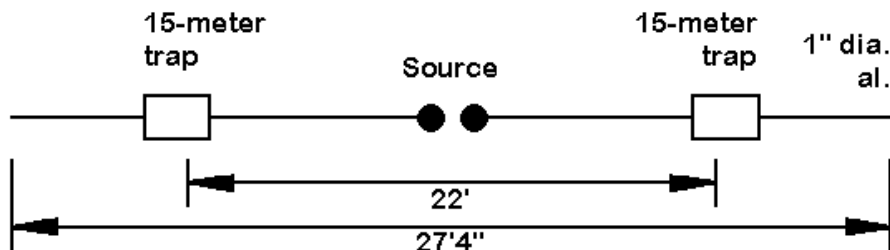


49. Traps

We have not so far had occasion to work with parallel R-L-C loads (LD1). The most notable use of such loads is to model traps, which we install to let an antenna be resonant on more than one frequency of operation. Let's go through an exercise and discover how we may convert traps into parallel R-L-C loads.



Examine the wire table for a test model, given in NEC-Win Plus form in **Fig. 49-1**. You will find a 5-wire assembly for 21.1 MHz that we shall also operate on 14.1 MHz. The wire table is non-standard. Wire 1 is the center section of the antenna—essentially the 15-meter portion. Wires 2 and 3 are the 1-segment wires on which we shall install the traps. Wires 4 and 5 are the outward extensions from the traps to the tip of the elements on 20 meters. **Fig. 49-2** shows the outline of the antenna with a set of dimensions. The overall dimension of 27' 4" corresponds to the wire table tips. However, the inner 22' dimension is the space between the traps themselves and not the space of the center section (wire 1) alone. See model 49-1.



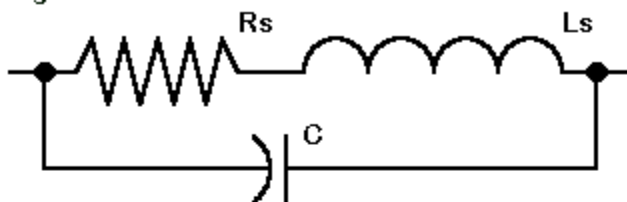
15-20-Meter Trap Dipole

Fig. 49-2

The antenna material is 1" diameter aluminum, and the environment is free space. Note that the trap wires are the same diameter as the remaining wires. Therefore, the model will not account for any effects created by the shape of the traps. We shall construct the 15-meter traps from the mathematical loading facility.

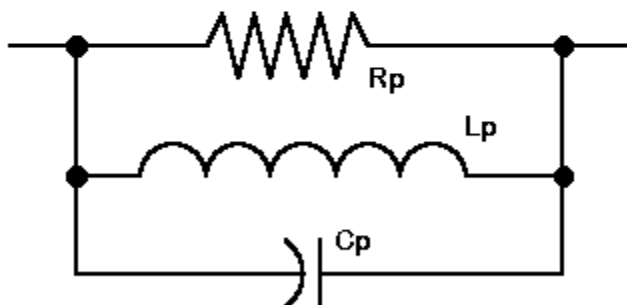
One problem with a trap is that it is not yet a parallel R-L-C circuit. As shown in **Fig. 49-3**, a trap consists of a capacitor in parallel with a series resistance-inductance leg. Before we can create a parallel R-L-C load, we must convert the trap configuration into a true parallel configuration. Moreover, we shall have to do the conversion for each frequency-band of operation.

Fig. 49-3



Equivalent circuit of a trap

Trap redrawn as a parallel R-L-C circuit



Two Representations of an Antenna Trap

In the following notes, we shall set up a procedure for calculating traps and converting them into parallel R-L-C loads. Basic to the procedure is the ability to convert inductances to inductive reactance and back, as well as capacitances to capacitive reactances and back. Therefore, as a quick reference, here are the basic equations:

$$X_L = 2 \pi f L \qquad L = \frac{X_L}{2 \pi f} \qquad (1)$$

where X is the inductive reactance, f is the frequency in hertz, and L is the inductance in henries. The same equations work if we use both MHz and μH .

$$X_C = \frac{1}{2 \pi f C} \qquad C = \frac{1}{2 \pi f X_C} \qquad (2)$$

where X is the capacitive reactance, f is the frequency in hertz, and C is the capacitance in farads.

For our small exercise in converting traps, we shall begin with an inductor only and carry you through the process. The inductor is a 3.3 μH coil with a measured Q of about 235. By standard equation, we can find the inductive reactance. However, we must know the trap frequency. Ordinarily, we design traps to be resonant at or just below the lowest frequency of operation on the upper band. If we set our trap at 21.0 MHz, the inductive reactance is $j\ 435.4$ Ohms. Since the Q is 235, the series resistance of the coil is 1.853 Ohms. We can use the capacitive reactance equation to calculate the capacitor, which will be about 17.41 pF to provide the matching reactance for the coil at 21.0 MHz.

We need to convert the series resistance and reactance values into parallel equivalents. The standard conversion equations for going from a series to a parallel combination of resistance to reactance are

$$R_P = \frac{R_S^2 + X_S^2}{R_S} \qquad X_S = \frac{R_S^2 + X_S^2}{X_S} \qquad (3)$$

where R and X are the desired parallel equivalents to R and X , the original series values of resistance and reactance. The parallel resistance for the trap at its resonant frequency is 102,325 Ohms. The parallel reactance is $j\ 435.4$ Ohms, which will return a parallel coil of 3.3 μH .

However, we do not intend to operate the trap at 21.0 MHz, but at 21.1 MHz. To determine the parallel values at the operating frequency, we need to take a few steps. First, we shall find the inductive and capacitive reactance of the inductor and capacitor at the operating frequency. We may return to basic equations, or we may take this shortcut:

$$X_{LB} = X_{LA} \frac{F_B}{F_A} \quad X_{CB} = X_{CA} \frac{F_A}{F_B} \quad (4)$$

where X_{LA} and X_{CA} are the reactance values at the resonant frequency, F_A , and X_{LB} and X_{CB} are the values of reactance at the new frequency, F_B . For operation at 21.1 MHz, we obtain an inductive reactance of $j 437.5$ Ohms and a capacitive reactance of $-j 433.4$ Ohms. The required parallel reactance of this combination we may call X_{NET} , which we may determine from this equation:

$$X_{NET} = - \frac{|X_L| |X_C|}{|X_L| - |X_C|} \quad (5)$$

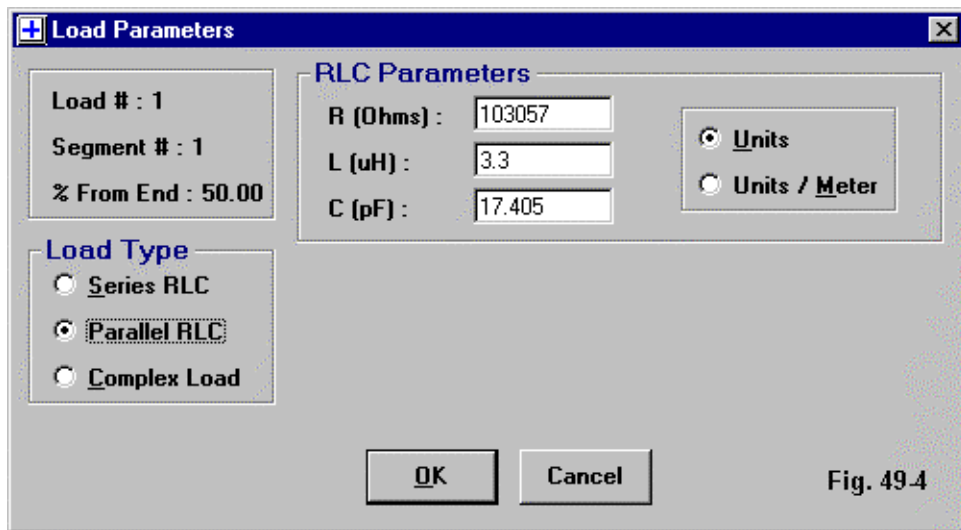
Note that the equation uses the absolute values of the reactances, not their originally signed values. For our test model at 21.1 MHz, the net or parallel reactance is $-j 45,829$ Ohms, although we do not have to enter that value, since we shall use the values of inductance and capacitance, 3.3 uH and 17.41 pF, respectively.

The parallel resistance for X_{NET} can be derived approximately from the parallel resistance at resonance using this equation:

$$R_{PB} = R_{PA} \left(\frac{F_B}{F_A} \right)^{1.5} \quad (6)$$

where R_{PA} is the parallel resistance at the resonant frequency, F_A , and R_{PB} is the parallel resistance at the new frequency, F_B . By raising the ratio of 21.1 over 21.0 to the

1.5 power—using the X^Y function of a hand calculator—we find a new parallel resistance of 103,057 Ohms.



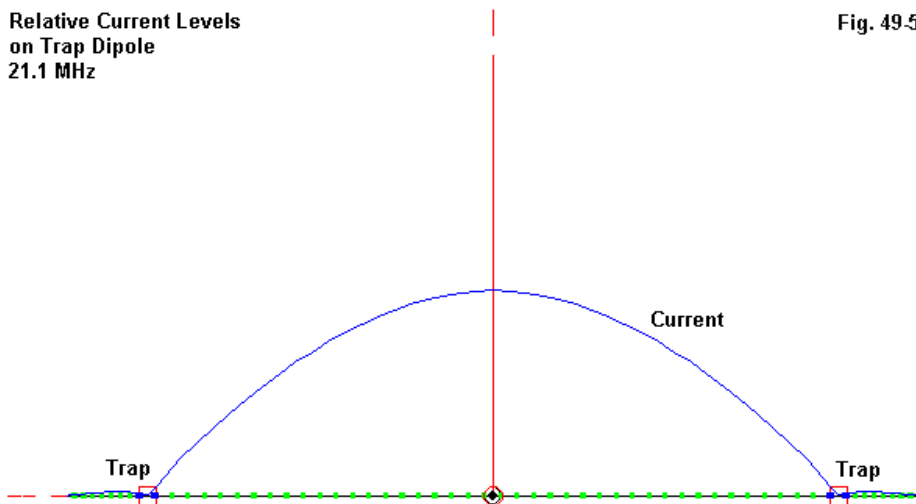
Now we are ready to install our approximate values into the parallel R-L-C load box for our test model. **Fig. 49-4** shows the NEC-Win Plus version of the entry. Remember that we have two traps and hence two parallel R-L-C loads to create. If we run the model at 21.1 MHz, we obtain a free-space gain of 2.05 dBi with a source impedance of about $71.9 - j 8.0$ Ohms. If we check the EZNEC load data output, we find less than 0.1-dB loss from the trap. If we check the NEC-Win Plus power budget table, we find an overall efficiency of almost 98%, despite the use of an aluminum element.

We may gauge the effectiveness of a trap in part by the degree to which it confines significant current levels to the 15-meter portion of the antenna. **Fig. 49-5** provides the EZNEC antenna view with the relative current magnitude showing. I have expanded the normal curve to show the just-visible low currents on the outer

ends of the wire, the portions designed to serve 20-meter operation. The fact that the source impedance is so close to the standard resonant 72 Ohms of a regular dipole further confirms the effectiveness of the trap.

Relative Current Levels
on Trap Dipole
21.1 MHz

Fig. 49-5



However, we wish to operate the antenna at 14.1 MHz as well. For this operation, we shall need to modify the test model. This version of the model will have loads that approximate the values seen at the lower frequency, well below the trap's resonant frequency. We must recalculate the applicable parallel combination of resistance and reactance that applies to the new frequency. At 14.1 MHz, the reactance of the 3.3-uH coil is about $j\ 292.4$ Ohms, and the reactance of the capacitor is about $j\ 648.5$ Ohms. Using the same two equations as we did for 21.1 MHz, we obtain for 14.1 MHz a parallel or net reactance of $j\ 532.2$ Ohms and a parallel resistance of about 56,297 Ohms. Of course, we shall use the values of inductance and capacitance that we started with, namely, 3.3 uH and 17.41 pF in the parallel R-L-C load, but with the new parallel resistance value.

For the revised model at 14.1 MHz, **Fig. 49-6** shows the values plugged into the NEC-Win Plus version of the load entry box. There are, of course, two traps to enter in parallel form. If we run the model at 14.1 MHz, we shall obtain a free-space gain of about 1.83 dBi, with a source impedance of about $66.8 + j 0.9$ Ohms. EZNEC's load data table shows a loss that slightly over 0.2 dB from the trap-equivalent load, while the NEC-Win Plus power budget table shows an efficiency of about 94.7%. Both supplementary values reflect the lower free-space gain at 20 meters.

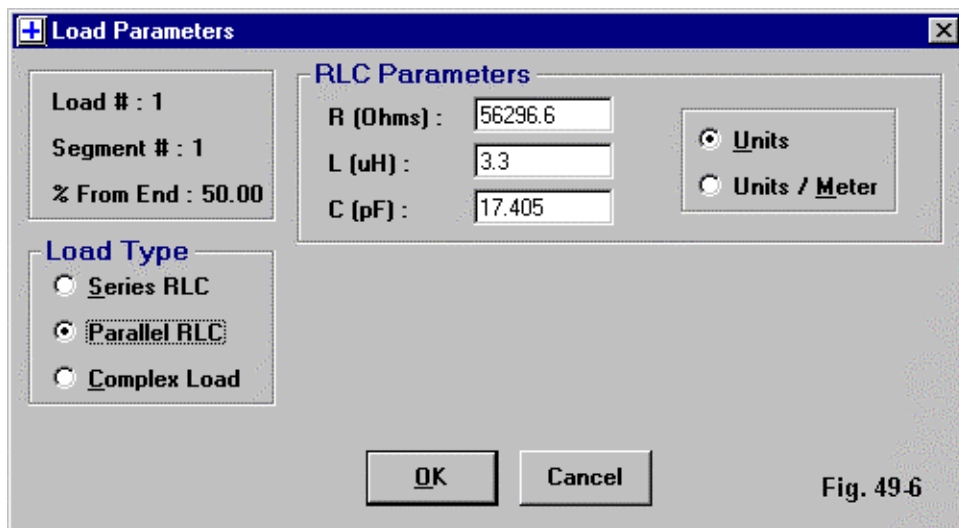
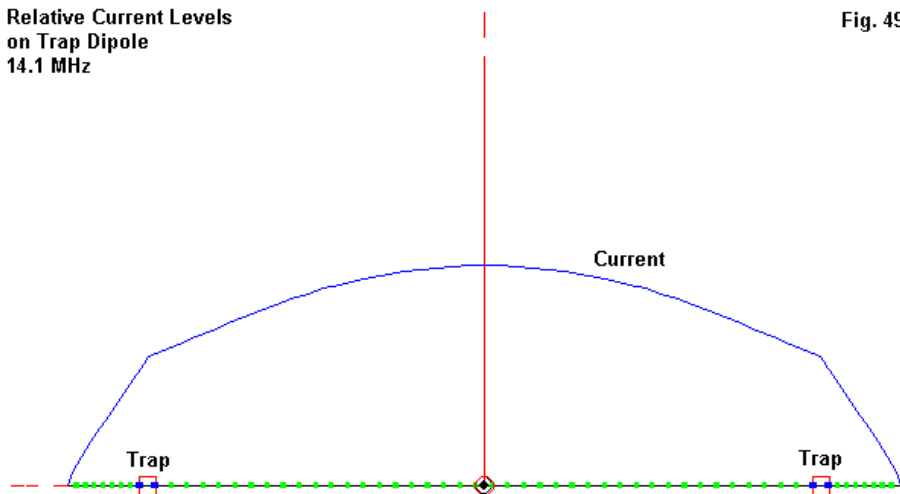


Fig. 49-6

Fig. 49-7 shows part of the reason for the reduced gain. The overall length of the trap dipole is shorter than a full-size version. The shortness is reflected in the source impedance, which is lower than normal for a dipole. In the antenna view, we can also see the sudden decrease in current past the trap positions on the antenna element.

Relative Current Levels
on Trap Dipole
14.1 MHz

Fig. 49.7



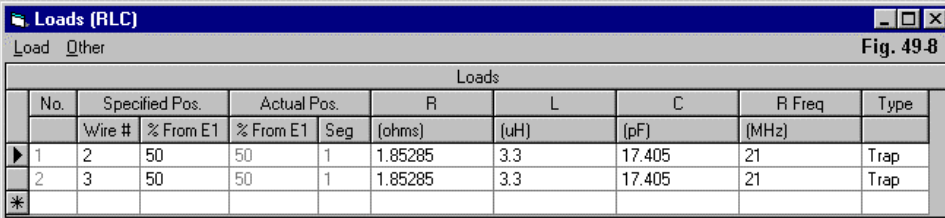
Part of the reduced efficiency is also due to the fact that the trap Q at 14.1 MHz is not the same as the coil Q that we used to estimate the parallel R-L-C load values. We may obtain the trap Q on 20 meters by reversing our calculations. We shall convert the parallel resistance and reactance into series values, using standard *ARRL Handbook* equations from Chapter 6:

$$R_s = \frac{R_p X_p^2}{R_p^2 + X_p^2} \quad X_s = \frac{R_p^2 X_p}{R_p^2 + X_p^2} \quad (7)$$

where the letters have the same meaning as they had in the series-to-parallel conversion equations. If we process our parallel values through these formulas, we obtain a series resistance of about 5.0 Ohms and a series reactance of about j 532.3 Ohms. Since Q is simply the reactance divided by the resistance, we obtain a value of about 106, somewhat lossier than the value we might obtain considering the coil alone. In fact, the entire trap must be considered at every frequency of use.

We cannot assume that, on frequencies below the resonant frequency of the trap, the coil alone determines the effect upon the antenna's performance.

The ability to transform a trap into a set of series values of resistance and reactance has a further benefit. If our interest in the trap antenna is confined to discrete frequencies, we may calculate the series values of resistance and reactance for each frequency, using the procedure that we have outlined. Then, we may use for each frequency a complex $R \pm jX$ (LD4) load instead of the parallel R-L-C (LD1) loads that we have used in the exercise. However, because LD4 loads do not change reactance with frequency, we cannot perform frequency sweeps with them. Although we can perform frequency sweeps with parallel R-L-C loads, we should limit the frequency excursions that we allow if the load is a trap conversion. Since the value of resistance changes with frequency, a given calculated value will return accurate result only over a limited frequency span.



Loads									
No.	Specified Pos.		Actual Pos.		R	L	C	R Freq	Type
	Wire #	% From E1	% From E1	Seg	(ohms)	(uH)	(pF)	(MHz)	
1	2	50	50	1	1.85285	3.3	17.405	21	Trap
2	3	50	50	1	1.85285	3.3	17.405	21	Trap
*									

Fig. 49-8

Those who may work with traps extensively and who have EZNEC can lighten the burden of modeling traps by using the special entry in the load list provided by the program. **Fig. 49-8** shows the entry box for a trap, using the series resistance and coil inductance, as well as the parallel capacitor value. Note that the frequency of the trap can also be specified. Under these conditions, through a related but somewhat different set of calculations, EZNEC calculates the requisite load values for each frequency at which the trap may be used, even if none of those frequencies happens to be 21.0 MHz.

EZNEC users may revise the load entry for the test model and run it at both 21.1 and 14.1 MHz. At the higher frequency, the gain should be 2.05 dBi with a source impedance of $71.9 - j 8.0$ Ohms. At 14.1 MHz, the corresponding values should be 1.83 dBi and $66.9 + j 0.9$ Ohms. The approximation system shown earlier for use

with any version of NEC-2, yields output values that are very usable compared to these. However, the appeal of the simple EZNEC trap entry system and of the ability to frequency hop without recalculation of load values is undeniable for individuals whose work requires extensive trap modeling.

In some ways, the degree of precision of the trap output data is related to more general questions of accuracy with respect to loads placed at some distance from the region in which the current changes slowly from one segment to the next. In our test model, the load is distant on 20 meters from the source, and from **Fig. 49-6**, we know that the current is changing fairly rapidly. Hence, the mathematical loads at the trap points will not calculate as accurately as loads placed closer in toward the source, and the inductor wire may have at least some affect on the total antenna length. Therefore, when working with trap antennas, allow considerable adjustment capability when moving from your model to the physical antenna.

We have not exhausted all that might be said about trap loads, but these exercises should enable you to proceed on your own.

* * * * *

Model included: 49-1. (All model dimensions in feet.)



50. The NEC-4 IS Card: Insulated Wires

From time to time, I shall look at some of the advanced features of both NEC-2 and NEC-4 programs. By “advanced,” I mean features not generally included on entry-level programs such as EZNEC 3.0 or NEC-Win Plus. Both of these widely used and user-friendly programs reduce the list of available geometry inputs and program control cards in the interest of effectively guiding the user through the modeling process.

However, both the NEC-2 and the NEC-4 core programs allow a considerable number of additional geometry and control functions. When NEC-4 appeared, it not only improved the accuracy of calculations for tapered-diameter elements, but as well added a number of new inputs. The one in which I am interested this month is the IS card or input. IS stands for “insulated sheath.” It provides a way for the user to analyze the performance of antenna wires with insulation.

For a long time, antenna builders have been aware that insulated antenna element wire has a velocity factor. The electrical length of an insulated wire will be longer than the physical length to a degree that depends upon the type and thickness of insulation. Expressed from a different perspective, a resonant dipole for some given frequency and wire diameter will be shorter if the wire is insulated than it will be if the wire is bare. How much shorter the insulated dipole will be depends on the insulation.

Unfortunately, there are no handy tables that are generally available to give us the velocity factors (VF) of insulated wires that are commonly used in wire antenna construction. However, experience has taught antenna builders that the values range from 0.99 down to 0.95 or so, depending on the type and thickness of the insulation. Perhaps the IS card of NEC-4 can give us some slightly better feel for insulated wire velocity factors, as well as introduce an advanced feature of a modeling program.

Modeling the Insulated Wire

An insulated wire, from the perspective of NEC-4, consists of a wire and an insulating sheath. The program assumes that the insulation begins at the exact surface of the wire and extends to some other point. The “other” point defines the radius of the sheath.

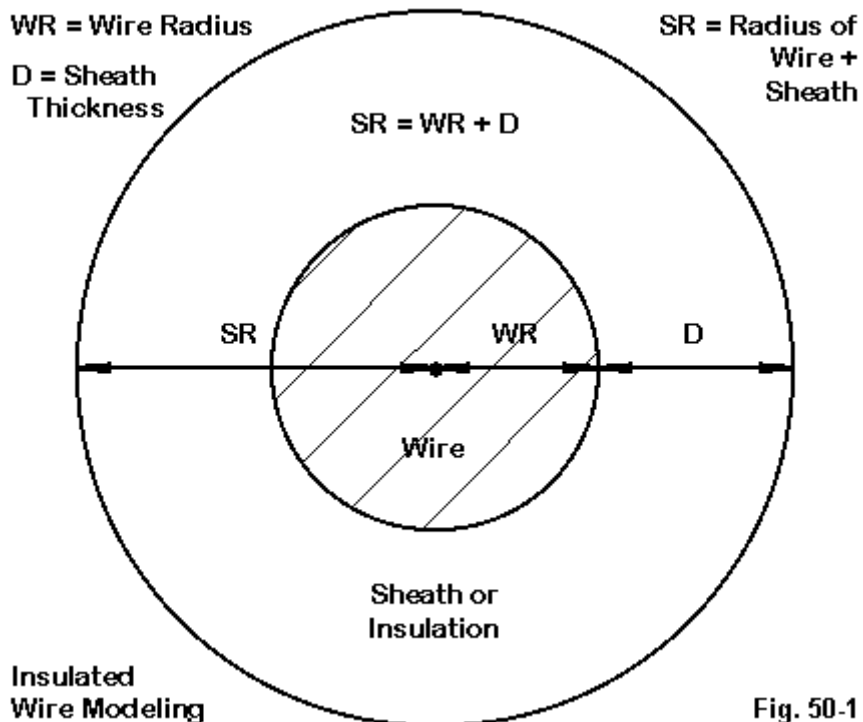


Fig. 50-1

Fig. 50-1 shows a sketch of the critical dimensions of an insulated wire and its model. We shall model the illustrated situation in GNEC, perhaps the only currently available commercial implementation of NEC-4 that allows the use of the IS input. Like the core itself, GNEC will expect that its wire geometry inputs list the wire radius and not its diameter. And the first step in setting up a model—without the insulation on the wires—is to set up the wire.

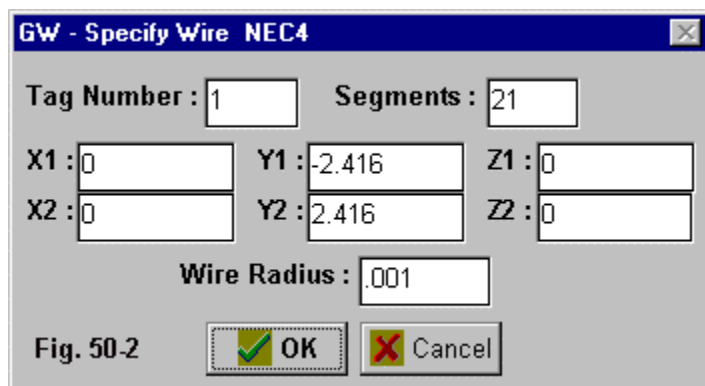
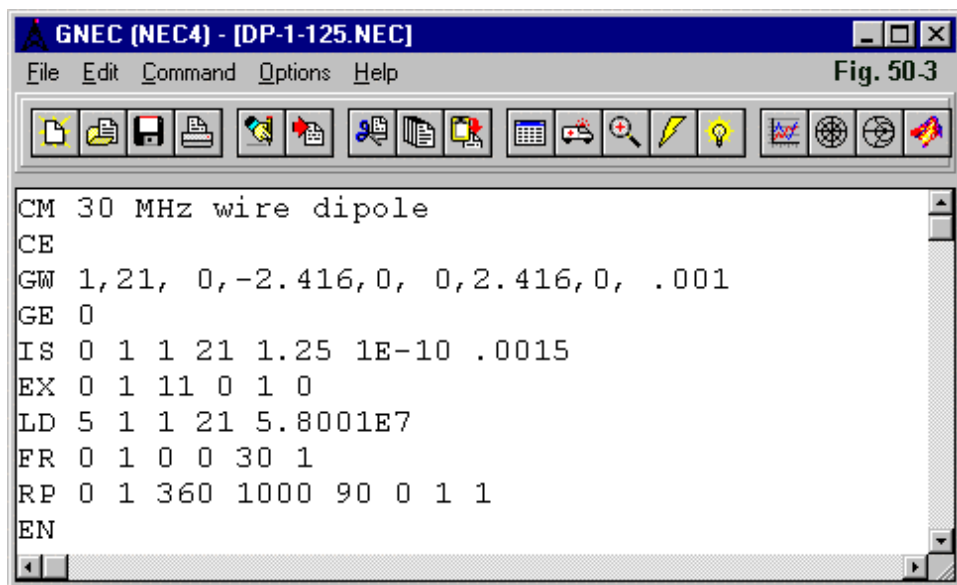


Fig. 50-2 shows the wire set-up panel from GNEC. The Tag number is simply the wire number. We shall give the wire 21 segments and place the source at its center (segment 11). In the examples that we shall explore, all dimensions will be in meters, the fundamental unit of measure of the NEC core. Hence, the single wire dipole—resonant at 30 MHz—will extend on each side of the X-axis along the Y axis ± 2.416 m. Likewise, the radius is in meters. $0.001\text{ m} = 1\text{ mm}$.

I selected the 0.001-m radius because 2-mm diameter copper wire is a very popular size for European antenna construction. A 2-mm wire is 0.07874" in diameter, just below the 0.0808" diameter of AWG #12 copper wire so popular with U.S. antenna builders.

Fig. 50-3 shows the basic antenna model in complete form for a free-space copper dipole resonated at 30 MHz. The CM or comment card is inaccurate because for the purposes of illustration, I have added a line that insulates the wire.

However, we should first trace the other lines of the model. The GW line shows the wire we created in **Fig. 50-2**, and the following GE line ends the geometry section of the model. The EX line specifies a voltage source placed at segment 11 of wire 1. The LD5 line provides the conductivity of copper as a material load on every segment of the wire. The FR or frequency request card shows a single frequency request of 30 MHz. The RP 0 line specifies a far-field azimuth (phi) pattern covering all 360 degrees around the antenna. See model 50-1.



If we ignore the IS line for a moment and return to the bare-wire model, the antenna will show a free-space gain of 2.10 dBi and a source impedance of 72.536 + j 0.178 Ohms. I have listed the impedance to many more decimal places than we might use operationally. However, at certain points in our work, we shall be interested in numerical progressions, and so I have given the data to the limits provided

by the program. The free-space source impedance of the bare-wire model will be important to us in more than one way as we proceed.

In Fig. 50-3, we inserted the IS line above the EX line. Let's see how to implement an insulated sheath for a wire.

IS - Insulated Wire NEC4

Type

- ☒ Specify Sheath
- ☐ Cancel Previous Sheath

Parameters

Tag #: First Segment:

Last Segment:

Sheath Radius (meters):

Relative Permittivity: Conductivity:

(S/m)

Fig. 50-4

Fig. 50-4 shows the line-assist screen for entering IS information. First, we must identify the wire to which the insulated sheath will apply, namely wire or tag 1 from the first to the last segment. Note that we have options here and may apply a sheath to only some or to all of the segments of a wire. Had we desired to leave the center segment bare, we could have specified 2 IS entries, one to cover segments 1-10 and the other to cover segments 12-21. The only restriction is that we cannot

apply two sheaths to any single segment. Hence, we cannot model the multi-layering of different types of insulation.

Beyond the segment-coverage of the shield, we have 3 significant variables to enter. One of them is the sheath outer radius, as measured from the wire center line to the sheath surface. The depth or thickness of the shield is the sheath radius minus the wire radius. In the illustration, the sheath is 0.0005 m (or 0.5 mm) thick (about 0.0197").

Note that the IS input is a program control card, not a wire geometry card. Therefore, we must input the value for the sheath radius in meters. If you have used the TL (transmission line) facility within a more basic program, you have sampled inputting dimensional values within a program control card. However, for user convenience, the programmers allow you to use the same units that you specified for the geometry section of your model. The program performs any necessary conversion for you. For NEC itself, the only acceptable input for all such program control entries will be in meters. In contrast, we could have specified the wire coordinates in any units of measure and then used a GS card to scale them to meters for the core run. I set up the basic model in meters so as not to require us to think in multiple systems of units within this exercise.

The inputs also call for a relative permittivity (or relative dielectric constant). The value shown is hypothetical and for illustration only. As I noted earlier, I do not presently have access to a handy list of relative dielectric constant values for wire insulation materials that we commonly encounter. One of the few guides available comes from the checking sources like *Passive Electronic Component Handbook*, 2nd Ed, edited by Charles A. Harper (McGraw-Hill, 1997). The capacitor chapter provides an interesting—although not wholly relevant—list of plastics used as capacitor dielectrics, along with their approximate dielectric constants.

Material	Approx. Permittivity
Polyisobutylene	2.2
Polytetrafluoroethylene (PTFE)	2.1
Polyethylene terephthalate (PET)	3.0-3.2
Polystyrene (PS)	2.5
Polycarbonate (PC)	2.8-3.0
Polysulfone (PSU)	2.8-3.2
Polypropylene (PP)	2.2

Common plastics, then, appear to have a range of relative permittivity values between 2 and 3. In contrast, the permittivity of a vacuum is by definition 1.0, and air is 1.0006. If we specify a relative permittivity value of 1.0 for any sheath, no matter how thick, we should obtain the performance of bare wire.

Note that we earlier specified that the two most interesting variables of insulation were its thickness and its type, which is expressed in the value assigned to the relative dielectric constant. In **Fig. 50-4**, we assigned the conductivity entry a very low value of 1E-10 S/m (or mhos/m). The assignment is arbitrary but not without reason. At any frequency of use, we assume that the insulation of an insulated antenna wire is highly effective. How ineffective must the insulating property be for the insulation to show some effect upon antenna performance?

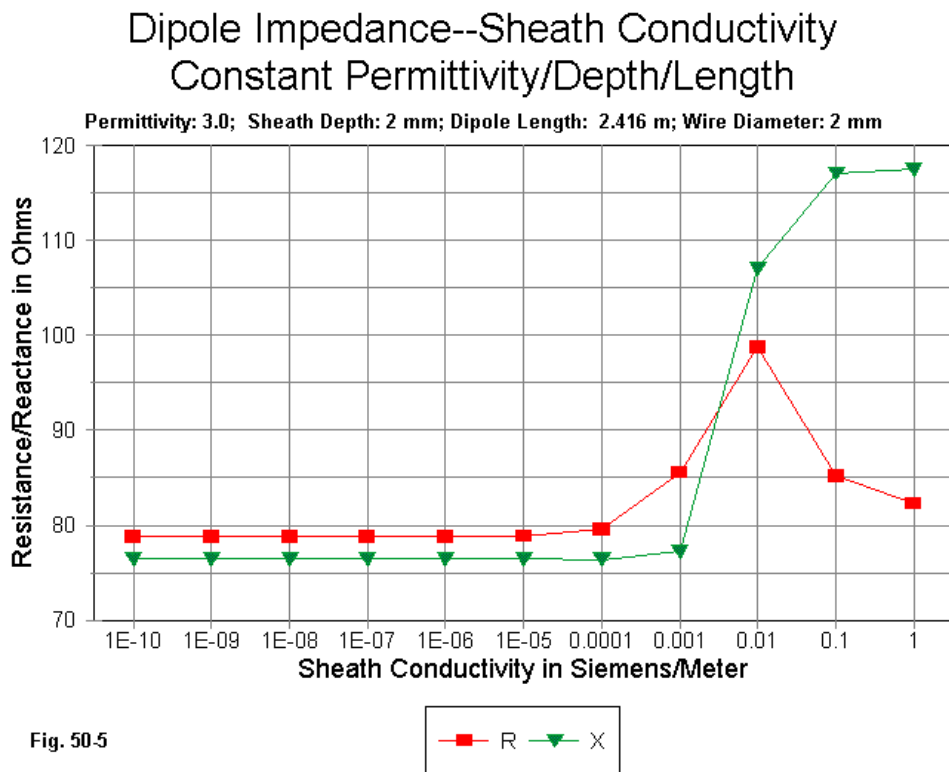


Fig. 50-5 suggests a partial answer. I took a particular situation and gradually increased the insulation conductivity. The original bare-wire dipole (+/-2.416 m) has a sheath that is 2 mm thick (for a total diameter of 6 mm or just under 1/4"). This relatively heavy insulation on a 2-mm wire has a permittivity of 3.0, the highest value scanned for these notes. I increased the conductivity in decades to produce the graph of source resistance and reactance in the figure.

Not until the conductivity passes the $1\text{E-}5$ S/m level (100,000 Ohms per meter resistivity level) do the values of source resistance and reactance show any change from the values at the lowest level of conductivity. At this level, the material is becoming a semi-conductor more than an insulator. Virtually all insulating materials have conductivity values of less than $1\text{E-}5$ S/m when used within their specified frequency and temperature ranges. Hence, setting the conductivity as a constant with the value of $1\text{E-}10$ S/m poses no problems. As well, it reduces the number of variables with which we must concern ourselves to a manageable value of 2.

Scanning the Range of Insulation Permittivity and Thickness

A specific modeling task for analysis might require that we have reasonably exact values for the insulation thickness and relative dielectric constant. Since we do not have access to such figures, let's perform a different sort of modeling task. Let's survey a variety of insulation thicknesses applied to our 2-mm bare wire and see how they affect dipole performance as we systematically increase the relative permittivity from 1.0 to 3.0.

We shall check 3 insulation thicknesses: 0.5, 1.0, and 2.0 mm (a 1-2-4 progression). A 2-mm thick insulation on a 2-mm wire yields a 6-mm overall insulated-wire diameter, close to 1/4". Here is what the dimensions will look like in tabular form:

Dimensions in Millimeters				
Wire Diameter	Wire Radius	Insulation Depth	Sheath Radius	Sheath Diameter
2.0	1.0	0.5	1.5	3.0
2.0	1.0	1.0	2.0	4.0
2.0	1.0	2.0	3.0	6.0

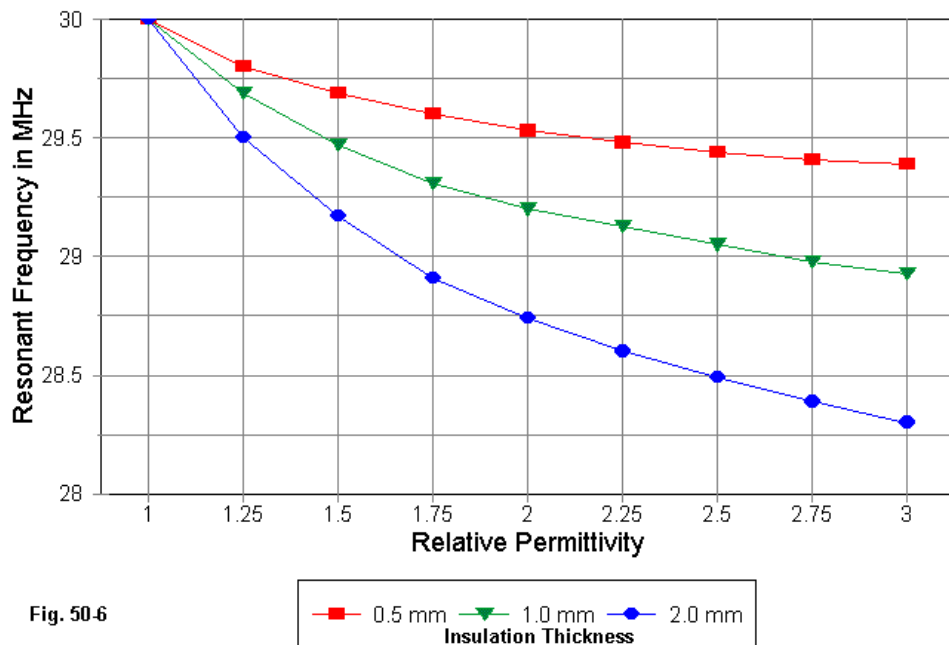
Dimensions in Inches				
Wire	Wire	Insulation	Sheath	Sheath

Diameter	Radius	Depth	Radius	Diameter
.07874	.03937	.01969	.05906	.11811 (< 1/8")
.07874	.03937	.03937	.07874	.15748 (5/32")
.07874	.03937	.07874	.11811	.23622 (< 1/4")

I have repeated the planned survey dimensions in inches for anyone not conversant with metrics.

Insulated Wire: Permittivity 1.0-3.0 Resonant Frequency at Bare Length

+/-2.416-m Long, 2 mm Diameter Copper Wire



We shall portray the results as a series of very similar graphs. Essentially, only the Y-axis will change as we check out various interesting parameters of antenna performance and size. **Fig. 50-6** graphs for each of the 3 insulation depths the resonant frequency of the original bare-wire antenna as we increase the permittivity. As expected, assigning a permittivity value of 1.0 to the sheath yields the original 30-MHz resonant frequency. However, for any given insulation depth, increasing the permittivity reduces the resonant frequency. In other words, the antenna becomes electrically longer than its physical length would indicate. Likewise, for any given value of permittivity, increasing the thickness of the insulation also reduces the resonant frequency of the antenna.

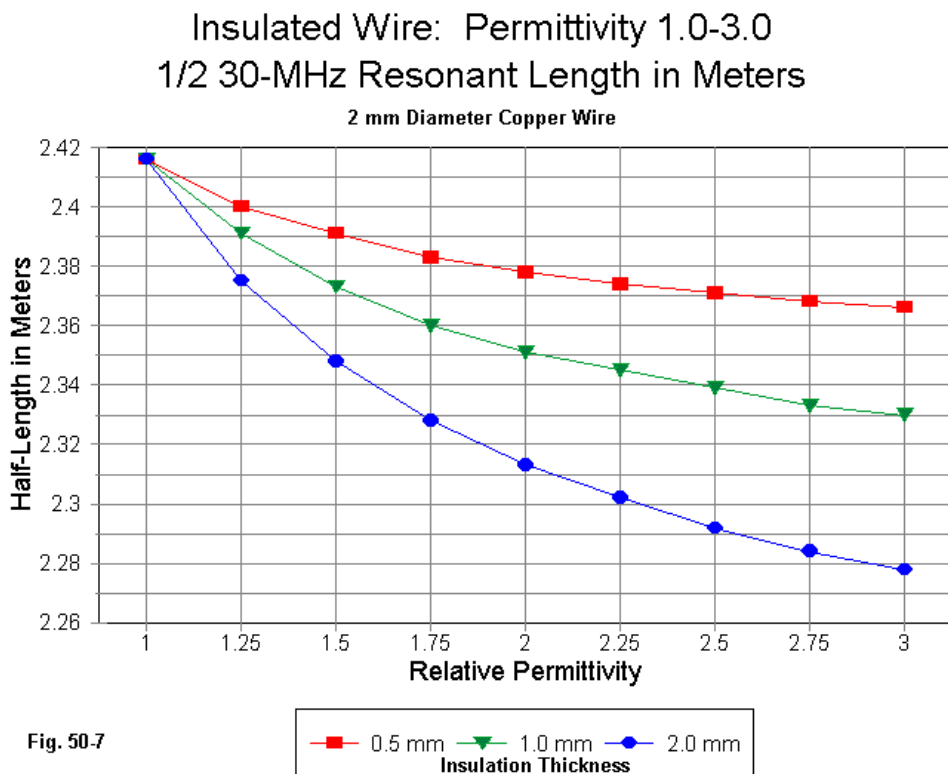
Note that for any insulation thickness, the highest rate of departure from the bare-wire resonant frequency occurs with the initial values of permittivity above 1.0. All three curves gradually flatten, although the thicker the insulation, the slower the rate of flattening. We may also look at the rates of change from the other perspective: for any given permittivity, the highest rates of departure from the bare-wire resonant frequency occur with the initial thickness increases. Each curve represents a doubling of insulation thickness, but the distance between the lower two curves is not twice the distance between the upper two curves.

Fig. 50-7 plots for each of the sheath thicknesses the resonant half-length of the dipole element versus the increasing permittivity. I re-resonated each dipole by changing its length until the source impedance again reached a value where the reactance was less than ± 1 Ohm. In fact, all of the checkpoints have reactances less than ± 0.6 Ohm. This amount of “play” in resonant lengths does limit the precision of the curves, although the general sweep is well within any desired scale of accuracy.

Since the antenna model extends its element on each side of the X-axis, the element half-length is the most convenient unit of measure. As we might expect, for the insulated dipole to be resonant at 30 MHz, we must reduce its length, with both the insulation permittivity and depth contributing to the shortening effect.

A convenient rule of thumb used by many antenna builders is to use the ratio of the measured insulated wire resonant frequency and the anticipated bare-wire resonant frequency as the amount by which to multiply the wire length to arrive at an insulated wire antenna that is resonant at the originally desired frequency. For prac-

tical purposes within the scope of insulation depths and permittivity values in this exercise, the rule of thumb will work. However, as the permittivity approaches 3.0 and the insulation thickness approaches 2.0 mm on a 2-mm wire, the actual element length needed for resonance will be slightly shorter than the frequency ratio suggests. Therefore, when calculating the insulated wire velocity factor, one should use the resonant wire length rather than the frequency offset.



In **Fig. 50-8**, we have the same data as in **Fig. 50-7**, but expressed in terms of a range of velocity factors for the insulated wire antennas. If we take the range of probable insulation permittivity values to run between 1.5 and 3.0, then 0.99 is about the lowest velocity factor that we encounter for wires with very thin, low permittivity insulation. However, wires with higher permittivity insulation that is also thick may have velocity factors that go well below the 0.95 value often cited as the approximate lowest value. Since a number of plastic materials have permittivities above 2.8, the antenna builder should be prepared to shorten the dipole more radically than indicated by rules of thumb wherever the insulation is thick.

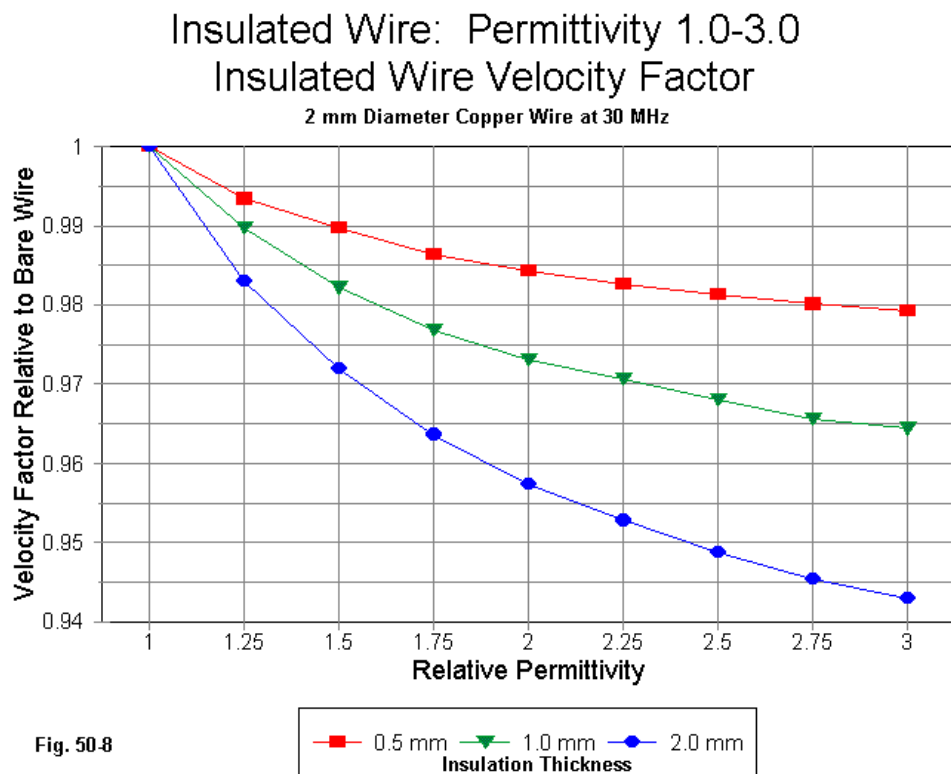
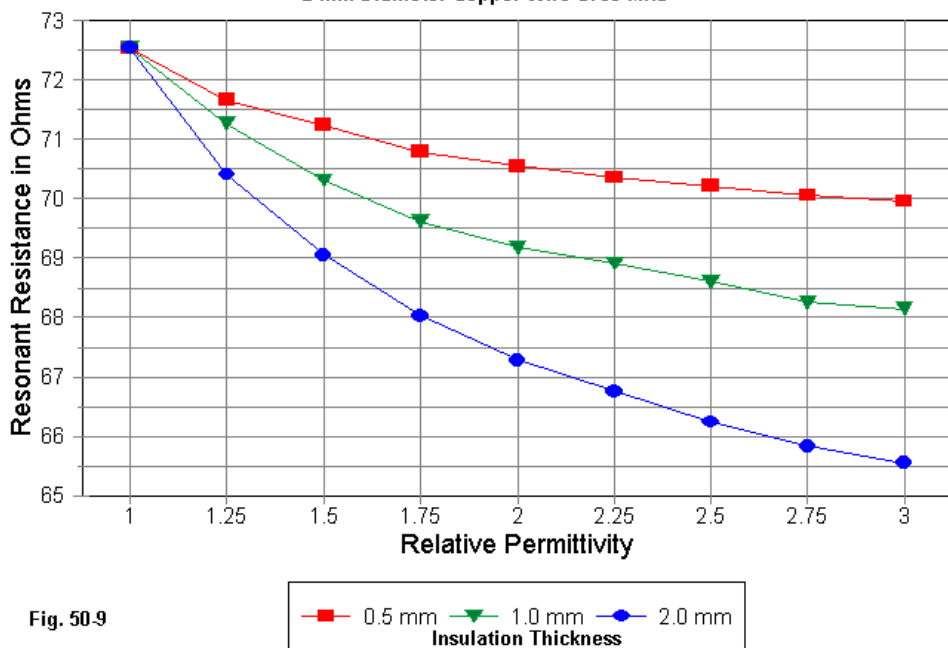


Fig. 50-9 calls to our attention an often overlooked aspect of the antenna wire's velocity factor. As we shorten a dipole for virtually any reason, the resistive component will decrease relative to its bare-wire resonant value. The bare-wire resonant resistance was just over 72.5 Ohms. All of the re-resonated 30-MHz sheathed dipoles yield resistive impedance values that are lower than the bare-wire value. The curves for the resistive impedance values track the curves in each of the other graphs shown here.

Insulated Wire: Permittivity 1.0-3.0 Resonant Impedance

2 mm Diameter Copper Wire at 30 MHz



For low values of relative permittivity or for thin insulation, the amount of impedance decrease is largely insignificant to antenna operation, especially as a dipole. However, the highest decrease shown, about 7 Ohms, may become a noticeable amount if thick wires of the highest permittivity value are used in a complex parasitic array. Such arrays may exhibit low bare-wire impedances, and 6 more Ohms of decrease may become objectionable relative to initial design plans for systems of matching the antenna source to a feedline.

Nonetheless, the small demonstration using the NEC-4 IS program control card does show a fairly close correlation between experiential rules of thumb and reasonable values of insulation thickness and permittivity as modeled for a dipole. Of course, this exercise has covered only 2-mm diameter wire. Amateur antenna builders very often use other wire diameters, ranging from AWG #18 to AWG #10 or so. Whether we can extrapolate the values from this exercise to these other cases is uncertain unless someone runs the same exercise for a reasonable sampling of the other wire sizes.

The curves may also serve to answer some questions often posed by those new to antenna work. For example, upon learning that the oxide of aluminum that forms on all antennas made from the material is an insulator, folks often ask whether that oxide has any significant effect on performance. We may use any one of the graphs to perform a crude extrapolation, even knowing that the tabulated permittivity of the material is 2.5-2.8: since the oxide thickness is only a few molecules, the graph line for the aluminum oxide material would be barely discernable at the top of **Fig. 50-6**.

Although the most common uses of the IS program control card may be connected with the use of insulated wire in antenna structures, these are not the only uses. The wire that we construct as the core around which to model a sheath need not be a highly conductive or even a thin wire. We might assign the wire a fairly low conductivity, and NEC-4 also permits us to assign a value of permeability so that we may account for any effects due to the wire's magnetic properties. We may also sheath the wire, using a uniform depth as a limitation, with any values we might like for conductivity and relative permittivity. Unlike the dipole, we do not need to place a source on the wire itself. Instead, we may use plane-wave excitation with either linear or elliptical polarization.

I can imagine numerous possible—but not necessarily real—applications for such an arrangement. There are as many applications as there are two-tiered physical structures where our interest may lie in the currents induced in the inner or “wire” layer. Bone-to-marrow, weather-insulation-to-pipe, and sheathing-to-mechanical-link-cable situations are but 3 possibilities among many.

The limiting factors for such modes of analysis are two. First, the situation must resemble an insulated wire so that a sheath covers a long inner element. We can create many shapes by linking such wires and sheathing all of them, although not necessarily with the same “material,” that is, with the same values of conductivity, permittivity, and thickness. The second—and perhaps more challenging—limitation is our knowledge of the conductivity and relative permittivity of a broad spectrum of materials. However, both conductivity and permittivity are subject to measurement.

Although not assured, it may be possible to use the IS input in conjunction with a wire and a cylinder created from direct wire inputs to model a coaxial cable. However, there are numerous issues connected with such a structure if it is to simulate an existing coaxial cable. These issues include the effective surface coordinates of the inner side of the cylinder relative to the wire radius, the sensitivity at the test frequency of the structure to close-wire modeling limitations—including closely spaced wires of different diameters, and the relative lengths of segments meeting at junctions within the cylinder structure. However, in principle, the IS entry may be used to simulate the dielectric between the center wire and the cylinder that represents the outer conductor.

In the end, antenna modeling software offers a great many more opportunities for RF analysis than the task of designing antennas can contain. The geometry input and the program control cards in the NEC-deck are simply tools to use in those processes. And, like all tools, they are subject to creative applications.

* * * * *

Model included: 50-1, .NEC format only. (All model dimensions in meters.)



Appendix: Antenna Models

This volume—the second of 3 volumes—of antenna modeling notes comes with 86 antenna models, almost all of which have text references (Model xx-x). I have included most of the models in 3 different formats: .EZ for users of EZNEC, .NWP for NEC-Win Plus users, and .NEC for NEC-Win Pro, GNEC, and generic NEC-2 core users. The folder (directory) structure simply follows this scheme.

N:\models\ez	for EZNEC format files
N:\models\nec	for generic ASCII NEC files
N:\models\nwp	for NEC-Win Plus format files

I recommend that you copy the most relevant set of files into your hard drive for use. NEC-Win Plus, for example, will store its output files in the same directory as the basic model file, and that requires a space to which the computer can write. Each file name follows the text by starting with the column number, followed by the model number within the chapter. So Model 34-3 is the third model used in conjunction with column #34.

The files are not likely to add to your collection of models in the sense of providing new or interesting antenna designs. For that purpose, I have assembled collections of interesting models from my own storehouse. These collections are available from *antenneX*. The files that go with this volume of antenna modeling notes are those referenced in the text. As such, they are illustrations of the principles discussed in the text. Hence, you may read along with your own modeling software active and investigate further the model under discussion.

You will find some discrepancy between many of the model outputs and the performance figures cited in the text. This situation has a number of sources, all related to the fact that I began the series in the last century (the late 1990s). In some cases, I simply could not find the file used for a column, and so I had to reconstruct as best I could the model under discussion. Sometimes, the text did not provide complete modeling data, so I approximated the text model as closely as

possible. Although the exact figures may not jive between text and model, the trends certainly do.

In other cases, software developments are the source of slight numerical deviance between the model as used when I wrote and the same model when you run it on your current software. When I began the series of columns, EZNEC was a DOS program, and now uses Windows. NEC-Win Plus did not yet exist. In the course of time and software development, the NEC cores have undergone customizing and enhancement for speed—with special reference to the latest Fortran compilers. In the process, there have been changes in the order of operations and rounding conventions, enough to create slight output differences. With respect to guiding construction, showing performance trends, or yielding reliable analysis, the changes make no noticeable difference relative to older outputs. However, in order to show trends as sensitively as possible, many parts of the output data cited in the text will be overly precise. That fact will create an illusion of difference where no operationally significant difference exists.

Models for columns 27, 28, 29, 30, and 32 require a model-by-equation facility. Hence, they appear only in the .NWP format. Model 50-1 requires NEC-4 and appears only in .NEC format.

I regret that I cannot include in this collection of models samples of MININEC files. I have and use several MININEC programs, including ELNEC, AO, MMANA, NEC4WIN, and the most recent and able version, Antenna Model. Each version uses a different file format, and there are few means of converting a MININEC file from one format to another except by writing the model from scratch. In contrast, I was able to convert files from one to another of the NEC formats. Conversion is not perfect, and so some EZNEC files given in English measures will appear in metric form in the generic NEC and NEC-Win Plus formats.

With these limitations in mind, I hope that the attached files enhance your safari through the topical jungle within this volume of antenna modeling notes.

Other Publications

We hope you've enjoyed this second of several volumes of the **Antenna Modeling Notes: Volume 2**. You'll find many other very fine books and publications by the author L.B. Cebik, W4RNL in the ***antenneX Online Magazine BookShelf*** at the web site shown below.

A Publication by
antenneX Online Magazine
<http://www.antennex.com/>
POB 271229
Corpus Christi, Texas 78427-1229
USA

Copyright © 2003 by **L. B. Cebik** jointly with ***antenneX Online Magazine***. All rights reserved. No part of this book may be reproduced or transmitted in any form, by any means (electronic, photocopying, recording, or otherwise) without the prior written permission of the author and publisher jointly.

ISBN: 1-877992-55-0
